Université d'Ottawa · University of Ottawa

CONSTANT VOLUME RING SHEAR TEST FOR SAND

Julio Angel Infante Sedano, B. Sc.A.

A Dissertation
Submitted to School of Graduate Studies
Under the supervision of

Dr. Vinod K. Garga, P. Eng., F. EIC.

in partial fulfilment of the requirements for the degree of

M. Sc. in Civil Engineering

Department of Civil Engineering
University of Ottawa
Ottawa, Ontario
Canada K1N 6N5

December 1998

The M. Sc. in Civil Engineering is a joint program between Carleton University and University of Ottawa, which is administered by the Ottawa-Carleton Institute for Civil Engineering.

0-612-38755-0

ABSTRACT

A ring shear device was designed to permit constant volume tests to be performed on granular materials. Constant volume ring shear tests can be used to simulate undrained conditions of shearing. The very large deformations allowed by the ring shear device are well suited to determine the steady-state strength of granular material. The steady state strength is an important parameter in evaluating the stability of sand deposits against flow sliding. The main contributions of this study are as follows:

- Tools and methods were developed to prepare annular samples of granular materials.
- Tools and methods were developed to verify the quality of the samples prepared.
- Tests on Unimin 2010 quartz sand showed that for this material, the steady state shear strength is independent of the presence of water, the rate of shear, and the fines content.
- There is good agreement in the steady state line obtained from constant load and constant volume ring shear tests with that obtained from triaxial tests.
- The constant volume ring shear test provides a lower steady-state friction angle than the undrained triaxial test.

ACKNOWLEDGMENTS

The author would like to express his most sincere appreciation to his research advisor, Dr. Vinod K. Garga, for his continuous support, invaluable advice, and guidance throughout the research program. The author also wishes to gratefully thank Dr. Erman Evgin, and Dr. Tim Law for serving as members of the examination committee.

The author would also like to gratefully acknowledge the financial support from the University of Ottawa and from the Natural Sciences and Engineering Research Council of Canada (NSERC).

Thanks to all the support staff in the department of Civil Engineering, and particularly to Mr. Richard Moore for his exceptional technical support.

TABLE OF CONTENTS

1 INTRODUCTION

1.1 STATEMENT OF THE PROBLEM

The widespread liquefaction that occurred in two major earthquakes in 1964 in the Prince William Sound, Alaska, and Niigata, Japan, focussed the attention of geotechnical engineers on the problem of seismic liquefaction. There is, at present, an increase of interest in the study of the steady state strength of granular soil which is the strength that the soil will mobilize even after very large deformations. The use of this strength parameter permits a rapid assessment of the post-seismic stability condition of an earth structure.

In 1939, Hvorslev, in his classical paper "Torsion shear tests and their place in the determination of the shearing resistance of soils", stated that the principal object of shear tests was the determination of :

(a) the maximum shearing resistance
(b) the bond resistance and the velocity of the slow plastic flow before failure
(c) the temporary or permanent decrease of the shearing resistance after failure and
(d) the stress-strain relationships and volume change characteristics due to shearing stresses.

In addition Hvorslev (1939) emphasized that consideration had to be given to simplicity in the construction and operation of the testing apparatus, to difficulties in sample preparation, and to the time required for testing. After examining the various tests available, including the direct shear test using the shear box, he concluded that objects *a*, *b*, and *d* could best be achieved in the triaxial apparatus. (Bishop et al., 1971).

As for item *(c)*, Hvorslev commented: "the fact that very large displacements often are required to produce this minimum value of shearing resistance seriously affects the suitability of various types of shearing apparatus. The data on the decrease of the shearing resistance after failure are required to determine the factor of safety of earth structures in which a localized failure of the soil is allowed or cannot be prevented." He concluded that this last item could only be achieved satisfactorily in a form of the torsion shearing that he called the *ring shearing apparatus*. The obvious advantages of a torsional shear apparatus to test soils at large strains is that there is no change in cross-section as the shearing progresses.

This research, therefore, has focussed on the determination of constant volume shear strength of granular soils at large strain, using the ring shear device. It was also of interest to compare the steady state (SS) strength obtained from constant volume tests using the ring shear apparatus to the values obtained by Zhang (1997) using the triaxial apparatus.

1.2 RESEARCH OBJECTIVES

The main objectives of this experimental study were:

1) To modify a ring shear test for constant volume tests
2) To assess the suitability of sample preparation methods
3) To verify the progress of particle breakdown at the sliding surface
4) To investigate the effect of the normal stress on the strength envelope
5) To compare the results of constant volume (CV) ring shear tests to those from triaxial tests
6) To assess the effect of shear rate on the undrained residual strength, S_{ur};
7) To assess the influence of fines on the undrained residual strength S_{ur};

1.3 SCOPE OF RESEARCH

In order to accomplish the research objectives experimental work was undertaken to cover the following aspects:

1. Develop tools to produce uniform sand samples in a ring cell

2. Investigate the uniformity of the samples produced.

3. Conduct simple comparative friction tests between aluminium rings and teflon rings to evaluate the relative importance of interannular friction in either case.

4. Conduct constant load and constant volume test using teflon as well as aluminium rings to study the impact of confining wall friction on ring shear results.

5. Conduct constant load and constant volume tests on sand specimens to evaluate the influence of the type of test on the results.

6. Conduct tests on saturated and dry sample to evaluate the influence of presence of water on the results.

7. Conduct tests at various shear rates to verify the influence of the shear rate on the residual strength.

8. Conduct tests with various fines contents to study the effect of the presence of fine particles on the shear strength of the soil.

1.4 OUTLINE OF THESIS

Chapter 2 presents a literature review on previous studies made on liquefaction and the ring shear device.

Chapter 3 describes the devices developed during this research.

Chapter 4 describes the steps involved in sample preparation and conduction of ring shear tests and sample density verification.

Chapter 5 describes the various verification tests and their results.

Chapter 6 describes the results obtained from ring shear tests.

Chapter 7 presents the conclusions of this study, and provides some recommendations for further research and development.

Appendix I presents a number of test results in graphical form.

2 LITERATURE REVIEW

The post-liquefaction shear strength is the strength that can be relied upon for stability even after liquefaction has been triggered. Castro's (1969) study of liquefied soils showed that even after liquefaction, many sands retain a significant shear strength. The undrained shear strength of liquefied soil is referred to as the steady-state strength by Poulos et al. (1985), residual strength by Seed (1987), and undrained critical strength by Stark and Mesri (1992)

The post-liquefaction shear strength is important when considering the stability of soil structures, such as dams, bridge foundations, storage tanks, docks, and any other case where soils prone to liquefaction might be present.

2.1 LIQUEFACTION

Liquefaction is the phenomenon in which a sand changes its behaviour from a solid state to a fluid state. It was recognized early in the century. In 1920, Hazen used the term "*liquefies* "to describe the flow slide failure of the hydraulic fill sands of the Calaveras Dam. Terzaghi and Peck (1948), in their classical text book *Soil Mechanics in Engineering Practice*, indicated that a slight disturbance such a mild shock could significantly decrease the volume of very loose fine sand while the overburden pressure remains unaltered. When such a decrease occurs below the ground water table, it is preceded by a temporary increase in pore water pressure to a value very close to the overburden pressure thus reducing the effective overburden pressure to almost zero, and causing the sand to flow as a viscous fluid. They defined the phenomenon as *spontaneous liquefaction*. Various definitions of the liquefaction phenomenon have subsequently been proposed by various researchers.

Casagrande (1975) presented the following definitions:

1. *Actual liquefaction is the response of loose, saturated sand when subjected to strain or shock that results in substantial loss of strength and in extreme cases leads to flow slides.*

2. *Cyclic liquefaction is the response of a test specimen of dilative sand to cyclic loading in a triaxial test when the peak pore pressure rises momentarily in each cycle to the confining pressure.*

Seed (1979) presented the following definition of Liquefaction:

> *Liquefaction denotes a condition where a soil will undergo continued deformation at a constant low residual stress, due to the buildup and maintenance of high pore water pressures, which reduce the effective confining pressure to a very low value; the pore pressure buildup leading to liquefaction may be due either to static or cyclic stress applications and the possibility of its occurrence will depend on the void ratio or relative density of a sand and the confining pressure; it may also be caused by a critical hydraulic gradient during an upward flow of water in a sand deposit.*

Castro (1982) defined liquefaction as follows:

> *Liquefaction is a phenomenon wherein a mass of soil loses a large percentage of its shear strength, when subjected to undrained monotonic, cyclic or shock loading, and flows in a manner resembling a liquid until the shear stresses acting on the mass are as low as the reduced shear resistance.*

Robertson (1994) proposed the following modified definitions, based on the understanding of the behaviour of particulate soils gathered in the last decade.

1. Flow liquefaction:

- *Requires strain softening response in undrained loading resulting in constant shear stress and effective stress, (i.e. ultimate steady or critical state).*

- *Requires that in-situ shear stress is greater than undrained residual or steady state shear strength.*

- *Flow liquefaction can be triggered by either monotonic or cyclic loading,*

- *For failure of a soil structure to occur, such as a dam or a slope, a sufficient volume of material must show strain softening response. The resulting failure can be a slide or a flow depending on the material characteristics and slope geometry. The resulting movements are due to internal causes and can occur after the trigger mechanism.*

- *Flow liquefaction can. occur in saturated, very loose granular deposits, very sensitive clays and loose loess deposits.*

2. Cyclic liquefaction:

- *Requires undrained cyclic loading where shear stress reversal or zero shear stress can develop (i.e. where in-situ static gravitational shear stress is low compared to cyclic shear stress).*

- *Requires sufficient undrained cyclic loading to allow effective confining stress to essentially reach zero.*

- *At point of zero effective confining stress no shear stress can exist, when shear stress is applied, pore pressure drops and a very soft initial stress strain response can develop resulting in large deformations. Soil will strain harden with increasing shear strain.*

- *Deformations during cyclic loading when effective stress is approximately zero can be large, but deformations generally stabilize when cyclic loading stops. The resulting movements are due to external causes and only occur during the cyclic loading. Subsequent movements can occur due to pore pressure redistribution. However, this will depend on ground condition and soil stratigraphy.*

- *Can occur in almost all sands provided size and duration of cyclic loading is sufficiently large. For dense sands, the size and duration of cyclic loading will be large and hence, the condition of zero effective confining stress may not always be achieved.*

- *Clays can experience cyclic liquefaction but deformations at zero effective stress are generally small due to the possible cohesive strength at zero effective stress and deformation are often controlled by rate effects (creep).*

Poulos (1997) gives the following definition for liquefaction:

> *Liquefaction is the undrained shear failure of a loose sand or a soft clay tat results when (1) the in-situ driving shear stresses on the soil mass prior to failure exceed the undrained steady state shear strength of the mass (2) additional shear stresses are applied fast enough to cause undrained shear, and (3) the latter stresses are large enough to cause strains that exceed the strain at peak in the mass such that steady state deformation can be approached.*

From the previous definitions, it can be seen that the terms *liquefaction*, *actual liquefaction*, and *flow liquefaction* refer to the same phenomenon in which a large displacement of a soil mass results from the sudden buildup of pore pressure, and therefore a reduction in effective confining stress.

Cyclic mobility

Cyclic mobility is the progressive softening of a saturated sand when subjected to cyclic loading at constant void ratio. The softening is accompanied by high pore pressures, deformations, but it does *not* lead to loss in shear strength nor to continuous deformation, both of which are essential aspects of liquefaction.

2.2 POST-LIQUEFACTION BEHAVIOUR

The post-liquefaction shear strength was first defined by Casagrande (1936) while developing the critical void ratio concept. Because of this, Stark and Mesri (1992) termed this shear strength the undrained critical strength. They concluded that this is the shear strength available after liquefaction has been triggered and that it is applicable for the purpose of post-liquefaction stability analyses.

2.2.1 Stress-Deformation Characteristics

Poulos (1997) states that the term *post-liquefaction strength* should not be used to describe the Steady State Strength since it leads to the assumption that liquefaction *must* occur to reach this strength, while it can be reached, without the occurrence of liquefaction, if the strain conditions are sufficient to reach the Steady State.

In undrained conditions three typical stress-strain curves appear associated with the strain-softening (contractive), strain-hardening (dilative), and limited strain-softening (partly contractive) behaviours. These curves, illustrated in **Fig. 2.3**, are:

Strain-softening curves

This curve is more typical of loose samples. In this case, the deviator stress and the pore pressure both increase to a small axial strain. The sample then suddenly collapses, the shear resistance drops significantly and the pore pressure increases rapidly. After having reached this point, the sample continuously deforms (**Fig. 2.3**)

Strain-hardening curves

In the case of a dense sand, the pore pressure and the deviator stress increase until the phase transformation is reached. At that point, the initially contractive behaviour of the sand becomes dilative, the pore pressure continuously decreases as strain progresses, while the deviator stress keeps increasing. The stress-path follows a straight failure envelope. (**Fig. 2.3**) For a sand with strain hardening behaviour, flow liquefaction is not possible, since the resistance of the sand increases continuously during undrained loading (Zhang & Garga, 1997 (a))

Partly strain-softening curves

If the sand sample is medium loose, the sample will initially behave much like the loose sample, that is, the deviator stress and pore pressure will initially increase with axial strain until the stress path reaches the ***collapse surface***. At this stage, a rapid deformation occurs, much as in the strain-softening behaviour, and the pore pressure increases while the deviator stress decreases. With further straining, however, the pore pressure will start decreasing while the deviator stress will increase, and, once again, the stress-path will follow a straight failure envelope.

Flow structure

Casagrande (1971) developed the concept of flow structure to explain stress paths of the type of (**Fig. 2.1**). He explained that a sand can change its static grain structure to a flow structure where the relative position of the grains is constantly changing to offer a minimum of resistance. This change of structure would start in a nucleus and spread though the sand mass in a chain reaction.

2.2.2 Critical State

Casagrande demonstrated that under conditions where volume changes can occur and for any given confining pressure, loose sands compress shear and dense sands dilate, leading to the postulation of a critical void ratio, e_{crit}, for which no volume change would occur during loading (Seed & Lee, 1967). This void ratio can be reached from either loose or dense conditions. If no drainage is allowed, dense sands will tend to gain strength when volume changes are prevented, while loose sands will tend to lose strength. The critical void ratio is one at which shearing under constant volume condition leads to no strength change (Taylor, 1948).

Roscoe et al. (1958) extended Casagrande's concept of void ratio to the critical state: the critical void ratio state.

> *In a drained test, the critical void ratio state can be defined as that ultimate state of a sample at which any arbitrary further increment of shear distortion will not result in any change of voids ratio. In any series of drained tests the set of critical void ratio points so defined can be expected to lie in or near a line on the drained yield surface.*
>
> *In an undrained test, the sample remains at a constant void ratio, but he effective stress will alter to bring the sample into an ultimate state such that the particular*

void ratio, at which it is compelled to remain during shear, becomes a critical void ratio. In any series of undrained tests the set of critical void ratio points so defined can be expected to lie in or near a line on the undrained yield surface.

This definition implies that an element of soil undergoing uniform shear distortion can eventually reach a critical state at which it can continue to deform without further change of void ratio and the effective stresses q' and p' (Roscoe and Burland, 1968). The critical state points from drained and undrained tests lie on a unique line (called the critical state line) (Roscoe et al., 1958, 1963).

2.2.3 Steady State of Deformation

The steady state of deformation was originally defined by Castro and Poulos (1977) as the state in which a will flow under constant shear stress at constant effective minor principal stress and at a constant volume, and modified in 1981 by Poulos to include the requirement of constant velocity. This last definition states:

The steady state of deformation for any mass of particles is that state in which the mass is continuously deforming at constant volume, constant normal effective stress, constant shear stress, and constant velocity. The steady state of deformation is achieved only after all particle orientation has reached a statistically steady-state condition and after all particle breakage, if any, is complete, so that the shear stress needed to continue deformation and the velocity of deformation remain constant.

Finn (1971), describes the steady state as:

When the sand is strained beyond the point of peak strength, the undrained strength drops to a value that is maintained constant over a large range in strain. This is called the undrained steady state or residual strength.

This steady state is only reached at large strains after the effect of the initial conditions, soil fabric and stress-strain history have been has been erased, after all particle orientation has reached a statistically steady state, condition and after all particle breakage is complete.

The steady state of deformation occurs during undrained tests on saturated loose sands after liquefaction has been achieved, or in drained conditions on sands at large strains. The steady state is not a static condition; it exists only during shear deformation. If the shear deformations are stopped, the specimen develops another, static, structure. In order to reach steady-state again, large enough deformations must be applied.

Steady-state deformations can also occur in clay in drained shear when the *residual* strength is reached, at very large strains. In this case the particles in the shear zone are oriented as well as they can be under the applied stress state, and the specimen therefore displays a minimum resistance to shear deformation. Essentially, the steady state can occur in any particulate mass, in any loading and drainage condition in which the initial structure is broken down and a new *flow* structure develops.

Poulos also suggests that the flow structure and corresponding shear strength for any particulate mass are not dependent on the original structure (which is destroyed), but is "*a unique relationship between void ratio, effective normal stress, and shear stress during steady-state deformation*"

Poorooshab (1989) indicates that the "*Critical State*", as originally intended, and the term "*Steady State of Deformation*", are identical. His objection to the use of "steady state of deformation" is that if the specimen is in a steady state of flow, with constant velocity, this flow velocity must be specified, and admitted as a state parameter, which would limit the usefulness of the method. If however it is postulated that as long as the velocity remains constant it is not required as a state parameter, this interpretation allows zero velocity to be considered as a constant velocity.

The use term of "*Ultimate State*" was suggested since all samples sheared far enough would tend to this terminal or ultimate state, and it does not involve the conceptual confusion that might be cause by the use of "steady state of deformation".

2.2.4 Critical State and Steady State

The concepts of steady state of deformation and critical state are closely related, and ultimately originate from Casagrande's concept of critical void ratio. Although steady state of deformation is mainly used to describe the collapse behaviour of sands, and used in the evaluation of liquefaction, while the critical state is used mainly for clays and is an important concept in Critical Soil Mechanics, they both indicate an ultimate state, at which a mass is continuously deforming at constant void ration, constant normal effective and shear stress (Poulos, 1981 on the steady state); or any further increment of shear distortion will not result in any change of void ratio, and the critical points will lie in or near a unique line on a yield surface (Roscoe et al., 1958 on the critical state). Many authors have mentioned the similarity between these two concepts for which Poorooshasb (1989) wrote: *Thus it is clear that the "Steady State of Deformation" and the "Critical State" as intended originally are identical.*

2.2.5 Phase transformation

Negussey et al. (1987) state that only very loose granular packings of granular material at very high confining pressures contract continuously to critical state during shear. In most cases there is an initial contraction, but the final approach to the critical state is through dilation. In most cases (dilative), therefore, undrained shearing shear causes an initial rise in pore water pressure, but since the approach to the steady-state is done by dilation, it is followed by a decrease in pore water pressure. The point of maximum pore water pressure is called the phase transformation state (Ishihara 1975).

Vaid and Chern (1985) have shown that the friction angle at phase transformation and at steady state of contractive sands are identical, and unique for a given sand. Luong (1980) has also suggested that the friction angle at maximum contraction in drained shear is identical to the friction angle at phase transformation.

2.2.6 Quasi-steady state

Alarcon-Guzman et al. (1988) called *quasi-steady state* the temporary steady state of deformation found by Castro (1969). Zhang & Garga (1997 (a)) describe the quasi-steady-state as follows:

> *in the case of the quasi-steady-state behaviour, a sample first collapses and reaches a temporary steady state of limited liquefaction termed quasi-steady state (QSS). On further shearing, the sample shows a strain hardening behaviour. Hence, there is no unique ultimate shear resistance in the QSS behaviour.*

Zhang & Garga (1997 (a)) also note that to their knowledge, there is no published field evidence of the existence of QSS behaviour. For such an occurrence inf the field, the soil mass would suddenly undergo a large strain of the order of 10 to 20% and stop. Based on triaxial test on Unimin sand, Zhang & Garga (1997 (a)) postulated that the apparent post-phase transformation increase in deviator stress in the QSS behaviour can result from: the dilation potential in the end zones due to end restraint; the undrained volume change due to the variation of membrane penetration and the compression of pore fluid; the conventional area correction.

2.2.7 Steady State Line

Been & Jefferies (1985) define steady state as:

> *The SSL is defined as the locus of all points in void ratio-stress space at which a soil mass deforms under conditions of constant effective stress, void ratio and velocity.* (see **Fig. 2.5**)

Poulos (1981) provides the following precision on the SSL:

the steady-state line is a locus of points at which the soil can deform continuously at the steady state. It is not a line connecting static states of a soil.

Castro and Poulos have presented experimental evidence indicating that the position of the steady-state line is a unique soil property, but also that the position and inclination of that line may vary widely even for apparently similar soils. The slope of the SSL in such that in many instances, a small variation of the void ratio may lead to large variations of the steady-state effective stress. They also suggest that the steady-state line marks the boundary between conditions in which a sand is, or is not ,susceptible to liquefaction.

The steady state concept has been incorporated into proposed procedures to evaluate the potential of liquefaction. Casagrande (1976) proposed that the liquefaction potential of a sand be expressed by:

$$L_p = \frac{\sigma'_{3i} - \sigma'_{3f}}{\sigma'_{3f}} \tag{2.1}$$

where σ'_{3i} is the initial effective minor principal stress, and σ'_{3f} is the effective minor principal stress during the steady state flow. Castro and Poulos (1977) rewrote this equation in terms of the angle of friction of the sand and the pore pressure parameter A:

$$L_p = A\frac{2\sin\phi}{1-\sin\phi} \tag{2.2}$$

From these equations, it can be concluded that for a given density, the liquefaction potential is a function of the relationship between the initial and steady-state confining pressures. If the density remains unchanged, the liquefaction potential increases as the confining pressure increases.

Poulos et al. (1985) described a method to estimate the field shear strength of a sample at a given void ratio (**Fig. 2.14**). First, the steady-state line in e-log S_{us} space is obtained from tests on reconstituted samples. This steady-state shear strength can easily be used to determine a factor of safety against liquefaction using:

$$FS = \frac{\textit{Undrained steady-state strength}}{\textit{Shear stength required for static equilibrium}} \quad \textbf{(2.3)}$$

2.2.7.1 State boundary surface

Roscoe et al. (1958) defined as a state boundary, a boundary above which no stress state is possible. Alarcon-Guzman et al. (1988) showed that collapse, the point where a granular material rapidly strain softens after having reached a peak resistance, was initiated when the stress state reached the effective stress path defined by the postpeak portion of the monotonic undrained loading test. Further more, Sasitharan et al. (1993) have demonstrated that the monotonic constant volume drained loading tests yields the same stress path as the monotonic undrained test at the same void ratio.

The postpeak portion of the monotonic constant volume test can therefore be considered a state boundary. When considered in the *effective normal stress - deviator stress - void ratio* space, the state boundary defines a surface which can be called the state boundary surface.

2.2.7.2 Collapse surface

For sample which lie above the steady state line, a sand sample collapses when its stress path reaches a peak, followed by a rapid deformation and a corresponding increase in pore water pressure. Sladen et al. (1985) defined the collapse surface by connecting the locus of peak points and the corresponding steady-state strength for undrained monotonic loading. Although this is not strictly speaking a state-boundary surface, since the actual stress paths can travel slightly above this linear surface, it can be used to avoid the complexity of modelling the curved state boundary surface.

2.2.8 State parameter

Poorooshasb (1989) defines the *state* of a sample as the complete set of the *pertinent* state parameters. In that context, a state parameter is a quantity associated with the sample and can directly be measured at the moment of examination.

Been & Jefferies (1985) remarked that the properties of sands cannot be expressed in terms of relative density alone since the confining pressure modifies can modify the material behaviour of sands that even a dense sand, under sufficiently high confining pressure will behave as a loose sand. A description of the stress level must therefore be included as well as the sand's void ratio.

They further explain that the same sand, tested under very different combinations of void ratio and mean effective stress, behaves similarly if the test conditions provide an equal initial proximity to the steady state. They define the proximity to the steady state as the *state parameter*, defined as:

> *the void ratio difference between the initial sand state and the steady state conditions at the same mean effective stress.*

This state parameter, ψ, emphasises the fact that it is the *combination* of the density and the confining pressure that is physically relevant to the description of granular materials.

The state parameter's utility is as a normalizing parameter for sand behaviour, in which case it competes with the relative density, which is the normalizing parameter most frequently used for sands. In the relative density approach, the behaviour of sand is normalized in terms of reference densities. Its major drawback is that it does not accommodate of stress on the sand behaviour, and therefore may not explain the difference in behaviour of two sands with essentially the same initial density. A sample with a positive ψ would display a contractive behaviour, while a sample with a negative ψ would display a dilative behaviour.

2.2.9 Factors affecting steady state strength

Void ratio

Void ratio is probably the most important factor, other than the soil composition itself, to affect its steady state strength. Poulos (1997) states:

> *The undrained steady state shear strength of a given soil specimen is a function only of its void ratio prior to the start of undrained shear.*

Research (Casgrande, 1938; Watson, 1940; Roscoe and Schofield, 1958; Bishop, et al, 1965; Castro, 1969) has demonstrated that, for a given soil, as the void ratio decreases, the shear stresses and effective normal stresses at the steady state of deformation increase (Castro et al. 1982).

The specific effect of the initial void ratio on the behaviour of a specific sample will depend on its position relative to steady state line. If the initial void ratio of the sample is much larger than the critical void ratio, or in other words, its initial state is much above the steady state line, the sample will exhibit contractive behaviour under undrained loading condition, and a high induced pore pressure and a collapse failure are to be expected; if the initial void ratio is less than the critical void ratio, the sample will exhibit dilative behaviour, and no strain softening would occur (Casagrande, 1975).

Consolidation stress

Increased consolidation stress decreases void ratio, with differing amounts depending upon the gradation, fines content etc. Decreased void ratio means post-liquefaction shear strength increases, all else equal (Jefferies, 1997). For a given void ratio, a sample under lower confining stress may exhibit dilative behaviour, but may show contractive behaviour under high confining stress (Casagrande, 1975). In particular, confining pressure modifies material behaviour of sands to the point that even dense sand, if tested at sufficiently high confining pressure, will behave similarly to loose sand (Been & Jefferies 1985).

Particle distribution, or fines content

Riemer (1997) notes the complexity of the problem. Whereas a small percentage of silt rattling around within the void structure will have little or no effect on the post liquefaction shear strength, it can significantly alter the density of the soil. A high percentage of fines also makes it difficult to accurately replicate the fabric of field conditions through reconstituted laboratory specimens (Martin 1997).

Great care must be taken in drawing conclusions from comparisons of tests with varying fines contents, since it is difficult to establish what the appropriately comparable densities should be. Because of the much wider variety of possible fabrics, the presence of fines essentially precludes reconstituting specimens from bulk samples of a granular material with any hope of accurately replication field conditions (Riemer, 1997).

It has been observed that, if a sand-fines mixture has the same *standard penetration value* $(N_1)_{60}$ as the clean sands, the addition of fines increases its liquefaction resistance (Seed *et* al. 1985). This has led to an erroneous belief that the addition of fines to sands increases their liquefaction resistance. However, Troncoso (1990) established that if fines are added to sands, their resistance to liquefaction decreases if the soils are tested at the same void ratio. Neither Troncoso (1990) nor Seed *et* al. (1985) describe the nature of fines in sand (Prakash et al. 1998).

Recent laboratory studies indicate that, as the fines content increased, initially the steady state strength at the same void ratio decreased followed by an increase in shear strength with further increase in fines content beyond about 30 percent (Thevanayagam & Mohan, 1998)

Ishihara (1993) suggested that the effect of fines on post-liquefaction strength is likely best described by the plasticity index of the fines (Olson 1997). He concluded that: "plastic fines increase the cyclic strength of the fine-grained sand, but the nonplastic fines reduce the strength of the fine-grained sand (Ishihara, 1993).

Prakash *et* al. (1998) believe that an increase of plasticity in silts does not necessarily mean increased resistance to liquefaction. There appears to be a critical value of PI below which the increase of plasticity indexes lowers the Cyclic Stress Ratio for liquefaction and beyond this critical value, the increase of plasticity index increases the value of cyclic stress ratio for initial liquefaction. The effects of fabric, aging, and cementation are also not quantitatively known, It appears that the fabric and aging may slow down the pore pressure generation. Clearly the importance of fabric in fine grained soils, such as silts, needs to be recognized when evaluating the pore pressure generation. (Prakash *et* al., 1998).

Poulos (1997) is of the opinion that the fines content, or, more broadly, the particle distribution cannot be separated from the soil composition as a distinctly quantifiable parameter.

> *To ask the effect of fines is equivalent to asking whether soil composition affects the undrained steady state shear strength. Yes, soil composition is the primary factor that controls the undrained steady state shear strength.*

Also problematic is the question of the void ratio to use in steady state determination. Consequently in an idealistic sense, one could argue that it is not the global void ratio controlling the residual strength of silty soils but rather the skeletal void ratio of the dominant constituent (Martin 1997).

If at lower fines contents it is assumed that the fine particles do not actively participate in the transfer of contact frictional forces, or that their contribution is secondary, and if FC represents the fines content in percentage of the mass of solids, then if we neglect the influence of the relative density (or specific gravity G_s) the volume of fines in a unit volume of solids would be: FC/100, while the volume of the coarser grains is expressed as (1-FC/100). Accordingly the *intergranular (coarser-grains) void ratio* e_s is defined as the volume of inactive constituents (fines and voids) in the soil per unit volume of active (coarser-grains) solids (Thevanayagam & Mohan, 1998):

$$e_s = \frac{e + FC/100}{1 - FC/100} \tag{2.4}$$

If the fines content is increased, at some point, the soil may become completely governed by the contacts along the fines, whereas the coarser-grains float within the fines. The presence of coarser-grains has no effect on the internal force chain within the soil mass. Since it is neither a void nor its volume affects the nature of the force chain in the finer-grains, the presence of the coarser-grains can be safely ignored. Contrary to the earlier case where the finer-grains were considered to be *voids*, in the present case, the coarser-grains are considered to be of *zero volume*. The silty sand may behave similar to that of the host finer-grained silt at an interfine void ratio e_f defined as the volume of void per unit volume of active (finer-grain) solids (Thevanayagam & Mohan, 1998):

$$e_f = \frac{e}{\left(\frac{FC}{100}\right)} \tag{2.5}$$

Even though the relative density of a silty sand may be medium dense to dense its undrained strength is equivalent to that of the loose (clean) host sand. Density of a silty sand is a deceptive term to be used to characterized the undrained strength. It is the intergranular void ratio (es) and the confining stress that affect the undrained shear strength of a silty sand (Thevanayagam & Mohan, 1998).

Grain crushing

Barden & Proctor (1970) remarked that the most important material property influencing crushing is grain strength, with the particle shape, its rugosity and grading having also an effect. They also remarked that crushing is a function of the applied stress system, the greatest crushing resulting from systems with a high mean stress p and a high stress ratio $\boldsymbol{R}$, the high stress ratio being important considering the peak strength. Been et al. (1991) considered that this crushing at high stress levels might explain the fact that the SSL is not linear but seems to become flatter at lower stress levels.

Sampling

The steady state strength of liquefiable sands can generally not be determined by undrained tests on undisturbed samples from the field. Potentially liquefiable soils are very difficult to sample without disturbance. They are likely to densify during sampling , transportation, and the process of setting up the samples for testing. Therefore, tests cannot be conducted at the field void ratio (Finn 1998).

Poulos et al (1985) developed a procedure for correcting the residual strength measured at the laboratory void ratio to the void ration in the field. The steady state strength is very sensitive to minor changes in the composition of the sample and many tests are required to establish a reliable basis for selecting the residual strength for design. In addition, the corrections for disturbances can lead to order of magnitude changes in the measured residual strength (Finn 1998).

In an effort to overcome the difficulties with direct measurement of residual strength, Seed (1987) back-analyzed a number of case histories in which significant displacements had occurred during earthquakes. He published a chart relating the residual strength to the normalized penetration resistance for clean sand $(N_1)_{60c\text{-}s}$ (Seed 1987). **Fig. 2.6** shows a revised version of the chart by Seed and Harder (1990).

Peck (1979) indicated that because of difficulties in understanding and modelling all of the factors that affect the liquefaction resistance of a soil, in-situ penetration testing is the preferred method to estimate liquefaction resistance (Olson *et* al). In-situ penetration tests refer to both the cone penetration test (CPT) and the standard penetration test (SPT).

The cone penetration test, and especially the piezocone test, offers several advantages over the standard penetration test including better standardization, precision and accuracy, improved cost-effectiveness, and it provides a nearly continuous record of penetration resistance throughout a soil deposit. For these reasons, the cone penetration test has seen increasing popularity and use for liquefaction assessment (Olson *et* al).

Stress path

There is no consensus as to the effect of the stress path on the steady state strength. Castro et al. (1985) hold the view (shared by others) that the steady state strength is independent of the stress path. Vaid et al. (1989), based on an extensive test program, found that the steady state strength was greater in compression tests than in extension tests. Poulos (1997) believes that the difference between the extension and compression triaxial tests comes from the difficulty in maintaining a uniform void ratio in extension tests. The two lines would match if the void ratio was measured in the zone of failure.

Drainage condition

The constant void ratio stress paths followed under drained constant-volume and undrained conditions are identical (Sasitharan et al., 1993).

Shear localization

Soil failure is often accompanied by a localization of the deformation in thin zone undergoing intense shearing known as shear bands. Harris et al. (1995) performed tests using stereophotogrammetry to analyze the development of shear bands in triaxial tests on sand. The method allowed them to obtain quantitative observations from which they draw the following conclusions for triaxial tests:

1. *Strain localization is systematically progressive in nature, i.e., a gradual transition from homogeneous deformation to temporary diffuse modes of localized strain to a highly non-uniform strain field is observed.*

2. *Prior to strain localization, in the region where the final shear band eventually forms, the soil contracts more than the rest of the specimen.*

3. *As soon as the final band is fully formed and for continuing shear, the soil inside the band either remains at constant volume or dilates.*

Shear bands pose, of course a serious problem in the SSL method since their existence will undoubtedly create a difference between the global void ratio and the actual void ratio in the zone of failure. In a contractive specimen, the density in the shear band will be greater than in the remainder of the sample, and the global void ratio will be also be higher than in the shear band. This would lead to an error in the determination of the SSL in the non-conservative side.

Scale effect, and boundary conditions

Ishibashi et al. (1996), based on a series of tests on hollow cylinder samples have reached the conclusion that the preparation mould can create an ordered arrangement around the lateral boundary, and that the thickness of material influenced by this boundary increases as the grain size increases. The specimen thickness relative to the grain size will therefore be important in minimizing the impact of boundary effects on the specimen. Based on their observation, they also suggest that the minimum thickness of a hollow should be about 150 particle diameters.

Shearing rate

In order to explain rock avalanches, Humgr and Morgenstern (1984) have conducted ring shear and flume tests with a number of cohesionless soils and polystyrene beads. Their results are summarized in **Table 2.1**.

From these tests, conducted up to a shearing rate of 98 cm/s, they conclude that the rate of shear of the particulate medium does not affect the friction characteristics of the particulate medium. They had already demonstrated, in flume experiments, that granular material retains its frictional character under very high rates of shearing (Hungr & Morgenstern, 1984). The ring shear test allowed them to explore the phenomenon at high normal stresses. Indeed, the high velocity ring shear experiment by Bridgwater (1972) seemed to indicate the beginning of a rate effect in tests of glass beads at velocities of approximately 50 cm/s and normal stresses exceeding 25 kPa.

The conclusion of Hungr & Morgenstern (1984), after performing tests on various granular materials, was that the shear rate did not have any effect on the friction angle of the granular material for the stress range investigated (up to 200 kPa). In fact all the materials tested *exhibited straight linear residual strength envelopes with zero cohesion and unique angles of residual friction, practically unaffected by the speed of the test.* The normal stress therefore did not appear to affect the strength envelope of the tested materials.

The only case where a variation of strength envelope due to the shear strength was recorded, was when testing a mixture containing 25% rock flour and coarse sand, so that the flour would just fill the void space of the sand in loose static piling. The slow tests yielded a friction angle similar to that obtained in the tests with greater proportion of rock flour while the fast test yielded a friction angle comparable to that of the sand alone **Fig. 2.13 (*f*)**. A possible interpretation of this is that the more angular rock flour controls the friction angle at low rates, while the more rounded large particles dominate at high velocity, perhaps by virtue of their greater dispersive pressure (Hungr & Morgenstern, 1984).

2.2.10 Uncertainty in the SSL

The position of the steady-state line (SSL) is usually obtained from regression on triaxial compression results for a number of samples at various void ratios. Kramer (1989) remarks that: "*Scatter in the steady-state data to which a steady-state line must be fit may be considerable*". In many cases the slope of the SSL is so flat that a very small difference in density can lead to very large differences in steady-state shear strength.

Using the "steady-state procedure" as described by Poulos et al. (1985) (see **Fig. 2.14**) the in-situ void ratio for a soil sample may be computed from:

$$e_{in\ situ}=e_{lab}+\Delta e_{consol}+\Delta e_{sampling} \tag{2.6}$$

Where e_{lab} is the void ratio of the sample tested to steady-state, Δe_{consol}, is the change of void ratio during the consolidation phase, and $\Delta e_{sampling}$ is the change of void ratio during sampling. While the steady-state strength of the lab sample, and the consolidation change of void-ratio may be measured with a relatively high degree of accuracy, the difficulties in sampling cohesionless soils make the change in void ratio due to sampling uncertain. The scatter of the laboratory steady-state line also make slope of the SSL uncertain. The actual in-situ steady-state strength will therefore be correspondingly uncertain, and since shear strength is in a log scale, the uncertainty may be substantial.

Kramer (1989) provided an analysis of the uncertainties related to the steady-state approach and defined a reduction factor (***R***) of the form:

$$R=\frac{S_{det}}{S_{in\ situ}}=10^{[\Delta e_{sampling}+\Delta e_{consol}/C_{ss}-\Delta e_{consol}/\overline{C_{ss}}]} \tag{2.7}$$

Where S_{det} is the shear strength predicted by the deterministic method described by Poulos et al. (1985), and $S_{in\ situ}$ is the actual in-situ steady state shear strength. C_s, as described in **Fig. 2.14**, is the slope of the SSL in the *e-log S* plot. If S_p indicates the steady-state shear strength with probability p of being less than $S_{in\ situ}$, then the corresponding R_p is:

$$R_p = \frac{S_{\det}}{S_p} \tag{2.8}$$

Fig. 2.17 provides contours of reduction factors (equivalent factors of safety) with SSL, in function of the regressed slope of the SSL (C_s) and the coefficient of variance, V_c of the data used to obtain the SSL.

To illustrate the impact of the uncertainties in the SSL, Kramer analyzed a sand for which the probability of overestimating the in-situ steady-state strength (in situ) was calculated at 50%, for which the deterministic approach estimated an in situ of 53.8 kPa. Using the reduction factor for a probability of 1% of overestimating the Sin situ, the steady-state shear strength to use would have been of 10 kPa. Evidently, neglecting to take into account the impact of uncertainties in the estimation of the SSL can lead to overestimation of the steady-state strength in the field.

2.3 SAMPLE PREPARATION METHODS

Several methods are available to prepare reconstituted sand samples, namely: moist tamping, air pluviation and water pluviation are frequently used to produce sand samples in laboratory.

In the moist tamping method, consecutive soil layers of specified thickness are placed into a sample mould, and each one is tamped flat with a specified force, after which the next layer is placed and tamped. The moist tamping method best model the soil fabric of rolled construction fills. It also offers the advantage of allowing soil densities lower than the minimum density obtained from the standard test (Ishihara, 1993).

In the air pluviation method, sand is dry sand is pluviated into a sample mould, while the height of fall is kept constant. It is possible to obtain different density values, by changing the height of fall. This method best models the natural deposition in aeolian environments.

The water pluviation method resembles the air pluviation, except that the medium in which the sand is pluviated is de-aired water instead of air. The sample is also sometimes boiled to ensure its saturation. The terminal velocity of soil particles in water is reached at a height of 0.2 cm (Vaid and Negussey 1988), and therefore the height of fall does not influence the sample density. Because the terminal velocity is reached so fast, the water pluviation method is not suitable to obtain uniform samples of poorly graded or silty sand since it would result in particle segregation. Baziar and Dobry (1995) found that the steady state strength of a silty sand from the reconstituted homogeneous sample was much less than the strength of the sample reconstituted in layers, where the material was poured into a triaxial mould and allowed enough time for full sedimentation before the next layer was added. Some other methods, such as the slurry deposition method, have been developed to overcome this problem (Kuerbis and Vaid, 1988). The water pluviation method best simulates the deposition of sand through water deposition environments and mechanically placed hydraulic fills (Oda et al., 1978).

Ladd (1974) employed moist tamping method and air-vibration method to prepare sand samples to the same density and sheared them in triaxial tests. His results showed that the samples prepared by the dry-vibration method were significantly weaker in cyclic undrained testing than samples prepared with the moist tamping method. This suggests that the soil fabric may significantly influence the cyclic strength of sand.Mulilis et al. (1977, 1978), from tests on specimens compacted using eleven different methods, showed that the degree of influence of the preparation method is a function of the type of soil. In a study comparing the methods of air-pluviation, wet-tamping, wet-vibration and water-vibration, Tatsuoka et al. (1986) found that the wet-vibration provided the strongest samples and air-pluviation the weakest, although the other two methods also provided the strongest and weakest samples in some instances.

Since at steady state the original fabric of the soil is completely destroyed, the sample preparation method does not influence its value. Been et al. (1991) found that the steady state of Erksak sand was the same wether the sample had been prepared using the moist tamping or water pluviation. Negussey and Islam (1994) found that the steady state line was independent of the bedding orientation of the tested specimens.

2.4 RING SHEAR TEST

Several types of torsional devices have been developed to test the shear strength of soils at large strains. Bishop et al. (1971) completed a list of devices in this respect **Fig. 2.18 & Fig. 2.19**. They list a number of torsional shear devices, including some simple ones where a cylindrical sample is sheared between two platens. In regard to such devices, Bishop et al. (1971) remark that "the radial distribution of stress and strain is likely to be very non-uniform."

Several of the early designs also promoted the failure of the sample adjacent to the loading platen rather than in the body of the sample although the use of divided confining rings promoted the shearing of the sample near its middle, far away from the influence of the platens.

The earliest ring shear apparatus for testing soil appears to be that designed by A. Casagrande in collaboration with the U.S. Corps of engineers, Boston (Hvorslev, 1939). A hollow cylinder, confined by end platens, is loaded radially and rotated so that failure occurs on a cylindrical surface, ideally at mid-wall thickness. (Bishop et al., 1971)

In the most common type of ring shear test, an annular ring-shaped specimen is subjected to a normal stress, is confined laterally and finally ruptures along a plane of relative rotary motion, **Fig. 2.20**. Bishop et al., (1971) designed such a device for testing clay samples, while measuring the friction contribution of the confining rings.

Bishop et al. (1971), analyzed a number of alternate assumptions concerning the distribution of the normal stress and the shear stress. These are:

(a) that the normal stress σ_n' and the shear stress τ are uniformly distributed across the plane of relative rotary motion;

(b) that the normal stress σ_n' has a specified form of variation and the shear stress τ has a correspondingly similar distribution;

(c) that the normal stress σ_n' is uniformly distributed whereas the shear stress τ varies linearly with the radius (Cooling and Smith 1936);

(d) that the normal stress σ_n' is uniformly distributed whereas the shear stress τ is a function of the shear strain (Hvorslev, 1939; Payne and Fountaine, 1952; Nowacki, 1967);

Their analysis led them to believe that alternative *a* was the most realistic since it assumes that the soil is plastic, as does alternative *b*, although analyzing a number of different possible stress distribution for alternative *b* **Fig. 2.20**, suggested little error, an simpler calculations, in assuming a uniform distribution. Alternative *c* and *d*, since they assume an elastic soil are less realistic than *a* or *b*.

Using assumption *a*, the average normal stress, σ_n' si given by:

$$\sigma_n' = \frac{W}{\pi(r_2^2 - r_1^2)} \tag{2.9}$$

and the average shear stress is given by:

$$\tau = \frac{3M}{2\pi(r_2^3 - r_1^3)} \tag{2.10}$$

so that

$$\tan\phi' = \frac{3M(r_1 + r_2)}{2W(r_1^2 + r_1 r_2 + r_2^2)} \tag{2.11}$$

2.5 FIGURES

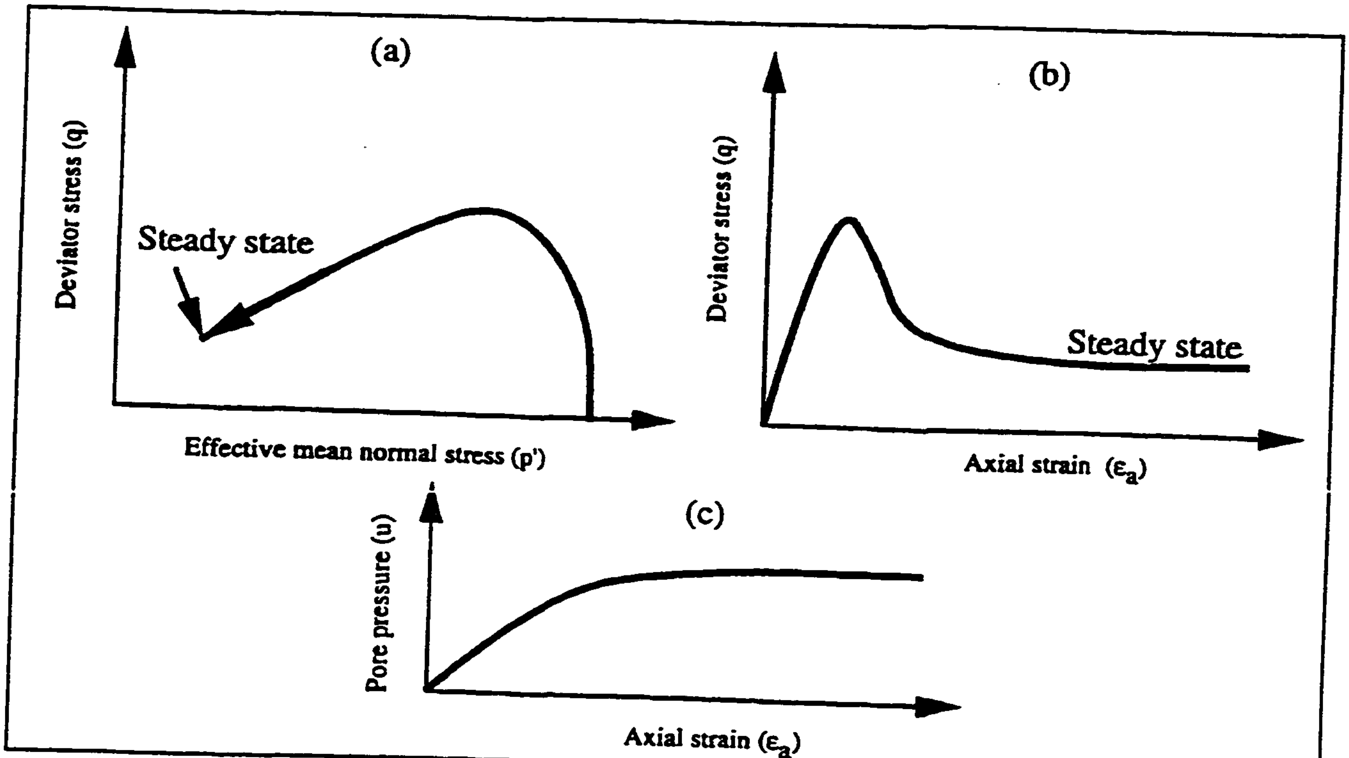

Fig. 2.1 Typical undrained monotonic triaxial compression tests results: (a) Stress path. (b) Stress-strain (c) Pore pressure. (after Sasitharan et al., 1993)

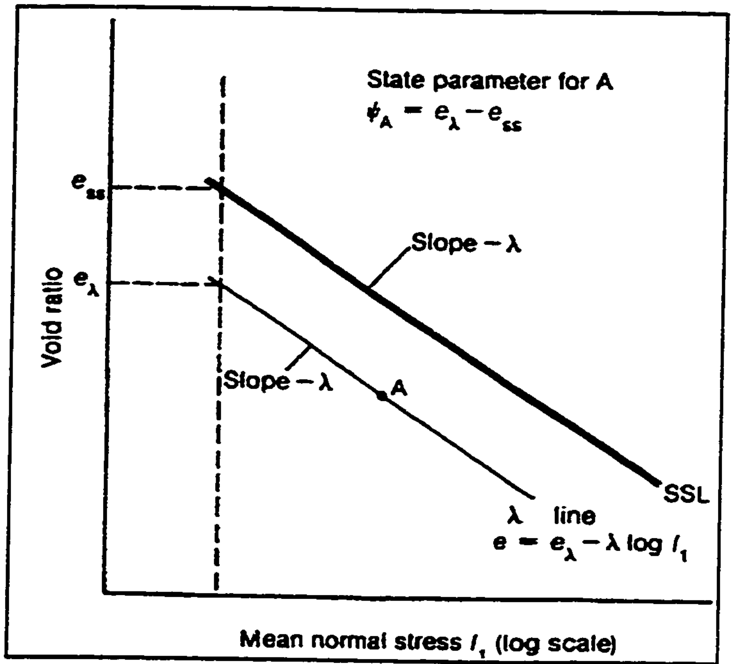

Fig. 2.2 Definition of state parameter ψ

(after Been & Jefferies, 1985)

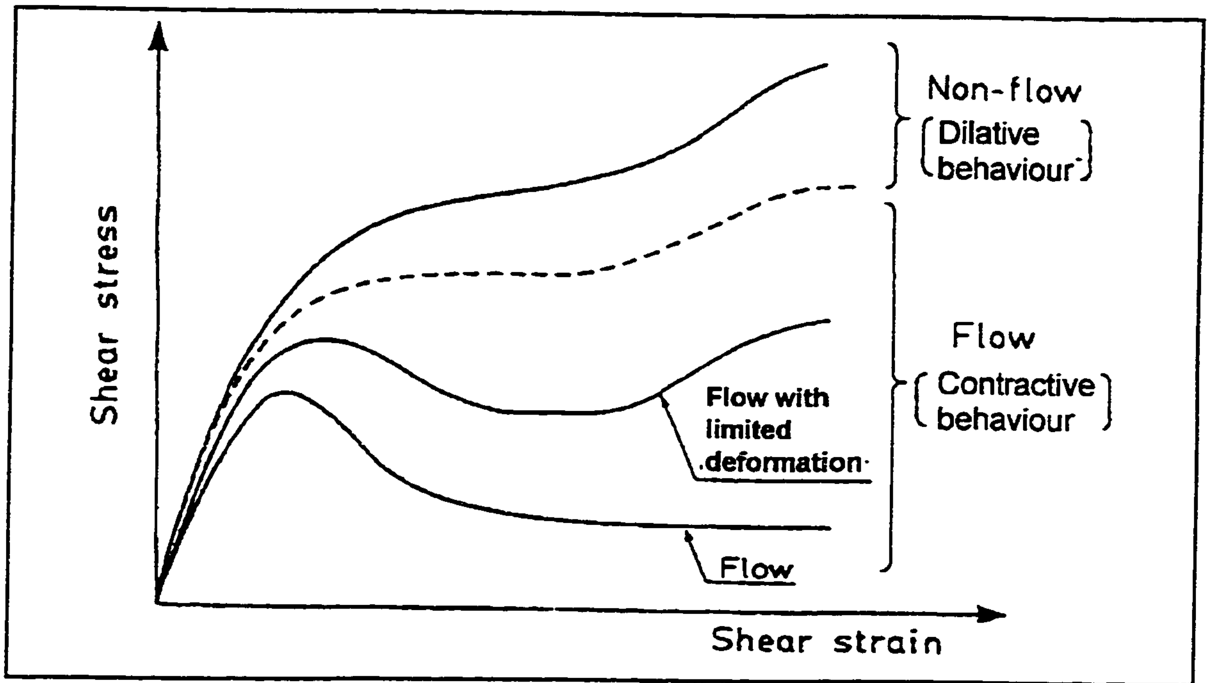

Fig. 2.3 Definition of flow and non-flow types of undrained deformation

(after Ishihara, 1993)

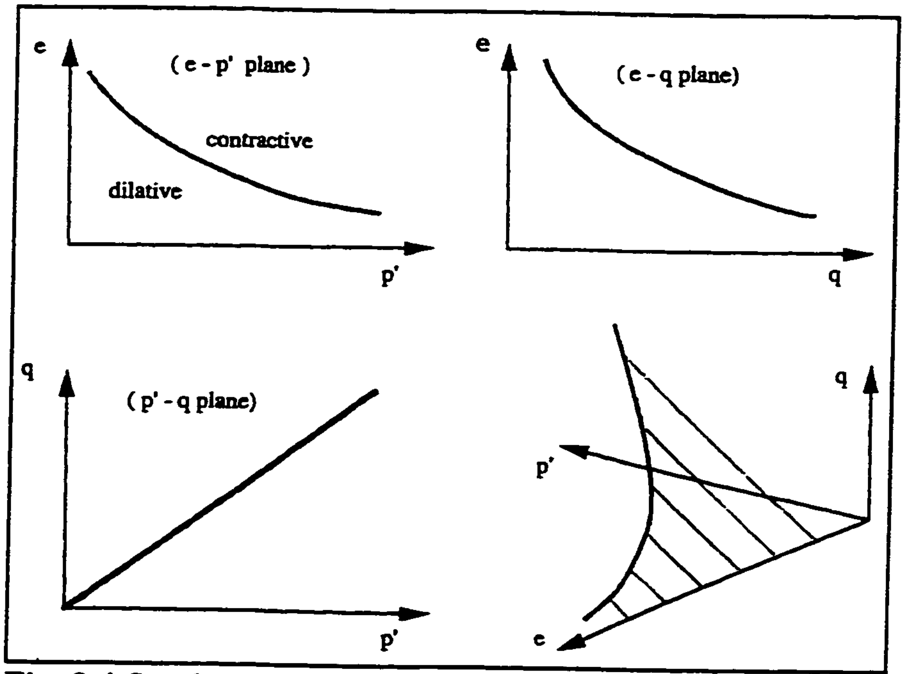

Fig. 2.4 Steady-state representation in *e-p'-q* space along with representation using *e-p'* , *e-q* , and *p'-q* planes.
(after Sasitharan et al., 1993)

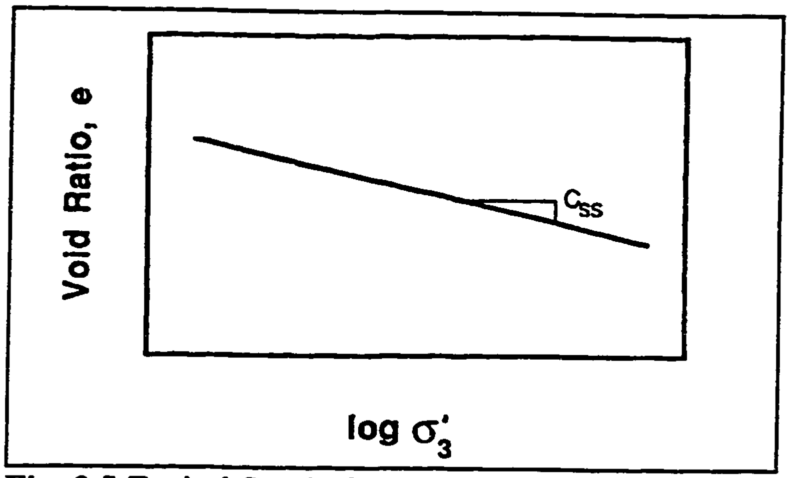

Fig. 2.5 Typical Steady-State Line
(after Kramer, 1989)

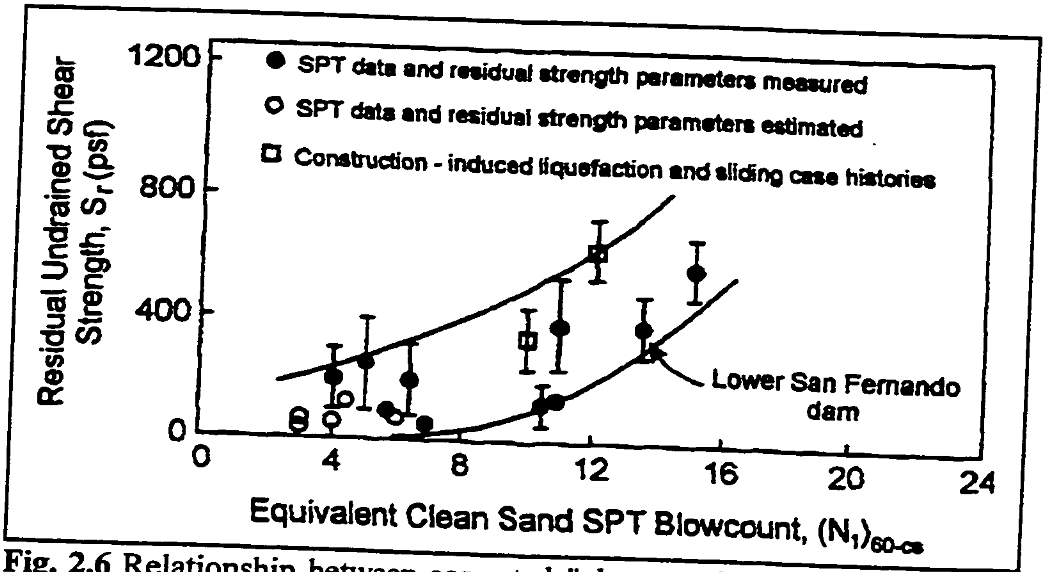

Fig. 2.6 Relationship between corrected "clean sand" blow count $(N_1)_{60c\text{-}s}$ and undrained residual strength, s_r, from case studies (after Seed and Harder, 1990)

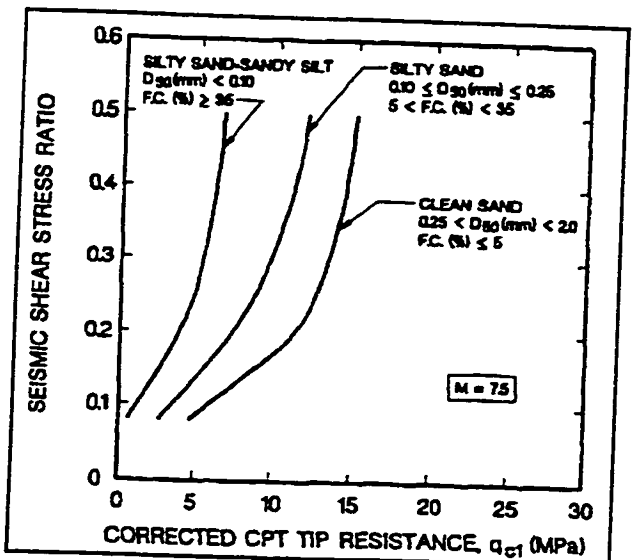

Fig. 2.7 CPT Based Liquefaction Resistance Relationships for Sandy Soils and M=7.5 Earthquakes (from Stark and Olson 1995)

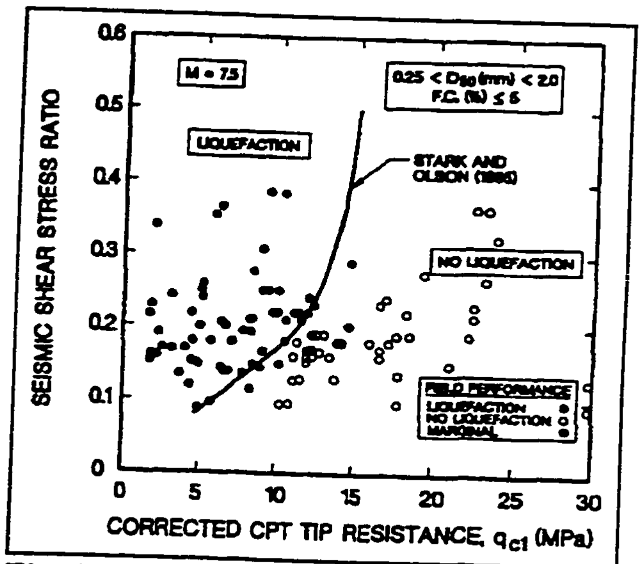

Fig. 2.8 Relationship between Seismic (Shear) Stress Ratio Triggering Liquefaction and q_{c1} values for Clean Sand and M=7.5 Earthquakes

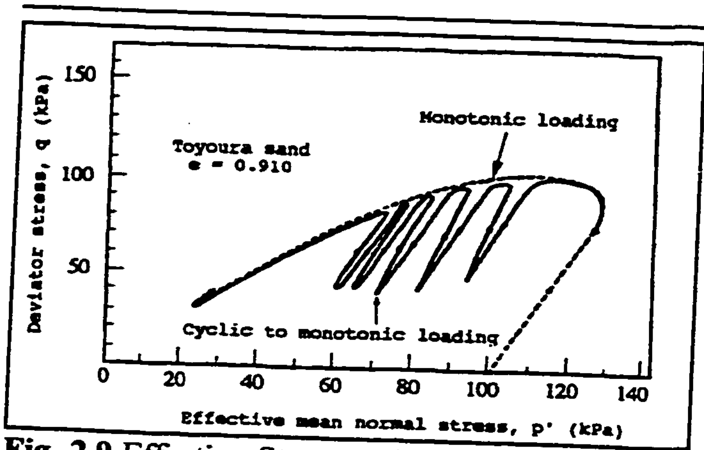

Fig. 2.9 Effective Stress paths for monotonic undrained loading and cyclic to monotonic undrained loading (modified from Ishihara et al. 1991)

(after Sasitharan et al., 1993)

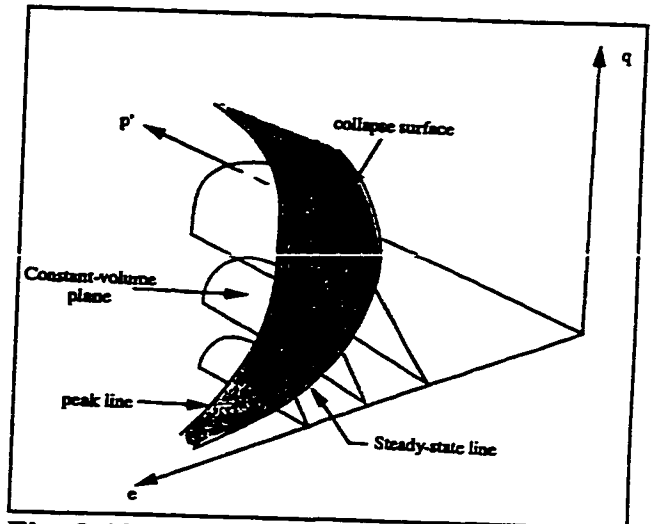

Fig. 2.10 Typical collapse surface in effective mean normal stress – deviator stress – void ratio space.

(after Sasitharan et al., 1993)

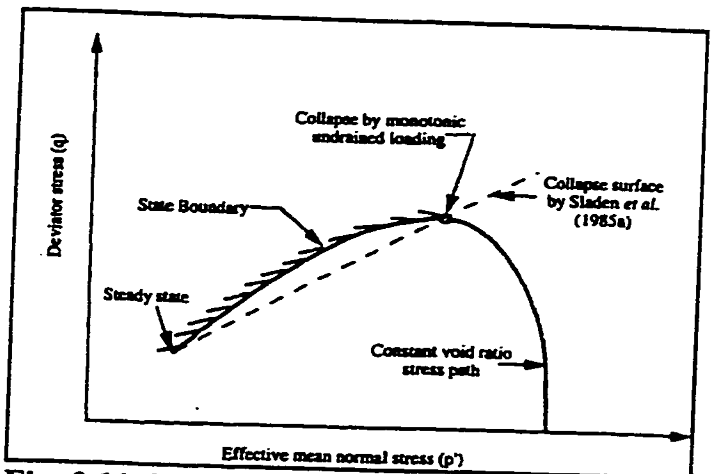

Fig. 2.11 Comparison of state boundary and collapse surface proposed by Sladen et al. (1985)

(after Sasitharan et al., 1993)

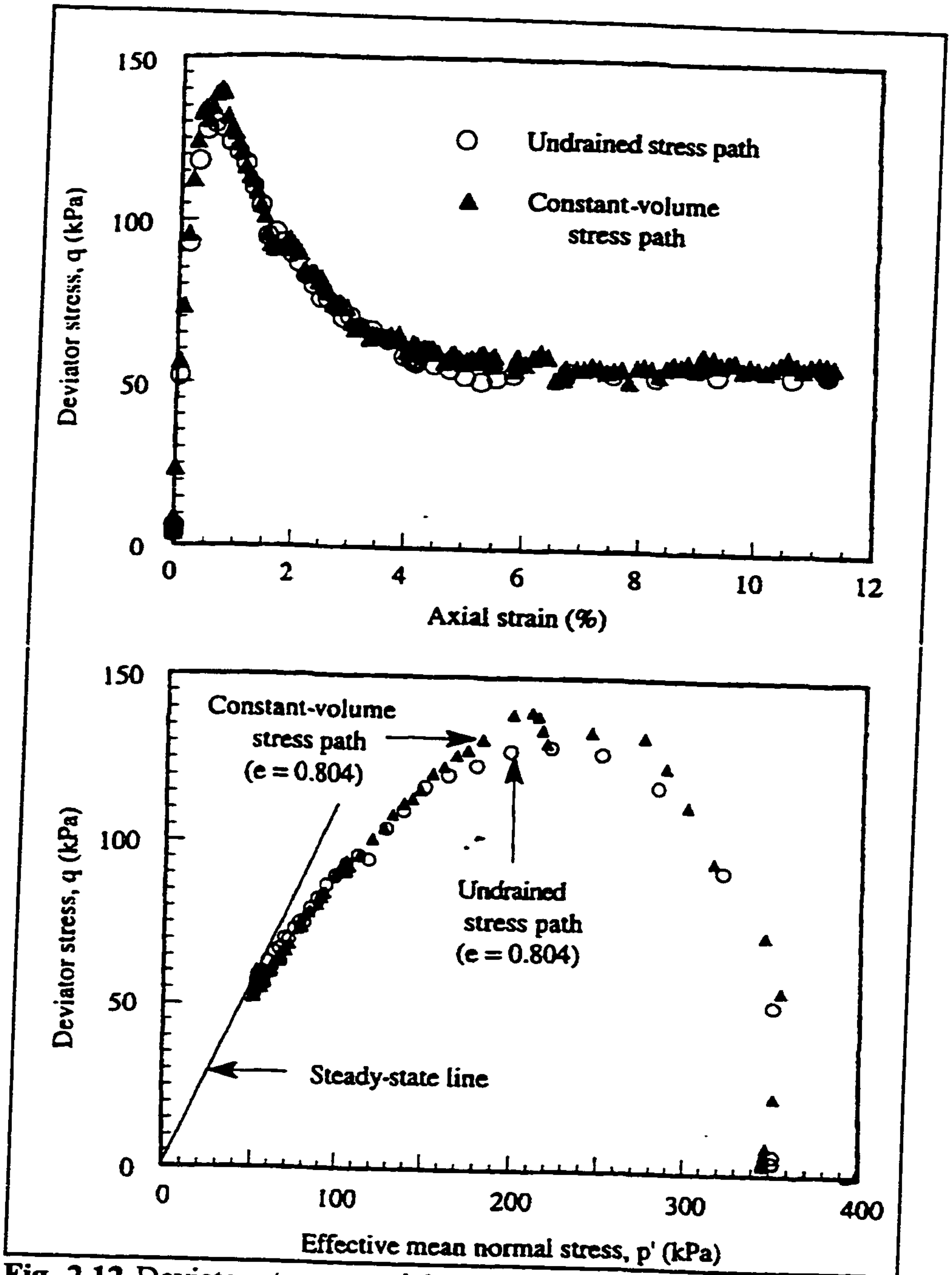

Fig. 2.12 Deviator stress – axial strain response and resulting stress paths of undrained and constant-volume tests.

(after Sasitharan et al.)

	Very slow: 0·1 cm/s	Slow: 16 cm/s	Fast: 98 cm/s
10–14 sand, dry	29	29	29
10–14 sand in water	26	26	26
4:1 sand–flour mixture	31	31	29
4:2 sand–flour mixture	31	31	31
8–10 sand, dry	30	30	–
Polystyrene beads	21	21	Stick slip
Ottawa sand in flume tests		25·5	
Polystyrene beads in flume tests		21·8 25	(2 m/s) (2 m/s)
Non-plastic silt*		26–30	
Uniform fine–medium* sand		26–30	

* Typical range of low velocity constant volume friction angles (Lambe & Whitman, 1979).

Table 2.1

Author	Materials tested	Sample volume cm^3	Maximum velocity m/s	Maximum stress kPa	Sample height cm	Power per cm: kW/cm^3	Rate effect
Healy (1963)	Ottawa sand	20	0.03	63	0.28	6.8	Slight
Novosad (1964)	Glass beads	254	0.5	2	3.0	0.3	None
Scarlett & Todd (1969	Sand	1200	0.03	6	4.0	0.5	None
Bridgwater (1972)	Glass beads and plastics	940	2.0	25	4.0	12.5	Yes
Hungr & Morgenstern (1984)	Coarse sand, sand and rock flour, sand and water	660	1.0	200	2.0	100	None

Table 2.2 Effect of shear rate on shear strength of various granular materials, by different investigators (after Hungr & Morgenstern, 1994)

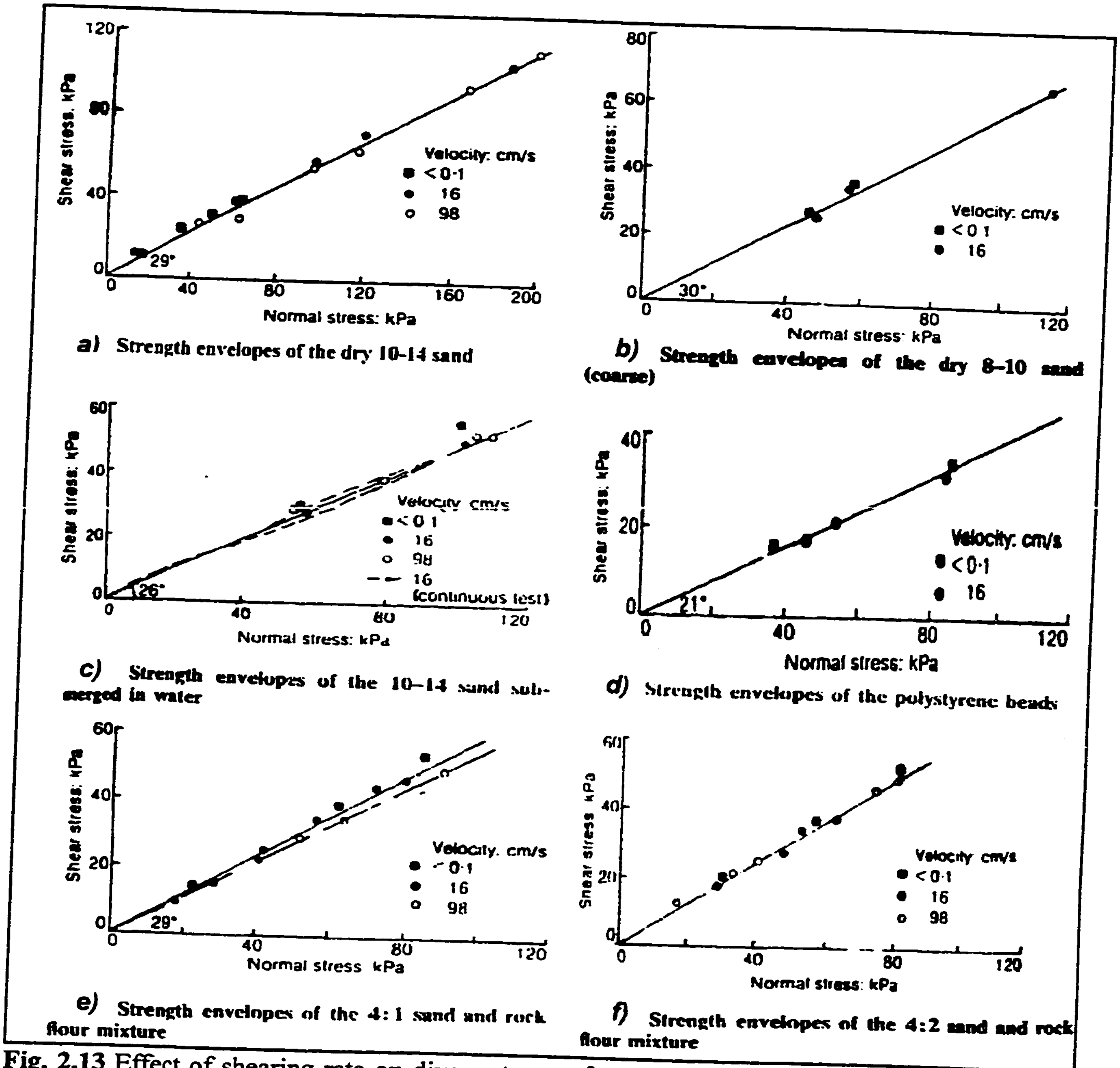

a) Strength envelopes of the dry 10-14 sand

b) Strength envelopes of the dry 8-10 sand (coarse)

c) Strength envelopes of the 10–14 sand submerged in water

d) Strength envelopes of the polystyrene beads

e) Strength envelopes of the 4:1 sand and rock flour mixture

f) Strength envelopes of the 4:2 sand and rock flour mixture

Fig. 2.13 Effect of shearing rate on diverse types of granular materials (after Hungr & Morgenstern, 1984)

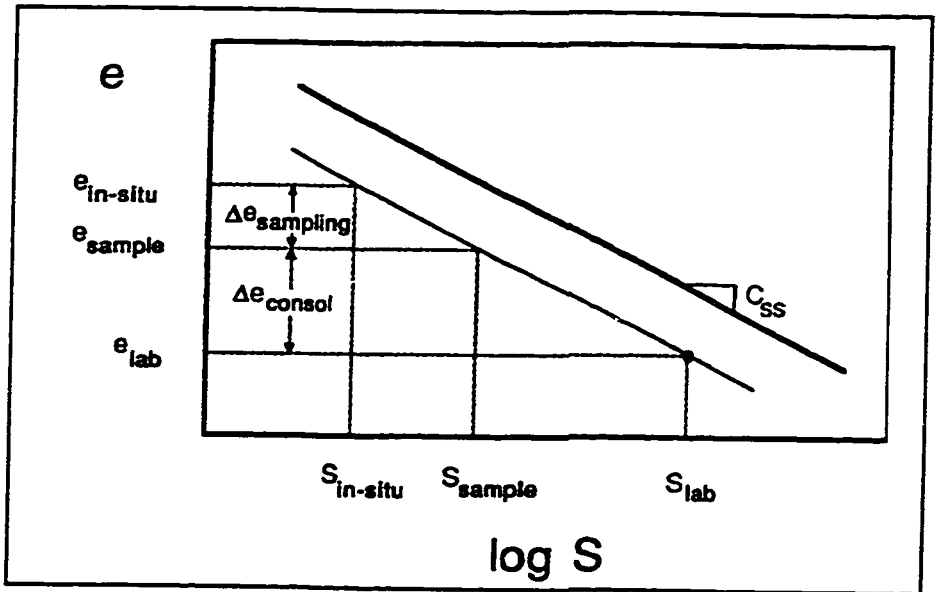

Fig. 2.14 Schematic illustration of Steady-State Procedure (after Kramer, 1989)

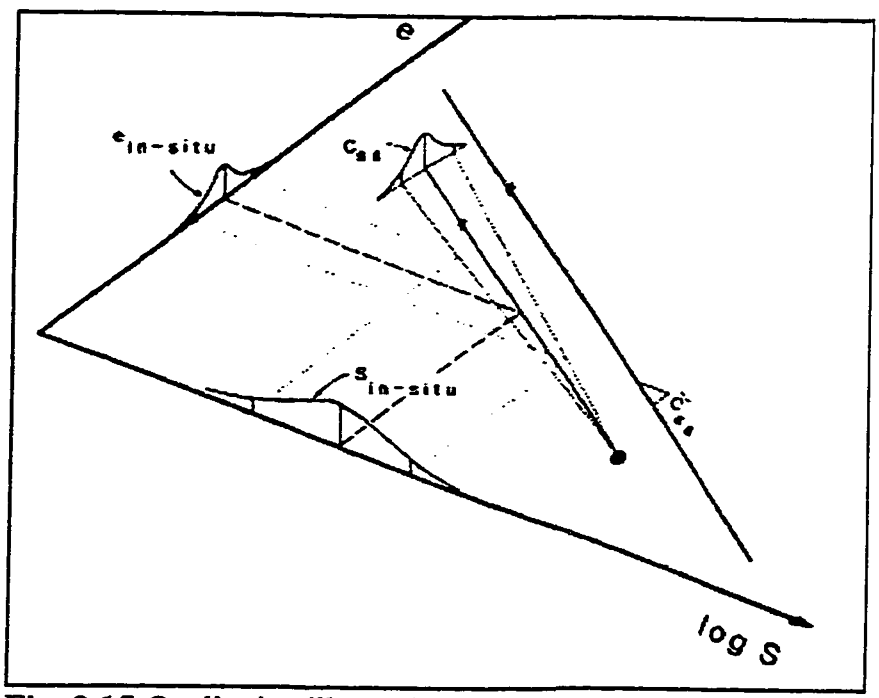

Fig. 2.15 Qualitative illustration of Influence of Uncertainty of *e*in situ on Uncertainty of Steady-State Shear Strength (after Kramer, 1989)

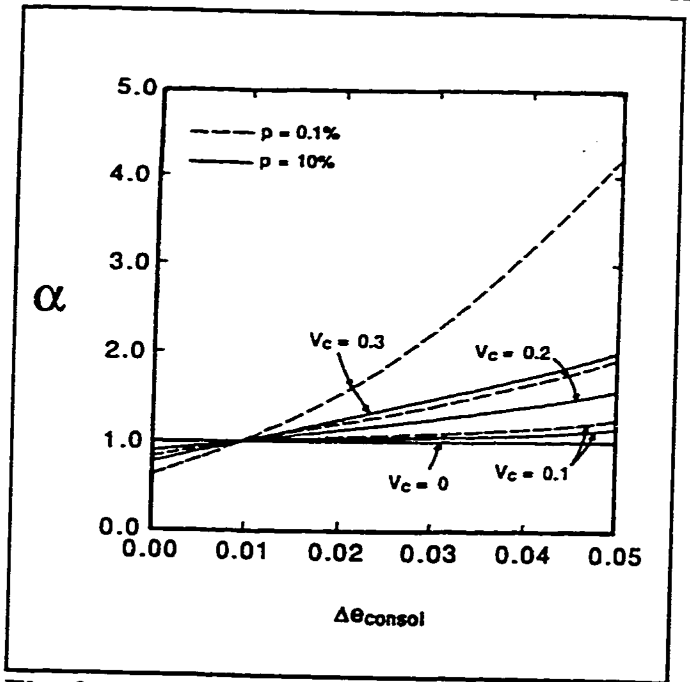

Fig. 2.16 Variation of Correction Factor α with $\Delta e_{console}$ and V_c (after Kramer, 1989)

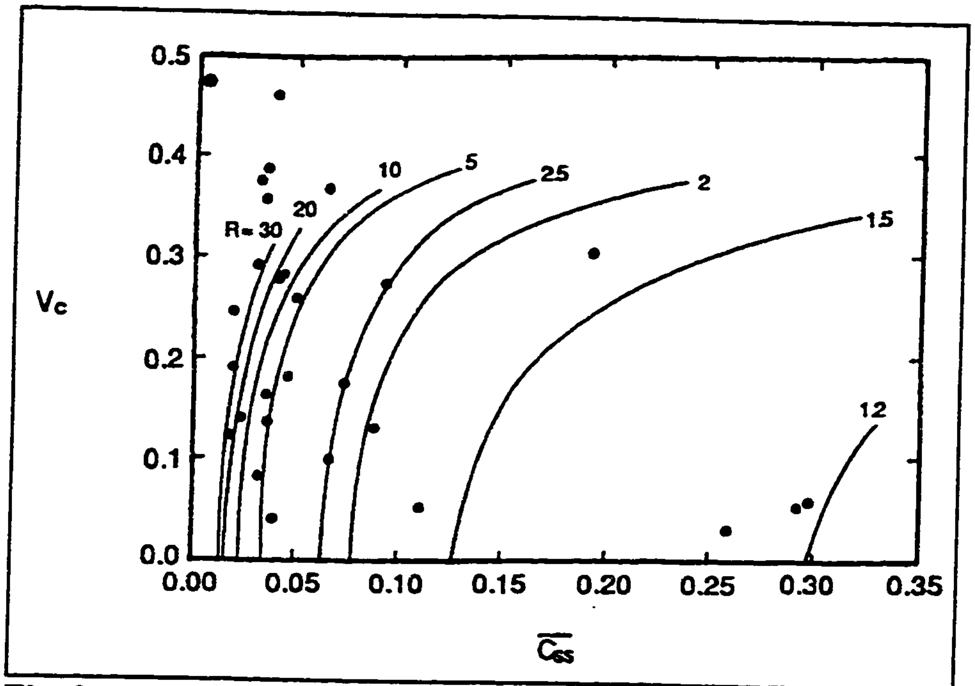

Fig. 2.17 Contours of Reduction Factor (Equivalent Factor of Safety) with Steady-State Line Characteristics of Sands of Table 2.1 for p = 1.0% (after Kramer, 1989)

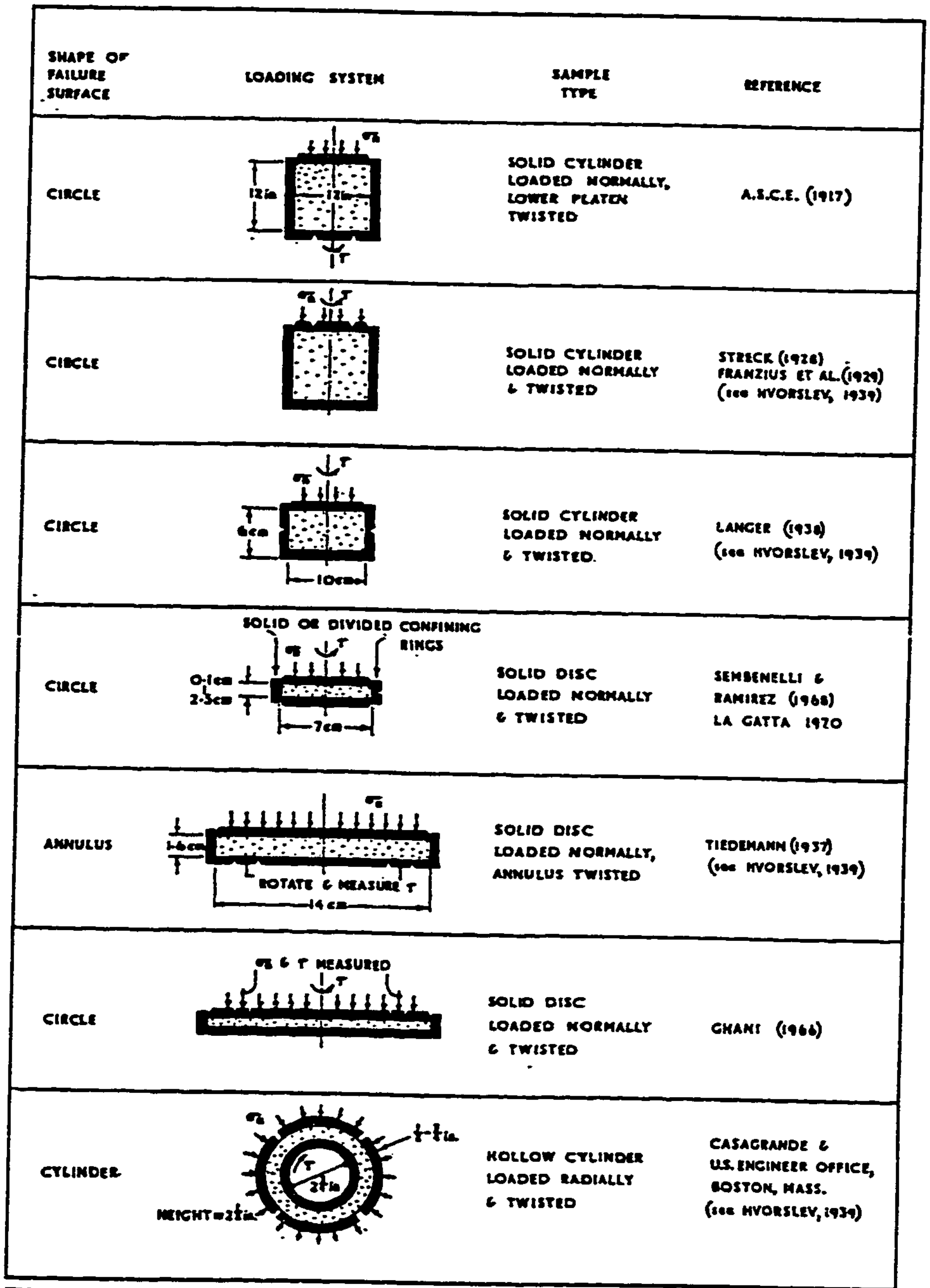

Fig. 2.18 Principal features of various forms of torsion and ring shear apparatus: **solid cylinder or disc or hollow cylinder** (after Bishop et al. 1971)

SHAPE OF FAILURE SURFACE	LOADING SYSTEM	SAMPLE TYPE	REFERENCE
ANNULUS	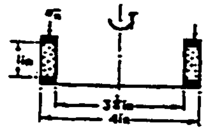	UNCONFINED ANNULAR DISC LOADED NORMALLY & TWISTED	COOLING & SMITH (1935, 1936)
ANNULUS	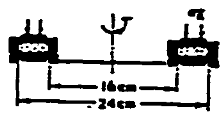	ANNULAR DISC LOADED NORMALLY & TWISTED	GRUNER & HAEFELI (1934) HAEFELI (1938) (see HVORSLEV, 1939)
ANNULUS	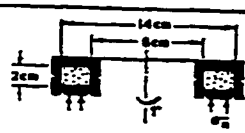	ANNULAR DISC LOADED NORMALLY & TWISTED	TIEDEMANN (1937) (see HVORSLEV, 1939)
ANNULUS	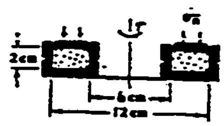	ANNULAR DISC LOADED NORMALLY & TWISTED	HVORSLEV (1937, 1939) HVORSLEV & KAUFMAN (1952) HERRMANN & WOLFSKILL (1966)
ANNULUS	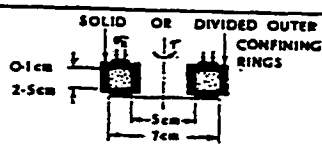	ANNULAR DISC LOADED NORMALLY & TWISTED	LA GATTA (1970)
ANNULUS	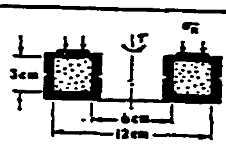	ANNULAR DISC LOADED NORMALLY & TWISTED	NOVOSAD (1964)
ANNULUS	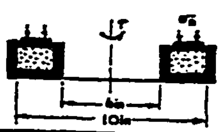	ANNULAR DISC LOADED NORMALLY & TWISTED	CARR & WALKER (1968)
ANNULUS	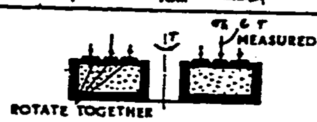	ANNULAR DISC LOADED NORMALLY & TWISTED	SCARLETT & TODD (1968)

Fig. 2.19 Principal features of various forms of torsion and ring shear apparatus: **annular disc** (after Bishop et al. 1971)

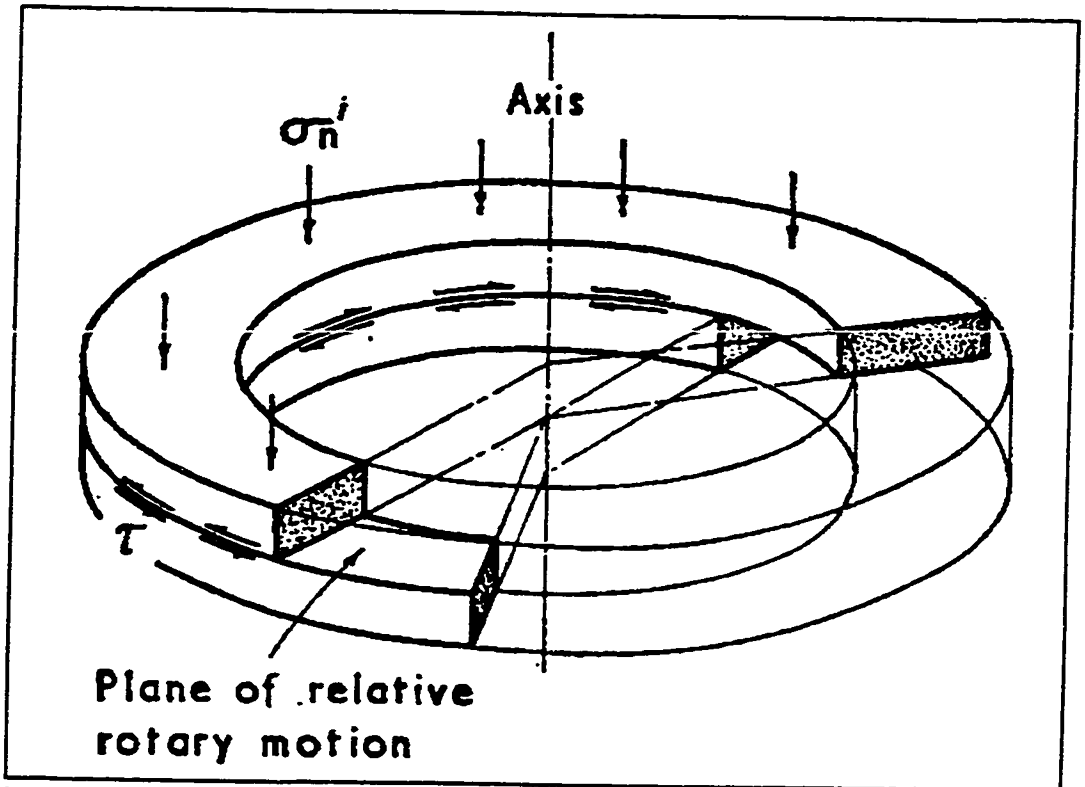

Fig. 2.20 Ring shear test sample (after Bishop et al., 1971)

Normal stress distribution	σ'_n	$\frac{p_{non\text{-}uniform}}{p_{uniform}}$	$\tan\phi'$	$\tan\phi'$ for $r_1 = 2{\cdot}01in$, $r_2 = 3{\cdot}01in$	$\frac{\tan\phi'_{non\text{-}uniform}}{\tan\phi'_{uniform}}$
Uniform 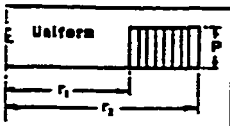	p	1·0	$\frac{3M}{2W}\cdot\frac{(r_2+r_1)}{(r_1^2+r_1r_2+r_2^2)}$	$0{\cdot}395\frac{M}{W}$	1·000
Linear I 	$\frac{p(r_2-r)}{(r_2-r_1)}$	2·14	$\frac{2M}{W}\cdot\frac{(r_1+2r_2)}{(r_2^2+2r_1r_2+3r_1^2)}$	$0{\cdot}424\frac{M}{W}$	1·075
Linear II 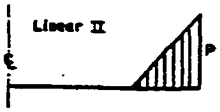	$\frac{p(r-r_1)}{(r_2-r_1)}$	1·87	$\frac{2M}{W}\cdot\frac{(2r_2+r_1)}{(3r_2^2+2r_1r_2+r_1^2)}$	$0{\cdot}372\frac{M}{W}$	0·943
Parabolic I 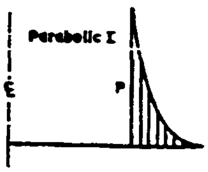	$\frac{p(r_2-r)^2}{(r_2-r_1)^2}$	3·33	$\frac{5M}{2W}\cdot\frac{(r_2+3r_1)}{(r_2^2+3r_1r_2+6r_1^2)}$	$0{\cdot}441\frac{M}{W}$	1·116
Parabolic II 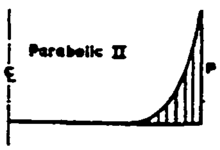	$\frac{p(r_1-r)^2}{(r_2-r_1)^2}$	2·73	$\frac{5M}{2W}\cdot\frac{(r_1+3r_2)}{(6r_2^2+3r_1r_2+r_1^2)}$	$0{\cdot}362\frac{M}{W}$	0·916
Parabolic III 	$\frac{4p(r-r_1)(r_2-r)}{(r_2-r_1)^2}$	1·50	$\frac{5M}{W}\cdot\frac{(r_2+r_1)}{(3r_2^2+4r_1r_2+3r_1^2)}$	$0{\cdot}397\frac{M}{W}$	1·006
Parabolic IV 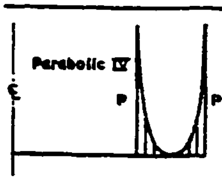	$\frac{p(2r-r_1-r_2)^2}{(r_2-r_1)^2}$	3·00	$\frac{5M}{2W}\cdot\frac{(r_2+r_1)}{(2r_2^2+r_1r_2+2r_1^2)}$	$0{\cdot}391\frac{M}{W}$	0·990

Table 2.3 Equations for angles of shearing resistance obtained from drained ring shear tests assuming different normal stress distributions (after Bishop et al. 1971)

3 APPARATUS

3.1 THE RING CELL

The ring shear apparatus used for the purpose of this research is based on the Bromhead design of the ring shear device (Bromhead, 1979) Since the original design was intended for tests on cohesive materials under drained conditions, the cell had to be modified to handle sand, and to allow constant volume test to be performed.

3.1.1 The Original Cell

The original Bromhead ring shear cell, is shown in **Fig. 3.1**. In this simple ring shear apparatus, the size of the annular sample is 5 mm (0.197 in) high, with inner and outer diameters of 70 mm (2.756 in) and 100 mm (3.937 in) respectively. It is confined in the vertical direction by two annular porous stones loading platens, and the normal stress is applied using a counter balanced lever loading system with a ratio of 10:1.

In the original design, the sample was made thin to ensure a sufficient drainage rate for plastic clay samples. The rate of rotation of the ring shear device can be selected to match the consolidation characteristics of the sample being tested in order to ensure drained conditions.

The base platen is rotated by means of a variable speed motor driving through a worm drive, while the upper loading platen is restrained. The torque during shear can be measured continuously by monitoring the forces at either end of the torque arm (**Fig. 3.1**), which is fixed to the upper loading platen. The rotation causes the sample to shear, producing a shear surface close to the upper platen. To prevent slippage at the platen/soil interface, the upper platen is artificially roughened.

3.1.2 The Modified Cell

A transverse view of the modified cell is shown in **Fig. 3.2**. The major modifications were as follows:

a) The sample size was altered to a height of 20 mm and external and internal diameters of 133 mm and 92 mm respectively. The extra height was deemed to be important in order to better control the placement density sand sample.

b) In order to reduce the friction at the confining walls , a series of 10 inner and 10 outer thin rings in which the sample was prepared was also provided **Fig. 3.2**. These rings were made either of finely machined Aluminium or teflon. The rings were 2 mm thick and 10 mm wide. The uppermost rings of the stacks were thicker (6 mm) to minimise sand penetration in this region which was observed in preliminary tests.

A pair of guard disks (**Fig. 3.3**) are screwed to the and keep the confining rings in place while the dummy sample is removed. Since the inner guard ring will later be inaccessible once the top platen is placed, the latter has been drilled with 6 holes which can be aligned with those of the inner guard ring.

3.2 THE ACTUATOR

The conventional ring shear test is carried out under a constant normal stress and the dimensions of the sample under drained shear are monitored. For the present research, however, it was necessary to modify the tests. In order to maintain constant volume, it was deemed necessary to modify the normal load by computer controlled servo actuator and feedback.

An air actuator assembly was installed in lieu of the conventional loading hanger attached to the loading lever arm. The load in the lever arm was therefore controlled by the air pressure in the actuator. Any change in the height of the sample during shear was monitored by a linear displacement transducer (with 10 mm travel) which could read to a precision of 0.02 mm. The computer controlled servo system automatically adjusted the pressure in the air actuator, and hence the normal load acting on the sample to maintain constant volume. The air pressure regulator which controls the air pressure in the actuator provides a minimum air pressure of 14 kPa (2 psi).

Two types of air actuators were used; one for low normal stress (up to 130 kPa) and the other for normal stresses up to a maximum of 660 kPa. The high pressure actuator was a sealed bellofram cylinder (Illinois Pneumatics, model: 4DAL-1-FF) with a piston area of 31.7 cm^2 (4.9 in^2).

No actuators of sufficiently small diameter and long enough stroke were commercially available to provide low normal loads for the required air pressure range. Hence a special air cylinder with an inner diameter of 34.9 mm (1.475") and a stroke of 100 mm (3.937") was fabricated. This actuator was designed as a leaking type cylinder in which air pressures are supplied at the bottom and top of the piston.

The pressure in the lower chamber of the actuators was maintained constant at 14 kPa (2 psi), and only the air pressure in the upper chamber was controlled to vary the load applied on the loading lever arm. **Fig. 3.4** shows a view of the actuators used in the test.

3.3 TRANSDUCERS

For automation provision of constant volume conditions and for continuous monitoring of data, a number of transducers were provided as follows (**Fig. 3.5**):

1- A vertical linear displacement transducer, to measure the vertical deformation of the sample is placed on the loading yoke, which is in turn on top of the loading platen.

2- Two load cells are used to measure the forces acting on the ends of the loading arms of the cap. Those readings can be used to determine the torque, and therefore the shear stress transmitted through the sample.

3- A third load cell is placed between the air cylinder, and the loading rod; which pulls on the loading lever arm. This load cell is used to measure the load applied to the loading yoke. The load applied to the sample is 10 times the load acting on the load cell due to the moment arm ratio.

4- A rotary potentiometer is connected to the axle of the turning table in order to automatically record the rotation of the base platen. It offers a resolution of a third of a degree.

All these transducers are connected to a PC-based data acquisition system, thus allowing the samples state to be continually monitored.

3.4 ADDITIONAL TOOLS

The preparation of sand samples in an annular volume presents particular difficulties. Because of the narrow width of the annular space, it is not possible to simply place some material in the cell for tamping purposes, as might be done for triaxial samples. Experience showed that dry sand pluviation through a series of sieves also presents problems with the uniformity of the sample. The sand accumulated much faster in on one side of the cell than the other, however well centred the ring cell might have been.

To solve this problem, it was decided to use a dry deposition method, in which sand could be gently deposited in the ring cell by means of a tube filled with sand, while the base platen was rotated.

3.4.1 Elevator Assembly

For the purpose of sample preparation, special tools have been designed. The main device for dry deposition of a sand sample consists of an elevator assembly, as shown in **Fig. 3.6** , with a sand deposition tube. This device permitted dry placement of sand under controlled conditions in the ring shear cell.

This elevator assembly consists essentially of a frame, with a screw driven elevator on which other devices, such as the sand deposition tube, and a sand scraper can be attached. A handle is fixed to the head of the lifting screws and used to raise or lower the tool elevator, or the dial gauge. A second lifting screw, is used to change the position of a dial gauge relative to the tool base. Once set-up, this dial gauge serves to establish the position of the sample surface relative to the bottom of the cell.

3.4.2 Alignment Pendulum

Preliminary experiments revealed that improper alignment of the top platen at the beginning of the test can cause sand to penetrate, between some of the confining rings. Initiation of sand penetration allows more sand to displace, and the void ratio calculations can therefore be seriously in error.

It was therefore decided to use a pendulum to ensure that upper, loading the platen, was horizontal when placed on the sample. It is also necessary to verify, using a level, that the rotating table on which the cell is placed is horizontal.

The pendulum assembly (**Fig. 3.7**) can be fixed to the vertical shaft (**Fig. 3.5**), and the vertical displacement transducer. It consists essentially of an horizontal arm terminated by a gimbal joint in which the pendulum, a 15 mm diameter and 25 cm long, sharp-ended, steel bar is fixed. The gimbal joint maintains the steel rod vertical, so that pointed end can be inserted on the conical seating of the centring pivot of the turning table (**Fig. 3.7**).

The pendulum assembly remains locked in position during the subsequent placement of the cap (although the pendulum rod itself can rotate and slide within the gimbal joint). The cap can then be allowed to gently slide down the vertical pendulum rod to rest on the sample horizontally.

3.4.3 Verification Device

The preparation of uniform samples is essential to obtain meaningful results from the ring shear tests. A special device was therefore designed to verify the density distribution of the samples prepared. This device was also used to assess the repeatability of the procedures adopted for sample preparation. The details of the sample preparation are presented in section 4.1. After preparation of the sample, a gelatine solution was circulated to semi-solidify the sand sample. This made it easier for thin slices to be cut for density determination.

The density verification device is shown in **Fig. 3.8** and **Fig. 3.9**. The device consists essentially of an acrylic version of the ring shear cell, with sliding lower platen, mounted on a large moveable piston. The piston enables the prepared sample to be extruded in a controlled manner which permits the material to be sampled for density determination.

Although the samples prepared in the density cell are of the same dimensions as standard samples, the density cell itself was made about 2 cm taller than the ring shear cell. This allows a sliding porous base platen to be inserted at the bottom of the cell.

Eight L-shaped channels were drilled in the outer wall of the acrylic cell. The horizontal section of the channels lead to the base of the cell and the porous bottom platen. These channels are the conduits that will allow the gelatine to infiltrate the sample from the bottom.

Open syringes, of 20 ml capacity, are used to deliver the gelatine solution into the channels. (**Fig.3.10**). The syringes can be plugged with flexible tubes of 1.5 mm diameter. This prevents premature flow of the gelatine solution into the sample. These flexible tube plugs can be pulled out together to start the flow to the sample simultaneously. Simultaneous delivery is necessary to avoid the creation of air bubbles that could disturb the specimen and therefore introduce an error in the measurement of the density variation through the sample.

Once the gelatine solution has percolated through the whole sample and solidified it (after 24 h), the extrusion tool can be rotated to extrude the sample in a controlled manner. A finely machined screw thread, with a pitch of 1 mm, is used to push the piston and the porous base platen of the cell. The screw thread is connected to a 120 mm diameter brass ring which is engraved with 10 divisions. The rotation of each division extrudes the sample by 0.1 mm. Hence, a very precise control can be exercised on the length of the sample.

3.5 FIGURES

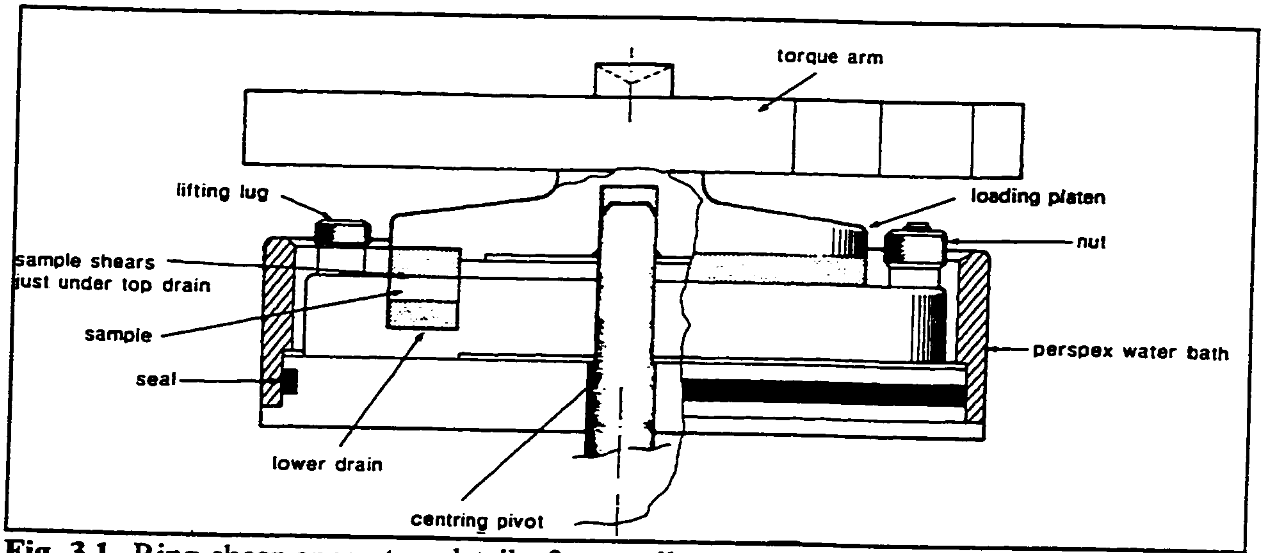

Fig. 3.1 Ring shear apparatus: detail of test cell (after Bromhead, 1986)

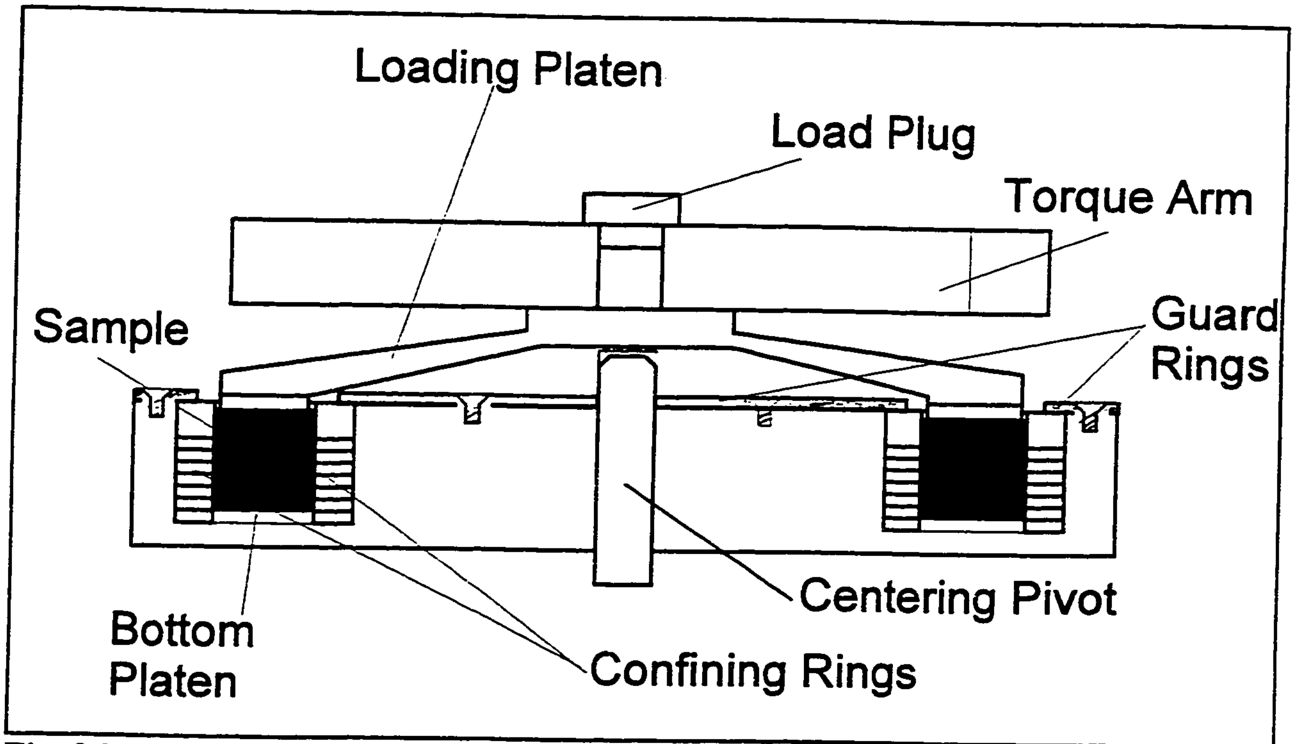

Fig. 3.2 Details of modified ring shear cell.

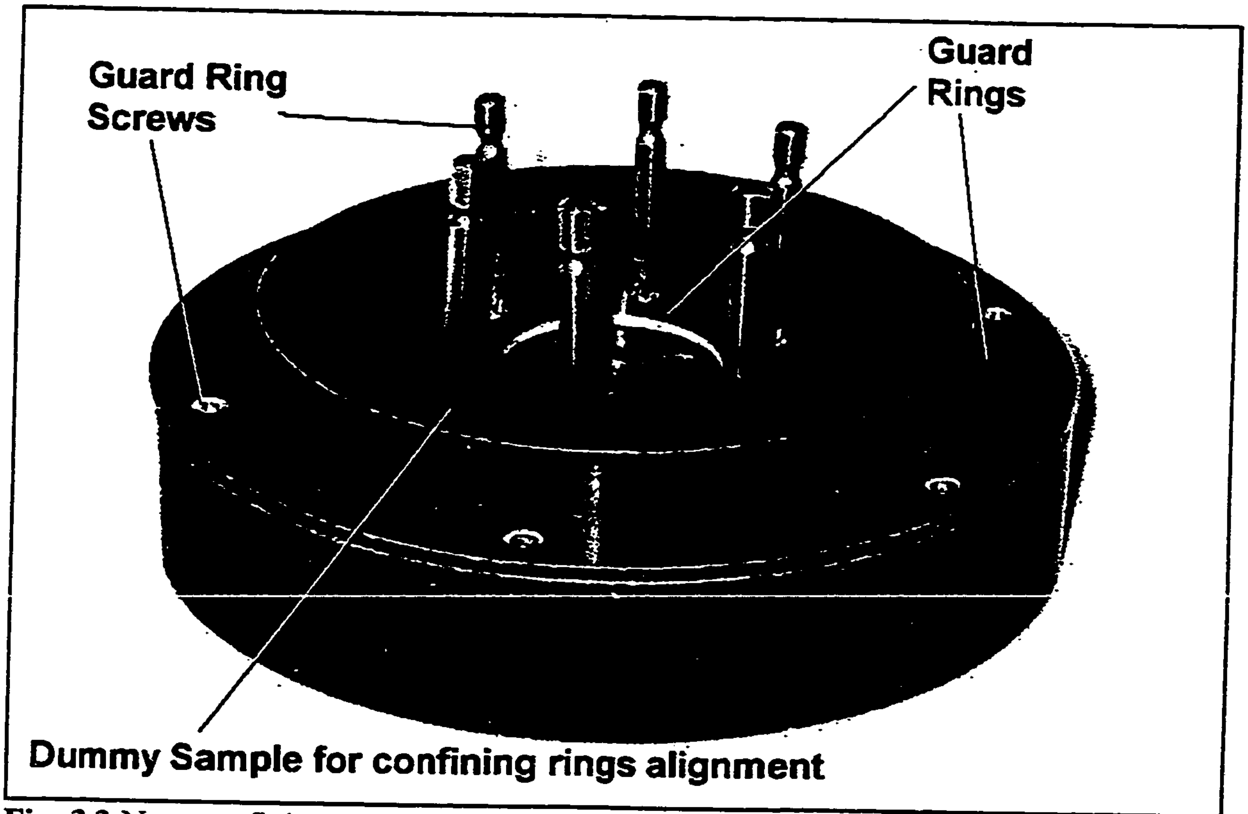

Fig. 3.3 New confining ring, with alignment sample, and guard rings tightened.

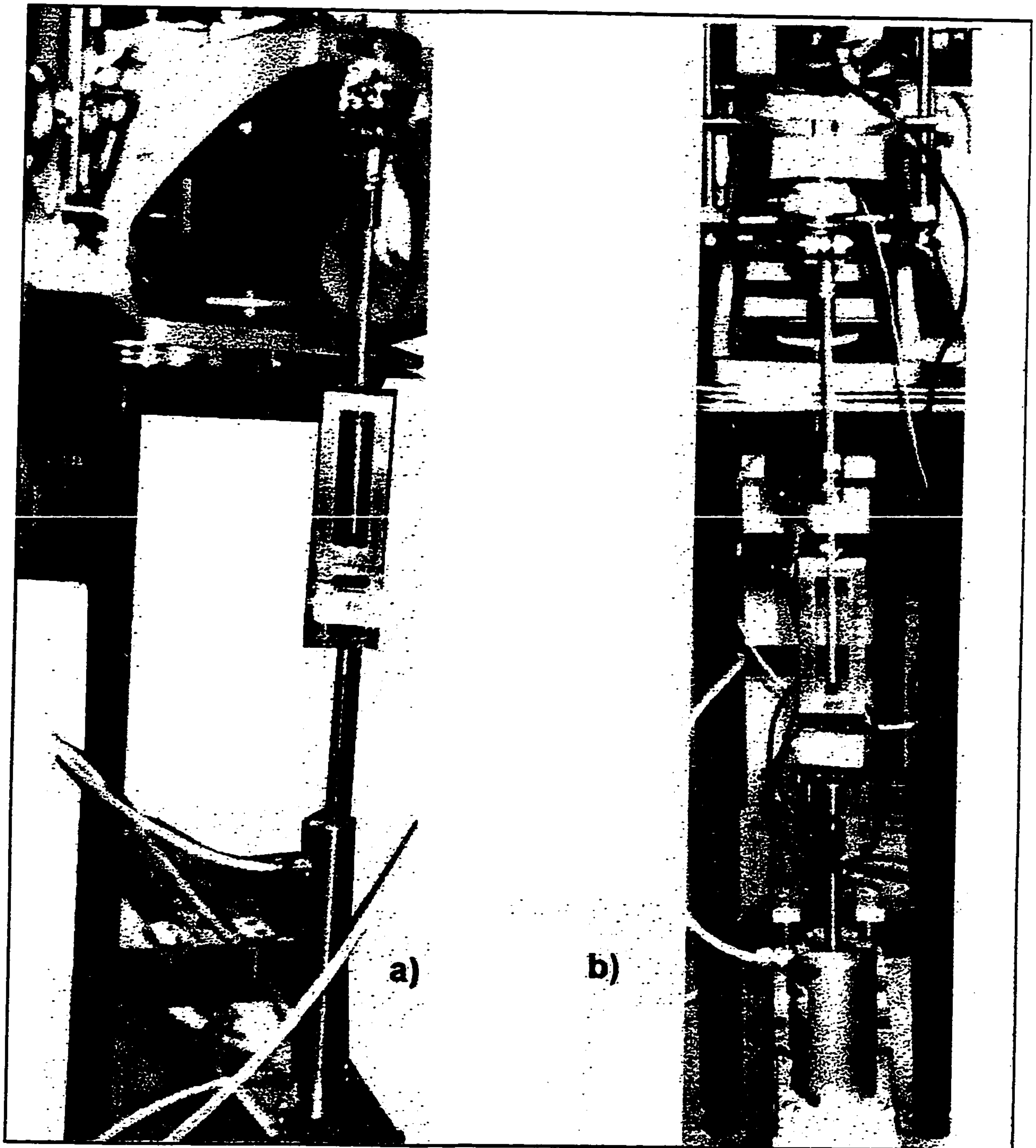

Fig. 3.4 View of the low pressure, (a), and high pressure, (b), actuators.

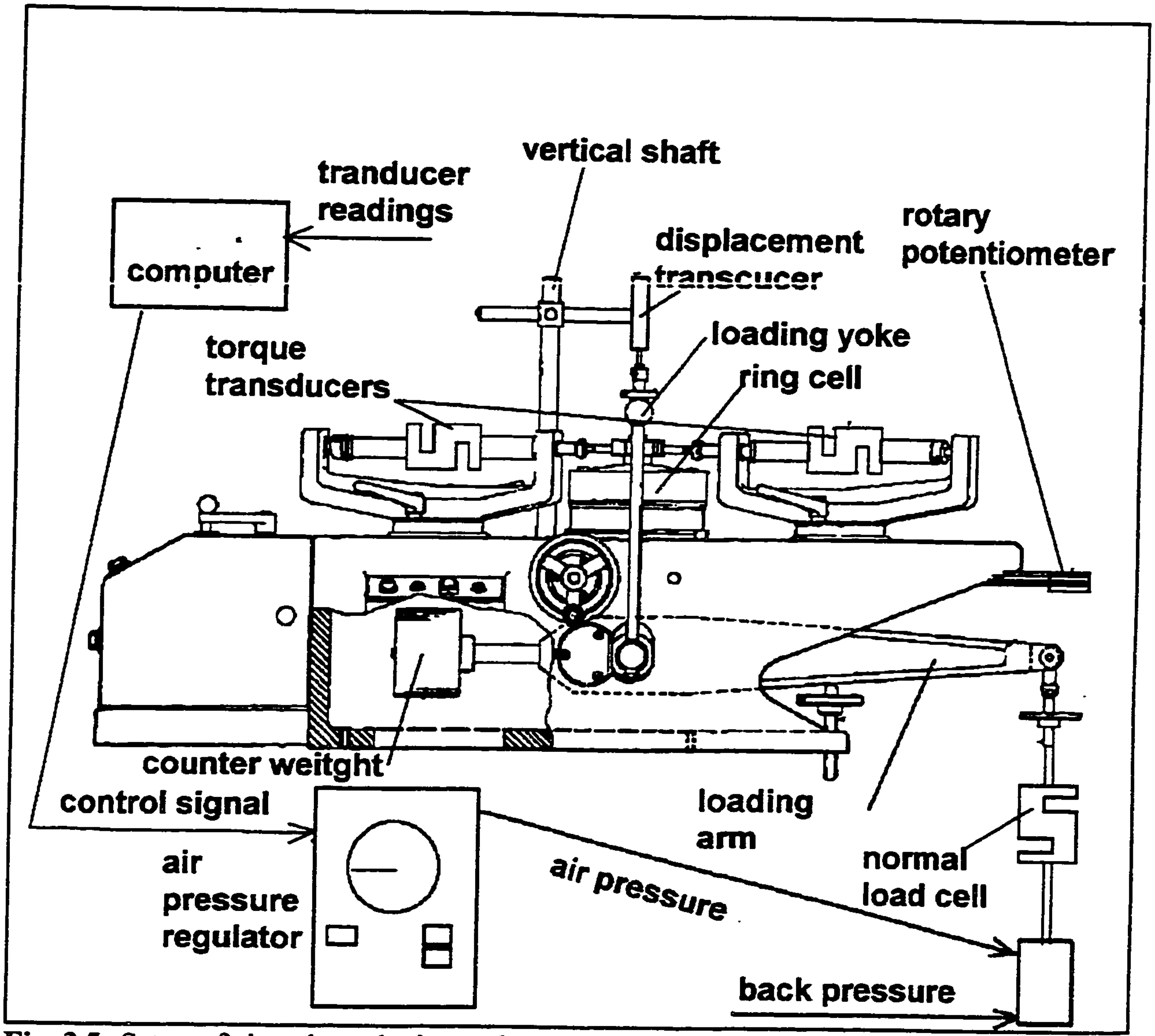

Fig. 3.5 Setup of ring shear device and transducers for automated control.

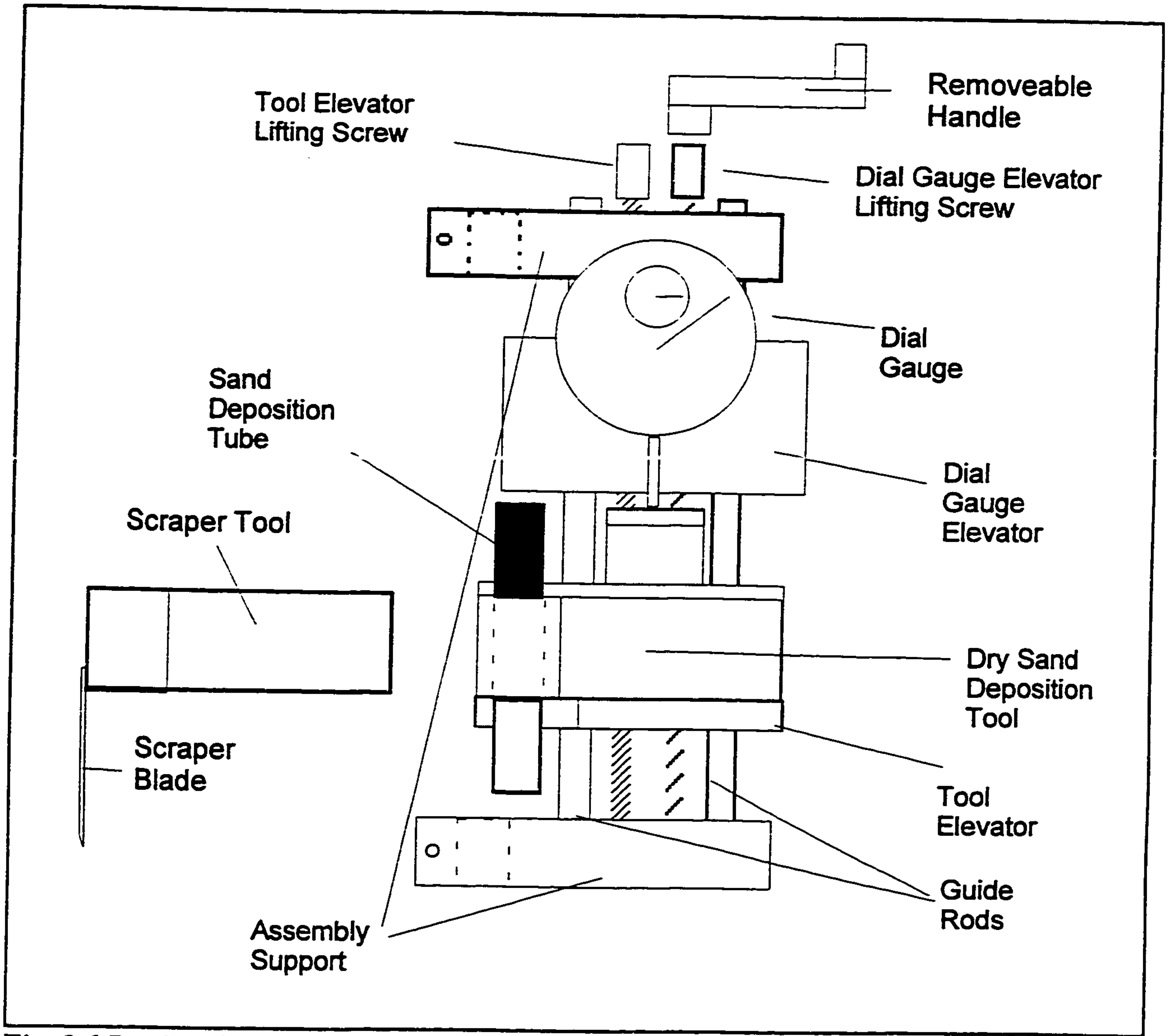

Fig. 3.6 Details of sample preparation tool assembly.

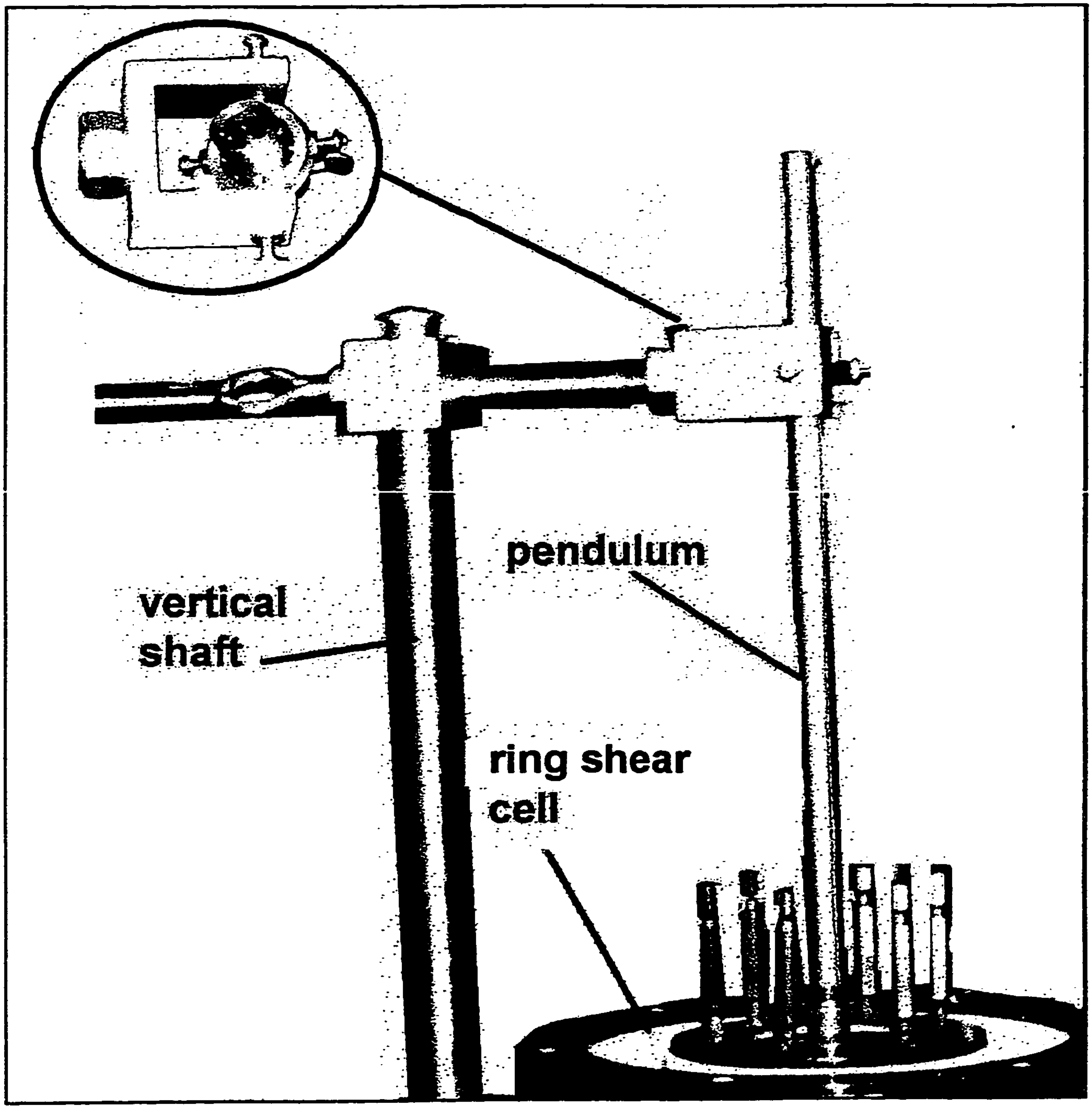

Fig. 3.7 Pendulum assembly

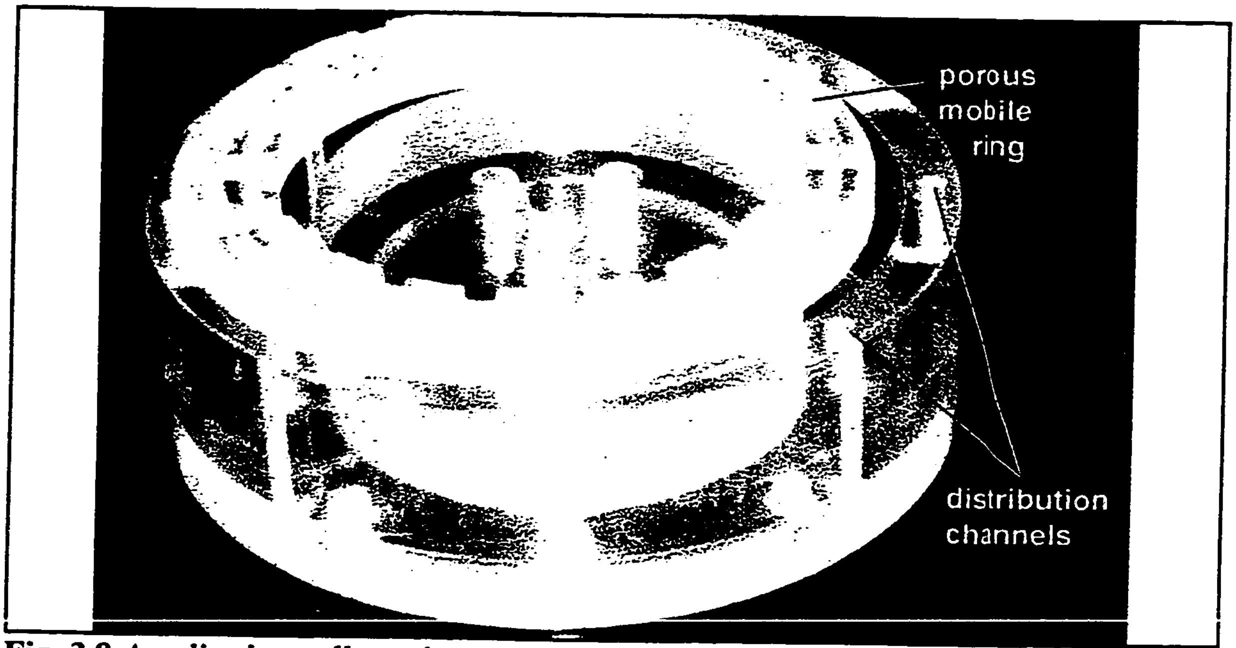

Fig. 3.8 Acrylic ring cell mock-up with the lifting bottom ring removed.

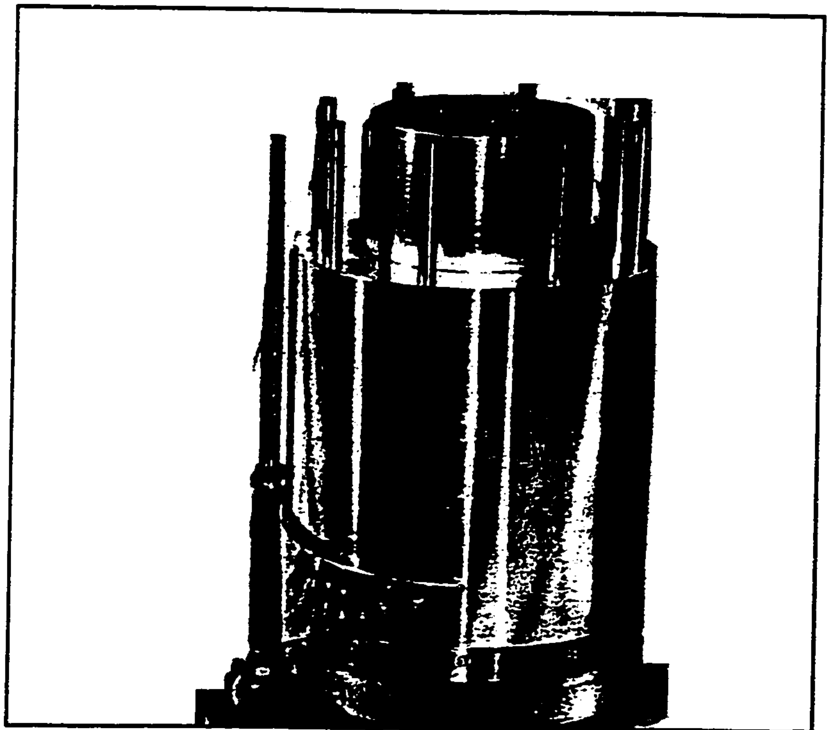
Fig. 3.9 Sample extruder piston

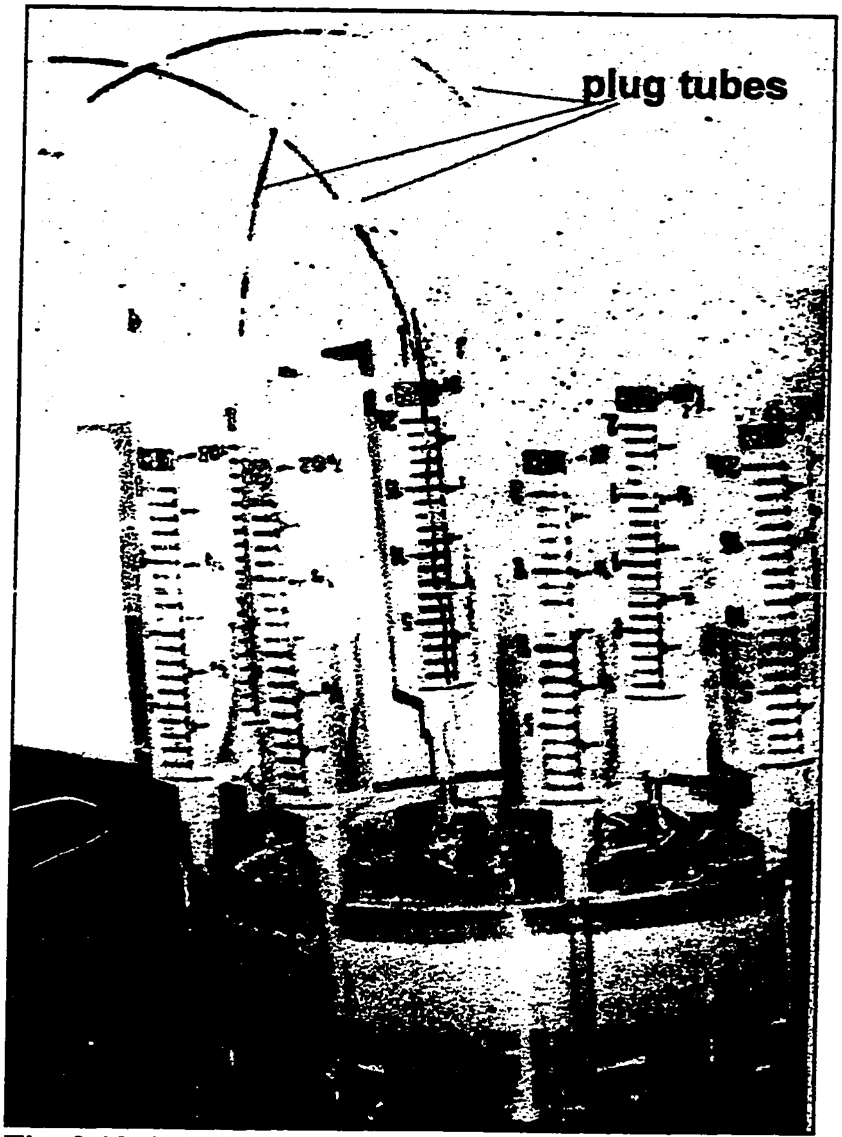

Fig. 3.10 Gelatine delivery system

4 SAMPLE PREPARATION METHODS AND TEST PROCEDURE

4.1 SAMPLE PREPARATION

For the purpose of this study, samples have been prepared using dry deposition method, for dry tests, and water pluviation for saturated conditions. The details of both sample preparation methods will be discussed in more detail in subsequent sections.

4.1.1 Preliminary Details

The first step in the sample preparation process consists of stacking up the confining rings that form the side walls between which the sample is formed. These rings, whether aluminium or are first stacked onto a dummy aluminium sample which allows them to be properly aligned (Fig. 4.1).

The dummy and rings set is then placed into the ring shear cell and the guard rings are screwed in place to keep the confining rings aligned. Once the dummy sample has been removed, a caliper is used to measure the depth of the ring cell from the top of the uppermost ring. This measurement is subsequently used to determine the thickness of the sample for volume and voids ratio calculations.

4.1.2 Sample Placement

4.1.2.1 Dry Deposition

As mentioned in the previous chapter, the dry deposition method has required the design of special tools in order to provide samples of uniform density.

The dial gauge is zeroed when the deposition tube is in contact with the lower platen, and a funnel is appended at the top of the tube. The funnel and tube are filled with sand and the turning table is used to fill the whole channel as the tube is raised in fixed increments (**Fig. 4.2**). When all the remaining sand fits entirely in the tube, a scaled cylinder is used to measure the amount of sand used for one revolution of the turning table (**Fig. 4.3**). This information can be used to select the last elevation of the tube so that the sample may be completed in one full revolution of the ring shear cell. The samples produced in this way are at the minimum density.

4.1.2.2 Water Pluviation

For the water pluviation method, a sample is boiled, an de-aired, in a pycnometer (**Fig. 4.4**). This pycnometer is filled to the brim with water and overturned into the ring shear cell which was itself filled with distilled water. The pycnometer must be moved smoothly along the ring shear cell's channel to permit the formation of a uniform sample.

Because the length to reach terminal velocity in water is very short, this method of sample preparation may discriminated samples with material that does not have a uniform particle distribution.

4.1.3 Placement of the Top Platen

Once the sample has been formed, the top platen can then be brought to rest on the sample (**Fig. 4.5**) using the pendulum assembly described in section 3.4.2. The loading yoke is then brought to bear on the top platen. Elevation difference between the top platen and the upper ring can be measured and comparison with the distance between the lower platen and the upper ring yields the height of the sample.

4.1.4 Loading the Sample and Starting the Test

Once the loading yoke is in place, all the transducers can be placed in their assigned positions. An initial load is applied to the sample. After allowing consolidation to occur, the screws that tighten the guard rings on the confining rings are removed. The drive gear of the ring shear device is engaged, and the shear test can begin.

4.2 DENSITY VERIFICATION

Density verification tests have been carried out on samples prepared with both dry deposition and water pluviation methods. The sample is prepared in the acrylic cell and the gelatine is injected. After 24 h, the sample is solid enough to be extruded in slices of 2.5 mm (**Fig. 4.6**). Each slice is recovered by first breaking it up into 8 sections for easy retrieval (**Fig. 4.7**).

The material recovered is placed in beakers. These are filled with water, well mixed and their contents are filtered under vacuum (**Fig. 4.8**). Preliminary tests have shown that 3 such mixing and filtering phases are required to thoroughly remove the gelatine present in the sample. The samples, left to dry in an oven, can be weighed after 24 h to determine their mass, and placement density.

4.3 PREPARATION OF FINES

In order to study the influence of the fine particles on the residual CV shear strength, a number of samples of Unimin sand were prepared with different concentrations of fine particles. The fines were produced by crushing Unimin sand. The crushing was done using mortar and a pestle attached to a drill press. After crushing, the material was sieved to retrieve the particles finer than the #200 sieve. These were defined as the fines for the purpose of the current study. Since the production of fines was a slow process, the samples were sieved after each ring shear test to retain as much of the fines as possible for subsequent tests.

All tests using additional fines were conducted under dry conditions. The process of sample preparation and testing are the same as those described for clean dry sand in sections 4.1.2.1, 4.1.3 and 4.1.4.

4.4 FIGURES

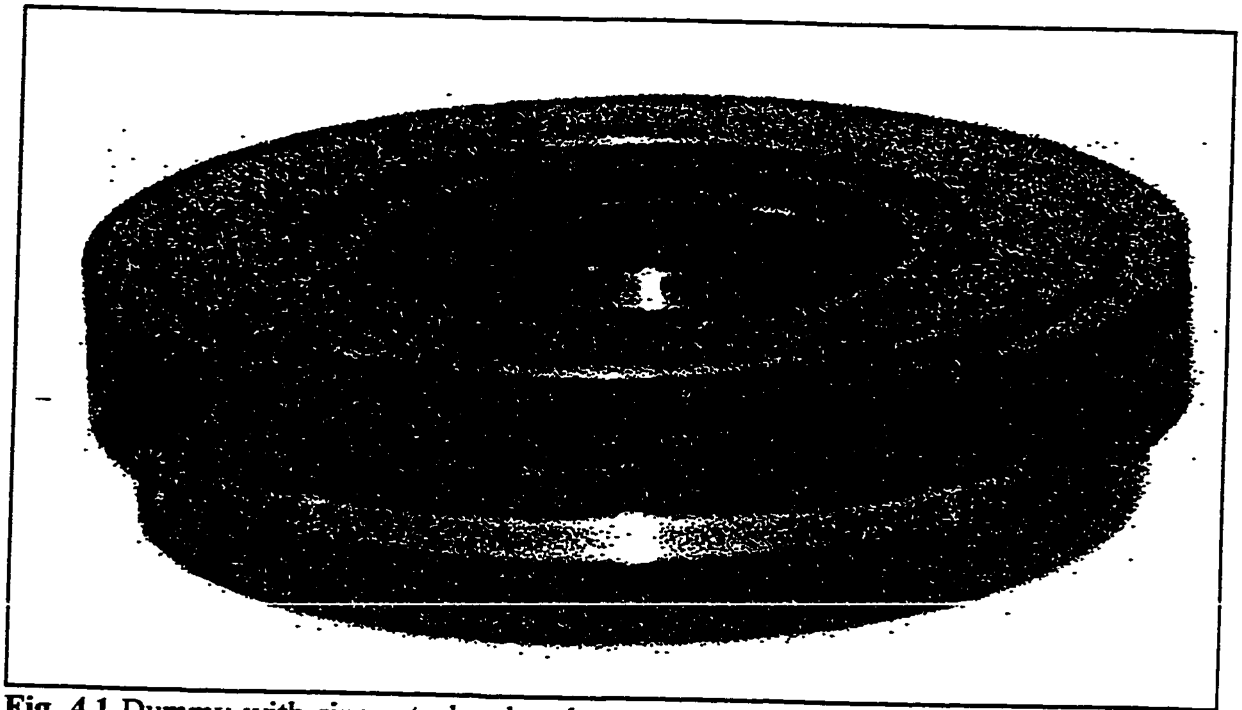

Fig. 4.1 Dummy with rings stacks placed.

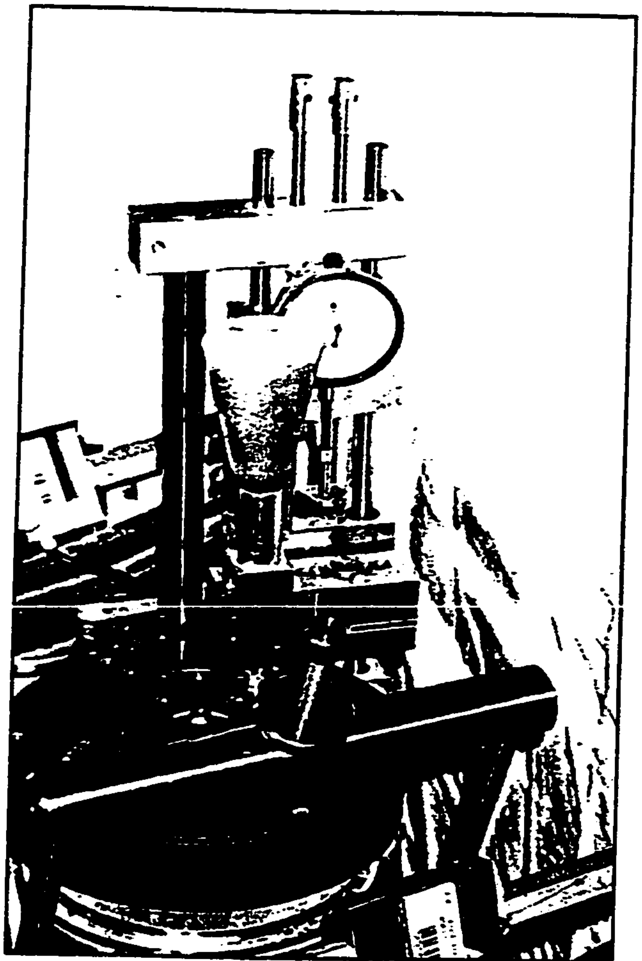

Fig. 4.2 Setup of dry deposition tool, with funnel filled with sand.

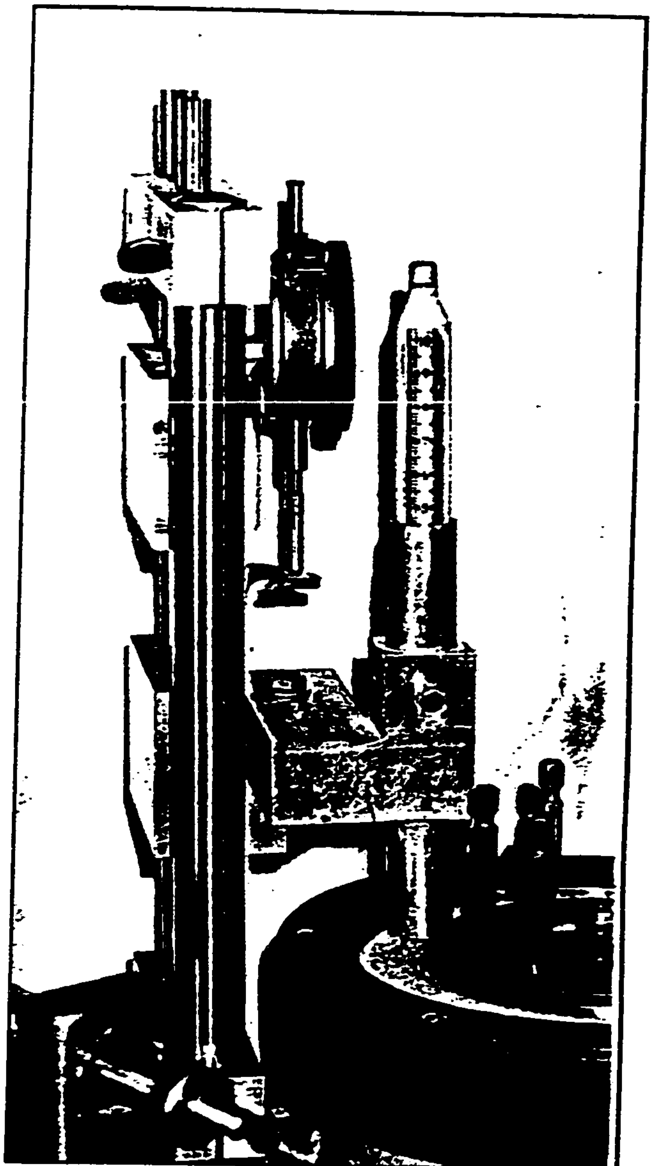

Fig. 4.3 Scaled tube used for placement of final layer.

Fig. 4.4 Boiling sand in a pycnometer for water pluviation of samples.

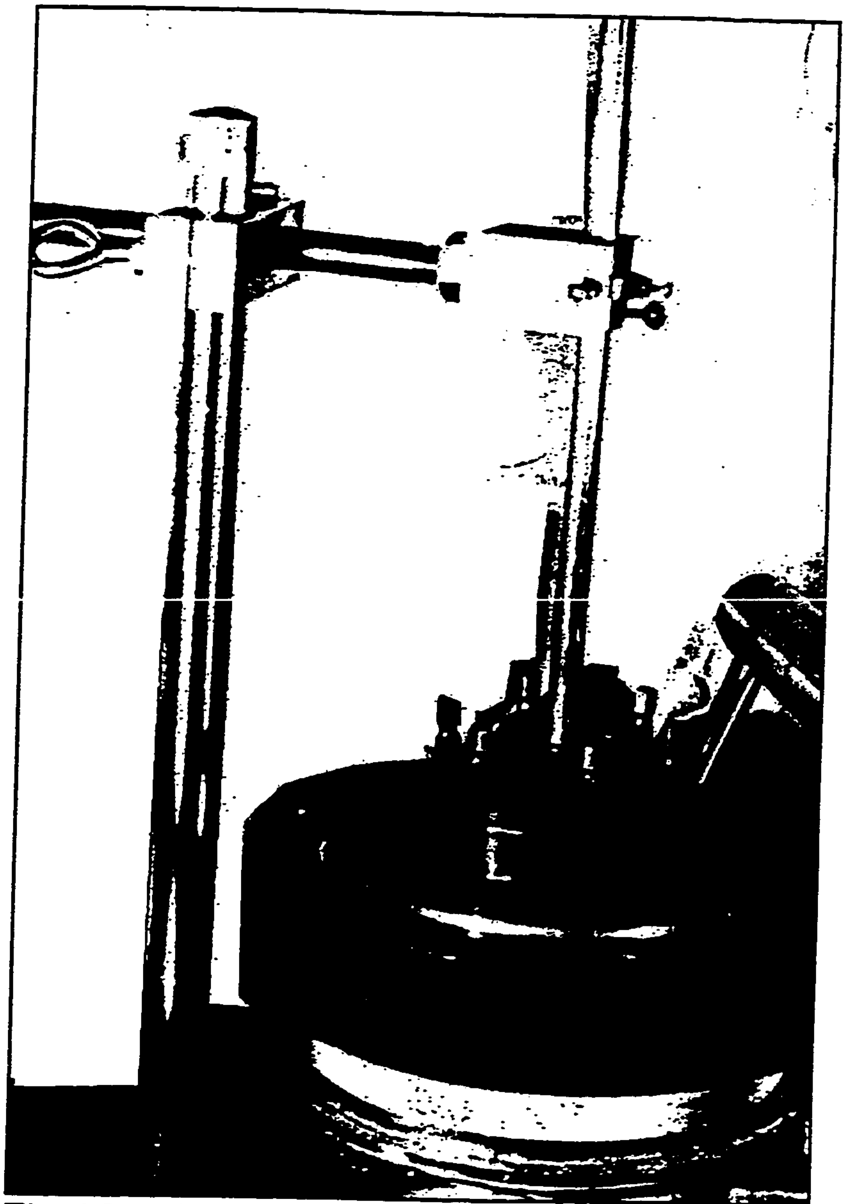

Fig. 4.5 Using the pendulum to centre the top platen on the ring cell.

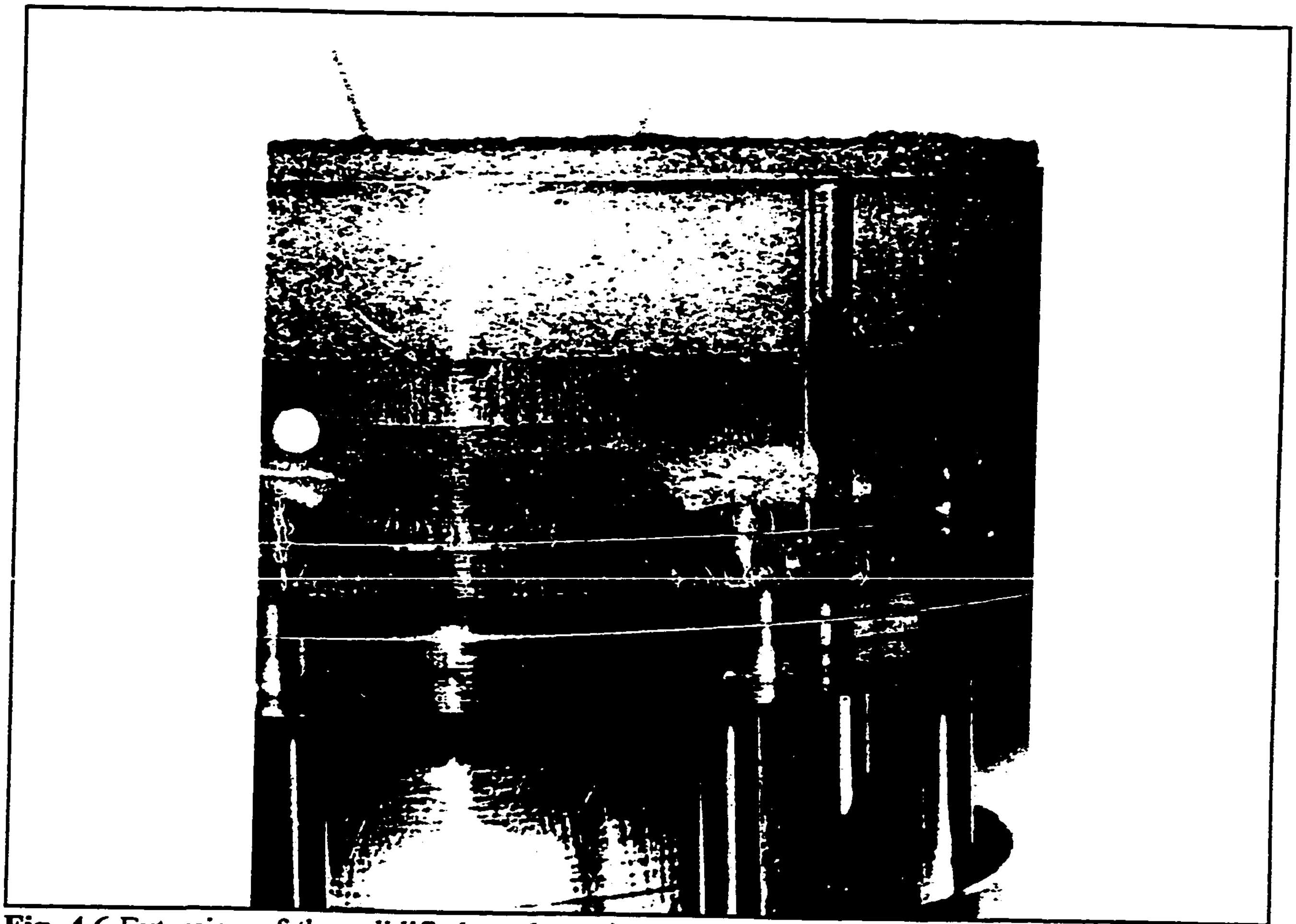

Fig. 4.6 Extrusion of the solidified sand specimen for density tests.

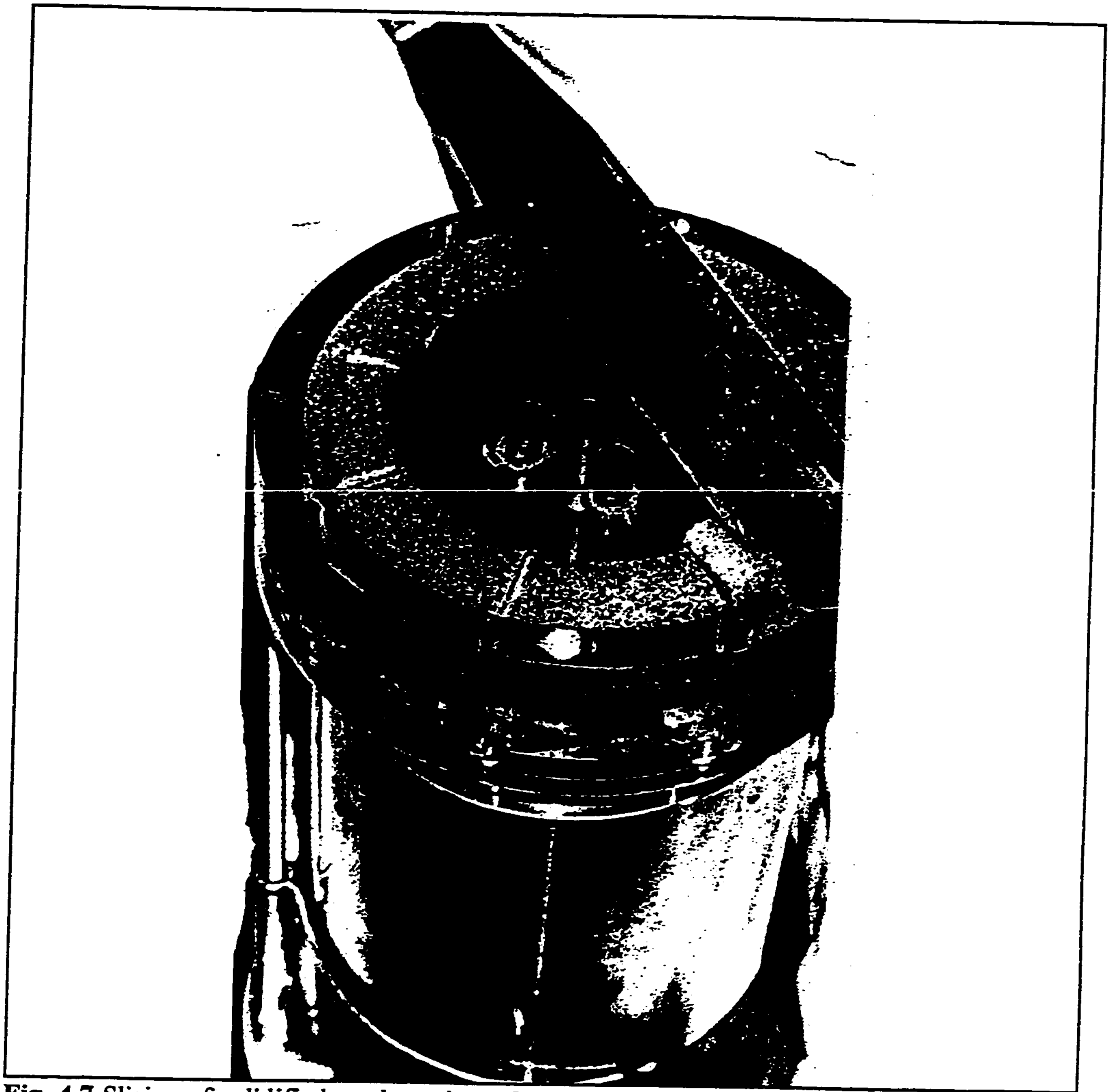

Fig. 4.7 Slicing of solidified sand specimen for density test.

Fig. 4.8 Vacuum filter setup.

5 VERIFICATION TESTS

This chapter describes the various tests carried out to verify the appropriateness of the sample preparation methods used. In particular, since density can significantly affect the S strength, considerable attention was focused on verifying the uniformity of density of the samples with depth (i.e. verification of the uniformity of the sample), and the repeatability of sample preparation.

In addition, considerable effort was also spent on assessing the mode of failure and the location of the shear plane in the ring shear apparatus, and also to assess the influence of friction between the confining rings on the measured constant volume strength.

5.1 DENSITY VERIFICATION TESTS

In order to verify the uniformity of the sample with depth, it is necessary to solidify it, without change in void ratio, in such a way that it becomes possible to take slices of the material without having sand grains falling apart. It is convenient to perform this solidification using a gelatine solution (Vaid and Negussey, 1988) that can then be injected into the prepared specimen. The saturation of the specimen with the gelatine solution is done through the base of the specimen, under a low head to ensure that it will not cause deformation of the specimen during the process. The verification tests were carried out in the density verification device described previously in section 3.4.4. The preparation of the gelatine solution itself, however, has required some particular considerations.

5.1.1 Gelatine Concentration

The first consideration in preparing the gelatine solution, is to make sure that it is thick enough to ensure a proper solidification of the sample while remaining fluid enough to easily flow through the specimen. Several qualitative preliminary tests were performed with this objective and an adequate concentration of gelatine material was found to be 1 g/10 ml. The samples produced are firm and easy to slice and recover since there is no loss of loose material. The gelatine solution used was prepared using commercial grade flavourless gelatine powder dissolved in hot water.

5.1.2 Gelatine Delivery System

The delivery system itself, as mentioned in section 3.4.3, has also required consideration. The first consideration was to ensure that the delivery head was not too high. When small diameter syringes were used, pore pressure buildup at the base of the sample made it bulge upwards (very visibly), to later collapse, thus leaving several pockets that were then filled with the gelatine solution. It is evident that such a condition is undesirable if a proper estimation of the density distribution is to be obtained from the test.

Subsequent tests revealed that the 20 ml syringes, with an inner diameter of 20 mm, providing a head of 70 mm of solution, were adequate as reservoirs for the specimen of Unimin sand 2010. The seepage conditions were such that the specimen was gently saturated without any visible deformation while saturation occurred.

5.1.3 Sample Recovery and Filtration

It is difficult to cut an entire slice of an annular ring shear sample. It was found useful to subdivide each annular slice into eight arc sections of 45° angle. These small sections proved very easy to recover, without noticeable loss of material when placing them into beakers. The detailed procedure for extruding the sample for slicing has been described in section 3.4.3.

The sliced samples were collected in a beaker, which was subsequently filled with water, vigorously mixed and the contents were placed in Previous tests on trial samples where the mass of sand and gelatine were both known allowed to determine that 3 washings were sufficient to clear all gelatin from the sample with losses of soil in the order of 0.01 g per 40 g of initial soil mass (or 0.025%). Less than 3 washings left too much gelatine, and, once dried, the sand grains tended to stick to each other.

It was also found impractical to perform the filtering operation on samples with added fines content since the filters promptly became clogged by the fine particles. The tests were therefore limited to the original Unimin sand.

5.1.4 Conclusion

Tests have been performed on both dry and saturated samples using the described gelatine solution delivery system. The results of tests on dry samples show a consistency with depth, to within 2 % of the average relative density (**Fig. 5.1**). The density variation is not systematic in nature. Samples prepared with the water pluviation method did not vary systematically with depth either. The error in the distribution of the densities was of 4%, systematically higher than the error recorded with the dry deposition method. These values are comparable to a 3% maximum variation obtained by Vaid and Negussey (1988) with pluviated sand samples. The greater variability in the preparation of water pluviated samples in the ring shear device may be explained by the difficulties in manually displacing the pycnometer at a regular velocity along the annular channel. The use of the scraper to level the surface of the sample after it was placed would also have an impact on the uniformity of the sample preparation.

5.2 LOCATION OF THE PLANE OF FAILURE

The ring shear, promotes the formation of an horizontal shear plane, much like the direct shear box. In many ring shear devices, such as the one described by Bishop et al. (1971), a gap exists between an upper and a lower ring which promotes shearing of the specimen near the middle of the sample, far from the influence of the upper and lower platen which might influence the results. The ring shear device described by Bromhead (1986), however, does not have such a gap since the confining ring is made of a single piece, and the sample shears along a horizontal plane near the loading platen.

The ring shear device used in this study also lacks a gap to direct the position of the shearing plane, but it dos not consist of a solid confining ring. As discussed in the chapter describing the apparatus, the confining walls consist of stacks of rings, made of aluminium or teflon, which easily slide over each other to reduce frictional contributions from the confining rings. As a result, the position of the shearing plane is not predetermined.

Visual inspection upon removal of specimen used in tests performed on saturated samples (particularly at normal loads at or above 200 kPa) showed a distinct failure surface a little above the middle of the sample, where the specimen showed a somewhat different colour, presumably due to the crushing of the particles in the shear zone. Similar observations were made for tests in dry conditions, although instead of a more pinkish colour, the shear zone appeared as a whiter horizontal band.

In order to obtain quantifiable data from such tests, a few samples were removed in layers, upon completion of the test, using a small vacuum cleaner and an interception jar with filter to prevent loss of material. The vacuum tube used in this procedure could be adapted quite easily to the dry deposition tube assembly, and the sample preparation tool elevator could then be used to regulate the increments of the sampling depth.

Once the specimen was collected in discrete layers in a number of beakers, a sieve analysis was performed on each layer collected in this fashion and the variation in the percentage of fines was recorded. **Fig. 5.2** shows the fines distribution within the specimen.

The fines distribution shows the degree of particle crushing within the sample. The degree of crushing is representative of the amount of shearing in the sample since at a constant effective normal stress, increased crushing would be expected to occur at the failure plane where the shearing is maximum.

The results of the test performed at 20 mm displacement (the shear displacement at which the peak strength is usually achieved) does not show any significant crushing compared to the sample where no shearing occurred. The fines distribution curves for shear displacements of 500 mm and 250 mm, also shown in **Fig. 5.2**, indicate considerable crushing at the failure plane located at the middle of the sample.

Another method used to depict the shearing process consisted of marking the confining rings along a vertical line at their inner surface. During shearing, each ring would slide with respect to its upper and lower neighbouring rings. After the test, the guard rings were tightened once again before the specimen was removed. The angular displacement between the marks on consecutive rings provided an estimate of the shearing deformations induced in the specimen. This method is limited by the finite widths of the rings. The results of these measurements are shown in **Fig. 5.3**, where the total deformation of the rings with the uppermost ring assumed fixed, is shown as solid circles. The slope of this curve provides an estimate of the degree of shearing (mm of shear / mm depth).

Independently of the method used to evaluate the shear deformation, it is evident that a definite plane of failure does occur close to the middle of the sample.

5.3 CONFINING RINGS

5.3.1 Influence of Confining Rings

When a vertical load is applied to a soil specimen through the loading platen, not all of it is carried by the specimen itself. As this vertical load is applied, the soil will apply a lateral pressure on its confining walls. Relative movement between the soil and a fixed boundary will generate some shear resistance, in the vertical direction. This shear resistance will have the result of relieving the soil below that level of a certain amount of normal stress.

The exact influence of the confining walls is difficult to determine. The amount of frictional resistance will be a function of the lateral pressure transmitted by the specimen, as well as the friction angle at the interface soil/wall. This is further complicated by the fact that the amount of mobilized interface reaction is dependent on the actual amount of relative displacement between soil and wall. The movement of the sample decreases with depth partly due to the variation of vertical normal stress acting on the specimen as a function of the interface reaction, but also because the settlement at the surface corresponds to the total sample settlement while the bottom of the sample remains stationary.

Since the change in normal effective stress is a function of the normal stress acting at a given depth and of the lateral pressure coefficient as well as the amount of interface friction mobilized, if it is assumed that the stress distribution at the surface of the sample is uniform, and if it is further assumed that loss of normal stress due to the friction with the side walls is uniformly distributed throughout the width of the specimen, then the vertical force acting on the sample lost at a given depth becomes:

$$d\sigma_z\, t\,(1) = -K_h \tan(\phi_i)\, \sigma_z\, dz(1) \tag{1}$$

where σ_z represents the normal vertical stress at depth, z, K_h is the coefficient of lateral pressure of the soil specimen, ϕ_i, is the interface friction angle (between soil and wall) mobilized at a given depth of the sample, while t is the thickness of the specimen (see **Fig. 5.4**), and in the case of the ring shear test, the width of the ring space, or channel. The value *(1)* represents the unit thickness of the sample considered.

If ϕ_i and K_h are assumed to be constant for the whole depth of the specimen, then equation **(2.12)** can be solved as:

$$\sigma_z = \sigma_o\, e^{-K_h \tan(\phi_i) \frac{z}{t}} \tag{2}$$

Fig. 5.3 schematically illustrates this simplified partial transfer of load to the side walls. The actual vertical shear strain mobilized will be greater near the top of the sample, where the total movement is observed, than at the bottom where it will be negligible, which will, of course, complicate the above expression. Equation **(2.13)** is nevertheless useful to provide an appreciation of the factors contributing to the transfer of load to the confining rings.

The amount of reduction in effective normal stress is therefore a function of the lateral earth pressure the mobilized friction angle between soil and side-walls, as well as the ratio of the depth to the width of the sample. Strategies to control the influence of the boundaries on test results would therefore include increasing the width of the sample substantially with respect to the thickness of the sample, as well as using a material offering little frictional resistance to make the confining rings.

Aside from the reduction in the effective normal stress, the confining walls could have an effect during the shearing itself. Indeed, if the confining rings were made of one solid ring throughout the whole thickness of the specimen, at the large longitudinal relative displacements occurring during shear between the soil and confining walls the full shear resistance at the interface would be mobilized and a non-negligible shear force would be added to the recorded shear resistance. As well, the rigid walls would probably favour the formation of the shear plane near the load platen, such as in the Bromhead design.

In an effort to reduce the impact of the walls on the specimen's behaviour, the side walls used during the experiments were made out of a series of rings. These rings, stacked on top of one another would, be free to rotate with the soil. This would therefore reduce the amount of relative movement between the walls and the soil, and thus the friction contribution from the confining rings should be dramatically reduced on the recorded torque. Ideally, the shear plane would form well within the body of the specimen.

Another factor affecting the recorded shear resistance may come from the vertical transfer of load from the soil to the confining rings. Although these rings can move freely with respect to each other, there will still be a frictional component attributable to their relative movements. This interannular friction would contribute to the recorded shear resistance of the specimen. It is therefore useful to reduce the interannular friction as much as possible, or to, at least, evaluate their impact, and possibly correct the results in consequence.

As a step to reduce the vertical load transfer, a compressible ring at the bottom of the stack, which would allow the stack to compress as easily as the soil, would contribute to reduce the amount of normal stress transferred to the ring stack since it would reduce the vertical relative movement between soil and side walls, and hence the vertical shear stresses. In practice, cardboard rings, about 1.5 mm in thickness have been placed below the outer and inner ring stacks.

5.3.2 Shear Contribution of Confining Rings

In an effort to obtain an appreciation of the contribution of the resistance of the confining rings to the recorded shear stress, a series of experiments was conducted using a set of teflon rings of the same dimensions as the original aluminium rings.

The teflon ring set will offer a lower resistance than the corresponding aluminium rings. By comparing the results obtained from the teflon rings tests to those obtained with the aluminium rings, it should be possible to evaluate the impact of the ring friction on the shear strength of the soil recorded during the test.

The failure envelopes obtained from tests using both aluminium and teflon rings are shown in **Fig.5.6.** The results show no variation of strength that could be attributed to the change in the confining material of the confining rings. The difference in friction is therefore essentially undetectable within the range of sensitivity of the instruments used in the test.

In order to appreciate the significance of these results, a very simple test was devised. The essential idea behind that test was the following:

> If the difference of friction between the teflon rings and between the aluminium rings is of a magnitude comparable to the magnitude of the friction between the teflon rings, then, since the difference of friction is undetectable to the instruments during the shear test, the friction contribution of the teflon rings themselves would be undetectable, and could therefore be neglected. Furthermore, since the difference between teflon rings and aluminium rings is undetectable, if the contribution of the teflon rings to the recorded torque is negligible, then the contribution of the aluminium rings would similarly be undetectable, and also negligible. If however the difference in friction is merely a small fraction of the friction between the teflon rings, then despite the fact that no difference is noted in the shear test, the contribution to the torque from the teflon rings could still

be important during the ring shear test. In that case, more sophisticated methods of measuring the contribution of the confining rings to the shear resistance would be required.

From this reasoning, two rings of each set were used. One was fixed in place, and the other ring placed on top of it, loaded with weights to press it against the bottom ring. A string was then tied to the top ring, at one end, and to a load cell ton the other. The load cell was then pulled manually, and through it the top ring, keeping the string always horizontal. The maximum load recorded using the aluminium ring was 29 N, while the maximum load with teflon rings was 12 N. The exact value of the load placed on top of the rings is not important, as long as it remains the same for both sets of rings. The essential element here is that the difference between the two friction resistances was 17 N, compared to the 12 N of friction recorded using the aluminium ring. The difference is of the same order of magnitude as the friction and it is even larger. If the difference in the contribution to shear resistance is undetectable during the ring shear test, it seems safe to assume that the contribution of the rings to the recorded shear resistance is negligible.

5.3.3 Conclusion

Despite the absence of a gap to direct formation of a failure plane, the new constant volume ring shear test leads the sample to fail on a defined horizontal failure plane near the middle of the sample, far from the influence of the end platens. This facilitates analysis since a direct shear mode of failure can be assumed, and Mohr circles determined from only from the normal vertical stress and shear stress acting on this plane.

Comparative tests on teflon and aluminium rings also indicate that the confining rings do not contribute significantly to the recorded shear strength of the sample. Both aluminium and teflon rings are suitable for the ring shear tests, although the aluminium rings may prove longer lasting in the abrasive sand environment.

5.4 FIGURES

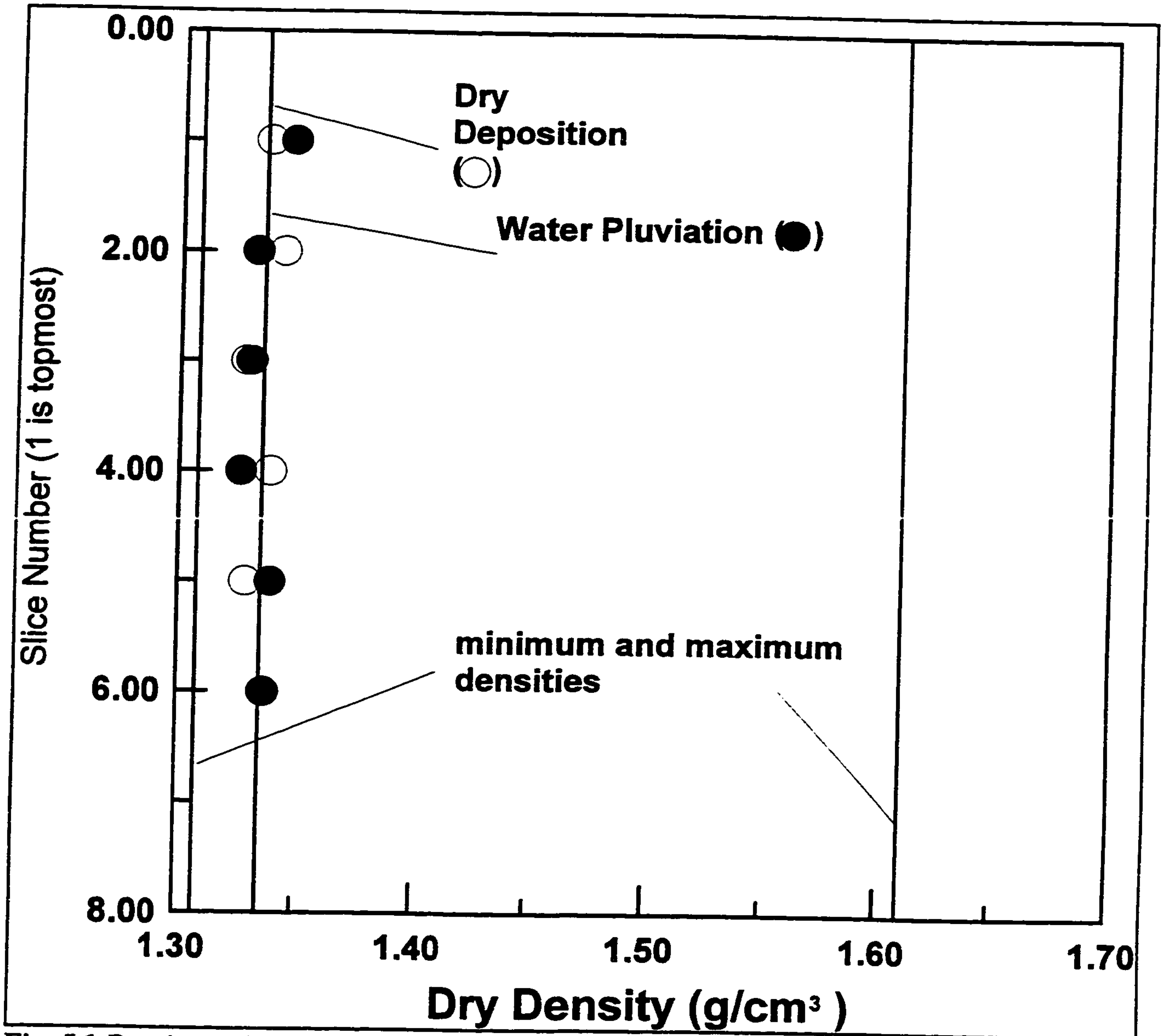

Fig. 5.1 Density variation with the sample using the dry deposition and the water pluviation methods.

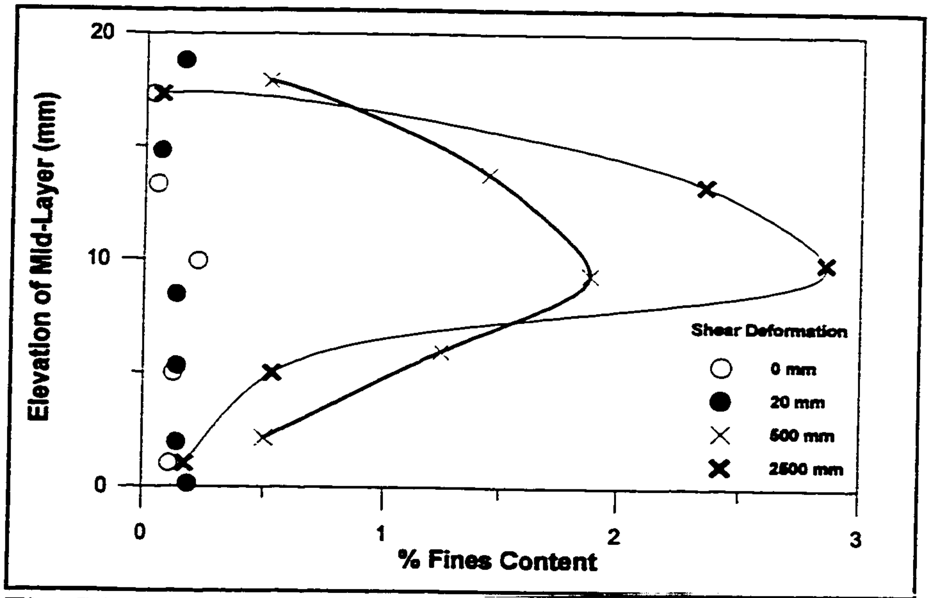

Fig. 5.2 Displacement of rings with depth, and displacement rate for a CV test at about 120° angular displacement.

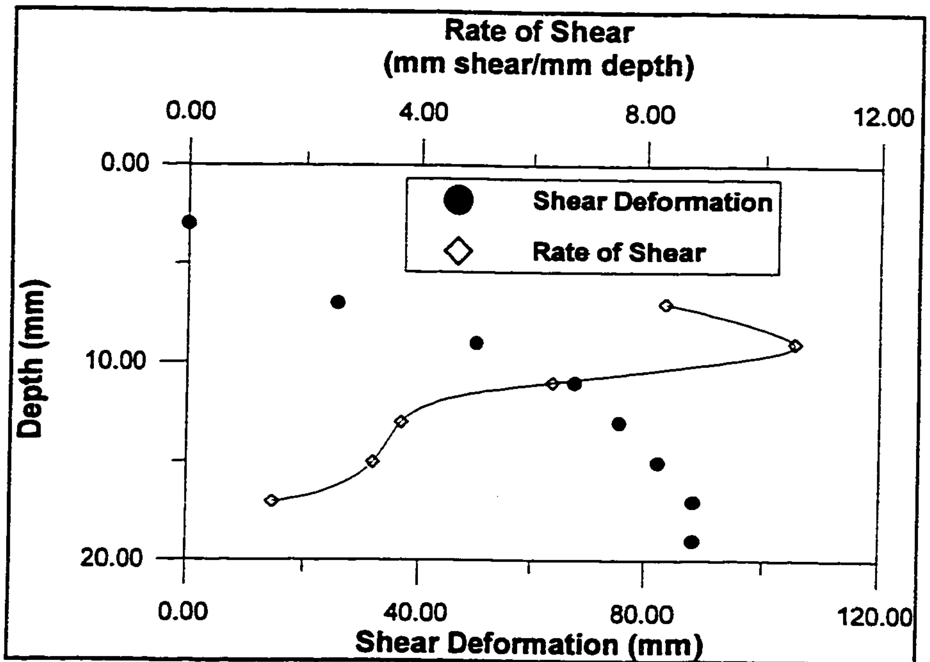

Fig. 5.3 Relationship between the ϕ, σ_{ff}, τ_{ff}, p, and q

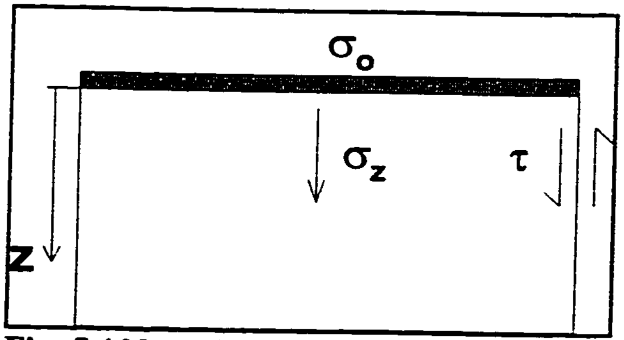

Fig. 5.4 Normal vertical stress lost due to friction with side wall.

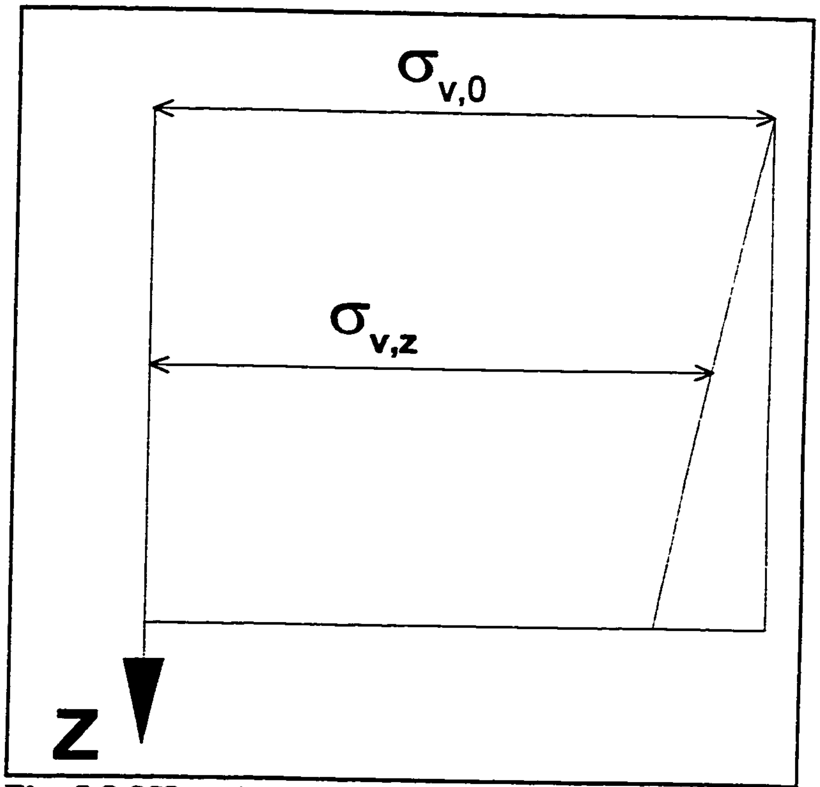

Fig. 5.5 SSL and residual strength envelope for tests using teflon and aluminium confining rings.

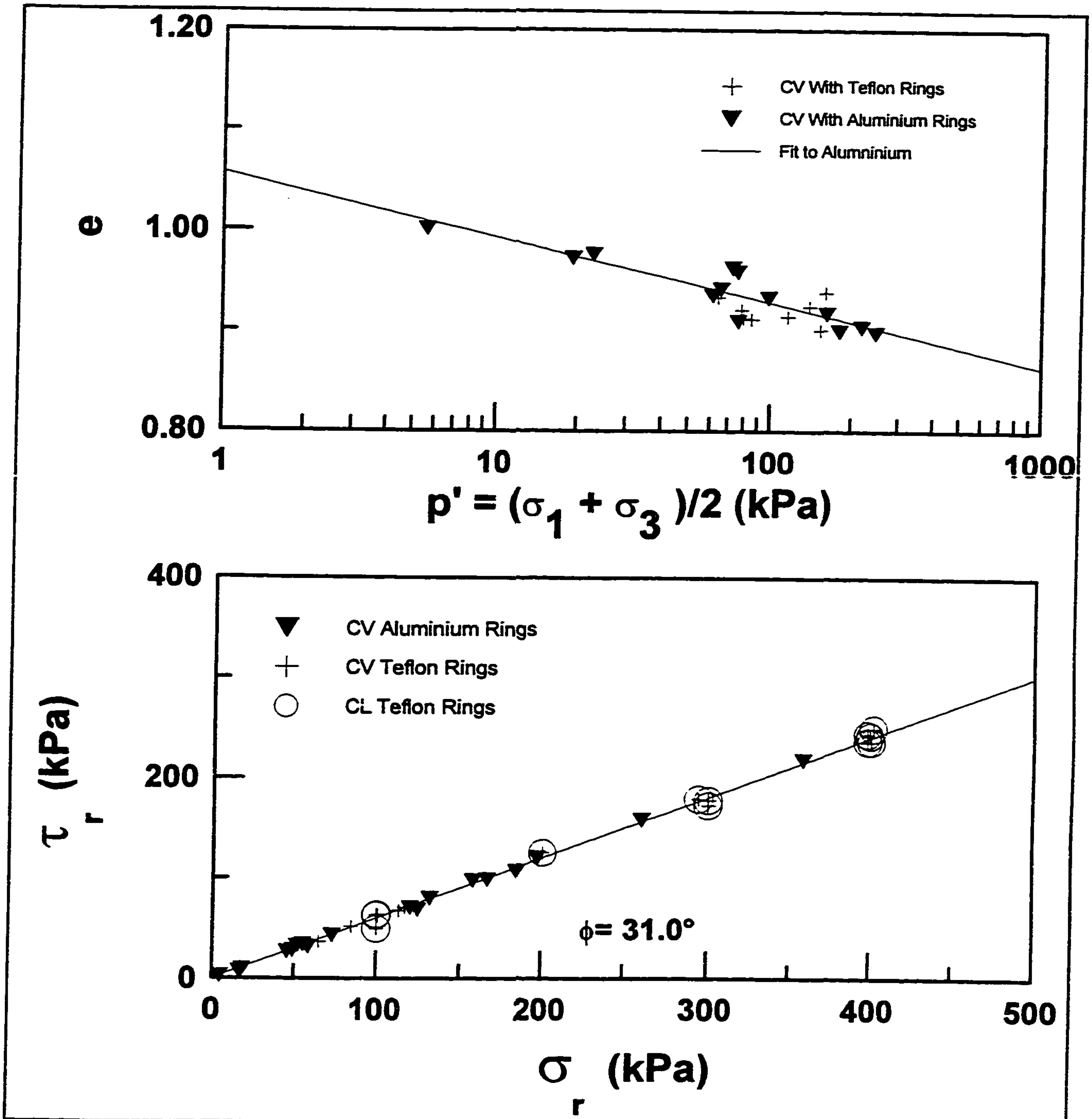

Fig. 5.6 Comparison of ring shear tests on Unimin 2010 sand using teflon or aluminium confining rings stacks.

6 TEST PROGRAM AND EXPERIMENTAL RESULTS

6.1 TEST PROGRAM

The test program undertaken is presented in Table 6.1

The test program was designed to investigate the flowing aspects:

a) the influence of shear rate on CV strength;
b) the comparison of CV strength for dry and saturated samples.;
c) the comparison of constant volume and constant load tests;
d) the evaluation of the influence of fines content;
e) evaluation of the influence of normal stress on CV strength;

All other testing was performed on Unimin sand. The specific gravity of the sand is 2.665, with a maximum and minimum dry density of 1.610 t/m^3 and 1.308 t/m^3 respectively. The grain size curve is show in **Fig. 6.1**. The Unimin sand 2010 was used since the same material had been used by Zhang (1997) for a detailed study of the steady state strength evaluation for the triaxial test. Hence, the S strength obtained for the ring shear tests have been compared to results presented by Zhang (1997).

6.2 EXPERIMENTAL RESULTS

6.2.1 Effect of Saturation

Fig. 6.2 compares the results of ring shear tests performed on both saturated and dry Unimin sand. Despite the greater void ratio scatter in the saturated test results, probably the result of the greater variability in sample preparation of water pluviated samples, the tests with both saturated and dry samples provide the same SSL. The residual strength envelopes using both sample preparation methods also agree. These results are consistent with the observations of Sasitharan et al. 1993, who concluded from a number of triaxial tests that the constant void ratio stress paths followed under drained constant-volume and undrained conditions are identical.

6.2.2 Constant Load/Constant Volume Tests

Fig. 6.3 shows the SSL and residual strength envelopes of specimen tested under constant volume and constant load conditions. Some of the CL tests were performed on samples having previously been sheared,to large deformations, at a higher normal load (included the other CL tests).

From the plot of the data in **Fig. 6.3 a)**, it can be concluded that the SSL is not influenced by the type of test since all points appear to be distributed about the same line. The scatter of the points about the SSL, however, is greater in the case of the CL tests. Also shown in **Fig. 6.4** is plot of *arctan*(τ/σ'_n) versus log of mean displacement in the ring shear. It is clear that steady state strength is reached at a displacement of 9 mm in both cases.

The comparison of the strength envelopes for both tests, depicted in **Fig. 6.3 b)**, indicates a systematic difference in the steady state strength achieved by CV tests and CL tests. The steady state friction angle of the CL tests is of 28.4° compared to the 31.0° of the CV tests. Also shown in **Fig.6.3**, are results of constant load tests on samples which had been sheared at a higher normal stress, and subsequently unloaded and re-sheared at a normal stress which was lower than during the first shear. The CL tests using teflon confining rings also show a steady state strength envelope with an angle of 31.0° (**Fig. 5.6 b)**).

These results suggest that there is a non-negligible transfer of normal load from the sample to the confining rings in a CL test. In a CV test the amount of vertical movement in the sample is very small (it is kept as close to 0 as possible), while it is permitted in a CL test. Thus, there is enough vertical movement generated in a CL test that the vertical interface friction resistance can be fully mobilized, which results in a loss of effective vertical stress on the specimen. The CV tests, on the other hand, do not promote transfer of normal effective stress to the confining rings. Since CV tests with aluminium and teflon confining rings as well at CL test using teflon rings, and unloaded CL tests using aluminum ring all result in the same steady state friction angle, it can be assumed that in those cases the vertical stress loss is negligible. The friction angle of 31.0° would therefore be representative of the strength of the Unimin sand 2010 under very large deformations. This can be compared to a triaxial S value of 33.6° for this sand (Zhang, 1997)

6.2.3 Influence of Rate of Shear

Fig. 6.5 shows the results of CL tests on saturated Unimin sand, using teflon confining rings, at various rates of shear. The data in **Fig. 6.5 a)** are uniformly scattered about the SSL defined by the constant volume tests at a rate of 15°/min. No shear rate related deviation is apparent. The only visible deviation from the CV SSL is observed at a vertical stress of 300 kPa. As it has been observed before, extensive particle crushing at those loads is the most probable factor influencing the incorrect evaluation of the steady state void ratio.

Fig. 6.5 b) shows the strength envelope obtained at the various shear rates. No appreciable variation of the strength envelope can be observed at the various shear rates. These results are consistent with those of Hungr and Morgenstern (1984).

6.2.4 Influence of Fines

For the purpose of this research, fines are defined as the particles finer than the #200 sieve opening. The fines used in this study are produced by crushing, and sieving, the Unimin sand 2010 used as the primary material for all tests. Since the fines have the same mineralogical composition as the skeleton material, only particle size distribution and possibly particle shape influence the behaviour of the tested material.

Because of the efforts required to initially produce, and then retrieve the fines after each test, both CL and CV tests were only performed on samples prepared with fines content of 10%. **Fig. 6.6 a)**, shows that, although the scatter is greater in the case of CL tests, the SSL obtained in both cases is the same. This confirms the results obtained for clean sand. The residual strength envelope of both types of test at 10% fines content have a friction angle of 31.0°; which is the same residual strength envelope obtained for clean sand. This suggests that the greater fines content in Unimin sand, while it does not affect the internal friction angle, results in a lower interface friction with the aluminium confining rings.

The sensitivity and capacity of the testing device being known, a range of testing vertical stresses can easily be selected for the purpose of CL tests. The equivalent steady state void ratio at those boundaries cannot be known until the CL tests have been performed, however. Since the results at 10% fines content suggested that at higher fines content the differences in the residual strength, between CV and CL tests, were much smaller than when using clean sand, CL tests were deemed adequate for the tests at higher fines contents. The results plotted in **Fig. 6.6 b)** show no variation of the friction angle due to the variation of the fine particles content.

Fig. 6.6 a) shows that with the initial increase of fines, the SSL is significantly lower than it was for clean sand. The transition from 30% fines to 40%, however, does not result in a further lowering of the SSL in the ***e-log p'*** plot, although the scatter of the results is increased. The lowering of the SSL means that for a given measured void ratio, the expected shear strength would be reduced as the fines content increases until some *critical* percentage of fines is reached, (the results suggests that the limit would be around 30%). The value of 30% fines content as a threshold is also reported by Thevanayagam & Mohan (1998).

This behaviour suggests that the coarser particles composing the skeleton control the behaviour of the sand at low fines contents. The fines are mostly inactive inside the voids while shearing occurs in the structure defined by the coarser particles. At high fines content, however, the fines particles, completely fill the voids, and become the matrix in which the coarser particles *float*. In this case, shearing occurs within the matrix. If the friction characteristics of the fines is different from the coarser material, the failure envelope would be expected to change as the amount of fines becomes sufficient for those particles to become active in the shearing resistance.

Using these assumption, the equation presented by Thevanayagan & Mohan (1998) can be used to correct for the void ratio of clean sand corresponding to a given fines content using equation **2.4** , the results of this analysis are applied to ring shear results of data up to 30% fines content (where presumably the limit of skeleton domination exists). The results are shown in **Fig. 6.8**, where it can be seen that the correction does indeed seem to agree with the test results up to a fines content of 10%. At 20% and 30% fines content, some other equivalent clean sand void ratio is achieved. Therefore, fines content at 20% already seems to have some influence on the compressibility of the soil.

6.2.5 Influence of Normal Stress

The results have consistently shown very linear failure envelopes throughout a large range of normal stresses. This linearity is confirmed when the *arctan* of the ratio of the residual shear strength over normal stress (the ϕ' angle) is plotted against the normal stress **Fig. 6.9**. The linearity of the failure envelope with the normal effective stress is consistent with the observations of Hungr & Morgenstern (1984) who performed an extensive series of constant load ring shear tests, at high shear rates, on a number of granular materials, including polystyrene beads an rock flour.

Comparing the ring shear results to those from the triaxial tests on Unimin sand (Zhang, 1997), **Fig. 6.8**, it can be observed that the latter show higher friction angles at low normal stresses. The ring shear tests, however, have a friction angle that remains constant for most of the range of confining pressures investigated. This suggests that the boundary conditions under which a test is performed is particularly important for loose samples, which reach steady state at low confining pressures, since both triaxial and ring shear test results seem to converge at higher confining pressures.

In fact, for the three constant volume tests performed on the loosest samples, the friction angle appears to be lower than the relatively constant values for the denser specimens. They do, however, show a marked increase in scatter if compared to the other test results. Two of those points are indeed not too far removed from the friction angle common to most other tests, while the third shows a clearly lower friction angle. In addition, **Fig. 6.9**, shows a typical volumetric strain curve for one of those "constant volume" tests, typical of the three cases, which shows dilatancy whereas constant volume was to be maintained by the system. the increase in scatter of the data together with the lack of a constant volume control suggests a systematic problem in maintaining test conditions constant at low stress levels. Whether the recorded values of strength are simply an artefact of the load cells' resolution, or the result of the difficulties in maintaining a constant pressure at low levels remains to be investigated. It would be useful for the purpose of such an investigation to use a sample with a larger surface area. This would allow finer control of the stresses applied since greater loads would be required to achieve them. As discussed in section 5.3.1, an increase in the sample width would also prove useful to reduce the relative vertical load transfer to the confining rings.

6.2.6 Comparison with Triaxial Tests

The results from CV ring shear test have also been compared to the triaxial test results on Unimin sand obtained by Zhang (1997). The results from both types of tests are compared in **Fig. 6.10**.

The steady state line, **Fig. 6.10 a)**, shows a close agreement between the triaxial CU compression tests and the CV ring shear tests. The regression lines from both tests are almost indistinguishable. Three data points from the CV ring shear tests (marked by circles) lie relatively far from the SSL. These point correspond to tests in which the vertical normal stress eventually went beyond the stress level of about 250 kPa, where crushing becomes so important that it significantly changes particle distribution of the sample. This increase of fines results, in a CV test, in a constant reduction of the normal stress as the device tries to compensate for the densification that the higher fines content promotes. If a steady state is eventually reached, it would be the steady state of a soil with higher fines content, not the original clean sand. None of the tests performed have shown a quasi-state or strain-hardening behaviour.

Fig. 6.10 a) shows more scatter in the ring shear test results than in the triaxial results. This may be attributed to the greater relative error in void ratio calculation caused by the smaller sample height used in the ring shear test. In a smaller sample, the same absolute error in the measurement of the height would result in a greater relative error.

Fig. 6.10 b) shows a difference of 2.6° between the residual strength envelopes of the triaxial tests and the ring shear tests. The ring shear test results have the lower friction angle, and even the points of continuous crushing lie on the same envelope.

6.3 FIGURES

Table 6.1

ID	Consol. State		Steady State					Comments
	e_o	σ_{vo} (kPa)	e_{res}	τ_{res} (kPa)	σ_{vr} (kPa)	$p' = (\sigma'_1 + \sigma'_3)/2$ (kPa)	$q = (\sigma'_1 - \sigma'_3)/2$ (kPa)	
CVD-01	0.983	3	1.001	2	4	6	3	CV Alum. Dry 15°/min
CVD-02	0.974	25	0.975	9	18	23	10	CV Alum. Dry 15°/min
CVD-03	0.958	143	0.958	32	58	75	36	CV Alum. Dry 15°/min
CVD-04	0.962	3	0.962	33	52	72	38	CV Alum. Dry 15°/min
CVD-05	0.909	113	0.909	34	55	76	40	CV Alum. Dry 15°/min
CVD-06	0.899	113	0.900	80	132	181	94	CV Alum. Dry 15°/min
CVD-07	0.762	115	0.770	69	125	163	79	CV Alum. Dry 15°/min
CVD-08	0.971	133	0.972	7	16	19	8	CV Alum. Dry 15°/min
CVD-09	0.943	18	0.941	28	49	65	33	CV Alum. Dry 15°/min
CVD-10	0.916	196	0.971	71	120	162	82	CV Alum. Dry 15°/min
CVD-11	0.988	13	0.989	27	46	61	31	CV Alum. Dry 15°/min
CVD-12	0.878	19	0.986	43	73	98	50	CV Alum. Dry 15°/min
CVD-13	0.897	344	0.952	107	184	247	124	CV Alum. Dry 15°/min
CVD-14	0.809	515	0.863	159	261	357	186	CV Alum. Dry 15°/min
CVD-15	0.726	491	0.726	218	358	491	256	CV Alum. Dry 15°/min
CVD-16	0.902	362	0.904	98	158	218	115	CV Alum. Dry 15°/min
CVD-17	0.881	385	0.880	121	197	271	141	CV Alum. Dry 15°/min
CVD-18	0.859	403	0.859	99	166	225	115	CV Alum. Dry 15°/min
CLD-01	0.941	49	0.979	32	50	70	37	CL Alum. Dry 15°/min
CLD-02	0.916	73	0.916	46	75	103	54	CL Alum. Dry 15°/min
CLD-03	0.922	97	0.919	61	100	138	72	CL Alum. Dry 15°/min
CLD-04	0.913	136	0.910	82	135	184	95	CL Alum. Dry 15°/min
CLD-05	0.926	21	0.931	12	20	27	14	CL Alum. Dry 15°/min (previously sheared under higher load)
CLD-06	0.920	55	0.922	32	50	71	38	CL Alum. Dry 15°/min (previously sheared under higher load)
CLD-07	0.915	77	0.917	47	75	105	56	CL Alum. Dry 15°/min (previously sheared under higher load)
CLD-08	0.906	102	0.909	63	100	139	74	CL Alum. Dry 15°/min (previously sheared under higher load)
CLD-09	0.940	35	0.979	18	30	41	21	CL Alum. Dry 15°/min
CLD-10	0.955	51	0.989	31	50	69	36	CL Alum. Dry 15°/min
CLD-11	0.947	72	0.992	46	75	103	54	CL Alum. Dry 15°/min
CLD-12	0.917	95	0.921	62	100	138	73	CL Alum. Dry 15°/min
CLSR03-01	0.985	99	0.926	48	100	123	53	CL Alum. Saturated 3°/min
CLSR06-01	0.992	19	0.937	10	20	25	11	CL Alum. Saturated 6°/min
CLSR06-02	0.990	48	0.937	25	50	63	28	CL Alum. Saturated 6°/min
CLSR06-03	0.975	97	0.921	51	100	126	58	CL Alum. Saturated 6°/min
CLSR15-01	1.005	18	0.954	9	20	24	10	CL Alum. Saturated 15°/min
CLSR15-02	0.961	110	0.949	62	100	138	72	CL Alum. Saturated 15°/min
CLSR15-03	0.797	310	0.790	160	300	385	181	CL Alum. Saturated 15°/min
CLSR30-01	0.969	96	0.920	56	100	132	64	CL Alum. Saturated 30°/min
CLSR30-02	0.941	98	0.944	62	100	138	72	CL Alum. Saturated 30°/min
CLSR30-03	0.770	299	0.763	166	300	392	190	CL Alum. Saturated 30°/min
CLSR60-01	1.011	21	0.957	9	20	24	10	CL Alum. Saturated 60°/min
CLSR60-02	0.937	100	0.941	61	100	137	72	CL Alum. Saturated 60°/min
CLSR60-03	0.919	202	0.880	103	199	253	116	CL Alum. Saturated 60°/min
CLSR60-04	0.850	306	0.830	162	301	388	183	CL Alum. Saturated 60°/min
CVDF10-01	0.718	575	0.718	141	242	324	163	CV 10% fines Alum. Dry 15°/min
CVDF10-02	0.738	262	0.739	63	111	147	73	CV 10% fines Alum. Dry 15°/min
CVDF10-03	0.760	147	0.760	46	82	108	53	CV 10% fines Alum. Dry 15°/min
CVDF10-04	0.780	105	0.780	25	43	57	29	CV 10% fines Alum. Dry 15°/min
CVDF10-05	0.802	22	0.804	13	23	31	15	CV 10% fines Alum. Dry 15°/min
CVDF10-06	0.699	255	0.700	132	224	302	153	CV 10% fines Alum. Dry 15°/min
CLDF10-01	0.769	25	0.801	12	20	28	15	CL 10% fines Alum. Dry 15°/min
CLDF10-02	0.798	49	0.807	31	51	70	37	CL 10% fines Alum. Dry 15°/min
CLDF10-03	0.705	72	0.722	48	74	105	56	CL 10% fines Alum. Dry 15°/min
CLDF10-04	0.790	96	0.799	61	101	138	72	CL 10% fines Alum. Dry 15°/min
CLDF10-05	0.789	110	0.805	71	114	157	83	CL 10% fines Alum. Dry 15°/min
CLDF10-06	0.709	125	0.721	81	129	180	96	CL 10% fines Alum. Dry 15°/min
CLDF20-01	0.737	26	0.715	12	20	27	14	CL 20% fines Alum. Dry 15°/min
CLDF20-02	0.728	50	0.702	31	50	70	37	CL 20% fines Alum. Dry 15°/min
CLDF20-03	0.690	62	0.656	46	74	103	54	CL 20% fines Alum. Dry 15°/min

ID	Consol. State		Steady State					Comments
	e_o	σ_{vo} (kPa)	e_{res}	τ_{res} (kPa)	σ_{vr} (kPa)	$p' = (\sigma'_1 + \sigma'_3)/2$ (kPa)	$q = (\sigma'_1 - \sigma'_3)/2$ (kPa)	
CLDF20-04	0.697	95	0.652	60	100	136	70	CL 20% fines Alum. Dry 15°/min
CLDF20-05	0.759	108	0.734	75	122	169	88	CL 20% fines Alum. Dry 15°/min
CLDF30-01	0.517	24	0.488	11	20	25	12	CL 30% fines Alum. Dry 15°/min
CLDF30-02	0.501	32	0.444	17	30	40	20	CL 30% fines Alum. Dry 15°/min
CLDF30-03	0.550	53	0.502	26	50	64	29	CL 30% fines Alum. Dry 15°/min
CLDF30-04	0.406	69	0.366	47	75	105	56	CL 30% fines Alum. Dry 15°/min
CLDF30-05	0.492	106	0.448	66	115	153	75	CL 30% fines Alum. Dry 15°/min
CLDF40-01	0.613	23	0.546	6	20	22	7	CL 40% fines Alum. Dry 15°/min
CLDF40-02	0.497	33	0.459	16	30	39	19	CL 40% fines Alum. Dry 15°/min
CLDF40-03	0.590	38	0.517	27	50	65	31	CL 40% fines Alum. Dry 15°/min
CLDF40-04	0.557	71	0.494	41	75	97	46	CL 40% fines Alum. Dry 15°/min
CLDF40-05	0.557	93	0.506	34	101	112	36	CL 40% fines Alum. Dry 15°/min
CLDF40-06	0.527	94	0.456	50	100	125	56	CL 40% fines Alum. Dry 15°/min
CLDF40-07	0.572	118	0.567	36	121	132	38	CL 40% fines Alum. Dry 15°/min
CLDF40-08	0.573	112	0.571	14	128	130	14	CL 40% fines Alum. Dry 15°/min
CLDT-01	—	405	—	126	201	279	148	CL Tefl. Dry 15°/min
CLDT-02	—	92	—	244	398	548	287	CL Tefl. Dry 15°/min
CLDT-03	—	100	—	64	100	141	76	CL Tefl. Dry 15°/min
CLDT-04	—	295	—	49	100	124	55	CL Tefl. Dry 15°/min
CLDT-05	—	404	—	180	295	404	210	CL Tefl. Dry 15°/min
CLDT-06	—	403	—	243	400	547	284	CL Tefl. Dry 15°/min
CLDT-07	—	402	—	237	401	540	275	CL Tefl. Dry 15°/min
CLDT-08	—	400	—	250	402	557	294	CL Tefl. Dry 15°/min
CLDT-09	—	100	—	64	100	141	76	CL Tefl. Dry 15°/min
CLDT-10	—	201	—	126	201	279	148	CL Tefl. Dry 15°/min
CLDT-11	—	100	—	49	100	124	55	CL Tefl. Dry 15°/min
CLDT-12	—	400	—	237	401	540	275	CL Tefl. Dry 15°/min
CLDT-13	—	399	—	250	402	557	294	CL Tefl. Dry 15°/min
CLDT-14	—	302	—	180	295	404	210	CL Tefl. Dry 15°/min
CLDT-15	—	403	—	243	400	547	284	CL Tefl. Dry 15°/min
CLST-01	—	100	—	63	100	139	74	CL Tefl. Sat 15°/min
CLST-02	—	200	—	178	300	406	207	CL Tefl. Sat 15°/min
CLST-03	—	400	—	237	398	539	275	CL Tefl. Sat 15°/min
CLST-04	—	298	—	173	300	400	200	CL Tefl. Sat 15°/min
CLST-05	—	401	—	237	398	539	275	CL Tefl. Sat 15°/min
CLST-06	—	300	—	173	300	400	200	CL Tefl. Sat 15°/min
CLST-07	—	100	—	63	100	139	74	CL Tefl. Sat 15°/min
CLST-08	—	296	—	178	300	406	207	CL Tefl. Sat 15°/min
CVST-01	0.914	90	0.914	51	84	116	60	CV Tefl. Sat 15°/min
CVST-02	0.993	400	0.993	27	49	64	31	CV Tefl. Sat 15°/min
CVST-03	0.911	399	0.911	36	65	85	42	CV Tefl. Sat 15°/min
CVST-04	0.901	397	0.901	68	114	154	79	CV Tefl. Sat 15°/min
CVST-05	0.924	403	0.924	62	101	140	74	CV Tefl. Sat 15°/min
CVST-06	0.911	295	0.912	35	58	80	41	CV Tefl. Sat 15°/min
CVST-07	0.920	197	0.921	35	56	78	41	CV Tefl. Sat 15°/min
CVST-08	0.937	405	0.938	71	117	160	83	CV Tefl. Sat 15°/min

Legend

CV	Constant Volume
CL	Constant Load
CLD	Constant Load, Dry sample
CLS	Constant Load, Saturated Sample
CLSR	Constant Load, Saturated, tests for variable shear Rates
CVDF	Constant Volume, Dry, tests for various Fines contents
CLDF	Constant Load, Dry, tests for various Fines contents
CLDT	Contant Load, Dry, with Teflon confining rings
CLST	Constant Load, Saturated, with Teflon confining rings
CVST	Constant Volume, Saturated, with Teflon confining rings

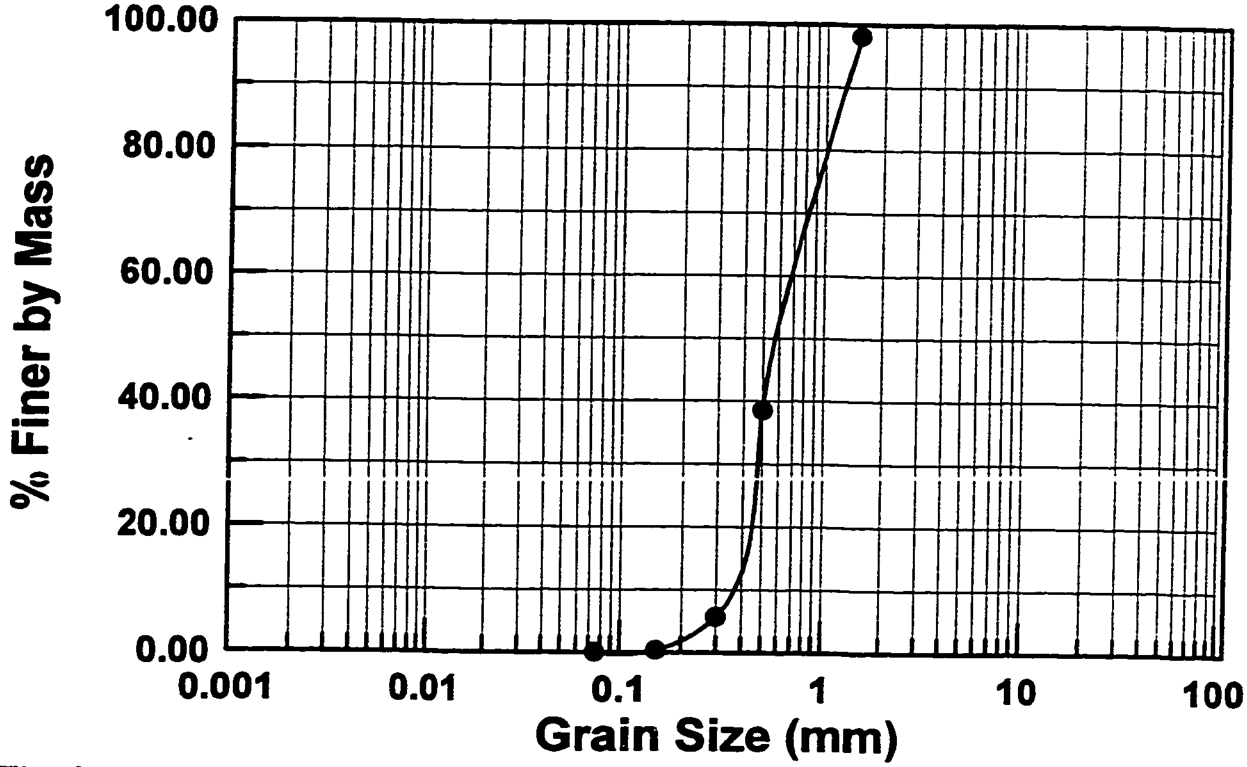

Fig. 6.1 Grain size distribution of Unimin sand 2010, C_u = 1.75

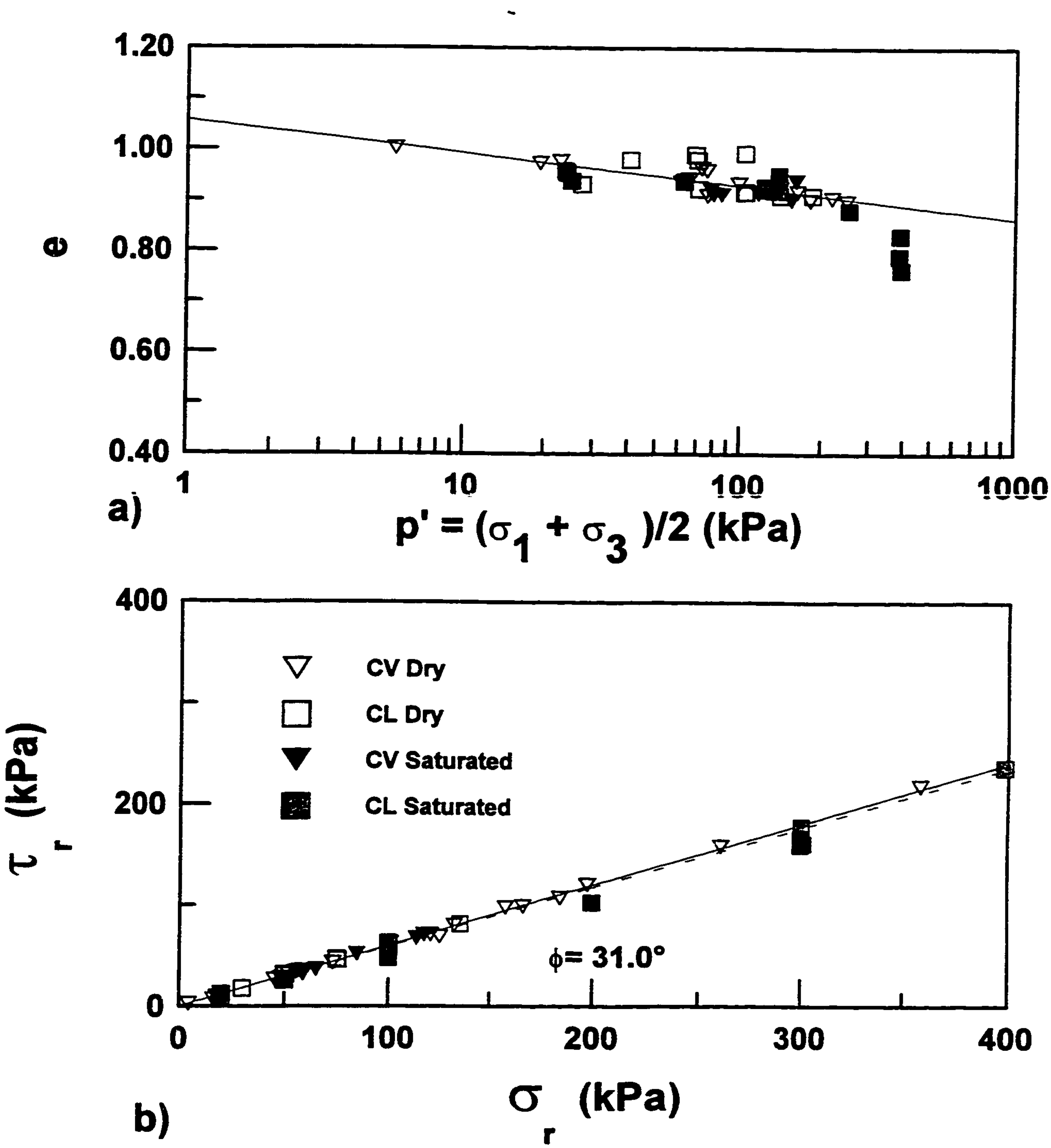

Fig. 6.2 Effect of saturation on ring shear tests of Unimin sand 2010.

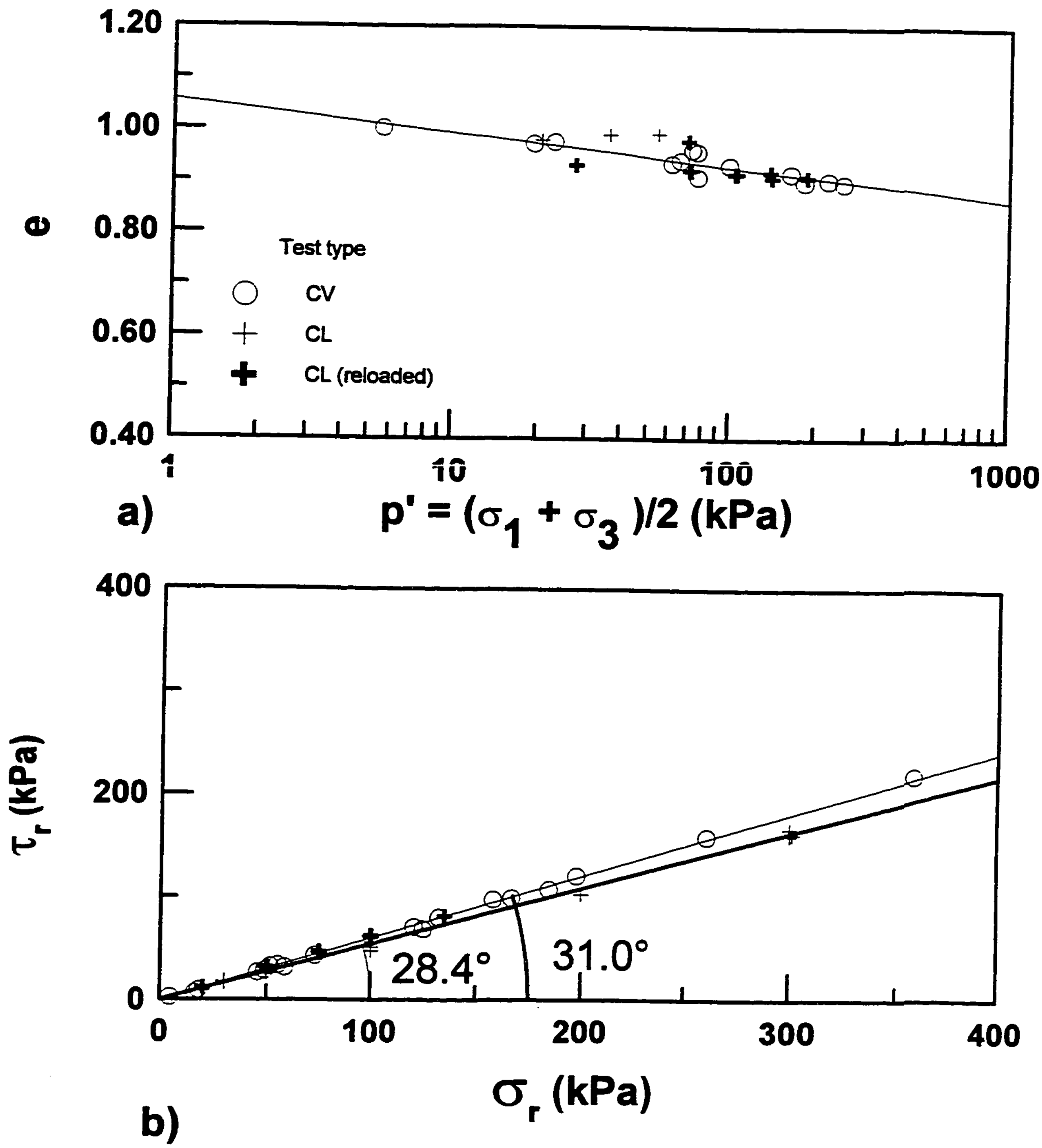

Fig. 6.3 Comparison of constant load and constant volume tests on Unimin sand 2010.

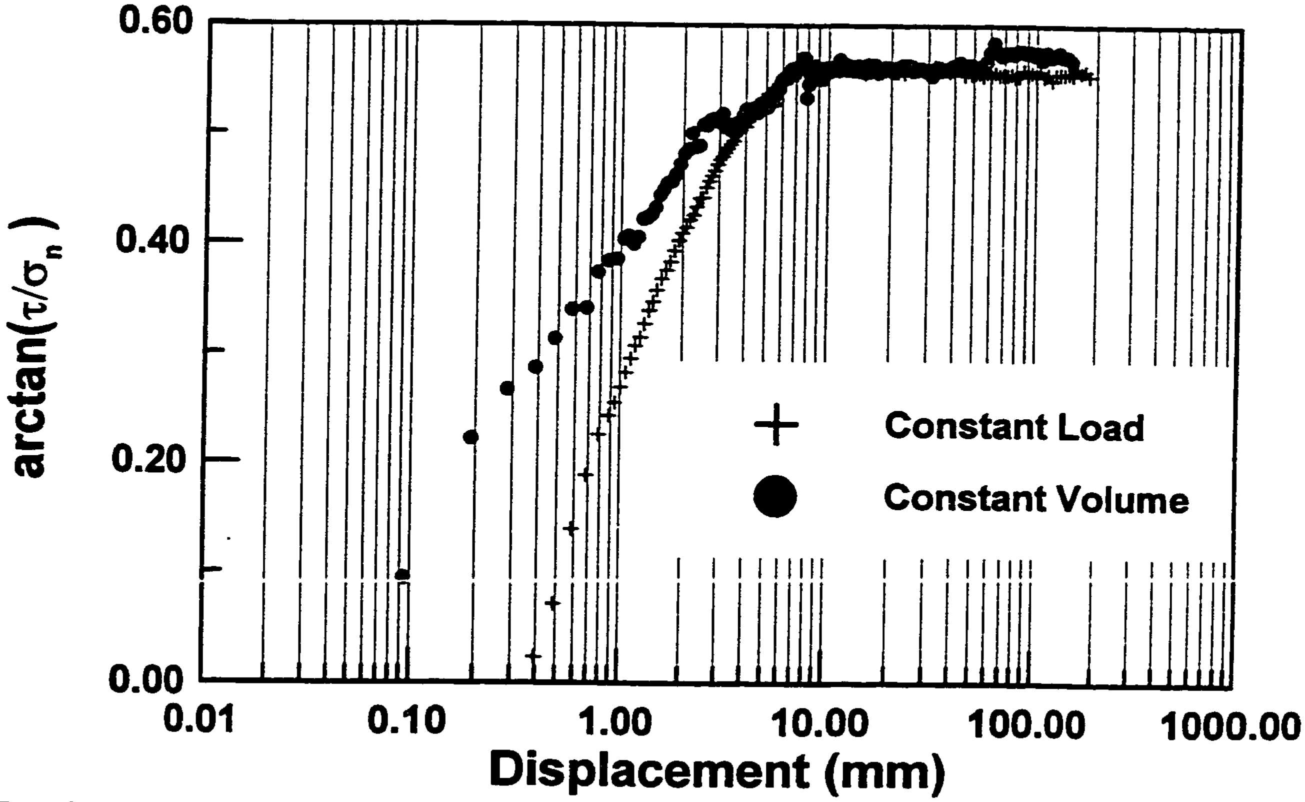

Fig. 6.4 arctan(τ/σ_n) versus log of displacement, showing the initiation of steady state at 9 mm displacement.

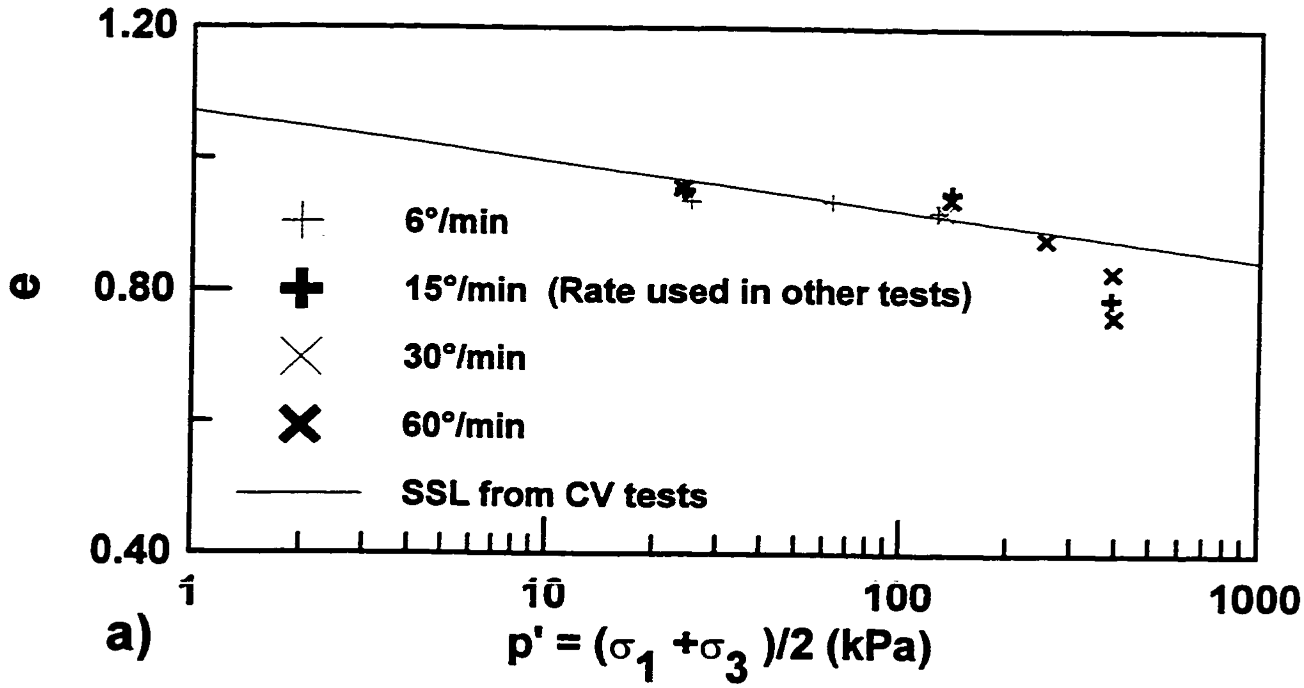

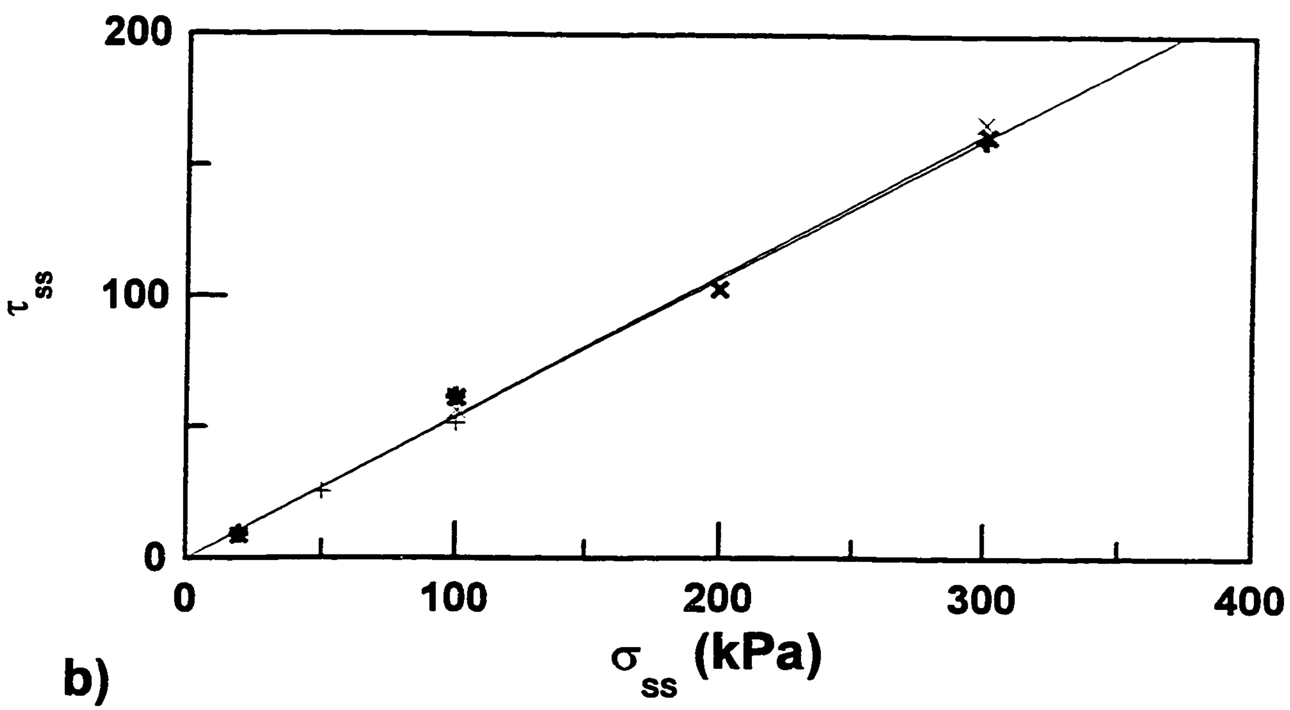

Fig. 6.5 Effect of the variation of the rate of shear on the steady state line and the strength envelope of Unimin san 2010.

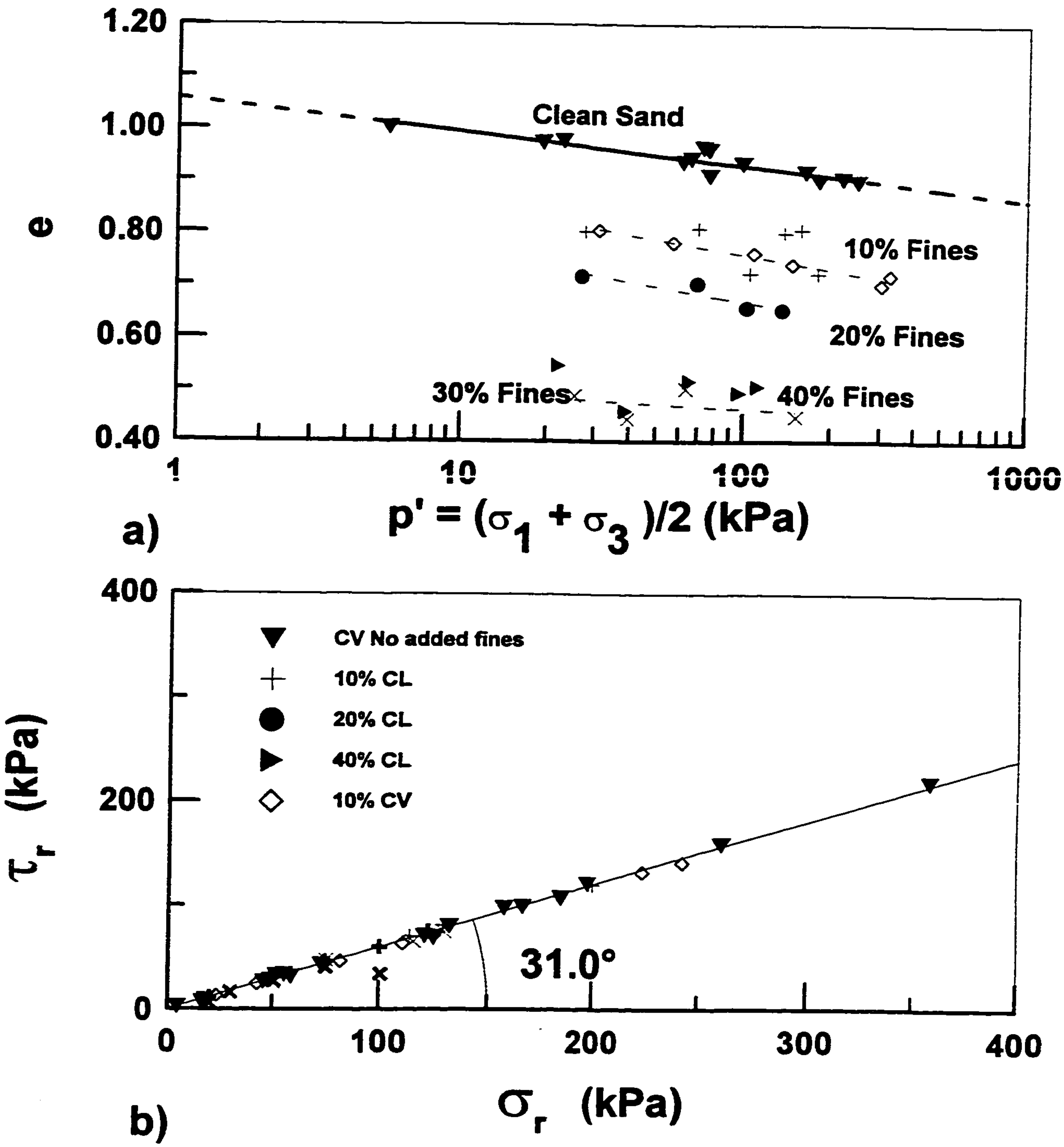

Fig. 6.6 Results of ring shear tests on specimens of Unimin sand 2010 with various fines contents.

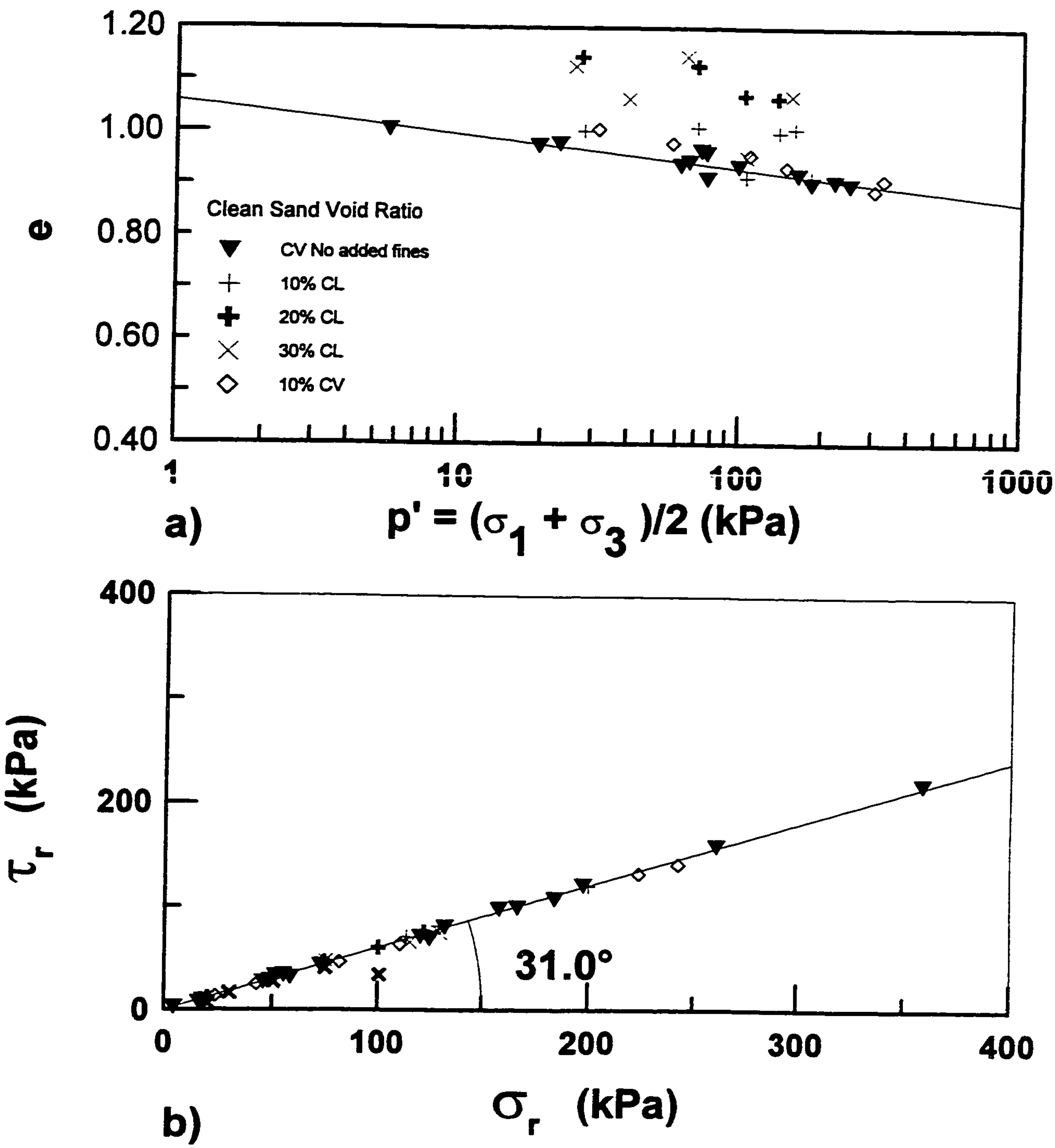

Fig. 6.7 Void ratio corrected for fines content.

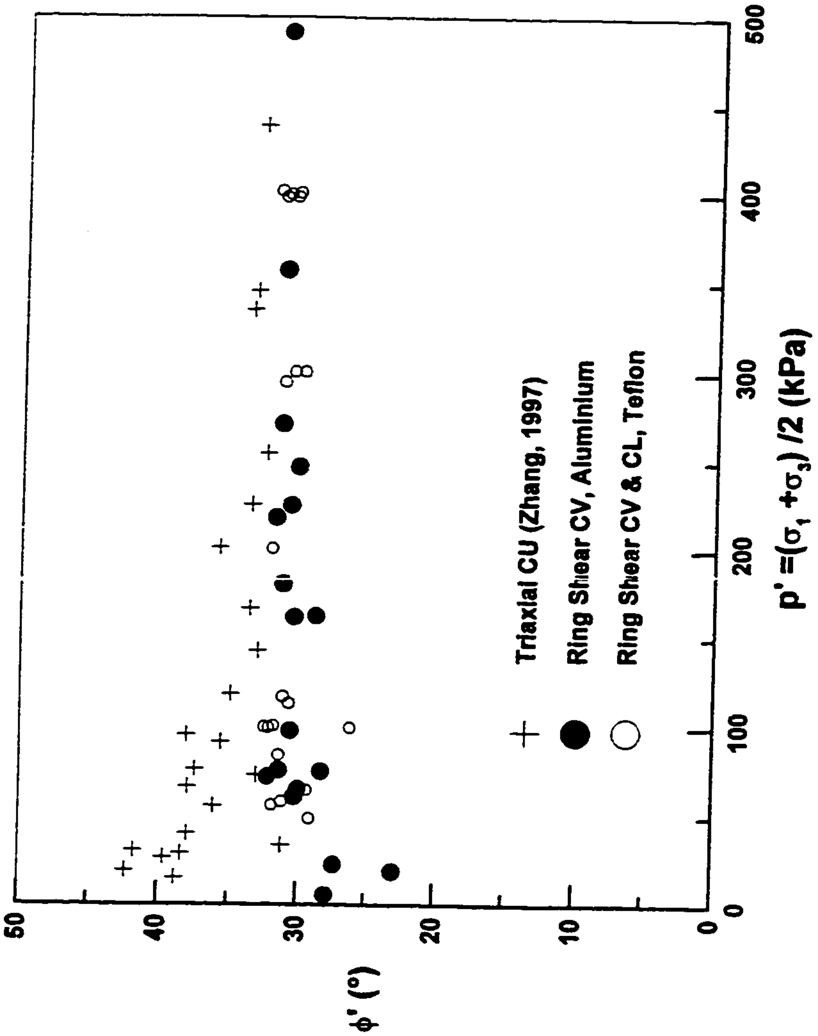

Fig. 6.8 Friction angle variation with normal stress: Triaxial CU tests and Ring Shear CV & CL tests.

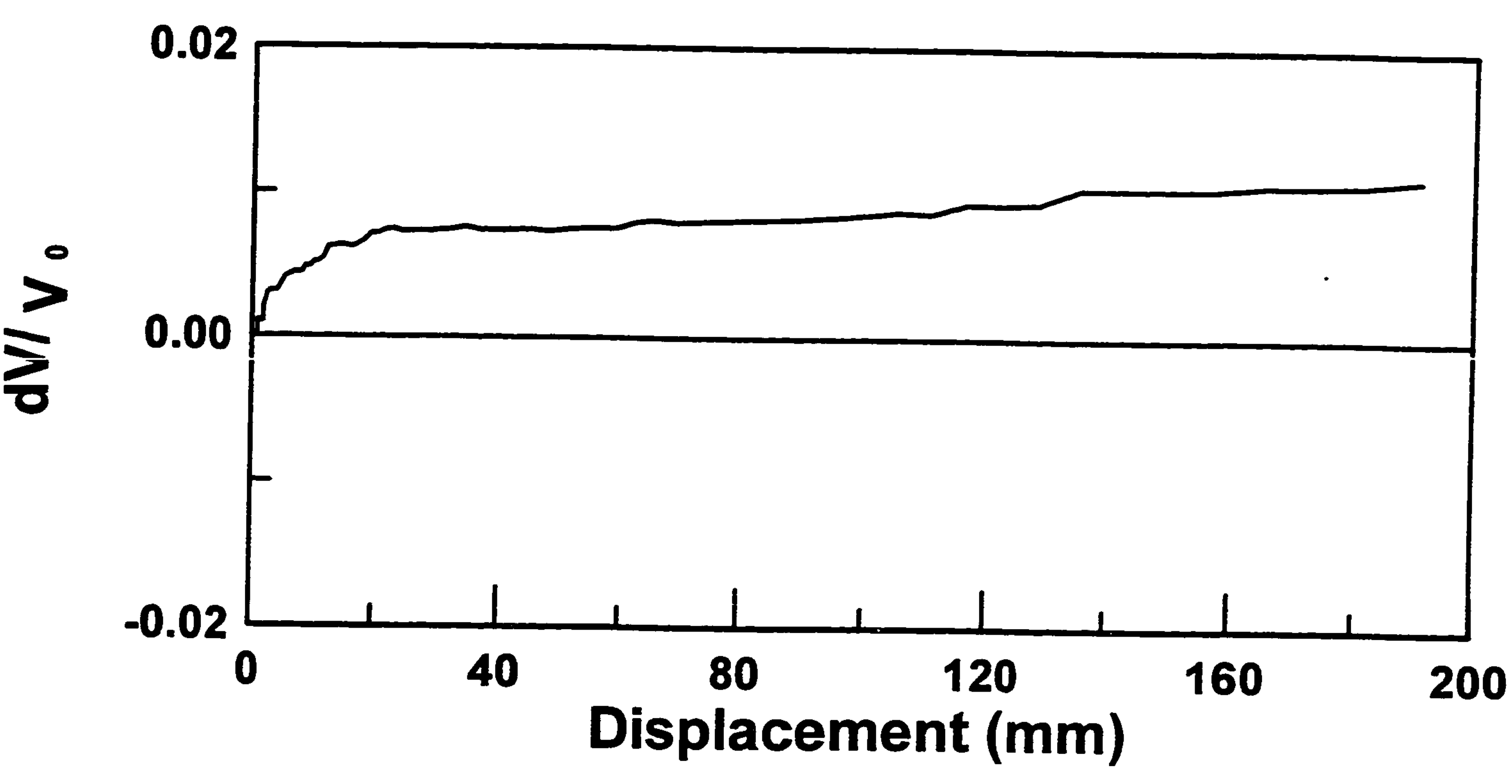

Fig. 6.9 Volumetric strain curve of a sample "constant volume" test with an unusually low friction angle

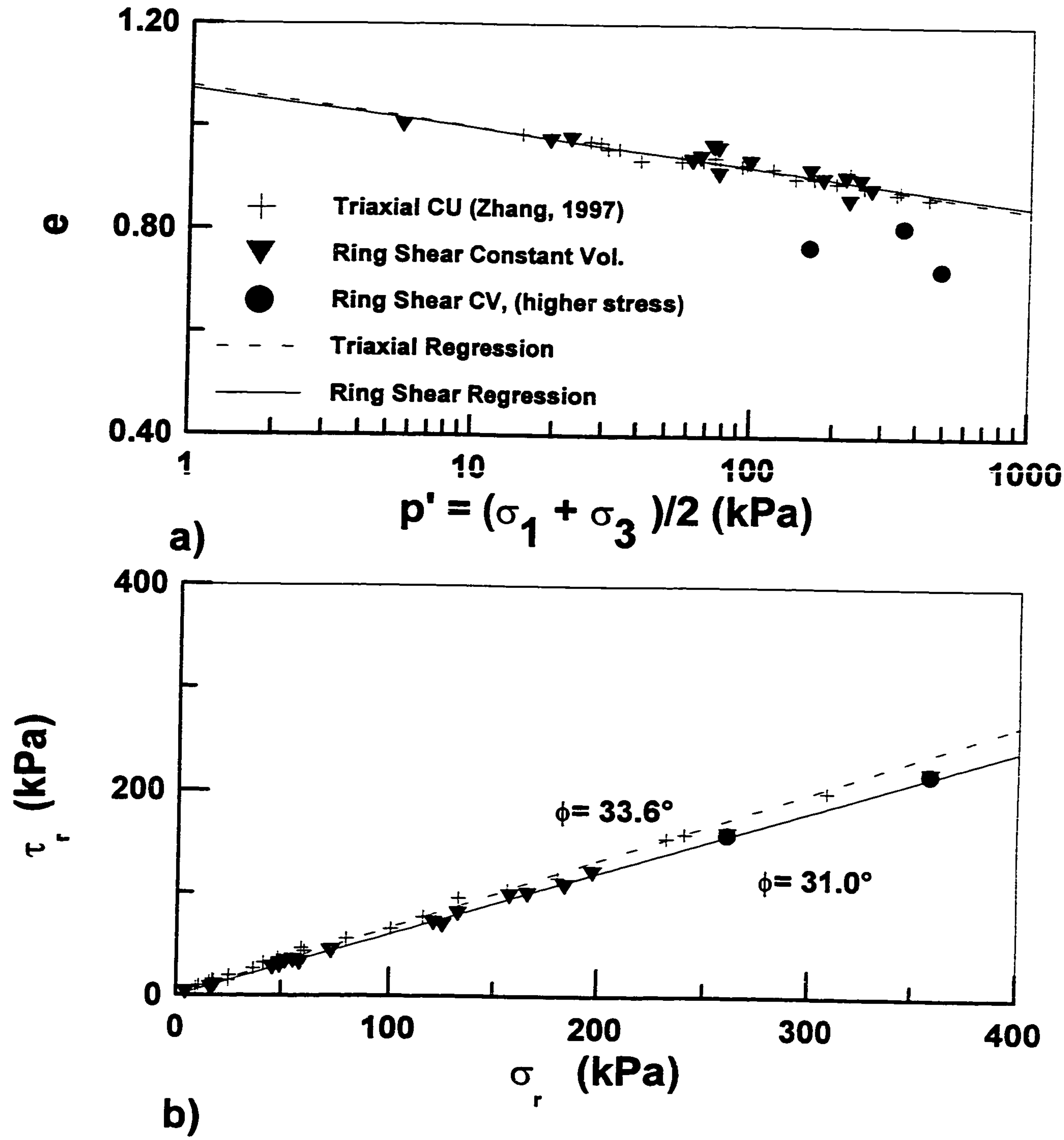

Fig. 6.10 Comparison of CV tests with triaxial CU tests (Zhang, 1997)

7 CONCLUSIONS

From the results of the tests performed, the following conclusions may be made concerning the Unimin quartz sand 2010, specifically:

1) The presence of water does not affect the constant volume strength results obtained from the ring shear test.

2) The low rates of shear used in this research do not affect the constant load residual shear strength of saturated samples.

3) Both the constant volume and the constant load tests result in the same steady state line

4) In contrast to the constant load tests, constant volume tests do not appear to promote normal load transfer to the confining rings.

5) The presence of greater amounts of fine particles affects the void ratio but does not seem to affect the post-liquefaction strength.

6) The steady state line of Unimin sand obtained in ring shear constant volume, and constant load, tests are similar to those obtained in the triaxial tests. The friction angle obtained from ring shear tests is 2.6° lower

7) The post-liquefaction friction angle obtained in the ring shear test is constant over a large rage of normal stresses, while the triaxial test results show an increase in friction angle at low confining pressures. Some indication that the friction angle may actually be reduced in the ring shear test at very low confining pressures needs to be verified since the system was

unable to maintain the original void ratio for the loosest samples, which indicates the existence of a systematic hardware problem at very low confining pressures.

7.1 Suggestions for further research

Further research on the following topics related to the ring shear device is suggested:

1) The development of a constant volume device which would allow testing to be performed effectively at low confining pressures.

2) Detailed study of the void ratio distribution throughout the sample after shear. This would involve recovering the sample without disturbing it for the purpose of calculating its void ratio, and particle distribution.

3) Development of tools to measure the normal load transfer to the confining rings.

4) Development of an undrained ring shear cell to compare the shear strengths at steady state, and the testing stress paths, to those of the constant volume ring shear cell.

5) A study of the effect of the modification of the fines content of the same mineral composition as the skeleton material, on the constant-volume residual strength. The types of granular materials should be varied in composition and particle angularity to show how the breakdown of such particles changes the frictional characteristics of the resulting material.

Alarcon-Guzman, A., Leonards, G.A. and Chameau, J.L. (1988), "Undrained Monotonic and Cyclic Strength of Sand". *J. Geotechnical Engineering* , ASCE, **114**(10): 1089-1109.

Arulmoli, K., Arulanandan, K., and Seed, H. B. (1985), "New Method for Evaluating Liquefaction Potential", *J. of Geotechnical Engineering,* ASCE , **111**(1): 95-114.

ASTM (1993b), D 4253-91, "Standard Test Method for Minimum Index Density and Unit Weight of Soils Calculation of Relative Density", ASTM Standards, Vol. 04.08, Soil and Rock; Dimension Stone; Geosynthetics, pp:674-681

ASTM (1993a), D 4253-93, "Standard Test Method for Maximum Index Density and Unit Weight of Soils Using a Vibratory Table", ASTM Standards, Vol. 04.08, Soil and rock; dimension stone; geosynthetics, pp:661-673

Barden, L. & Proctor, D.C. (1971), "The Drained Strength of Granular Material", *Canadian Geotechnical J.* **8**: 372-383

Baziar, M. H. and Dobry, R. (1995), "Residual strength and large deformation potential of loose sitly sands". *J. Geotechnical Engineering,* ASCE, **121**(12): 896-906

Been, K., Jefferies, M.G. and Hachey, J. (1991), "The critical state of sands.", *Géotechnique,* **41**(3):365-381

Been, K. & Jefferies, M. G. (1985), "A state parameter for sands", *Géotechnique* **35** (2): 99-112

Bishop, A.W., Webb, D.L. and Skinner, A.E., (1965), "Triaxial Testss on Soil at Elevated Cell Pressures". Proc. 6th Int. Conf. Soil. Mech., Montréal, vol. 1, pp. 170-174

Bishop, a.W., Green, g.e., Garga, v.K., Andresen, A. & Brown, J.D. (1971). "A New Ring Shear Apparatus", *Géotechnique*, **21**(4): 273-328

Blight, G.E. (1965),"Shear Stress and Pore Pressure in Triaxial Testing" , *J. of the Soil Mechanics and Foundations Division*, ASCE, **91**(6)

Bridgwater, J. (1972), "Stress-Velocity Relationships for Particulate Solids", ASME Paper No. 72-MH-21, New York.

Bromhead, E. N. (1979), " A Simple Ring Shear Apparatus", *Ground Engineering*, **12**(5):40-44

Bromhead, E.N. (1986), "The Stability of Slopes", Surrey University Press, Chapman and Hall, New York, USA

Casagrande, A. (1975), "Liquefaction and cyclic deformation of sands: a critical review". Presented at Fifth Pan-American Conference on Soil Mechanics and Fondation Engineering, November 1975, Buenos Aires, Argentina.

Casagrande, a. (1976), "Liquefaction and Cyclic Deformation of Sands -- A Critical Review", Harvard soil Mechanics Series, No. 88, Harvard University, Cambridge, Mass, USA.

Casagrande, A. (1936), "Characteristics of cohesionless soils affecting the stability of earth fills", Contributions to Soil Mechanics, 1925-1940.: 257-276, Boston Society of Civil Engineers, 1940 (originally published in the Journal of Boston Society of Civil Engineers, 1936)

Casagrande, A. (1971), "On Liquefaction Phenomena: A Lecture to the ENCOLD and the British Geotechnical Society," (Reported by P. a. Green and P. A. s. Ferguson), *Géotechnique*, **21**(3),

Casagrande, A. (1938), "the shearing resistance of soils and its relation to the stability of the earth dams.", Proc. Soils and Foundation Confere ce of th U.S. Engineer Department.

Castro, G. (1997),"Post-Liquefaction shear Strength from case Histories", NSF Workshop: Post-Liquefaction Shear Strength of Granular Soils Workshop, April 17, Urbana Illinois, USA, pp. 61-66

Castro, A. (1969), "Liquefaction of sands." Ph.D. thesis, Harvard University, Cambridge, Mass., USA.

Castro, G., Poulos, S.J., France, J.W. and Enos, J.L. (1982), "Liquefaction Induced by Cyclic Loading", Report to National Science Foundation, Washington, D.C.

Castro, G. and Poulos, S.J. (1977), "Factors Affecting Liquefaction and Cyclic Mobility", *J. Geotechnical Engineering*, ASCE, **103**(6):501-516

de Alba, P. (1997), "Post Liquefaction Shear Strength From Laboratory and Field Tests: Issures and Questions." NSF Workshop: Post-Liquefaction Shear Strength of Granular Soils Workshop, April 17, Urbana Illinois, USA, pp. 102-105

de Alba, P., Seed, H.B. & Chan, C.K. (1976),"Sand Liquefaction in Large-Scale Simple Shear Tests", *J. of the Geotechnical Engineering Division*, ASCE, **102**(9)

Dyvik, R., Berre, T., Lacasse, S. & Raadim, B. (1987), "Comparison of Truly Undrained and Constant Volume Direct Simple Shear Tests", *Géotechnique*, **37** (1): 3-10

Finn, W.D.L., (1990), "Analysis of post-liquefaction deformations in soil structures." H. Bolton Seed, Vol.2, Memorial Symposium Proceedings, May 1990, Editor J. Michael Duncan, Vancouver, B.C., Canada

Finn, W.D.L. (1998), "Seismic Safety of Embankment Dams: Developments in Research and Practice 1988-1998", *Geotechnical Earthquake Engineering and Soil Dynamics III* **2**, ASCE, 812-853

Finn, W.D.L., Pickering, D. J., Bransby P. L. (1971), "Sand Liquefaction in Triaxial and Simple Shear Tests", *J. of the Soil Mechanics and Foundations Division*, **97** (4):639-659

Frost, J.D. & Kuo, C.-Y. (1996), "Automated Determination of the distribution of Local Void Ratio from Digital Images", *Geotechnical Testing J.*, GTJODJ, **19**(2), 107-117

Frost, D.J., and Ashmawy, A.K.(1997), "Post-Liquefaction Strength - the Role of Soil Structure", NSF Workshop: Post-Liquefaction Shear Strength of Granular Soils Workshop, April 17, Urbana Illinois, USA, pp.69-74

Gan, J.K.M., Fredlund, D.G. & Rahardjo, H. (1988), "Determination of the Shear Strength Parameters of an Unsaturated Soil Using the Direct Shear Test", *Can. Geotech. J.* **25**: 500-510

Garga, V.K. Zhang, H. (1997), "Volume Changes in Undrained Triaxial Tests on Sands", *Canadian Geotechnical J.*, **34**(5):762-772

Hanzawa, H. (1980), "Undrained Strength and Stability Analysis for a Quick Sand", *Soils and Foundations*, JSSMFE, **20** (2): 18-29

Harris, W. W., Viggiani, G., Mooney, M. A. & Finno, R. J. (1995), "Use of Stereophotogrammetry to Analyze the Development of Shear Bands in Sand",

Hazen, A. (1920), "Hydraulic fill dams." ASCE Transaction, **83**: 1713-1745.

Hight, D. W., Gens, A., & Symes, M. J. (1983), "The Development of a New Hollow Cylinder Apparatus for Investigating the Effects of Principal Stress Rotation in Soils", *Géotechnique*, **33** (4): 355-383

Hungr, O. & Morgenstern, N.R. (1984), "High Velocity Ring Shear Tests on Sand", *Géotechnique* **34**(3): 415-421

Hvorslev, M.J. (1939), "Torsion Shear Tests and their Place in the Determination of the Shearing Resistance of soils.", ASTM, **39**:999-1022.

Hyodo, M. Tanimizu, H., Yasufuku, N. and Murata, H. (1994), *Soils and Foundations*, JSSMFE, **34** (1): 19-32

Ibrahim, A.A. & Kagawa, T. (1991), "Microscopic Measurement of Sand Fabric From Cyclic Tests Causing Liquefaction" *Geotechnical Testing J.*, GTJODJ, **14** (4): 371-382

Ishibashi, I., Jenkins, J. T., Choi, J. W., Parker, C. L. (1996), "The Influence of Boundaries on the Volumetric Behaviour of Solid and Hollow Cylindrical Specimens of Glass Beads", *Soils and Foundations*, JGS, **36** (2):45-55

Ishihara, K. (1993), "Liquefaction and flow failure during earthquake.", *Géotechnique*, **43**(3):351-415.

Ishihara, K., Tatsuoka, F. and Yasuda, S. (1975), "Undrained deformation and liquefaction of sand under cyclic stresses.", *Soils and Foundations*, **15**(1): 29-44.

Ishihara, K. (1994), "Evaluation of Residual Strength of Sandy Soils" *XIII ICSMFE*, New Delhi, India

Jefferies, M. (1997), "NSF Workshop on Post-Liquefaction Shear Strength of Granular Soils",NSF Workshop: Post-Liquefaction Shear Strength of Granular Soils Workshop, April 17, Urbana Illinois, USA, pp. 81-84

Kramer S.L. (1997), "Post-Liquefaction Shear Strength of Granular Soils: Pre-Workshop Written Statement", NSF Workshop: Post-Liquefaction Shear Strength of Granular Soils Workshop, April 17, Urbana Illinois, USA, pp. 93-101

Kramer, S. L. and Seed, B. S. (1988), "Initiation of Soil Liquefaction Under Static Loading Conditions", *J. of Geotechnical Engineering*, **114** (4)

Kramer, Steven L. (1989), "Uncertainty in Steady-State Liquefaction Evaluation Procedures", *J. of Geotechnical Engineering*, ASCE, **115**(10)

Kuerbis, R. and Vaid, Y.P. (1988), "Sand Sample Preparation -- The Slurry Deposition Method", *Soils and Foundations*, JSSMFE, **28** (4): 107-118

Ladd, R.S. (1974), "Specimen preparation and liquefaction of sands.", *J. Geotechnical Engineering*, ASCE, **100**(10):1180-1184.

Ladd, R.S. (1974): "Specimen Preparation and Liquefaction of Sands", ASCE, **100**(10): 1180-1184

Lade, P. V., Yamamuro, Jerry A. (1993), "Stability of granular Materials in Postpeak Softening Regime", *J. of Engineering Mechanics* **119**(1), 128-144

Lambe, T. William, & Marr, W. Allen (1979), "Stress Path Method: Second Edition", *J. of the Geotechnical Engineering Division*, **105**(6):727-738

Lindenberg, J. & Koning, H. I. (1981), "Critical density of Sand", *Géotechnique* **31** (2): 231-245

Martin, G.R. (1997), "Post Liquefaction Shear Strength from Laboratory and Field Tests" NSF Workshop: Post-Liquefaction Shear Strength of Granular Soils Workshop, April 17, Urbana Illinois, USA, pp. 46-60

Mesri, G. (1997),"Undrained Shear Strength of Liquefied Sands: Pre-Workshop statement", NSF Workshop: Post-Liquefaction Shear Strength of Granular Soils Workshop, April 17, Urbana Illinois, USA, pp.110-121

Miura, S. & Toki, S. (1982), "A Sample Preparation Method and its Effect on Static and Cyclic Deformation-Strength Properties of Sand", *Soils and Foundations*, JSSMFE, **22** (1): 61-77

Mulilis, J. P., Townsend, F.C. and Horz, R. C. (1978), "Triaxial Testing Techniques and Sand Liquefaction", *Dynamic Geotechnical Testing, ASTM STP 654:* 265-279

Negussey, D. and Islam, M.S. (1994), "Uniqueness of steady state and lieuqfaction potential." *Canadian Geotechnical J.*, **31**: 132-139.

Negussey, D., Wijewickreme, w.K.D. and vaid, Y.P. (1988), "Volume Changes During Drained Triaxial Tests on Granular Materials." *Geotechnique*, 7:17-34

Oda, M., Koishikawa, I. and Higuchi, T. (1978), "Experimental study of anisotropic shear strength of sand by plane strain test.", Soils and Foundations, **18**(1): 25-38.

Olson, S.M. (1997), "Discussion Group: Post-Liquefaction Shear Strength from Laboratory and Field Tests: Field Tests" NSF Workshop: Post-Liquefaction Shear Strength of Granular Soils Workshop, April 17, Urbana Illinois, USA, pp. 122-146

Olson, Scott M., and Stark, Timothy D. (1998), "CPT Based Liquefaction Resistance of Sandy Soils", *Geotechnical Earthquake Engineering and Soil Dynamics III*, ASCE, **1**: 325-336

Peck, R. B (1978), *J. of the Geotechnical Engineering Division*, ASCE, **105**(3):393-398

Pitman, T.D., Robertson, P.K and Sego, D.C., (1994), "Influence of Fines on the Collapse of Loose Sands", *Canadian Geotechnical J.*,**31**: 728-739

Poorooshasb, H. B. (1989), "Description of Flow of Sand Using State Parameters", *Computers and Geotechnics* **8**: 195-218

Poulos S.J. (1997), "Comments on Laboratory Determination of Undrained Steady State Shear Strength", NSF Workshop: Post-Liquefaction Shear Strength of Granular Soils Workshop, April 17, Urbana Illinois, USA, pp. 147-153

Poulos, S.J., Castro, G. and France, J.W. (1985), "Liquefaction evaluation procedure." *J. Geotechnical Engineering*, ASCE, **111**(6):772-792

Poulos, S.J. (1981), "The steady state of deformation.", *J. Geotechnical Engineering*, ASCE, **107**(5):553-562

Prakash, S., Guo, T. & Kumar, S. (1998), "Liquefaction of Silts and Sit-Clay Mixtures", *Geotechnical Earthquake Engineering and Soil Dynamics III*, ASCE, **1**: 337-348

Riemer, M. F., Seed, R.B., Nicholson, P.G., and Jong, H.L. (1990), *J. of Geotechnical Engineering*, **116** (2):332-337

Riemer, M. F., Seed, R. B. (1997), "Factors Affecting Apparent Position of Steady-State Line", *J. of Geotechnical and Geoenvironmental Engineering* **123** (3): 281-288

Riemer, M.F. (1997), "Discussion Group on Laboratory and Field Testing", NSF Workshop: Post-Liquefaction Shear Strength of Granular Soils Workshop, April 17, Urbana Illinois, USA, pp. 154-163

Robertson, P.K. (1994), "Design Considerations for Liquefaction", XIII ICSMFE, New Delhi, India.

Roscoe, K.H. and Burland, J.B. (1968), "On the generalized stress-strain behaviour of wet clay.", Proc. Conference on Engineering Plasticity, Cambridge.

Roscoe, K.H., Schofield, A.N. and Wroth, C.P. (1958), "On the yielding of soils",*Géotechnique*, **8**(1): 22-53

Sasitharan, S., Robertson, P.K., Sego, D.C. & Morgenstern, N.R. (1993), "Collapse behaviour of sand", *Can. Geotech. J.* **30**, 569-577

Sasitharan, S., Robertson, P.K., Sego, D.C. and Morgenstern, N.R. (1994), "State-Boundary Surface For Very Loose Sand and its Practical Implications", *Canadian Geotechnical J.*, **31**, 321-334

Seed, H. B., Tokimatsu, K., Harder, L. F., and Chung, R. M. (1985). "The Influence of SPT Procedures in Soil Liquefaction Resistance Evaluations", *J. of Geotechnical Engineering*, ASCE, **111**(12): 1425-1445.

Seed, H.B. (1979), "Soil liquefaction and cyclic mobility evaluation for level ground during earthquake.", *J. Geotechnical Engineering*, ASCE, **105**(2):201-255

Seed, H.B. (1987), "Design Problems in Soil Liquefaction", *J. of Geotechnical Engineering*, ASCE, **113**(7):827-845

Seed, H.B., Lee, K.L. (1967), "Undrained Strength Characteristics of Cohesionless Soils", *J. of the Soil Mechanics and Foundations Division*, ASCE, **93** (6): 333-360.

Sladen, J.A., D'Hollander, R.D. and Krahn, J. (1985), "The liquefaction of sands, a collapse surface approach.", *Canadian Geotechnical J.*, **24**:462-466

Stark, T.D, and Mesri, G. (1992), "Undrained Shear Strength of Liquefied Sands for Stability Analysis", *J. of Geotechnical Engineering Division*, ASCE, **118**(11): 1727-1747

Stark, T. D., Olson, Scot M., Kramer, S.L., and Youd, T. L. (1998), "Shear Strength of Liquefied Soil", *Geotechnical Earthquake Engineering and Soil Dynamics III*, ASCE, **1**:313-324

Tatsuoka, F., Ochi, K., Fujii, s. and Okamoto, M. (1986), "Cyclic Undrained Triaxial and Torsional Shear Strength of Sands for Different sample Preparation Methods", *Soils and Foundations*, **26**(3):23-41

Taylor, D.W. (1948), Fundamentals of Soil Mechanics, Chapter 14. John Wiley and Sons, Inc, New York

Terzaghi, K. and Peck, R.B. (1948), Soil Mechanics in Engineering Practice. 2nd edition, p.108, Chichester: Wiley

Thevanayagam, S., and Mohan, S. (1998), "Intergranular Void Ratio-Steady State Strength Relations for Silty Sands", *Geotechnical Earthquake Engineering and Soil Dynamics III* **1**, 349-360

Troncoso, J.H., (1990), "Failure risks of abandoned tailings dams," Proceedings, International Symposium on safety and Rehabilitation of tailings dams, ICOLD, Sydney, Australia, May, pp. 82-89.

Vaid, Y.P. and Chern, J.C. (1985), "Cyclic and monotonic undrained response of saturated sands", Advances in the art of testing soils under cyclic conditions, ASCE, Annual Convention, Detroit, Mich., pp. 120-147

Vaid, Y.P. & Negussey, Dawit (1984), "Technical Note: Relative Density of Pluviated Sand Samples", *Soils and Foundations* **24**(2):101-105, Japanese Society of Soil Mechanics and Foundation Engineering

Vaid, Y. P. and Negussey, D. (1988), "Preparation of Reconstituted Sand Specimens", *Advanced Triaxial Testing of Soil and Rock, 405-417, ASTM STP 977*, Robert T.

Donaghe, Ronald C. Chaney, and Marshall L. Silver, Eds., American society for Testing and Materials, Philadelphia.

Vardoulakis, I. (1996), "Deformation of water-saturated sand: I. uniform undrained deformation and shear banding" *Géotechnique* **46**(3), 441-456

Vardoulakis, I. (1996), "Deformation of water-saturated sand: II. effect of pore water flow and shear banding" *Géotechnique* **46**(3), 441-456

Wroth, C.P. (1987), "The behaviour of normally consolidated clay as observed in undrained direct shear tests", *Géotechnique* **37** (1), 37-43

Yan, L., Sasitharan, S., Lum, K.Y., and Ahlfield, K.O. (1988), "Laboratory Assessment of Residual Strength of Gravely Fill of an Earth Dam", *Geotechnical Earthquake Engineering and Soil Dynamics III, ASCE,* **2**: 974-985

Yoshimi, Y. & Goto, S. (1996), "Liquefaction resistance of silty sand based on in situ frozen samples", *Géotechnique* **46** (1), 153-156

Zhang, H. (1997), "Steady State Behaviour of Sands and Limitations of the Triaxial Test", Ph. D. Thesis, University of Ottawa, Ottawa, Ontario, Canada

Zhang, H. Garga, V.K.(1997), "Quasi-steady state: A real behaviour?", *Canadian Geotechnical J.*, **34** (5):749-761

APPENDIX I

PLOTS OF RING SHEAR TESTS

APPENDIX I

TEST: CVD-01

e_o : 0.983
σ_{vo} : 3 kPa

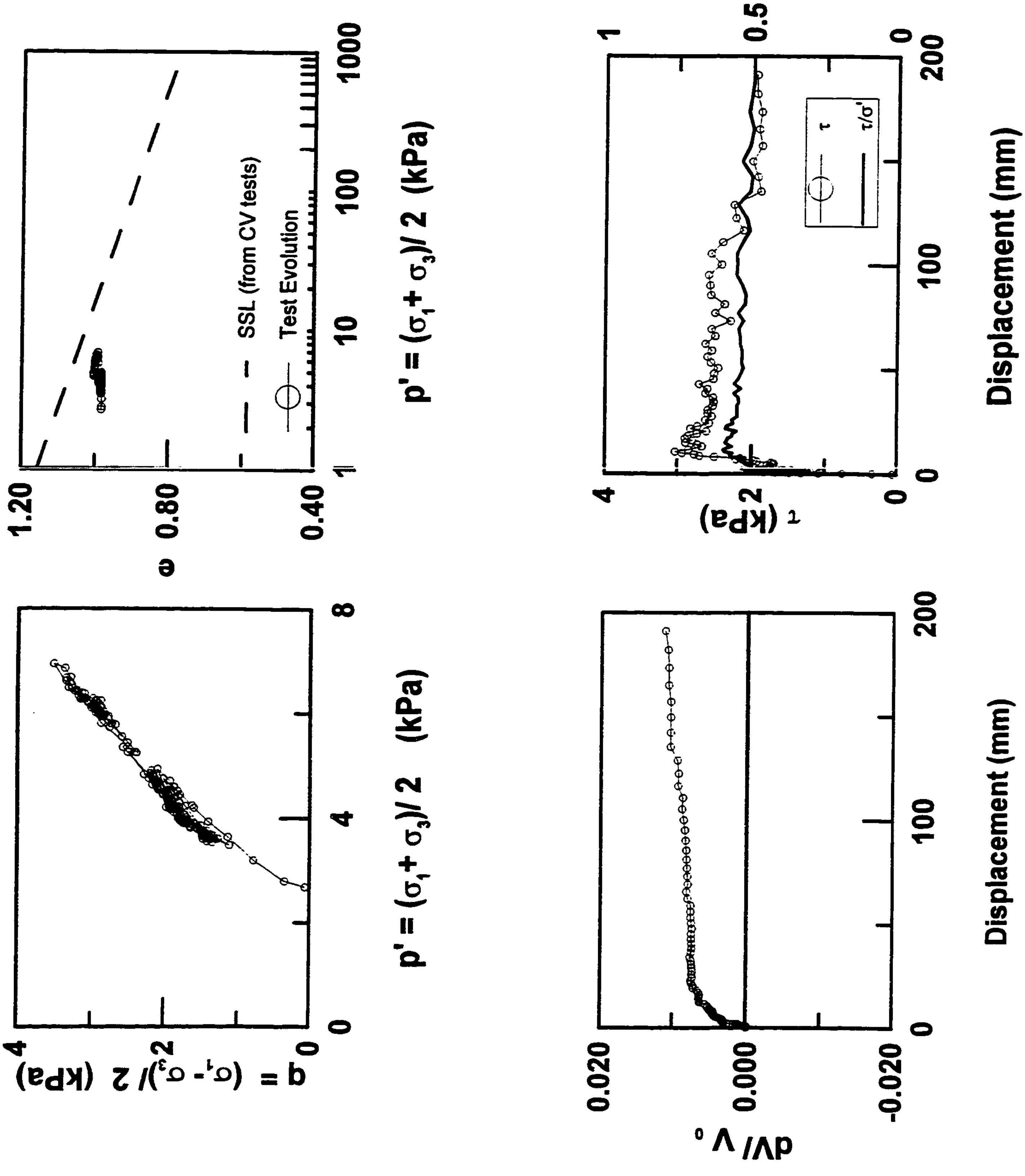

APPENDIX I

TEST: CVD-02

e_o : 0.974
σ_{vo} : 25 kPa

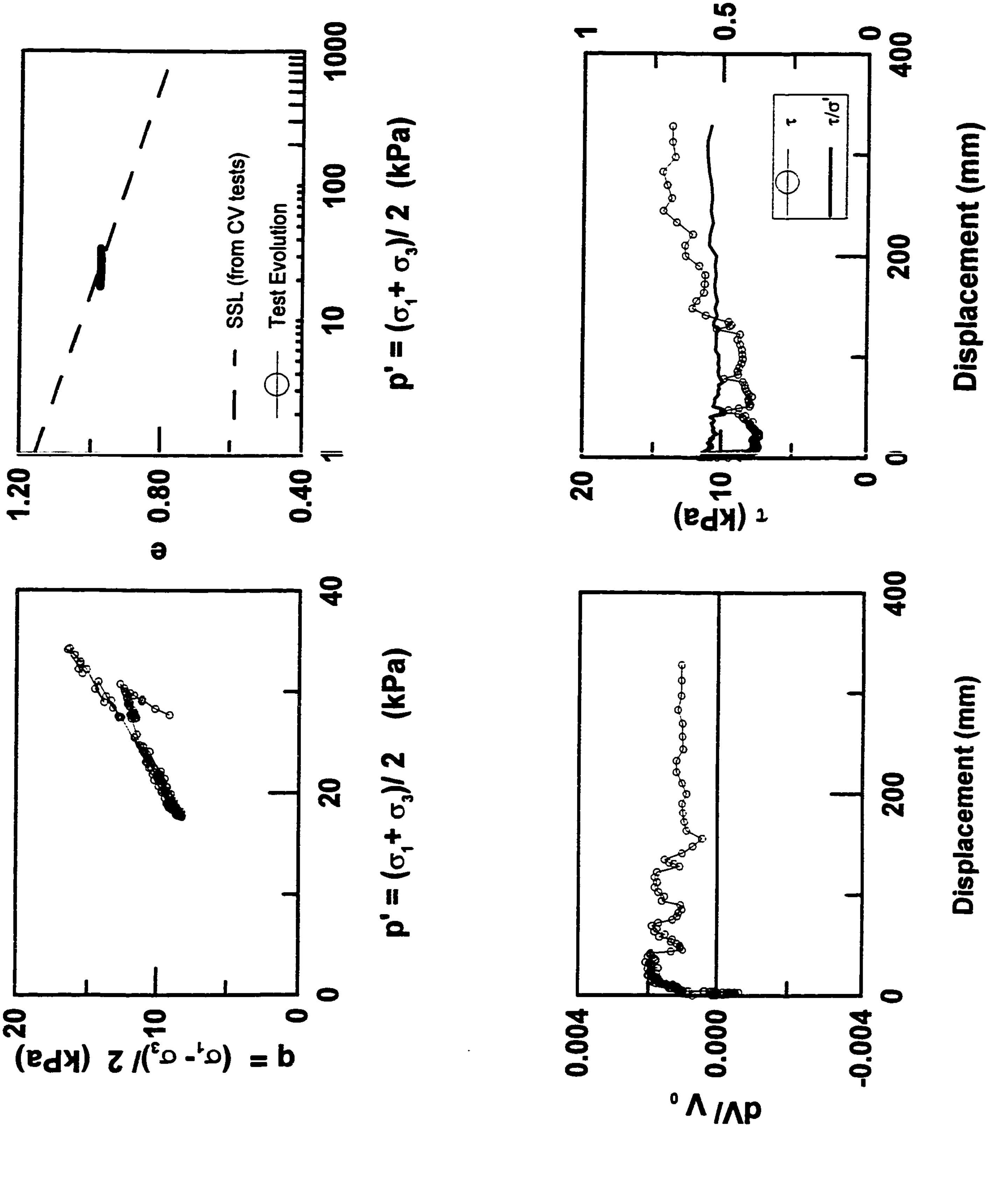

APPENDIX I

TEST: CVD-08

e_o : 0.971
$\sigma_{vo}{}^{o}$: 133 kPa

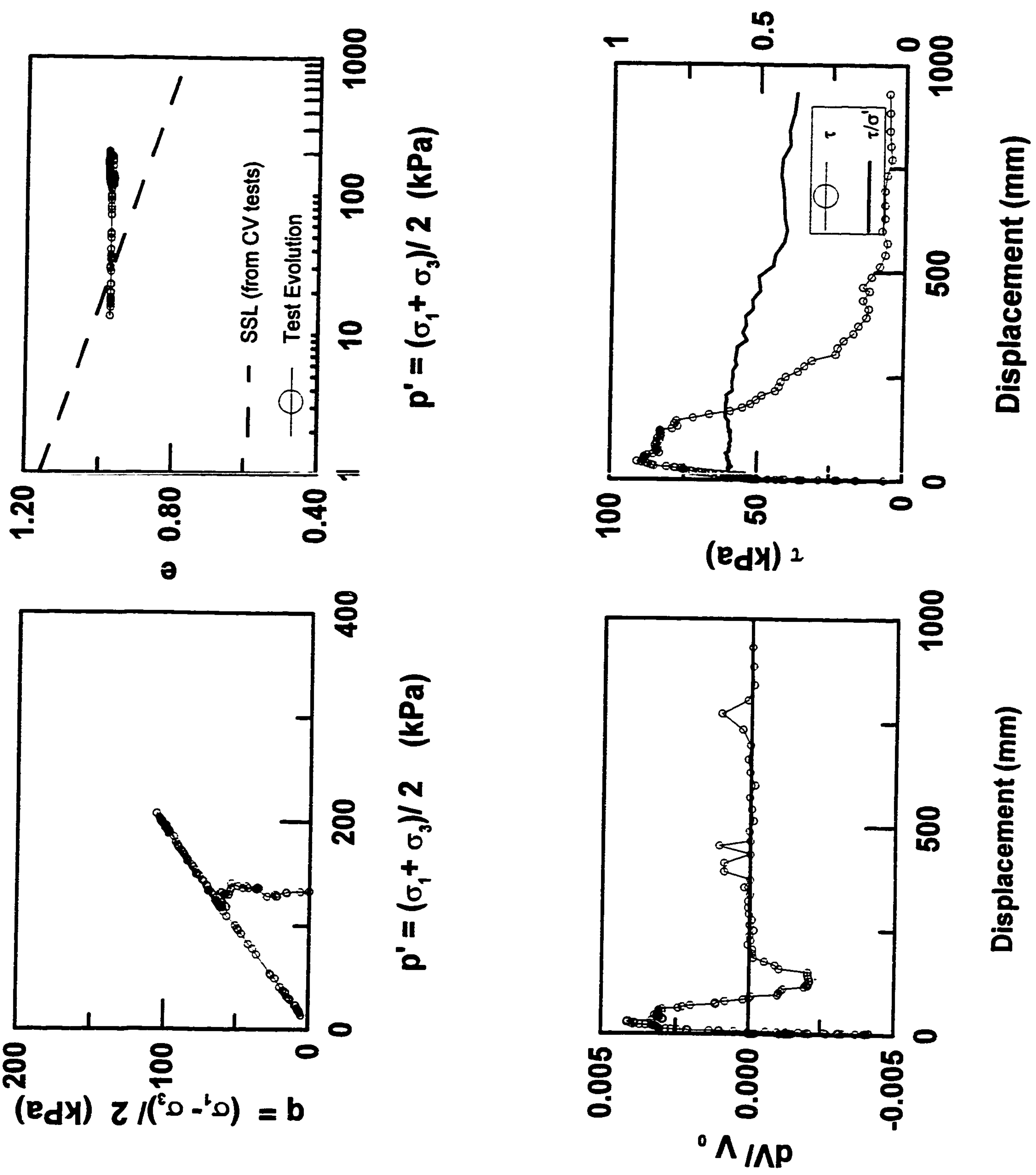

APPENDIX I

TEST: CVD-03

e_o : 0.958
σ_{vo}': 143 kPa

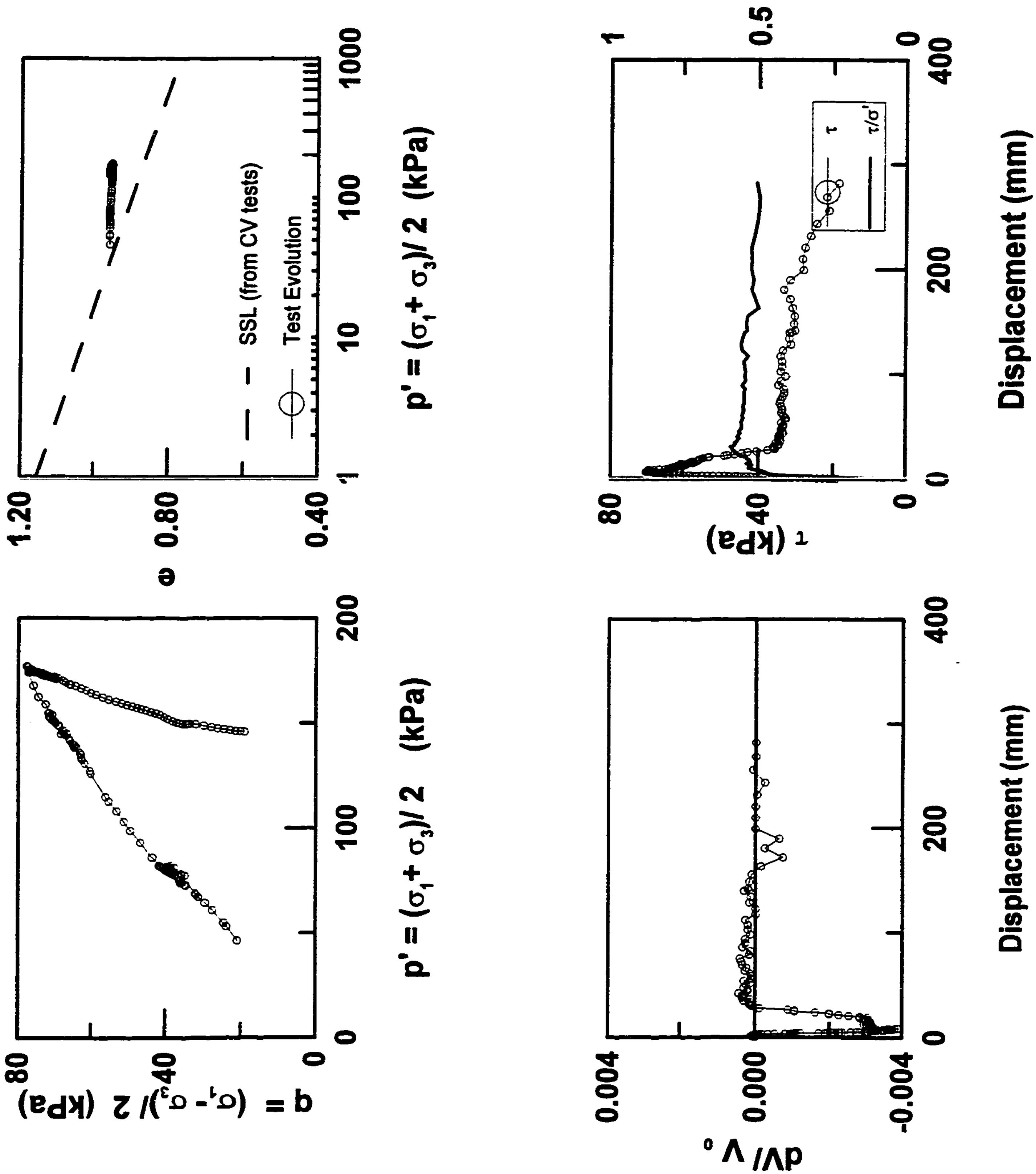

APPENDIX I

TEST: CVD-05

e_o : 0.909
σ'_{vo}: 113 kPa

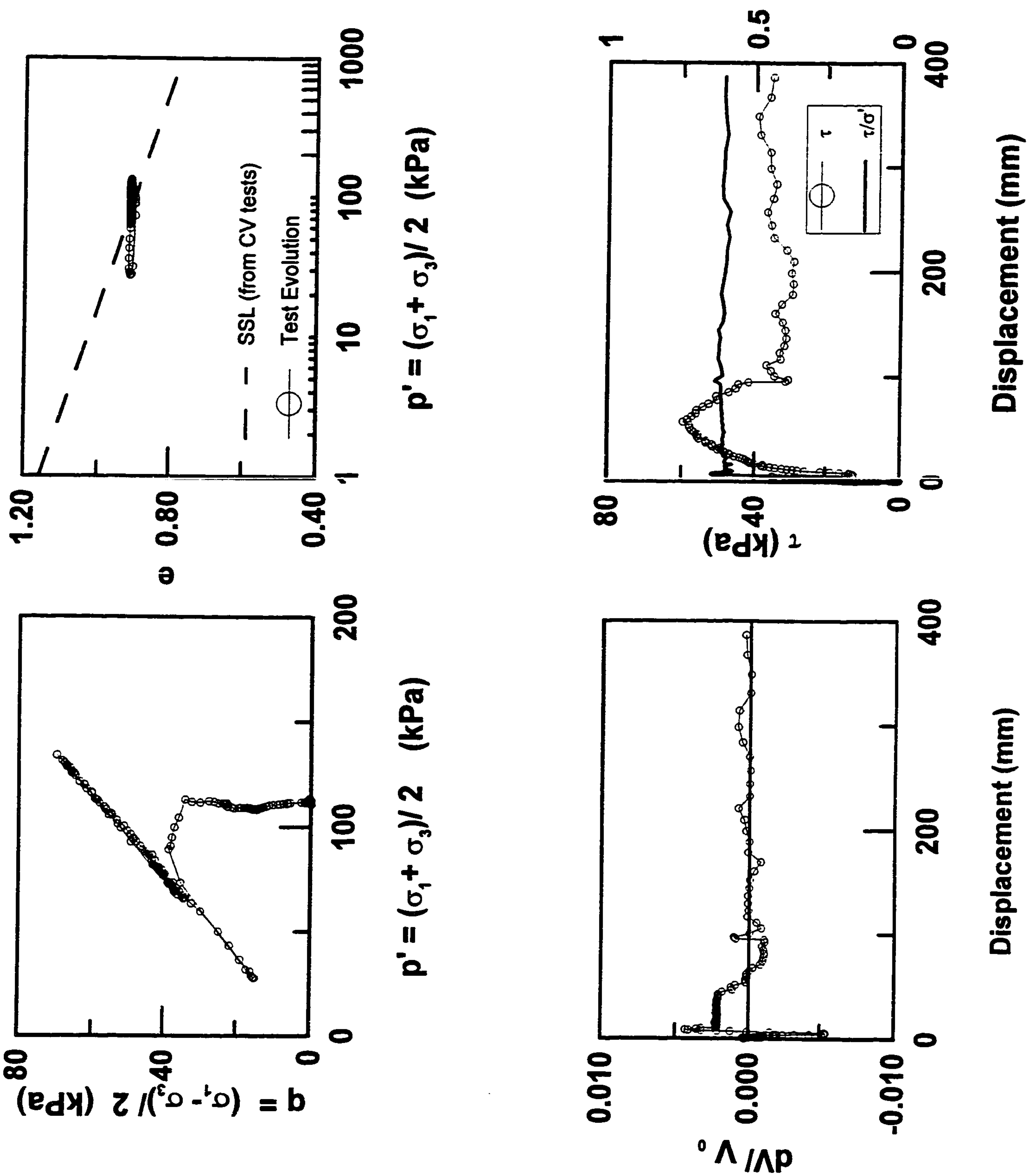

APPENDIX I

TEST: CVD-10

e_o : 0.916
σ_{vo}' : 196 kPa

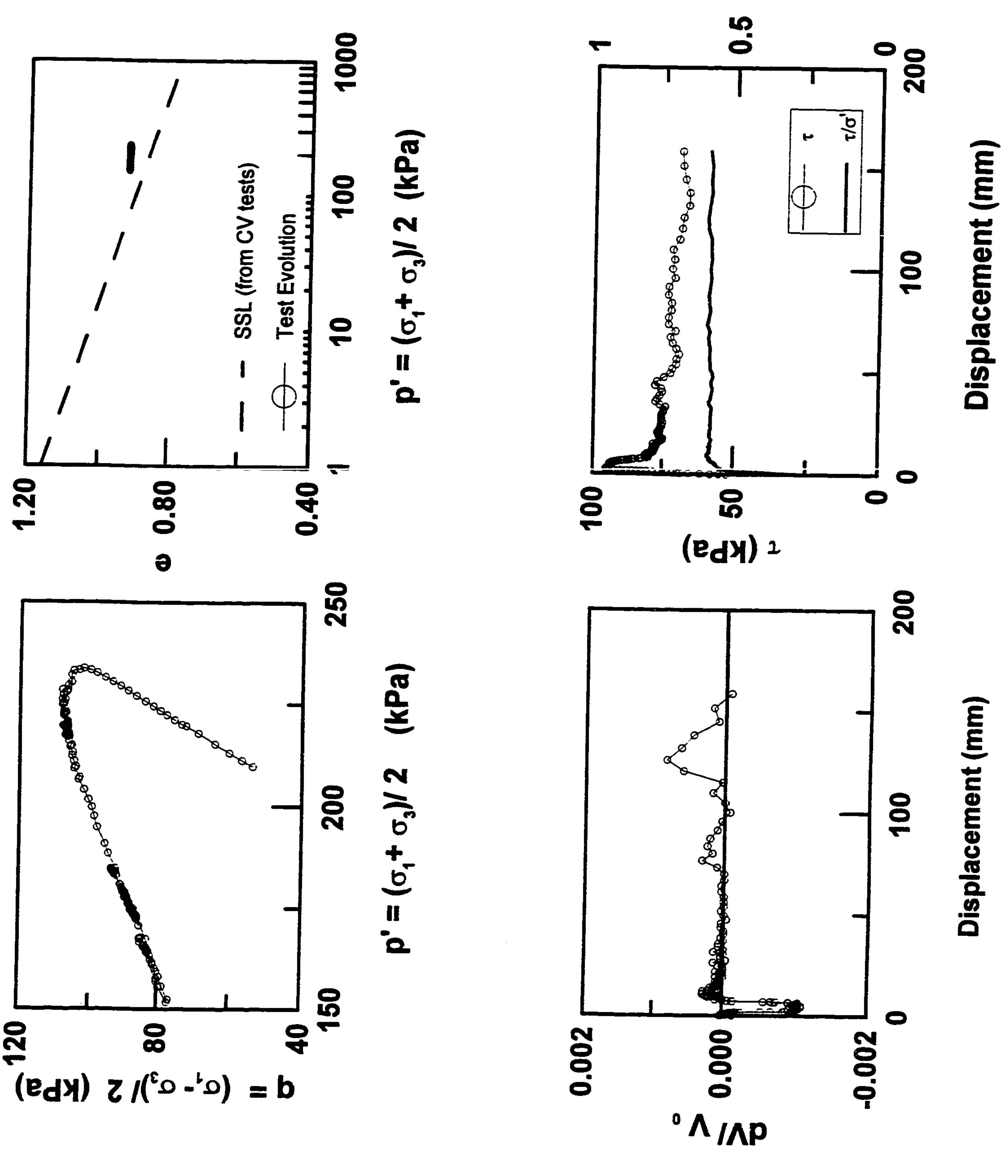

APPENDIX I

TEST: CVD-13

e_o : 0.897
σ_{vo}' : 344 kPa

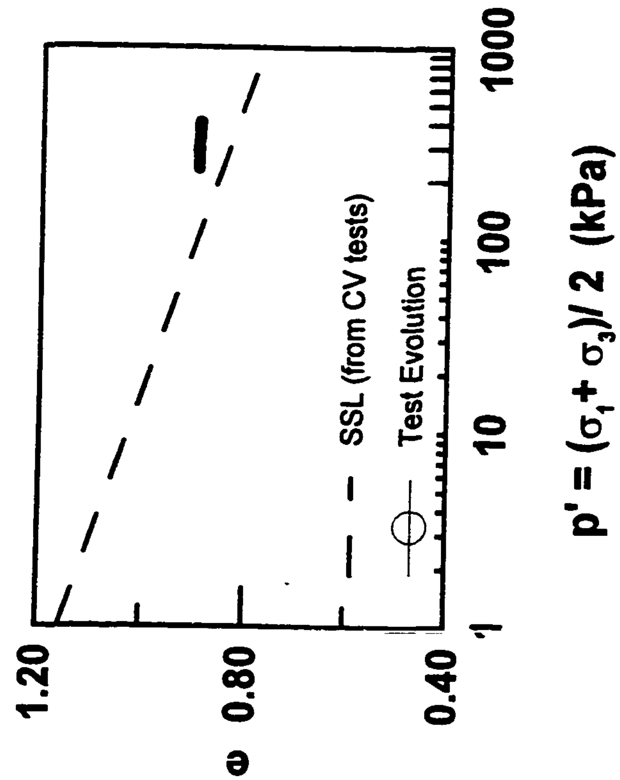

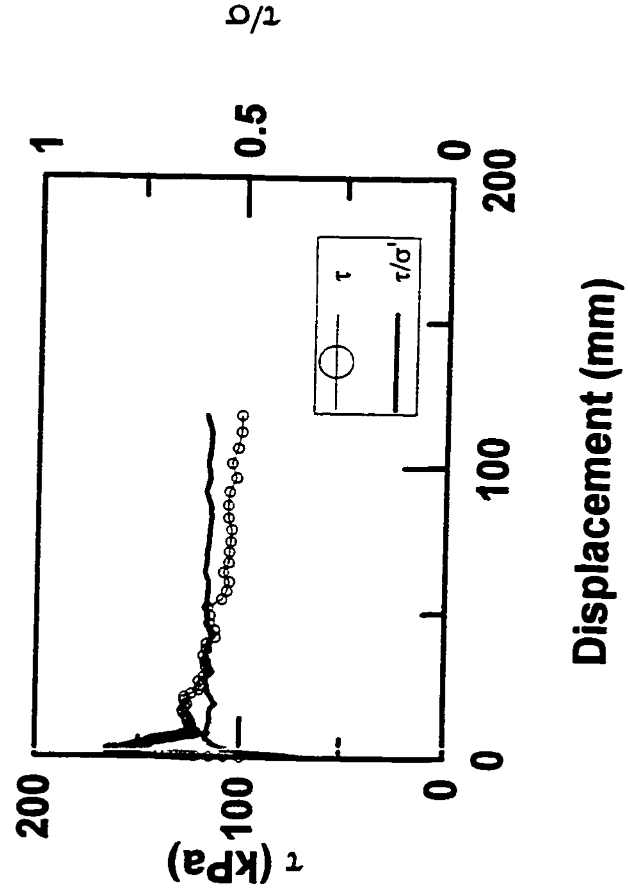

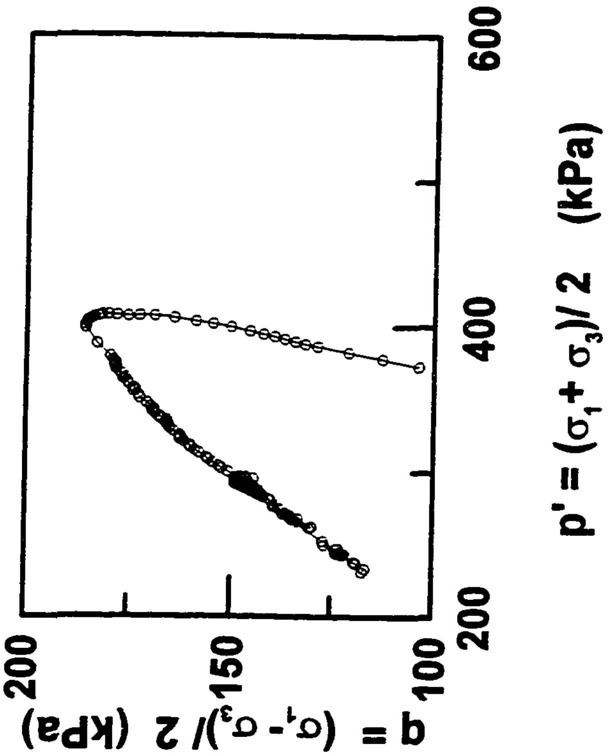

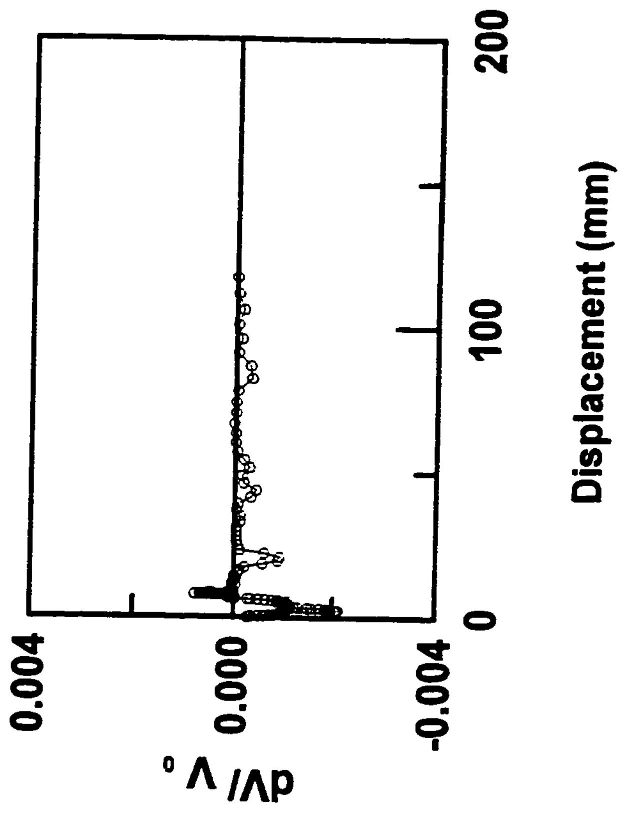

APPENDIX I

TEST: CVD-14

e_o : 0.809
σ_{vo}': 515 kPa

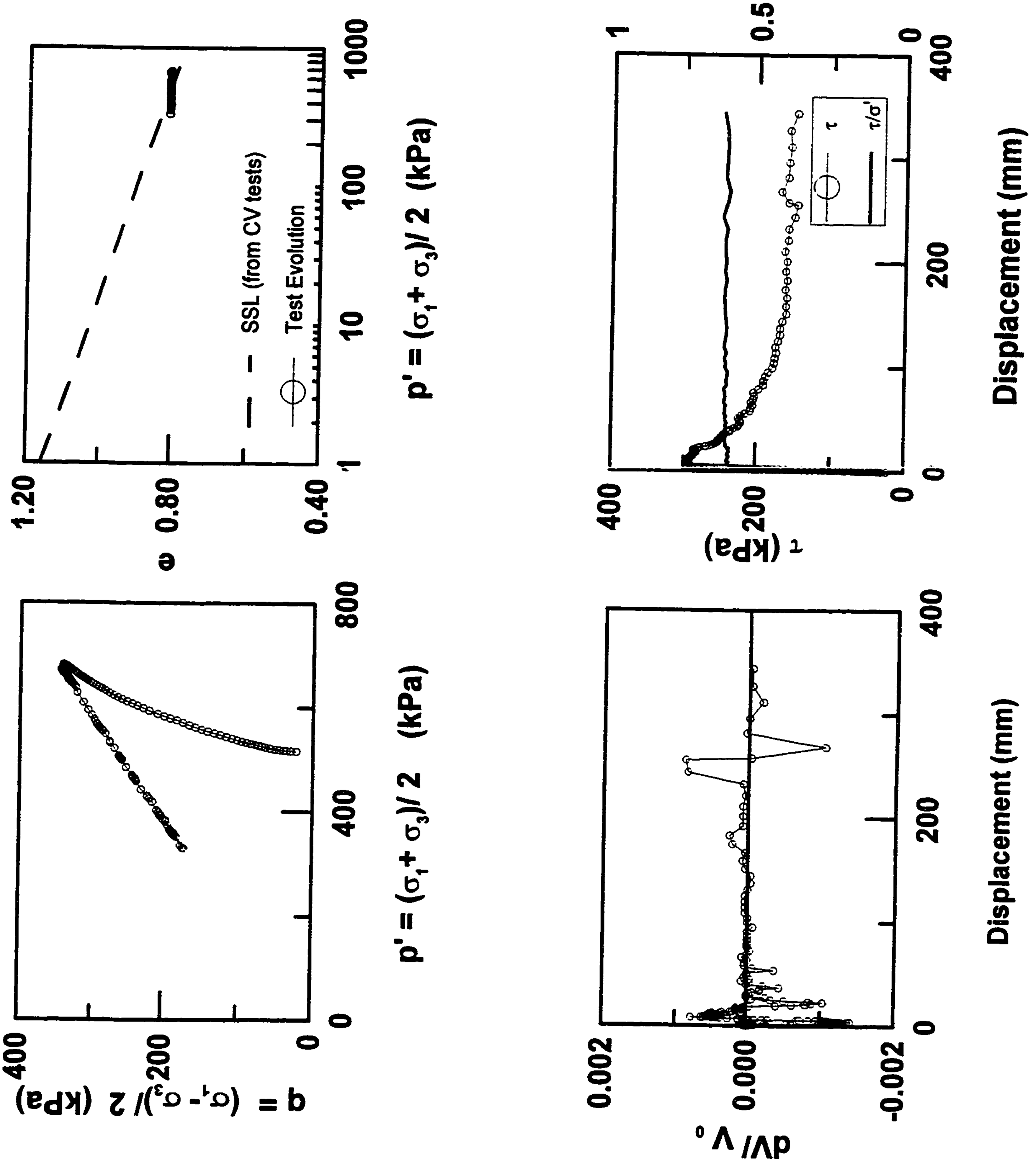

APPENDIX I

TEST: CVD-17

e_o : 0.881
σ_{vo}^{o}: 385 kPa

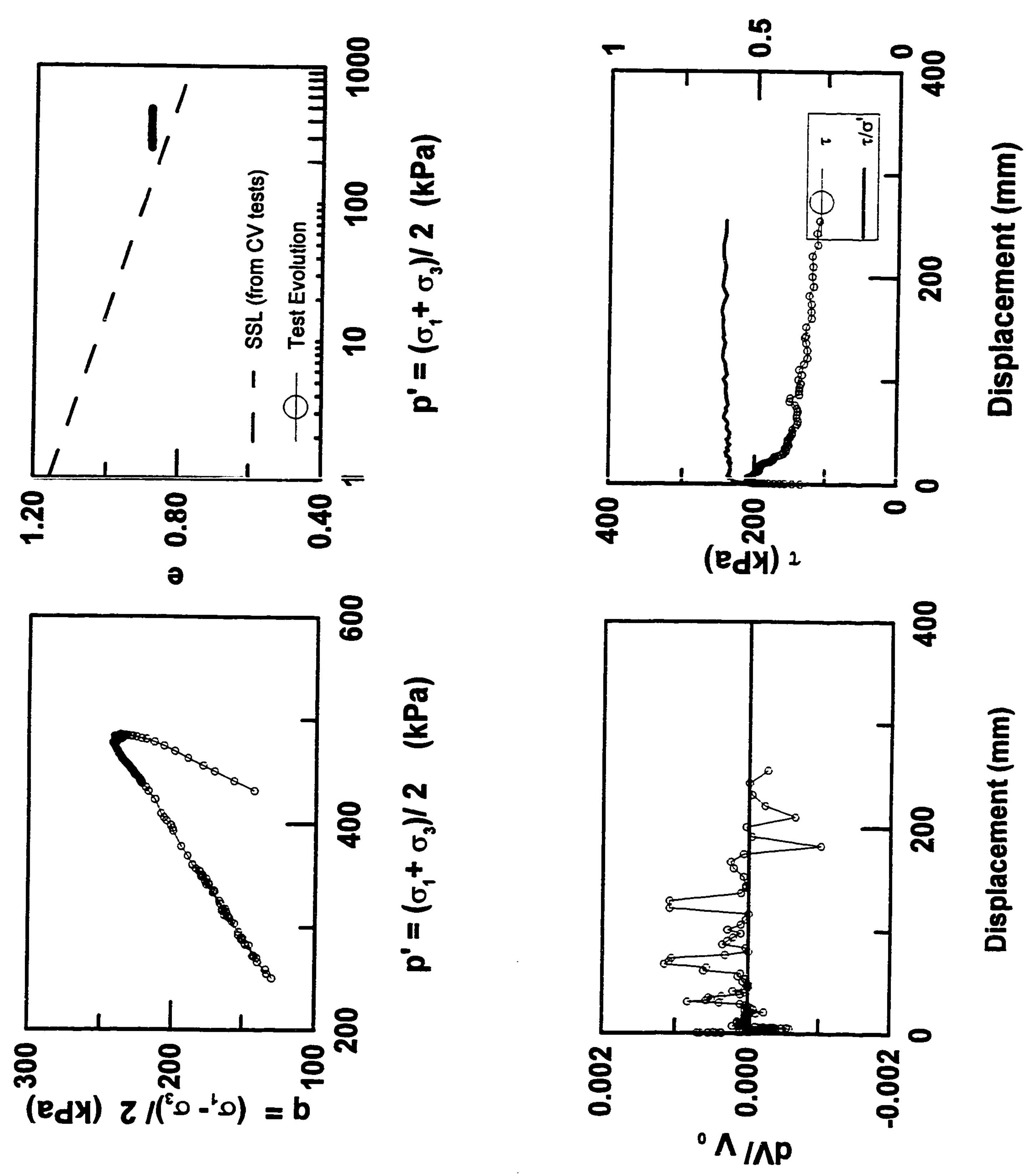

APPENDIX I

TEST: CLD-01

e_o : 0.941
σ_{vo} : 49 kPa

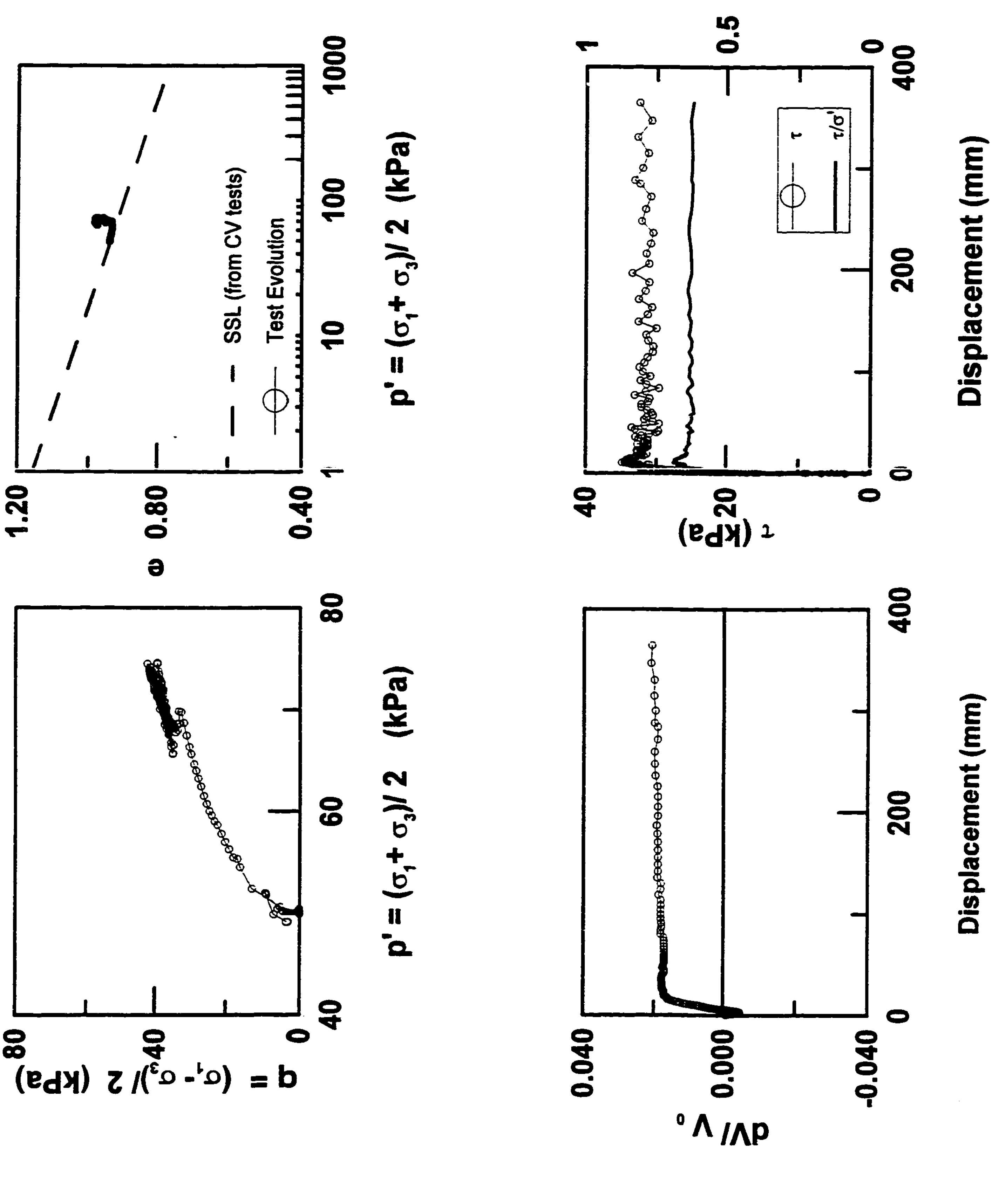

APPENDIX I

TEST: CLD-04

e_o : 0.913
σ_{vo} : 136 kPa

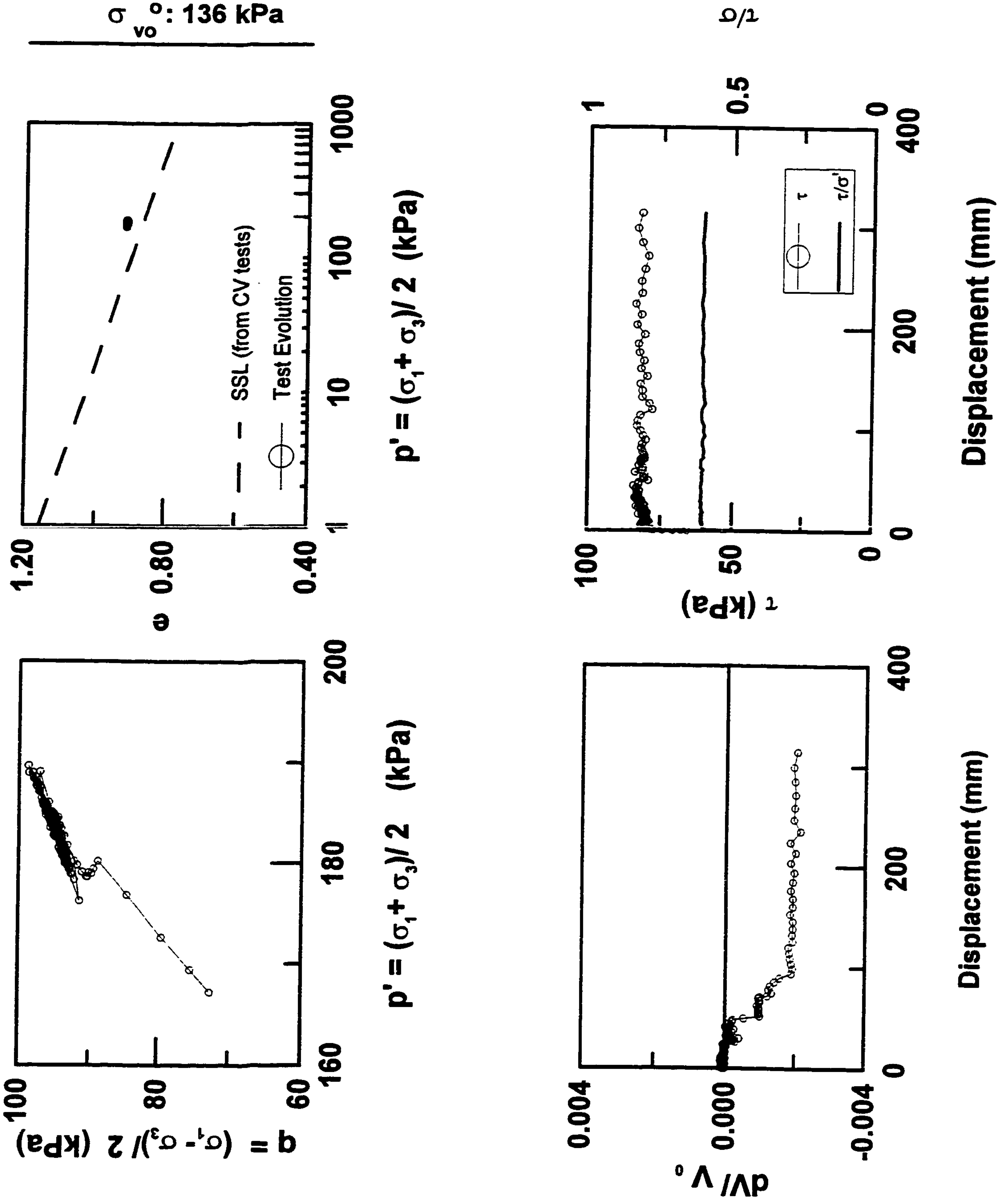

APPENDIX I

TEST: CLD-05

e_o : 0.926
σ_{vo} : 21 kPa

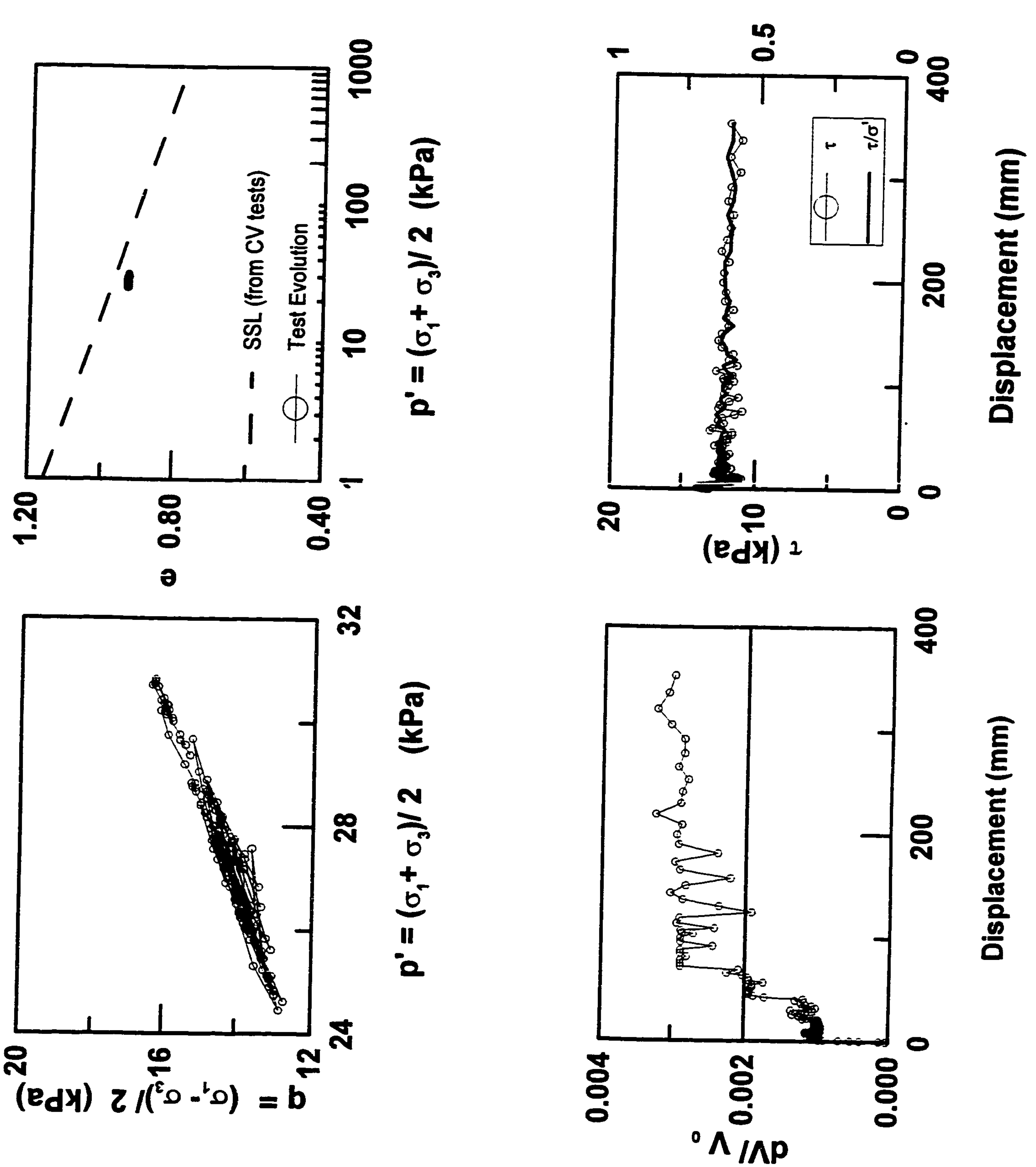

APPENDIX I

TEST: CLD-06

e_o : 0.920
σ_{vo} : 55 kPa

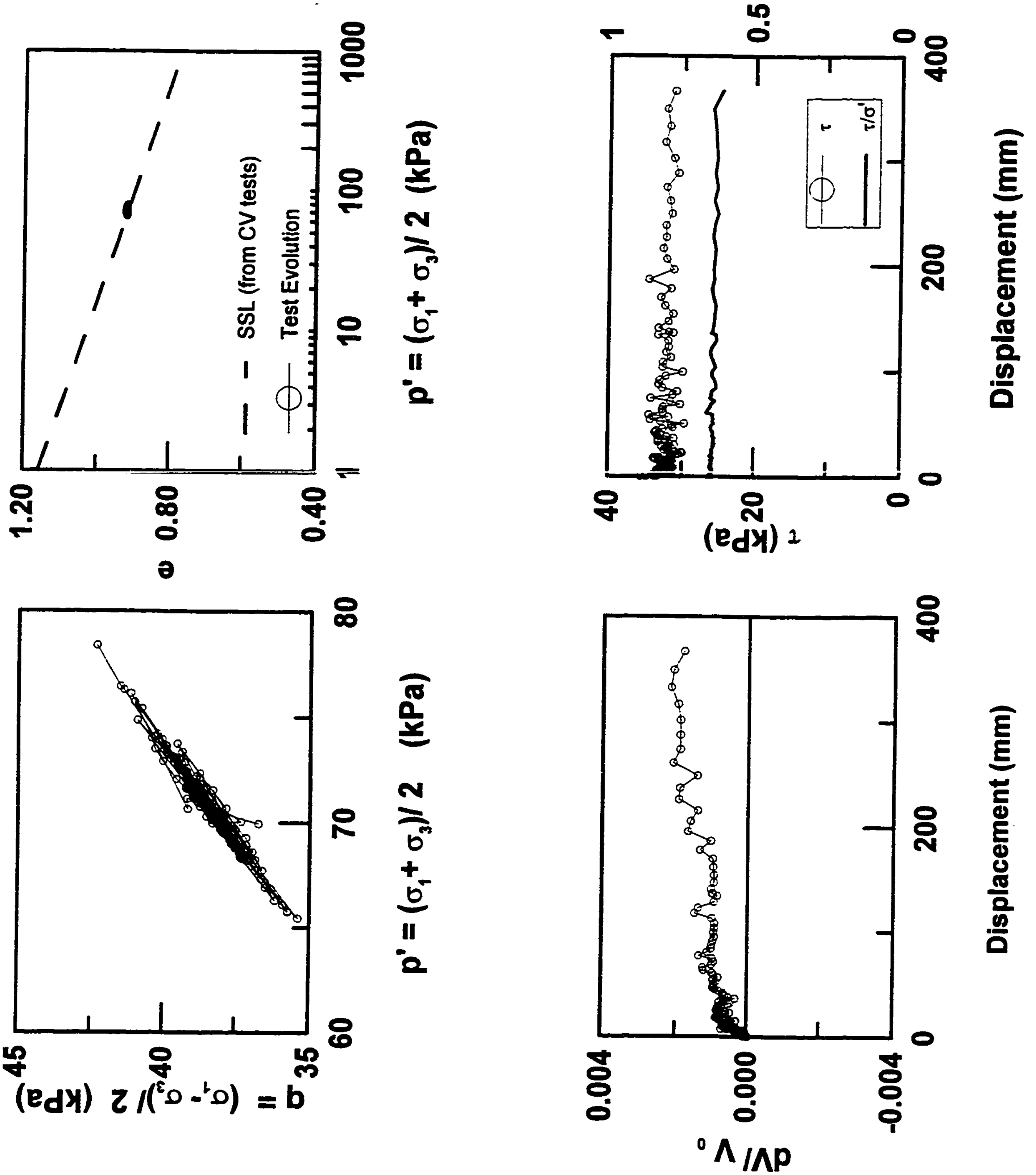

APPENDIX I

TEST: CLD-08

e_o : 0.906
σ_{vo}': 102 kPa

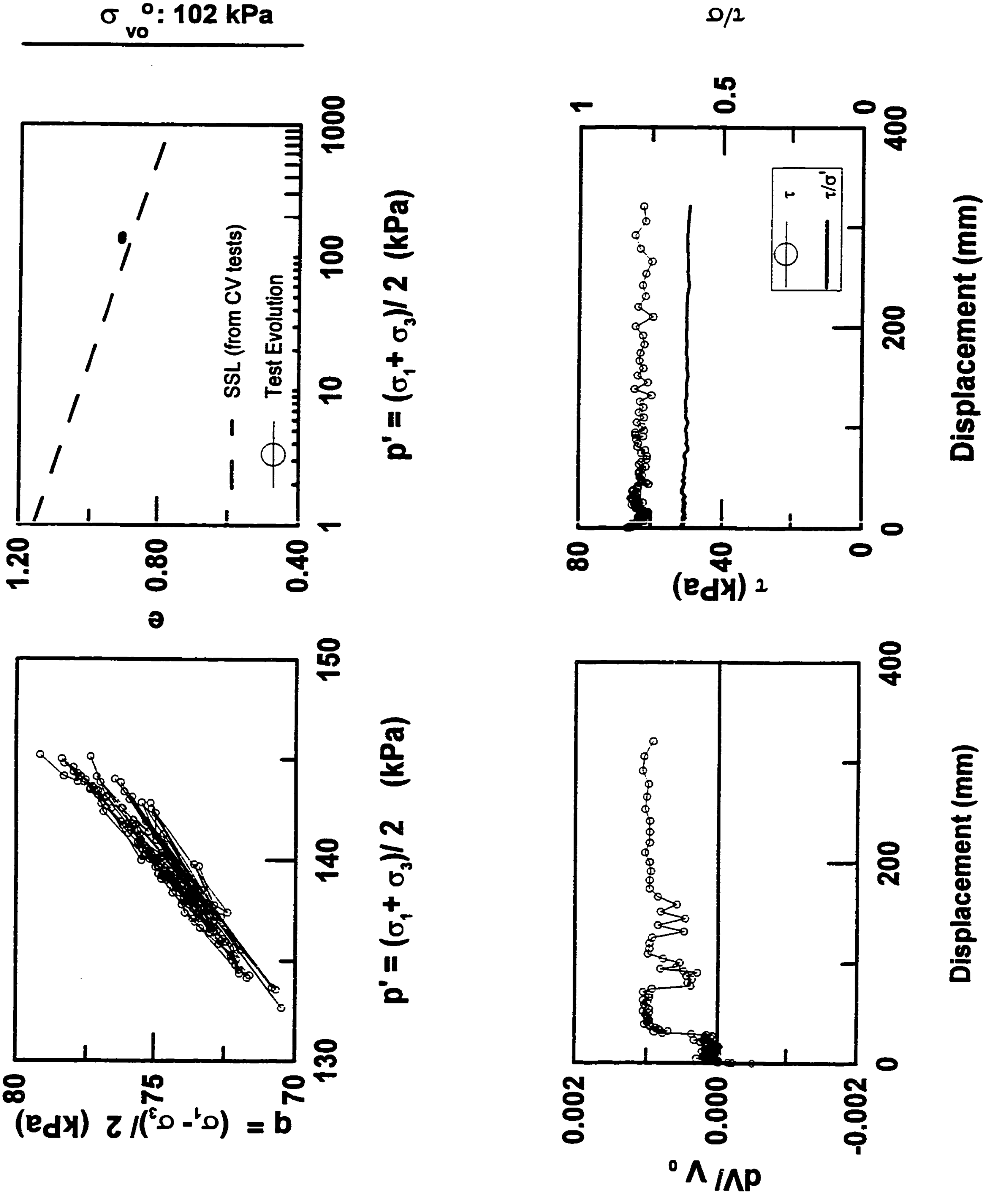

APPENDIX I

TEST: CVST-04

e_o : 0.901
σ_{vo}^{o}: 397 kPa

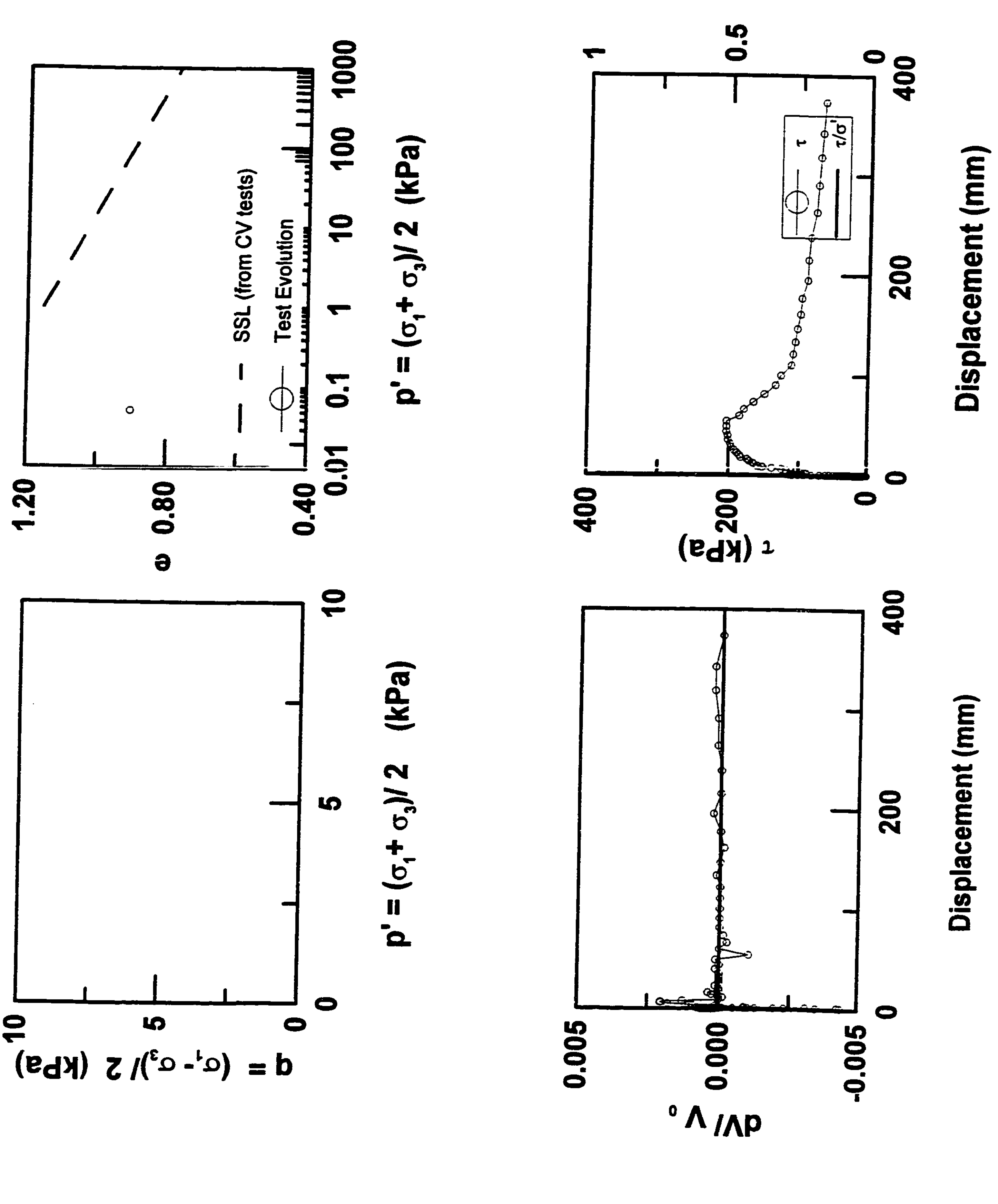

APPENDIX I

TEST: CVST-07

e_o : 0.920
σ_{vo}': 197 kPa

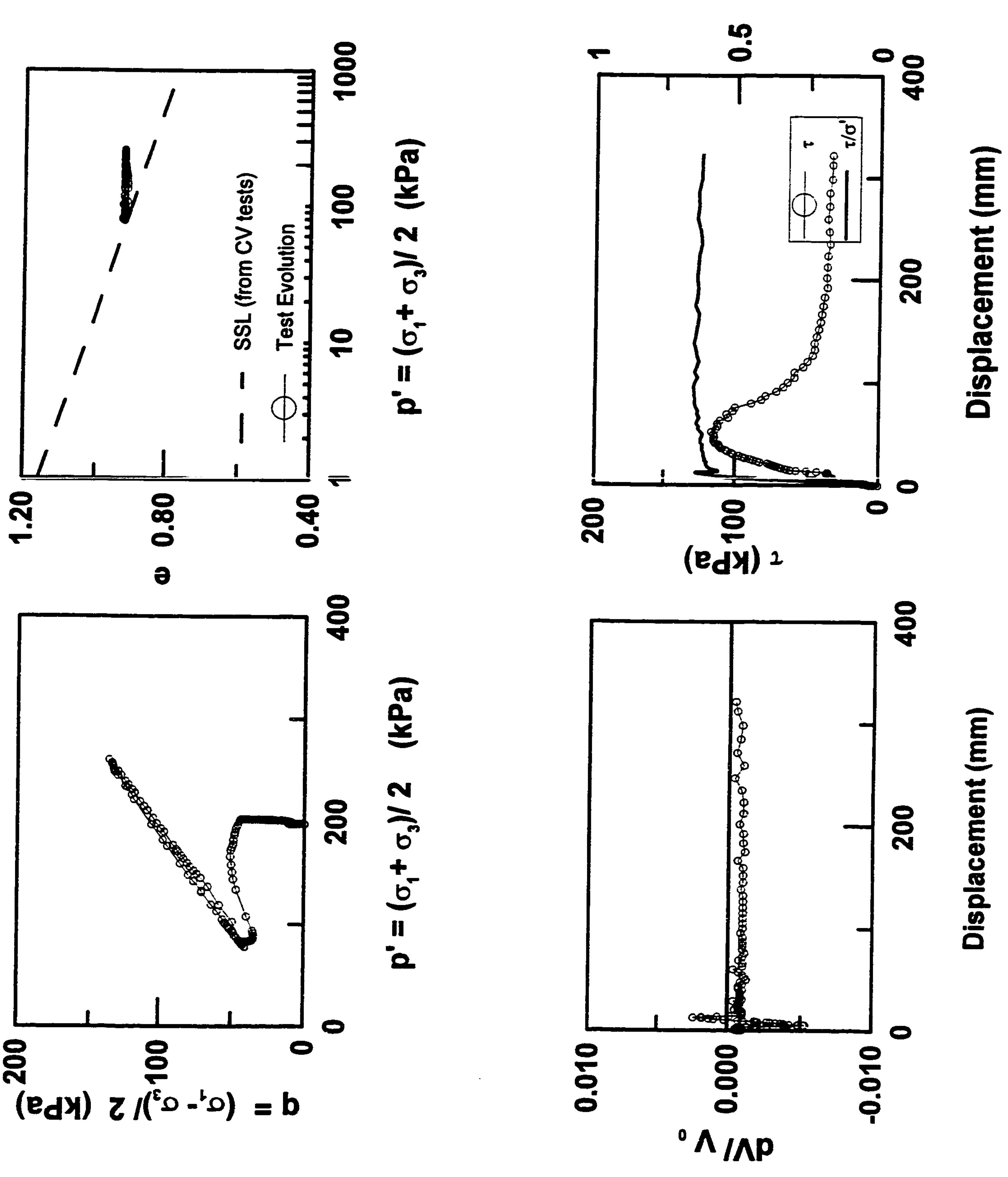

APPENDIX I

TEST: CVST-06

e_o : 0.911
σ_{vo}': 295 kPa

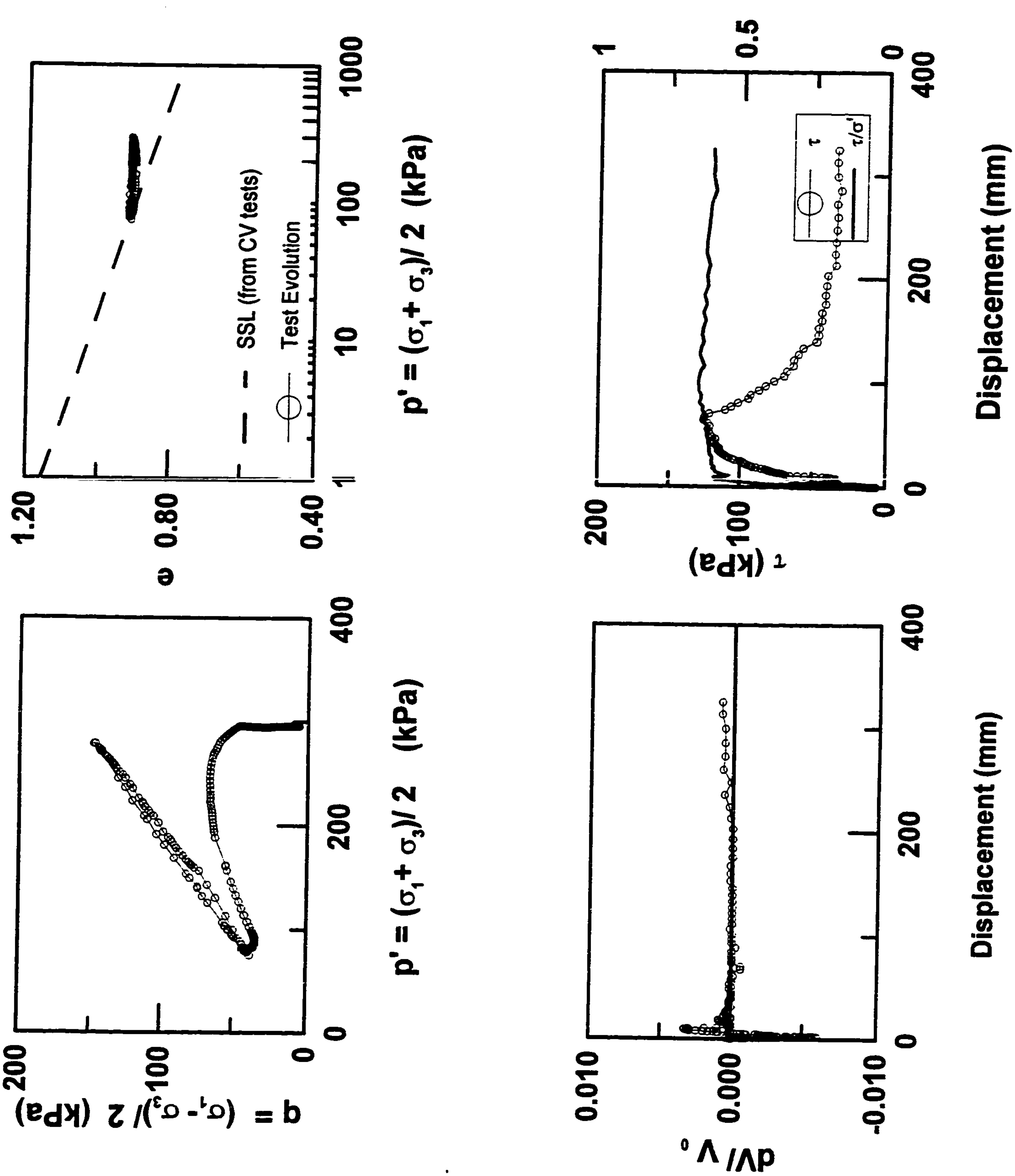

APPENDIX I

TEST: CVST-02

e_o : 0.993
σ'_{vo}: 400 kPa

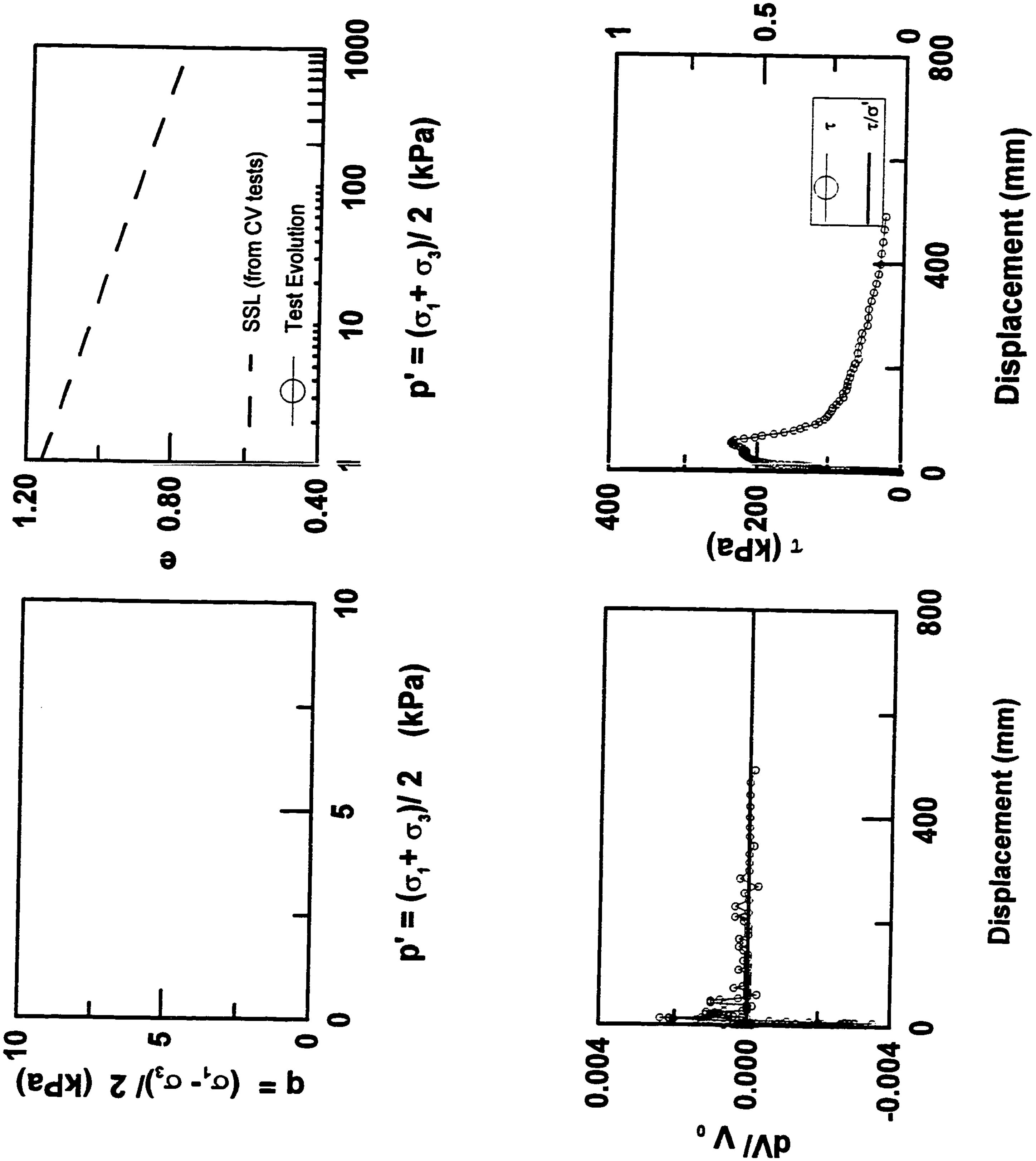

APPENDIX I

TEST: CLSR06-01

e_o : 0.992
σ'_{vo} : 19 kPa

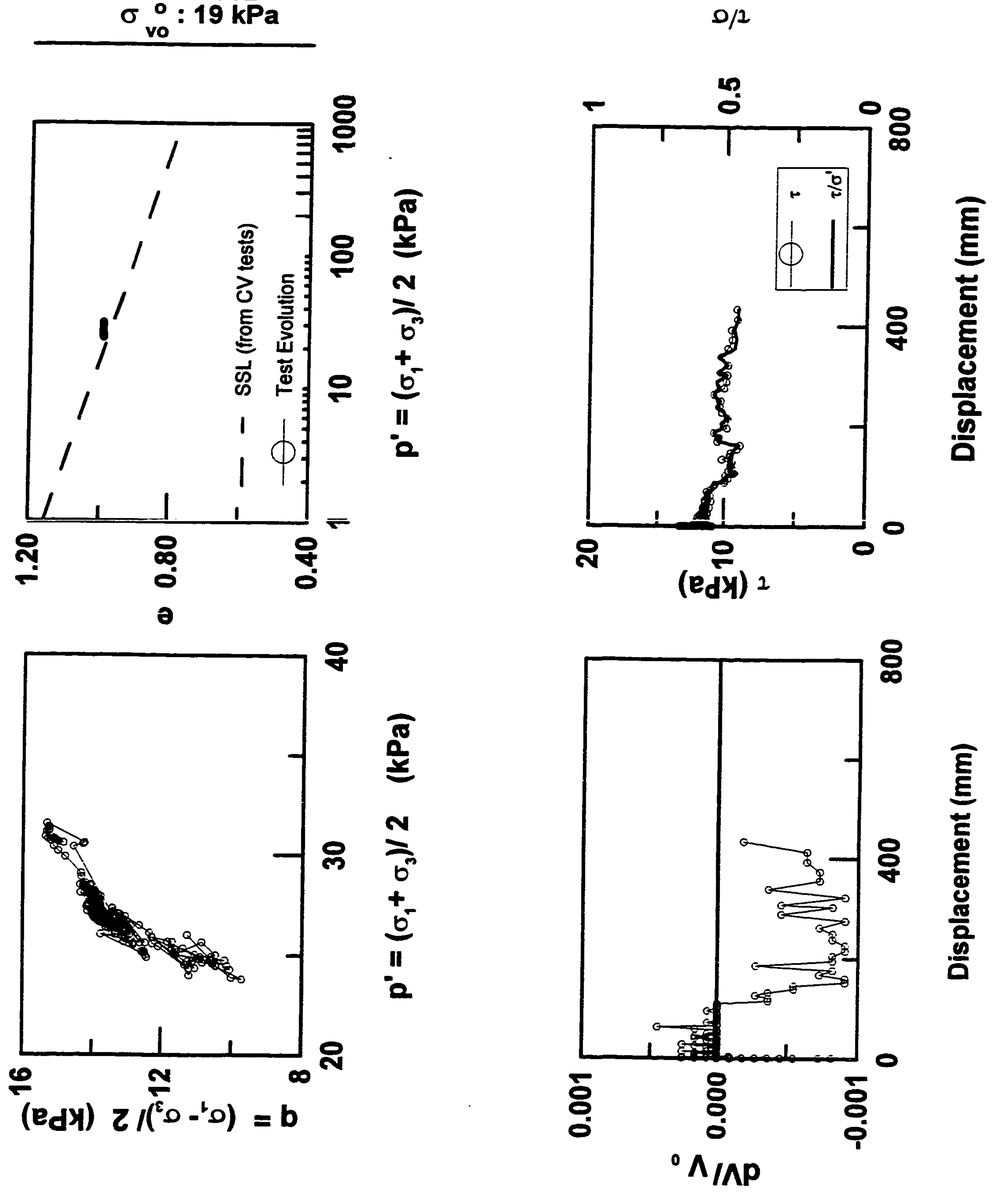

APPENDIX I

TEST: CLSR06-02

e_o : 0.990
σ_{vo}^{o} : 48 kPa

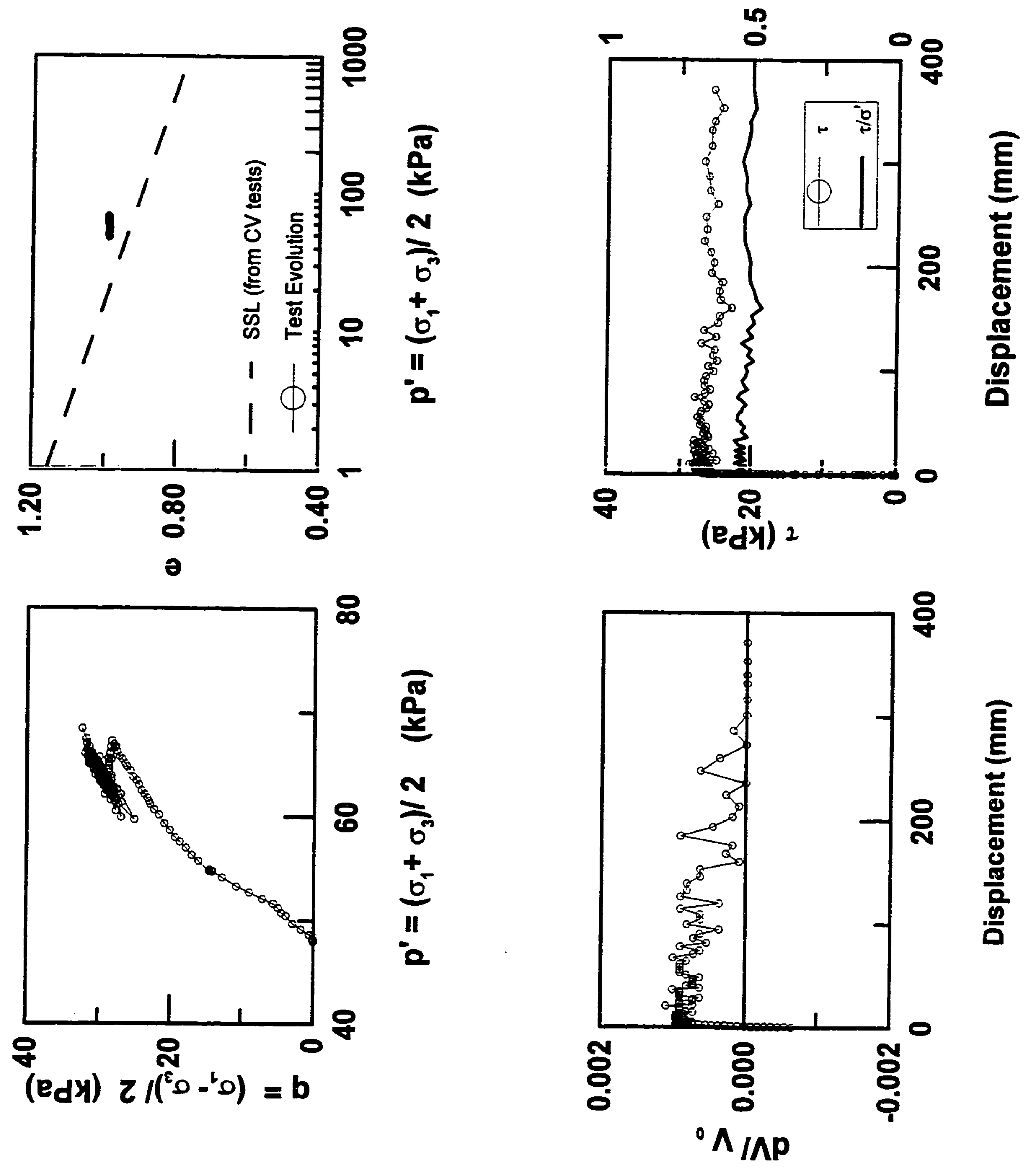

APPENDIX I

TEST: CLSR03-01

e_o : 0.985
σ_{vo} : 99 kPa

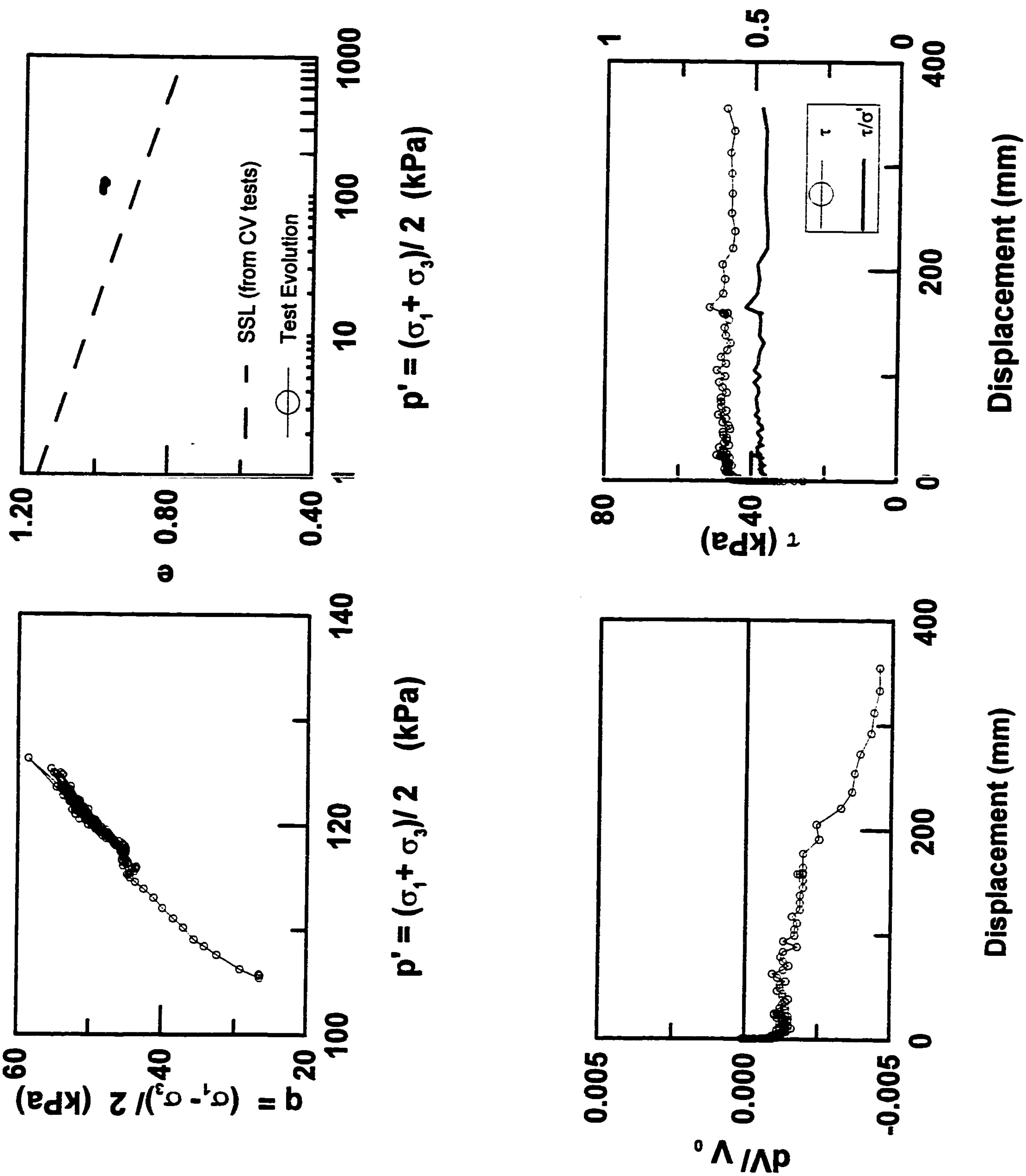

APPENDIX I

TEST: CLSR15-02

e_o : 0.961
σ_{vo}': 110 kPa

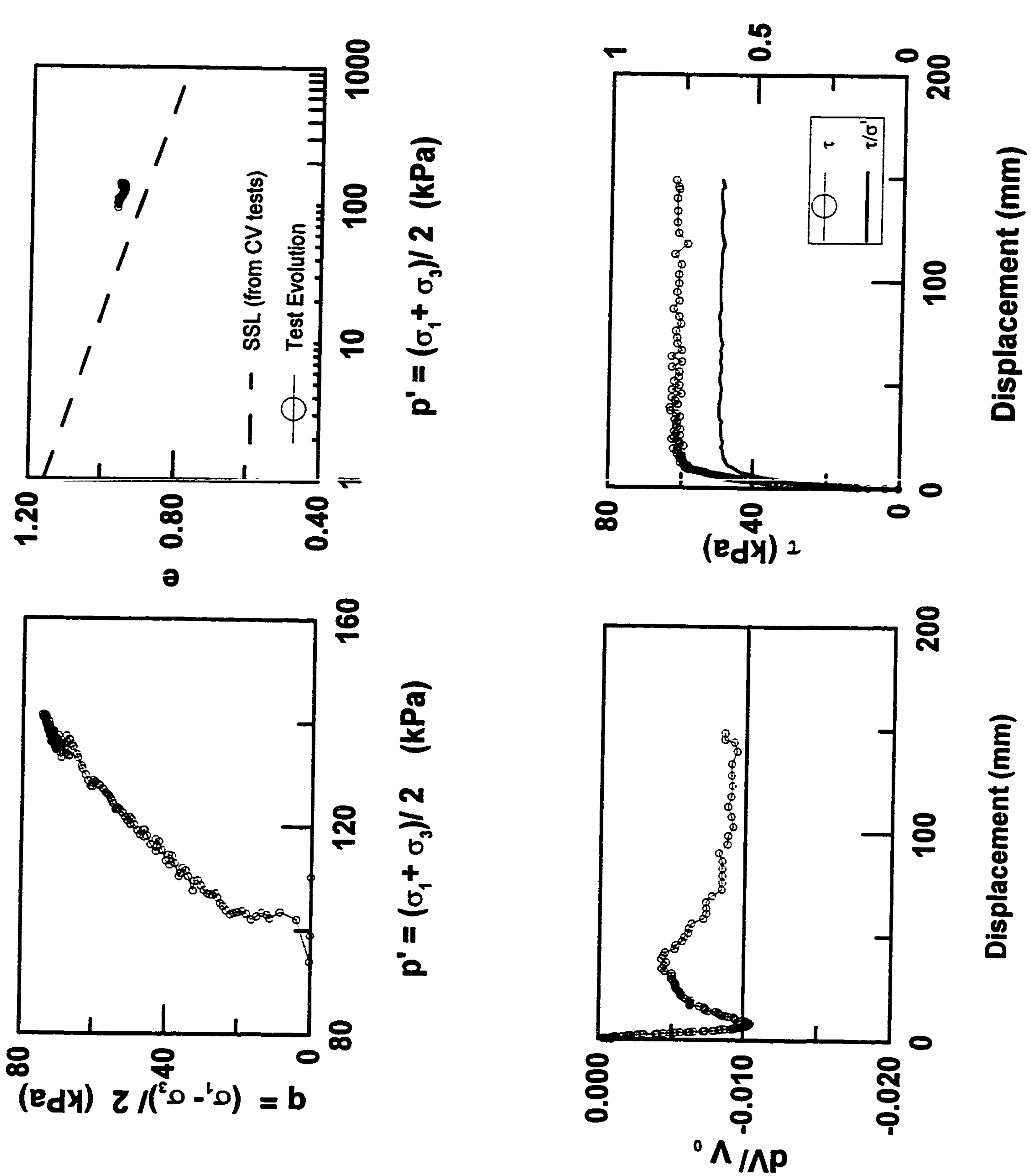

APPENDIX I

TEST: CLSR30-01

e_o : 0.969
σ_{vo} : 96 kPa

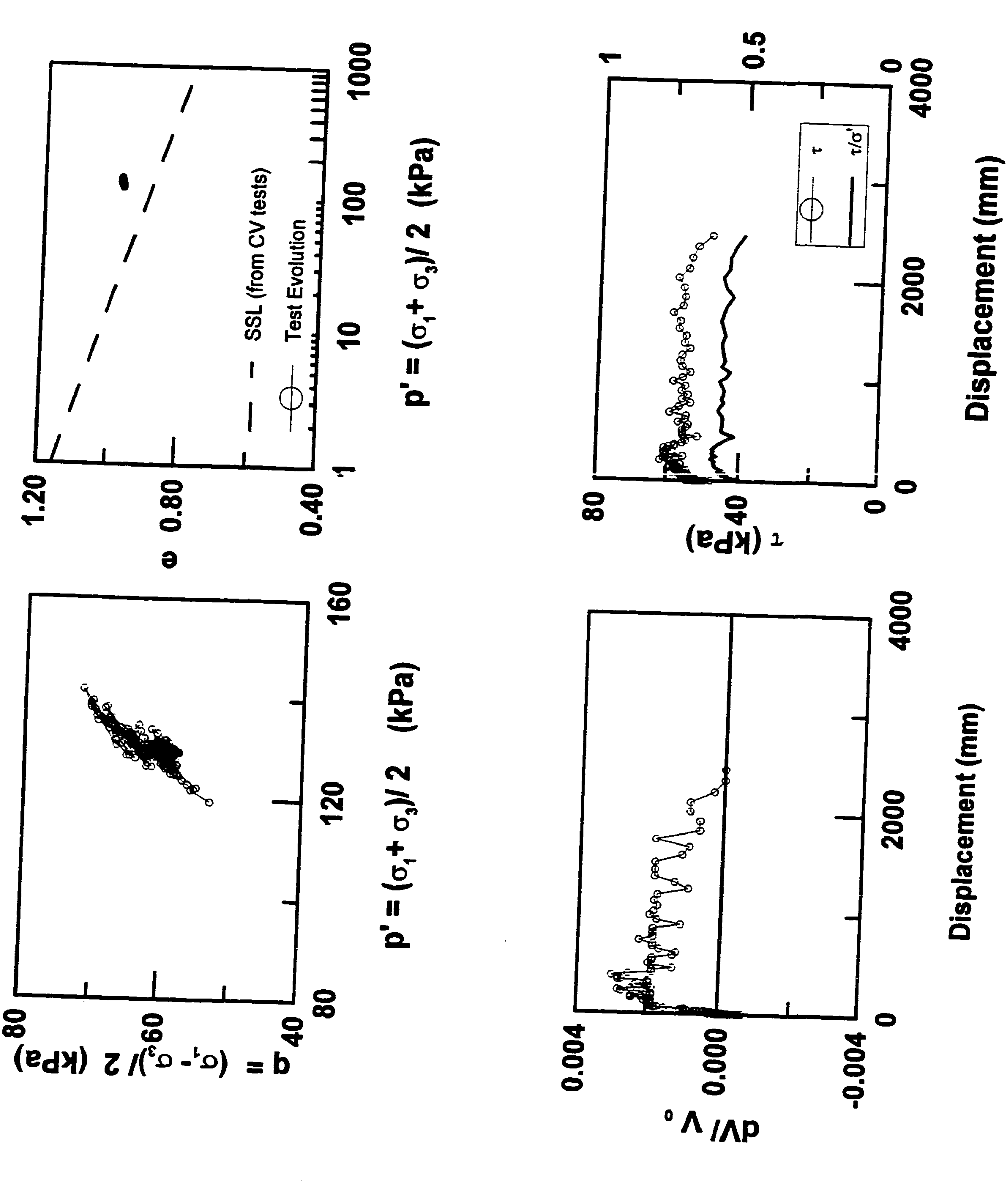

APPENDIX I

TEST: CLSR30-02

e_o : 0.941
σ_{vo} : 98 kPa

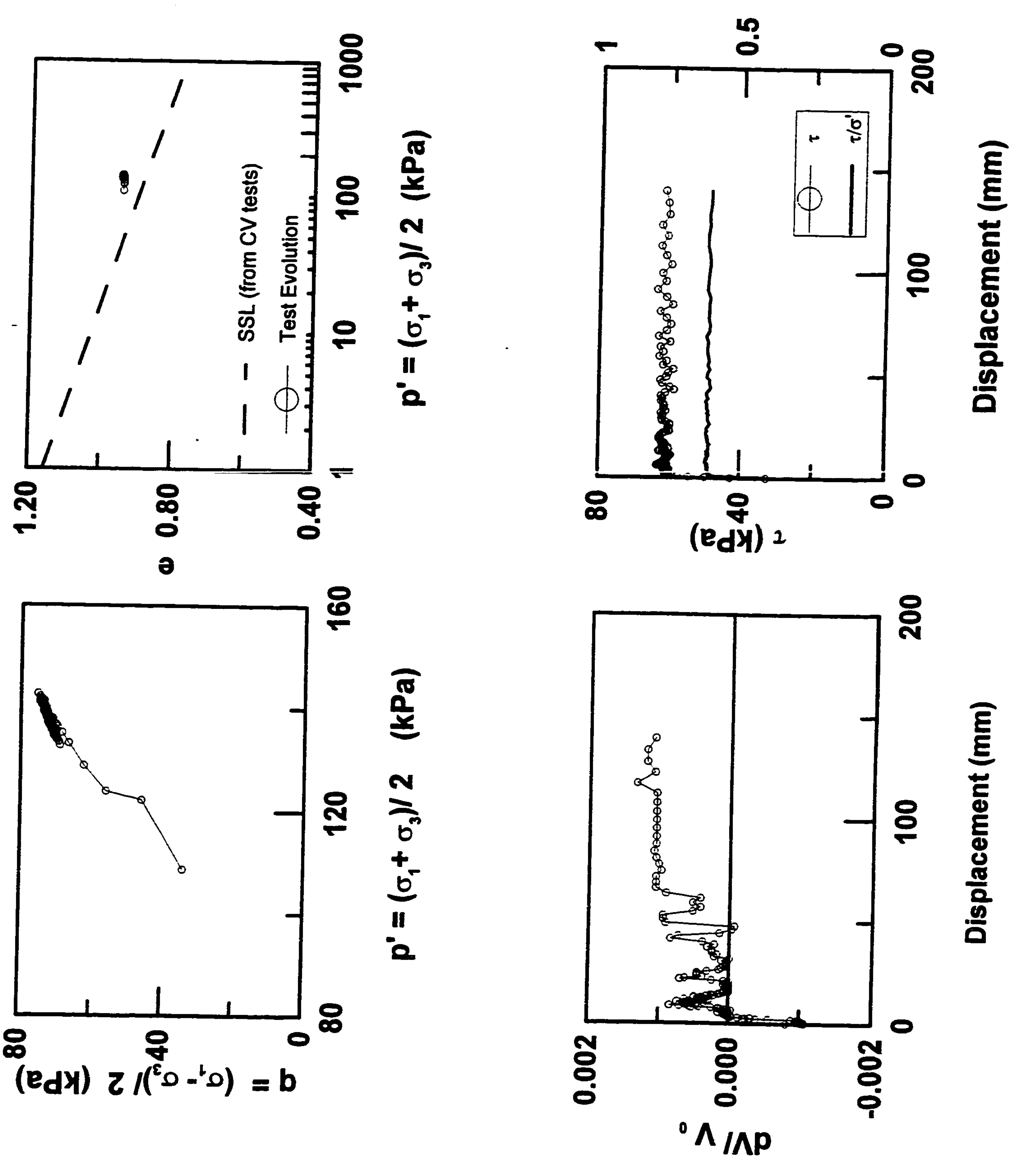

APPENDIX I

TEST: CLDF10-01

e_o : 0.769
σ_{vo} : 25 kPa

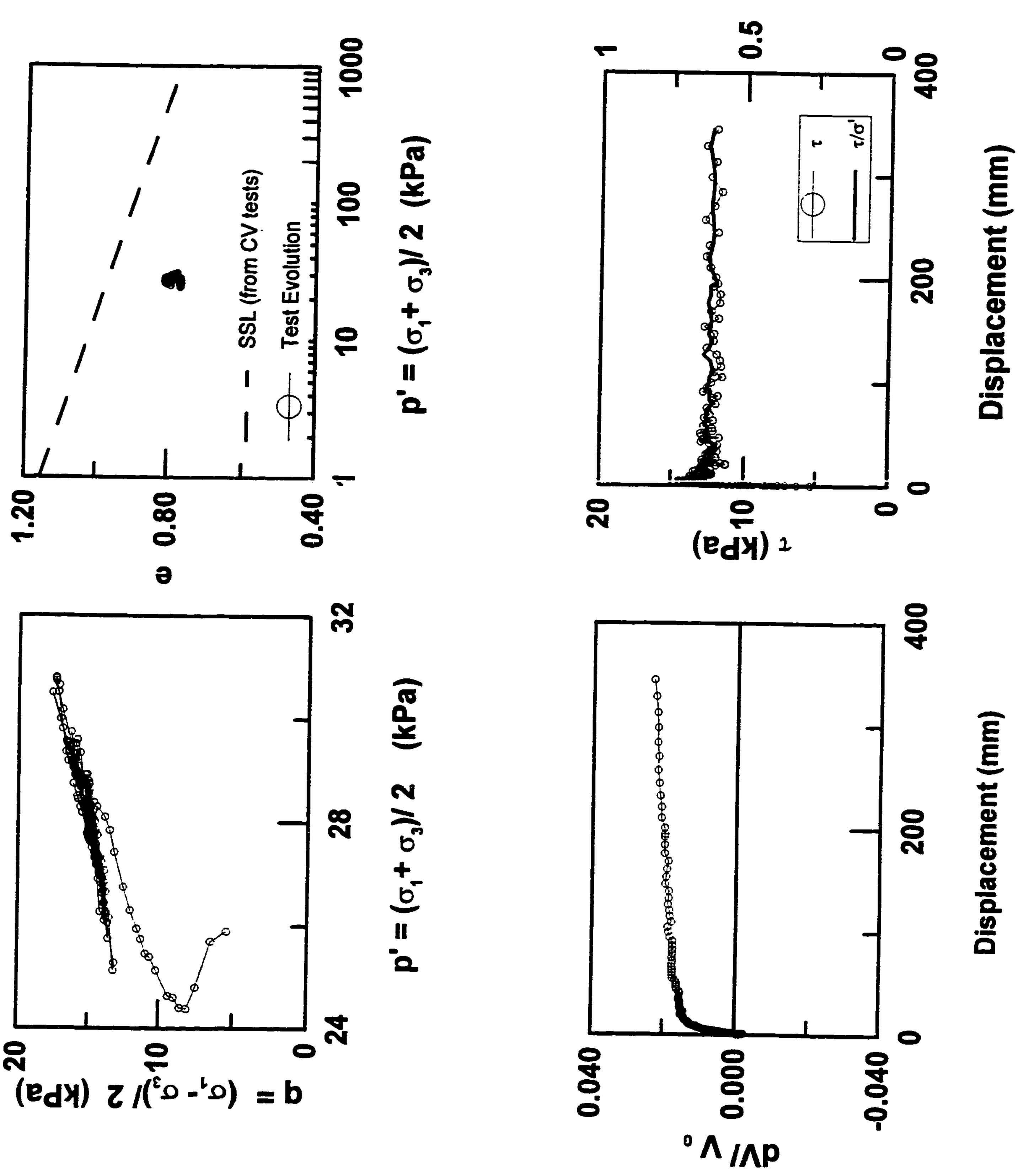

TEST: CLDF10-02

e_o : 0.798
σ'_{vo} : 49 kPa

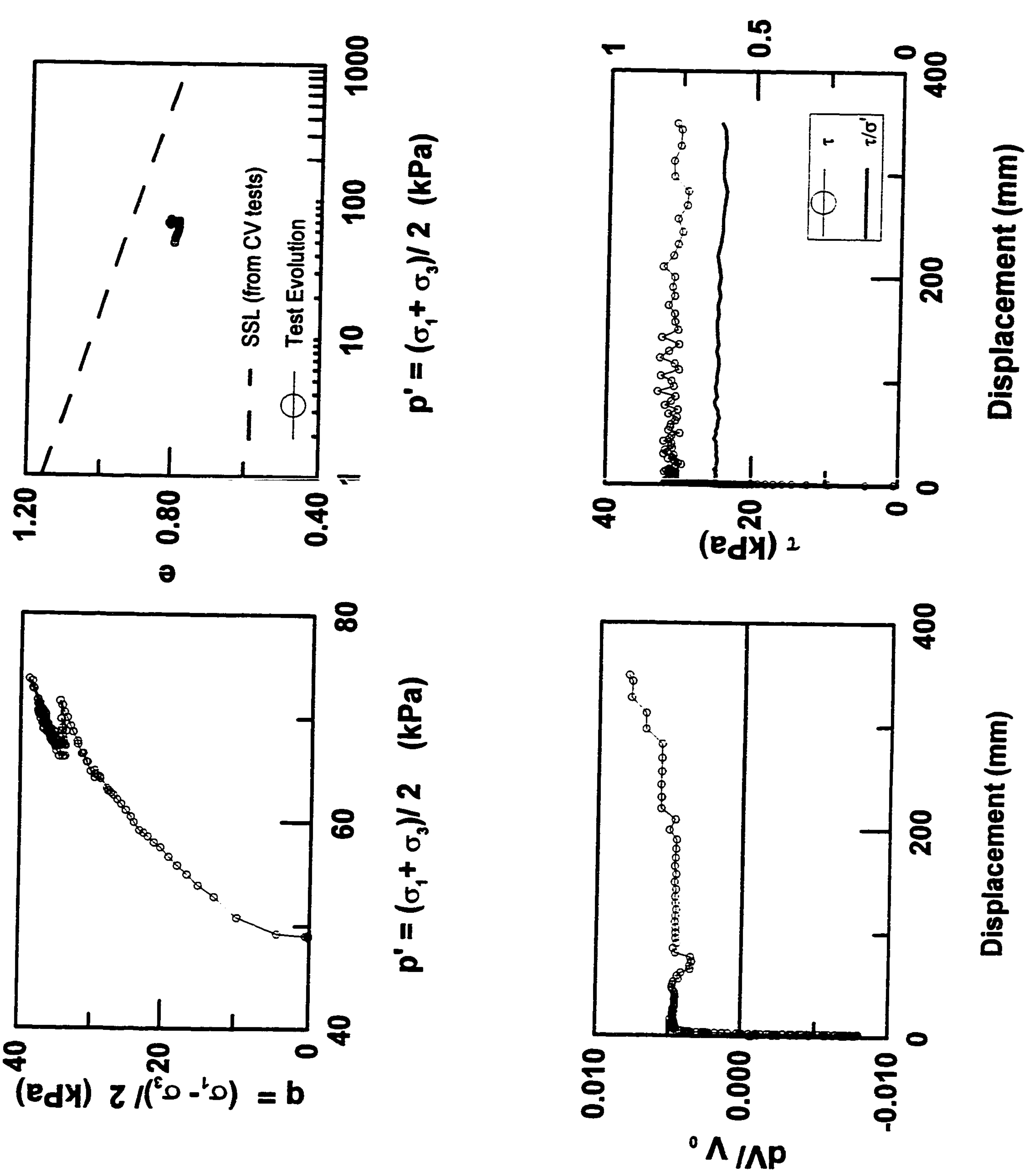

APPENDIX I

TEST: CVDF10-01

e_o : 0.718
σ_{vo} : 575 kPa

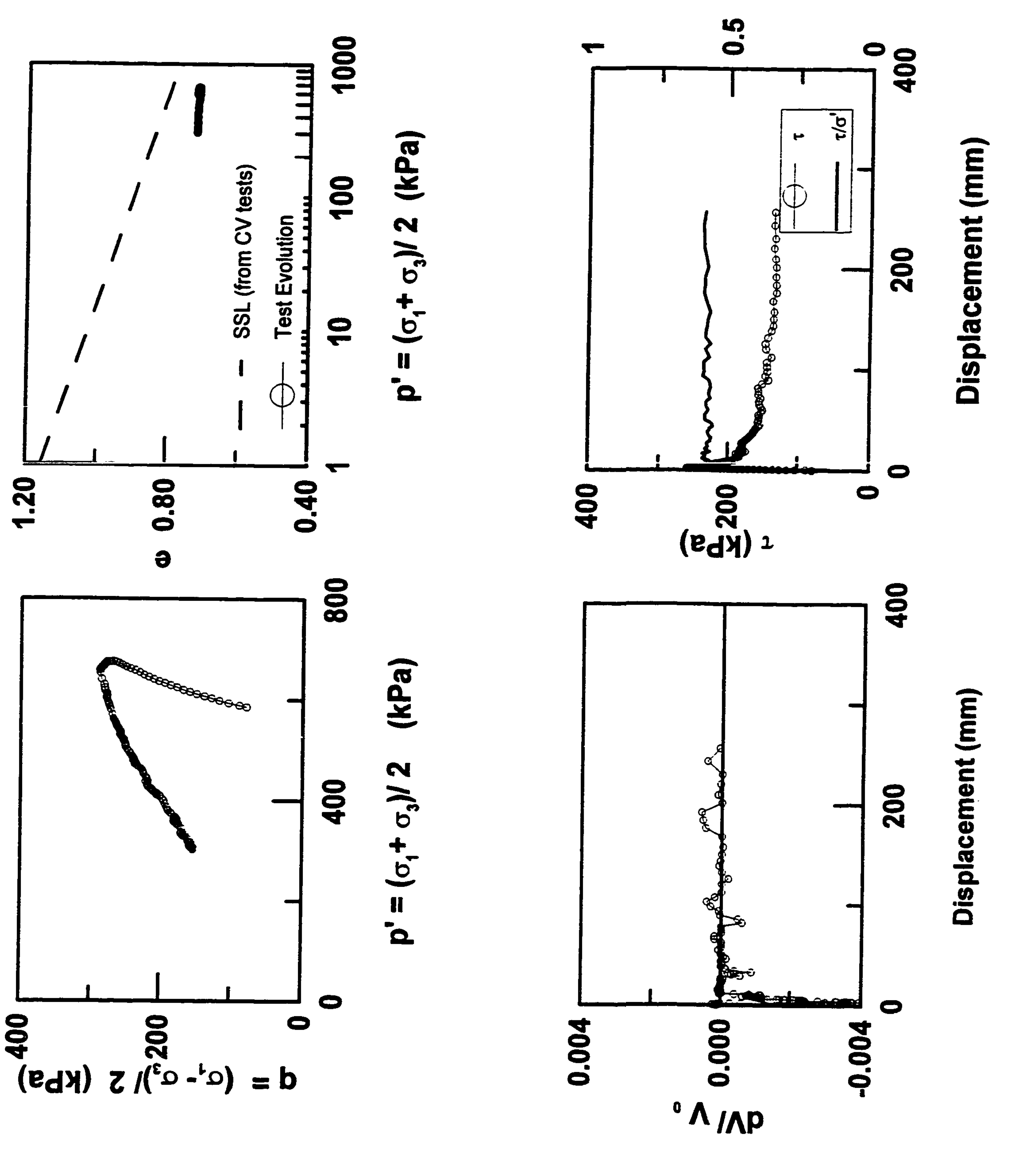

APPENDIX I

TEST: CVDF10-06

e_o : 0.699
σ_{vo}^{o}: 255 kPa

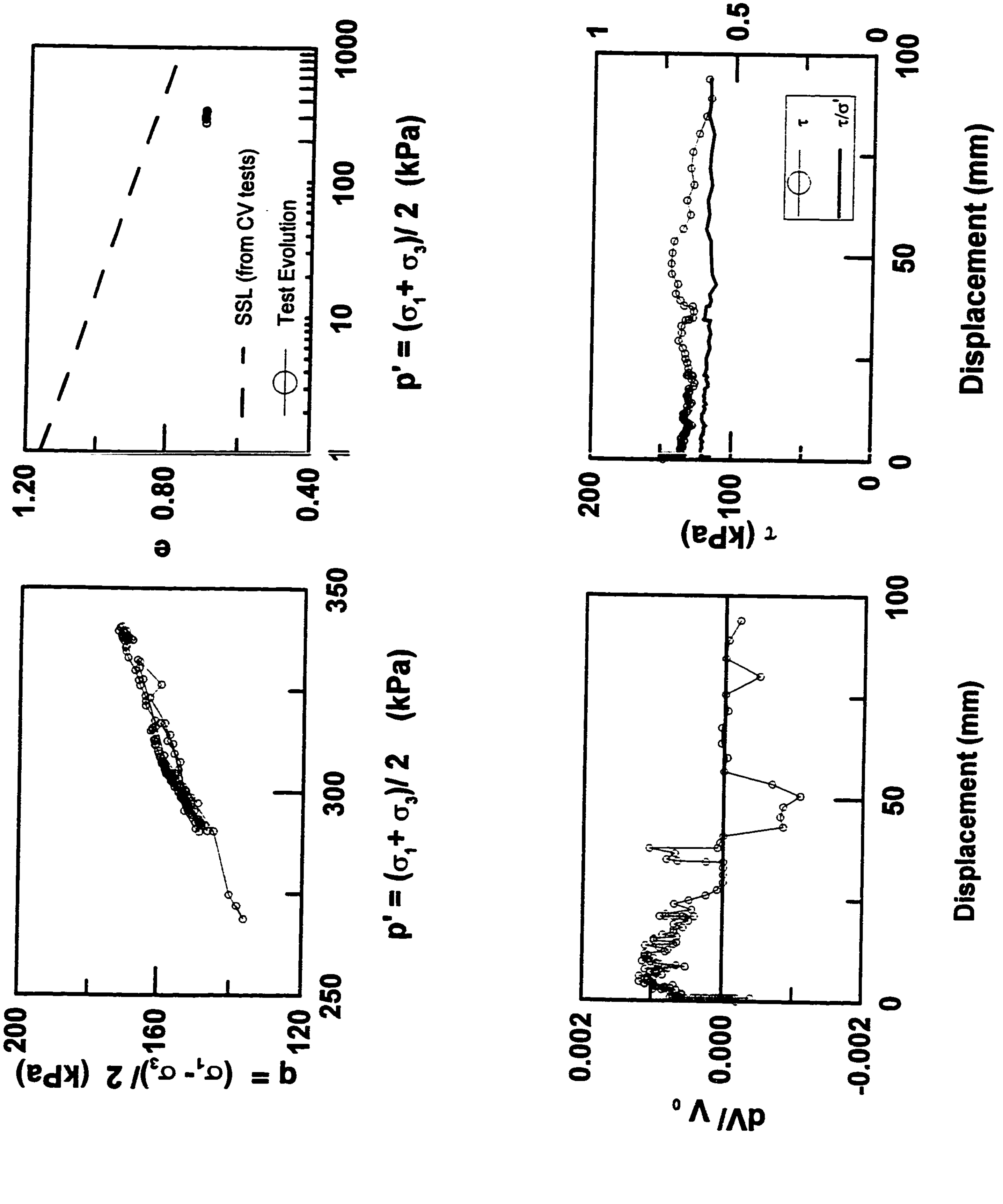

APPENDIX I

TEST: CVDF10-02

e_o : 0.738
σ'_{vo}: 262 kPa

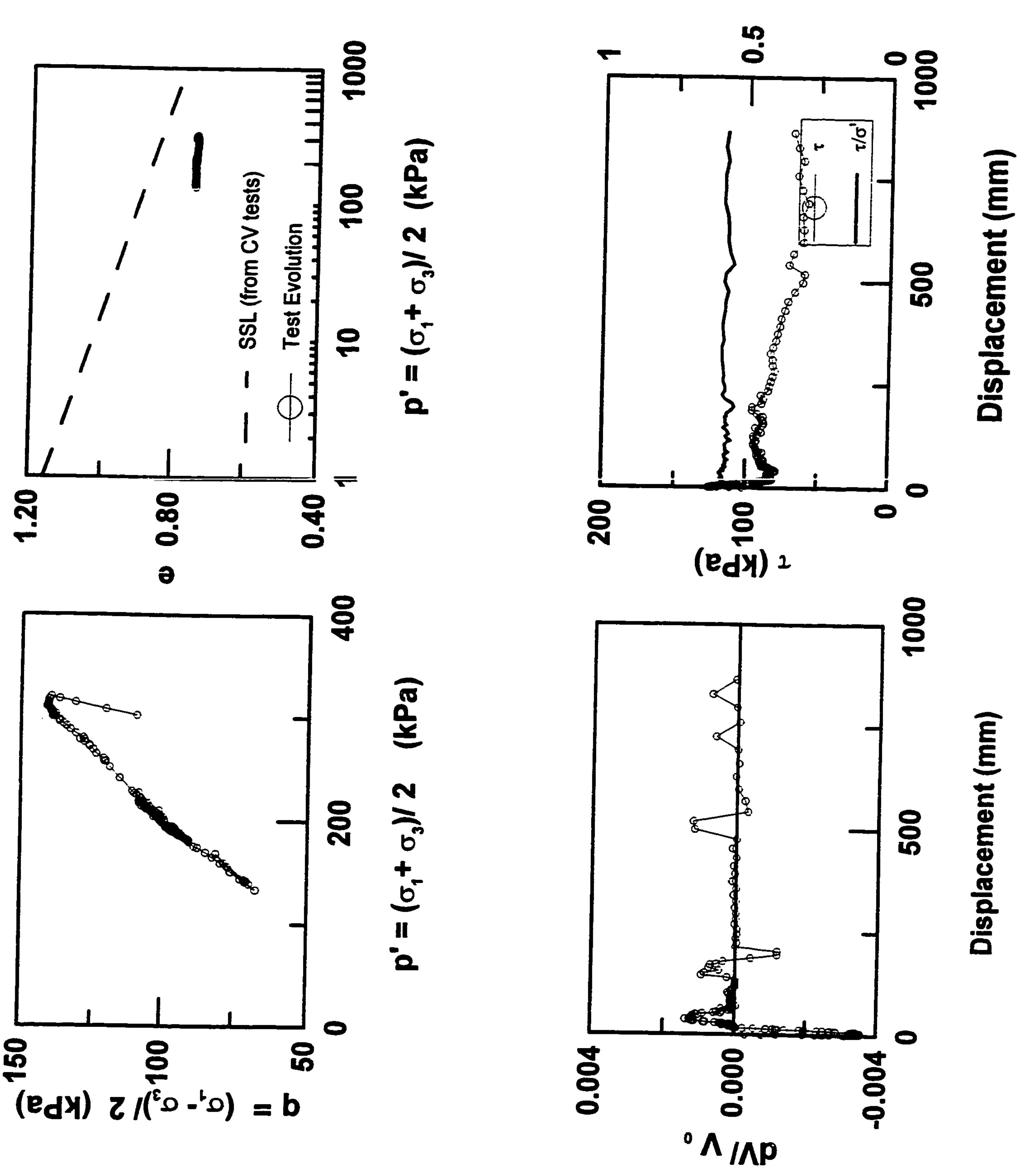

APPENDIX I

TEST: CVDF10-03

e_o : 0.760
σ'_{vo}: 147 kPa

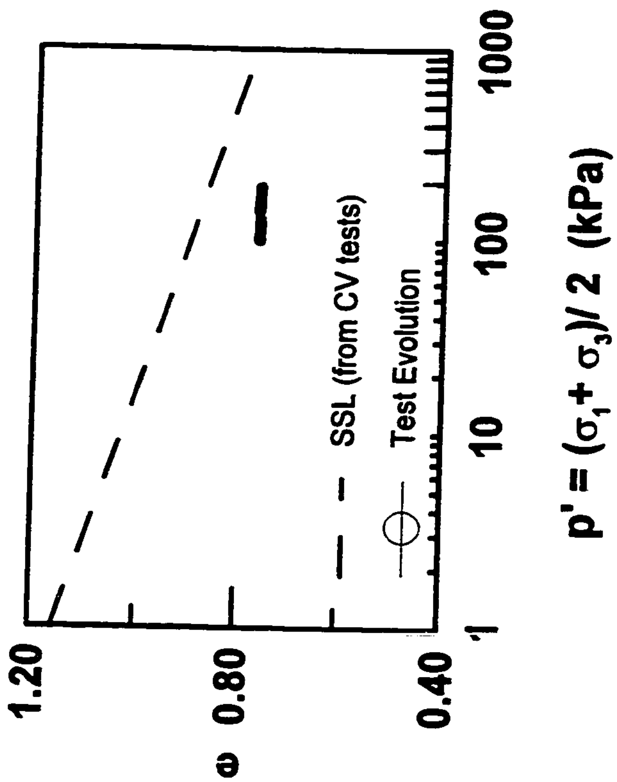

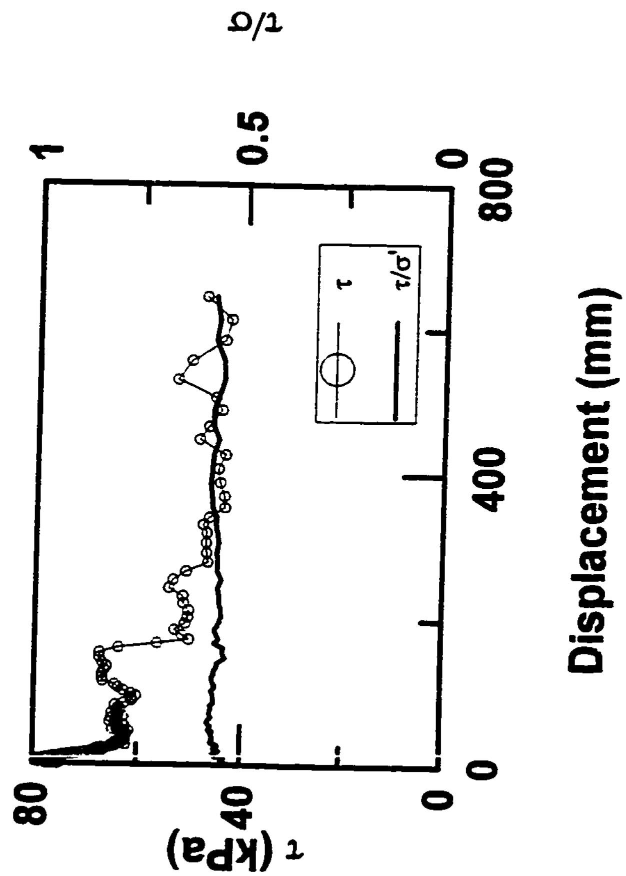

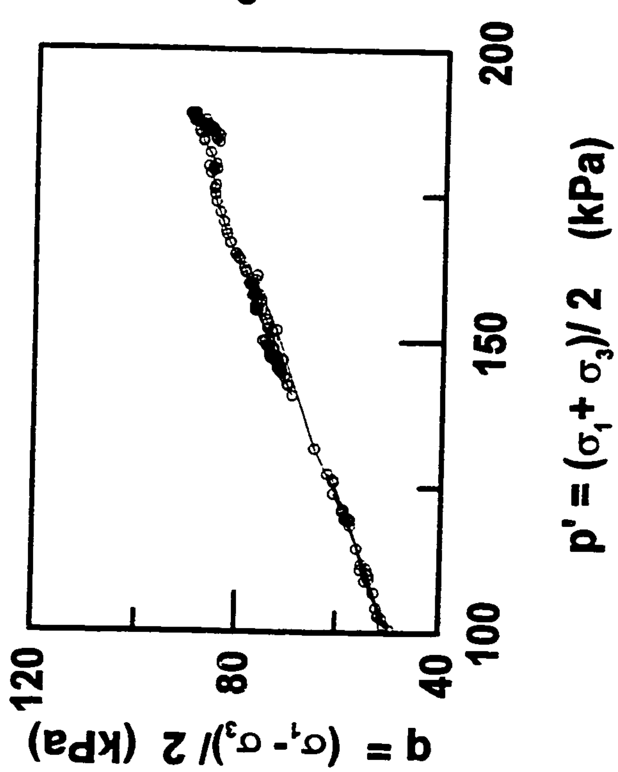

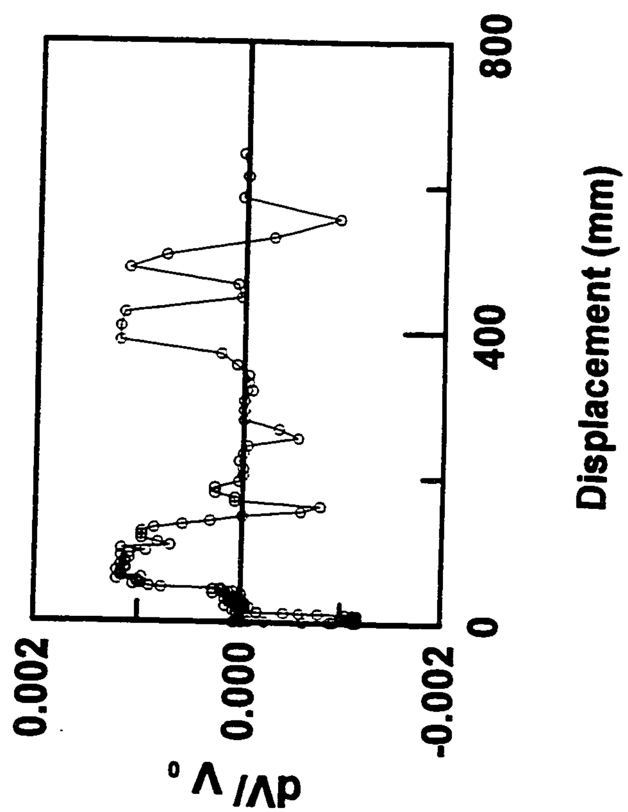

APPENDIX I

TEST: CLSR60-04

e_o : 0.850
σ_{vo}^{o}: 306 kPa

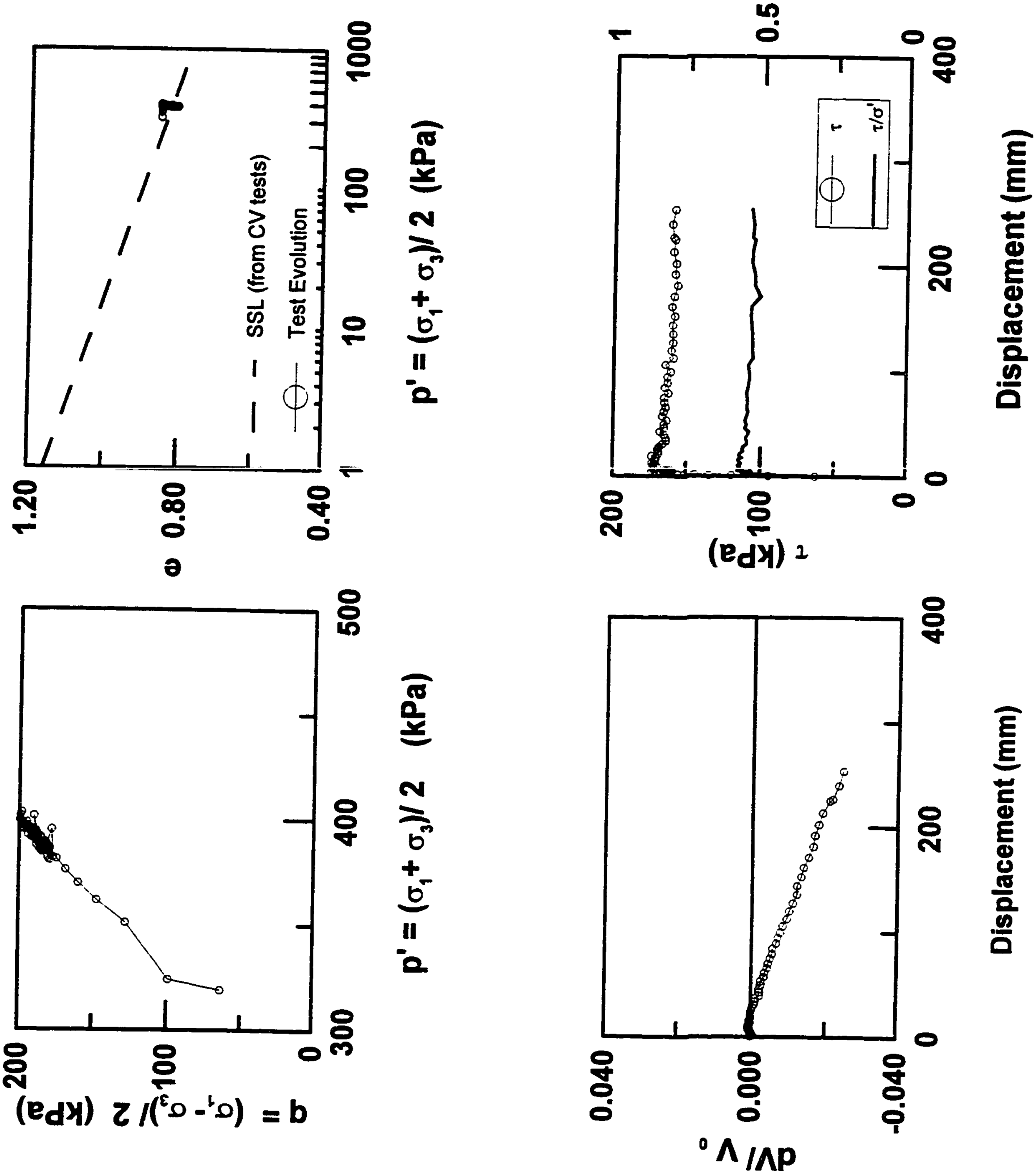

APPENDIX I

TEST: CVDF10-04

e_o : 0.780
σ_{vo}' : 105 kPa

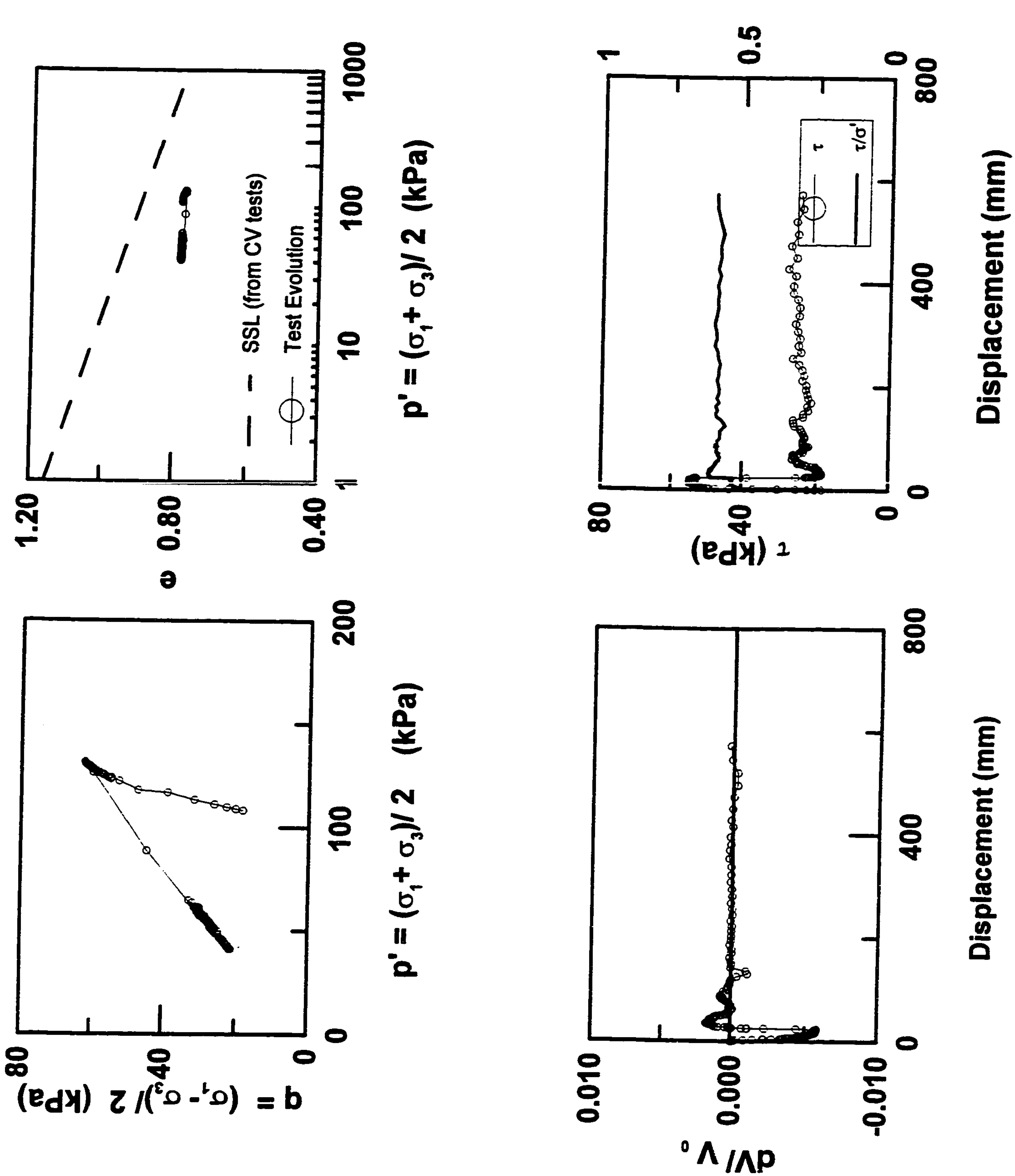

APPENDIX I

TEST: CVDF10-05

e_o : 0.802
σ_{vo} : 22 kPa

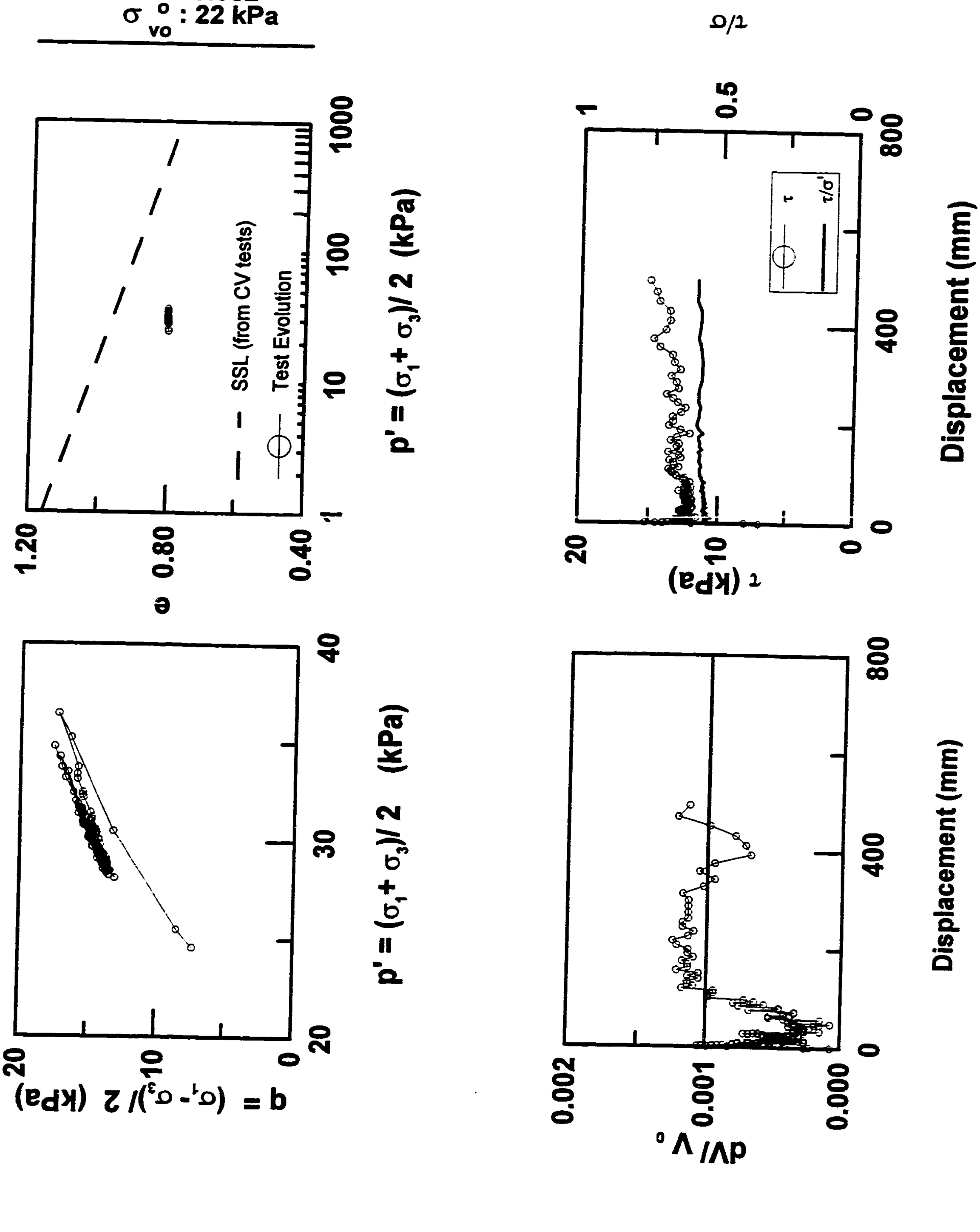

APPENDIX I

TEST: CLDF20-02

e_o : 0.728
σ_{vo} : 50 kPa

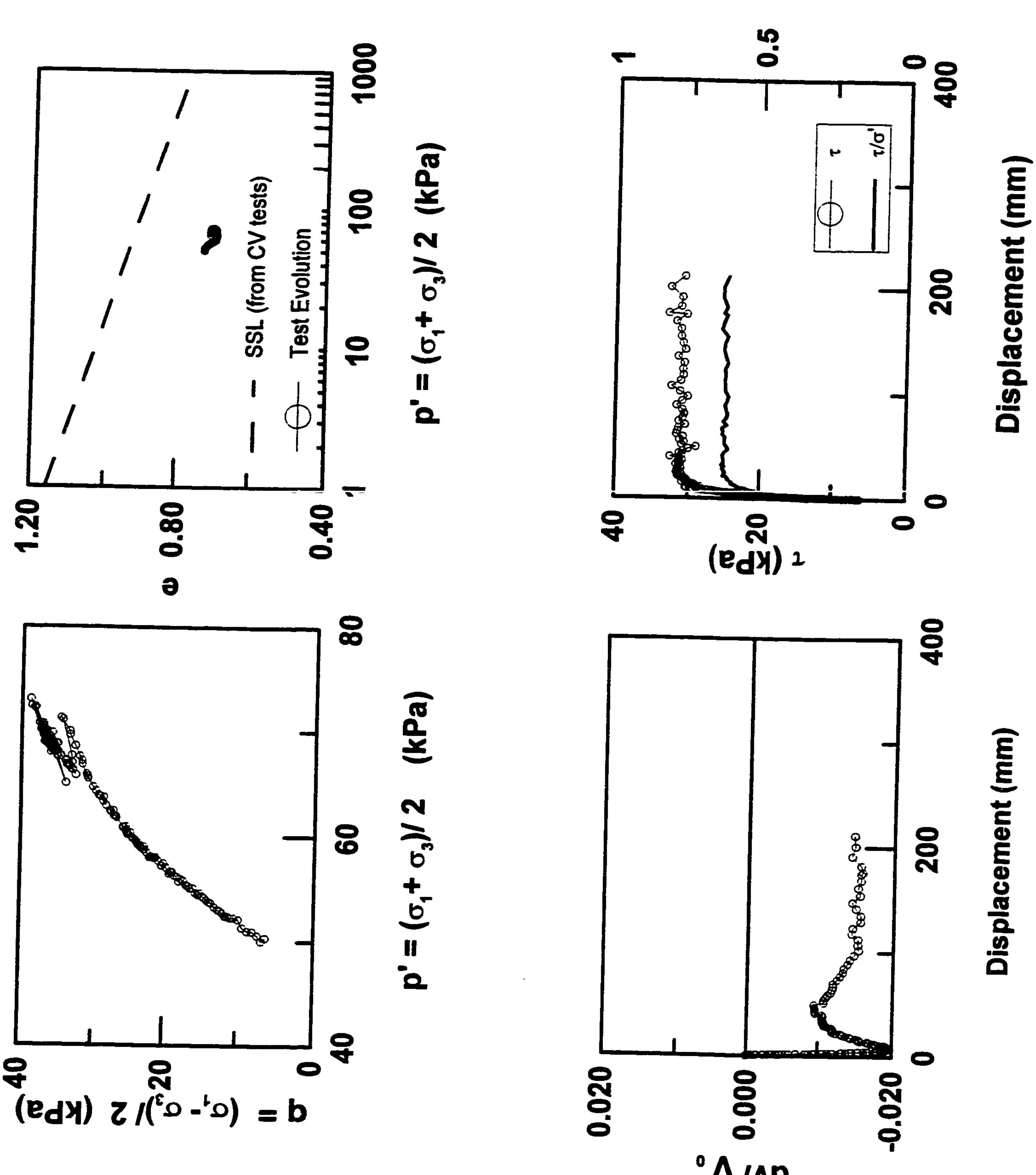

APPENDIX I

TEST: CLDF20-03

e_o : 0.690
σ_{vo} : 62 kPa

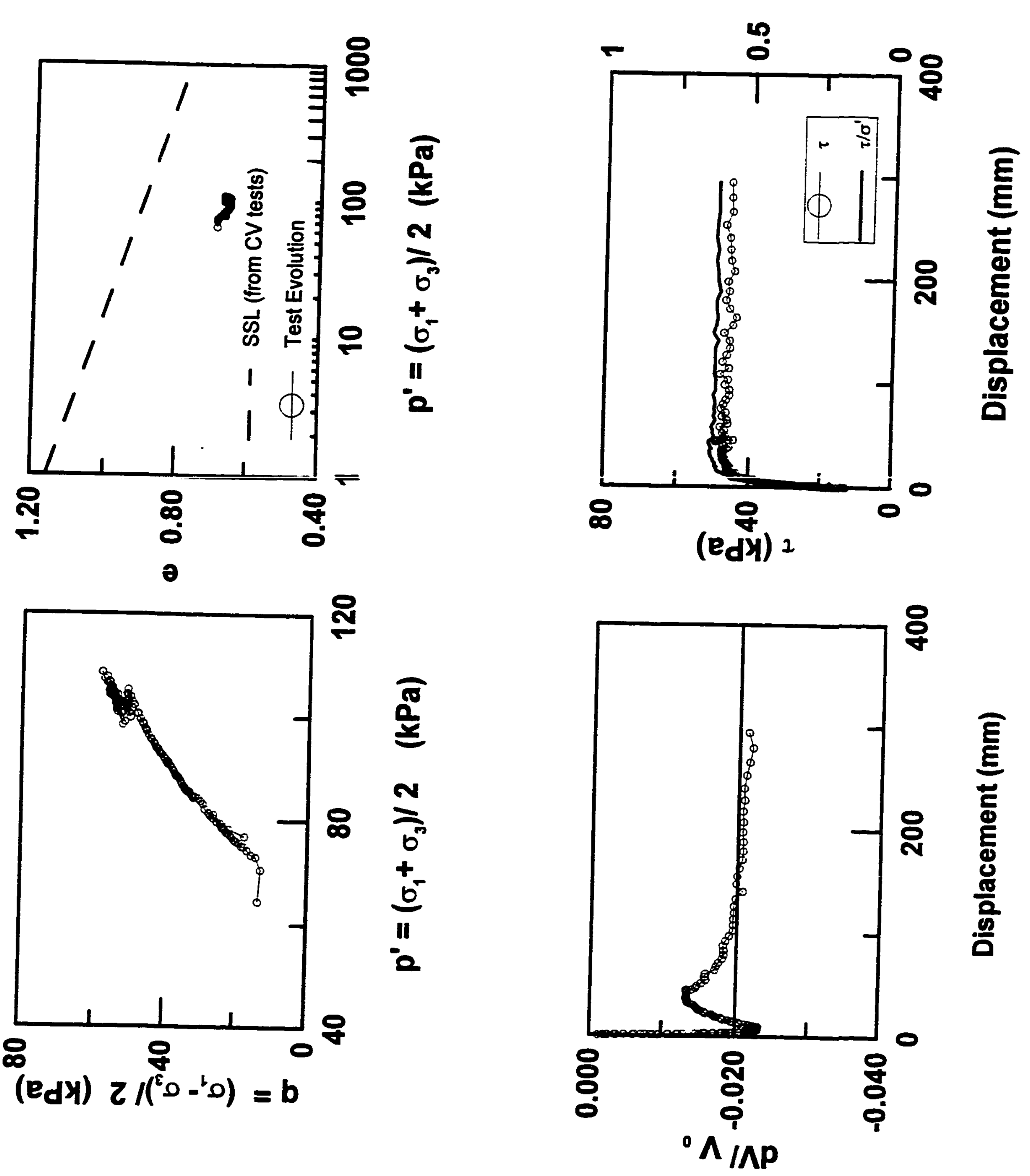

APPENDIX I

TEST: CLDF20-04

e_o : 0.697
σ'_{vo} : 95 kPa

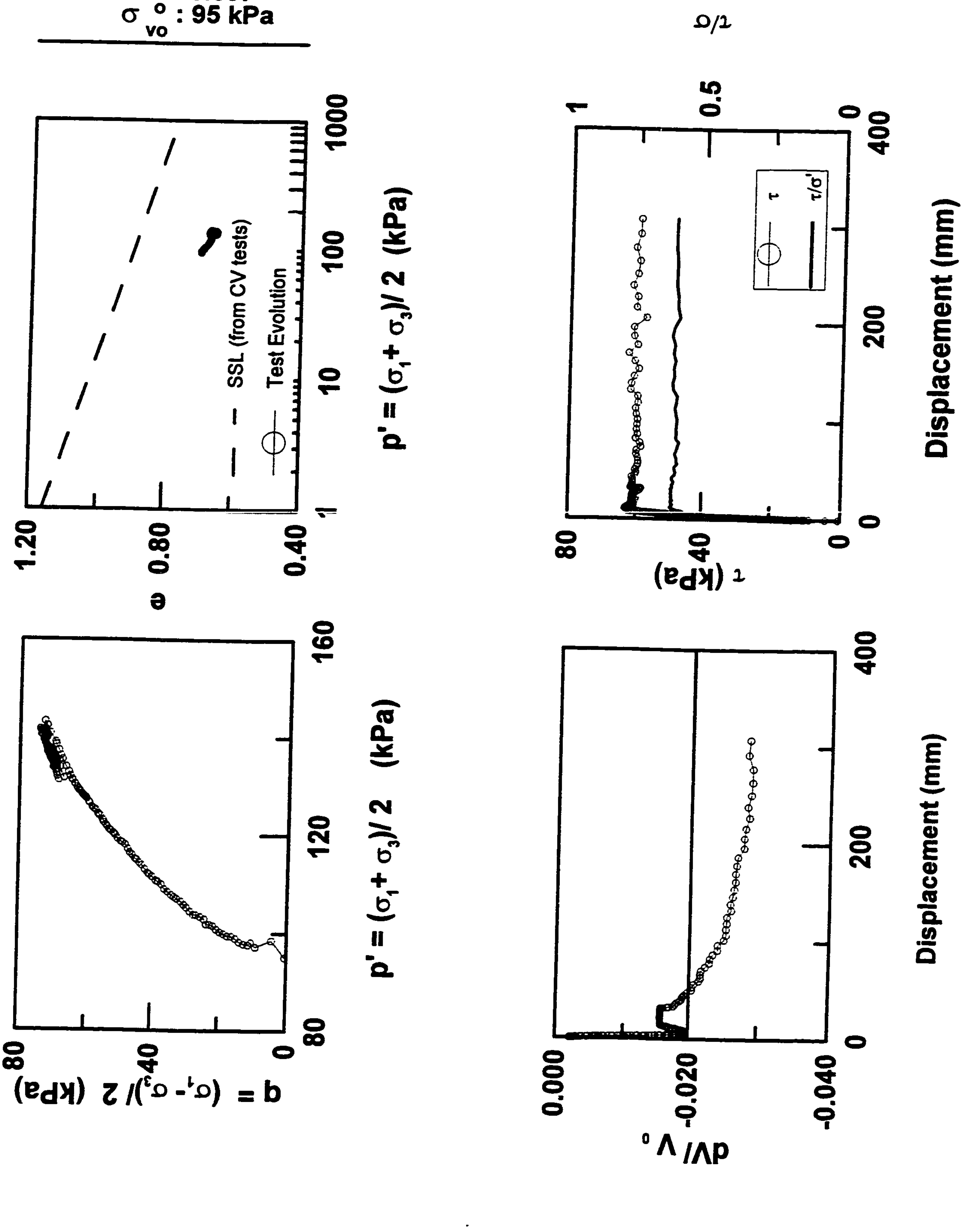

APPENDIX I

TEST: CLDF20-05

e_o : 0.759
σ_{vo}^{o}: 108 kPa

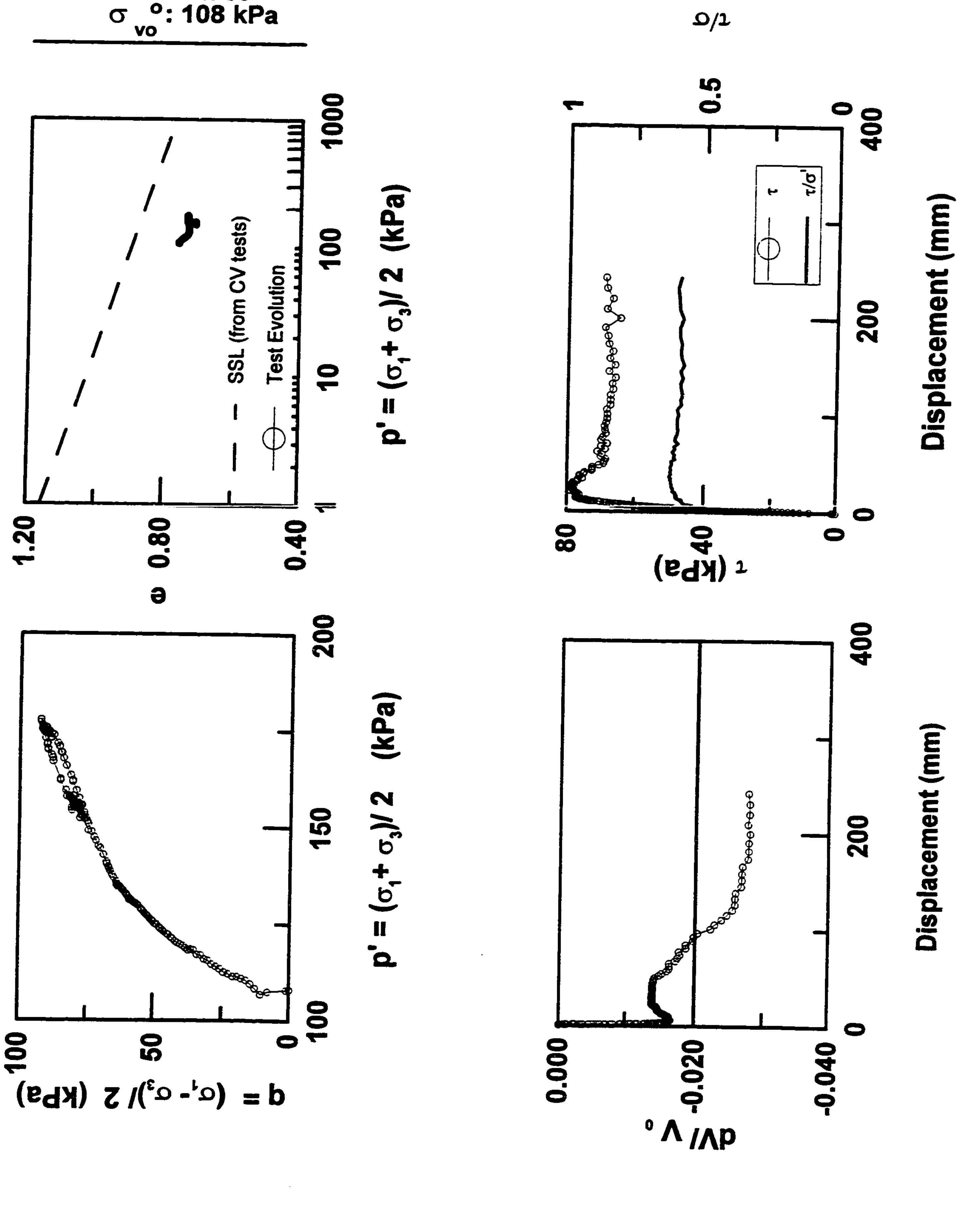

APPENDIX I

TEST: CLDF30-01

e_o : 0.517
σ'_{vo} : 24 kPa

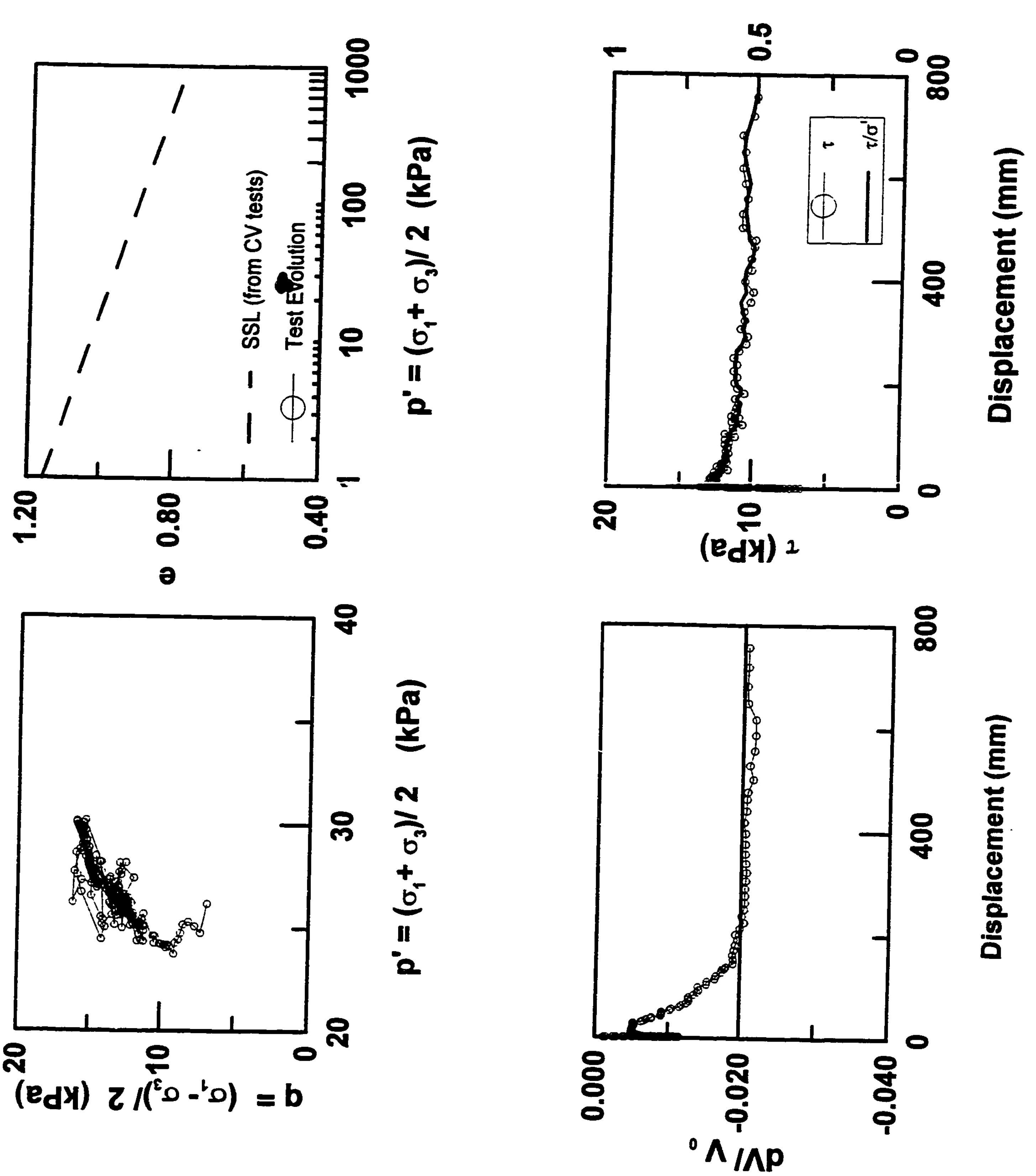

APPENDIX I

TEST: CLDF30-03

e_o : 0.550
σ'_{vo} : 53 kPa

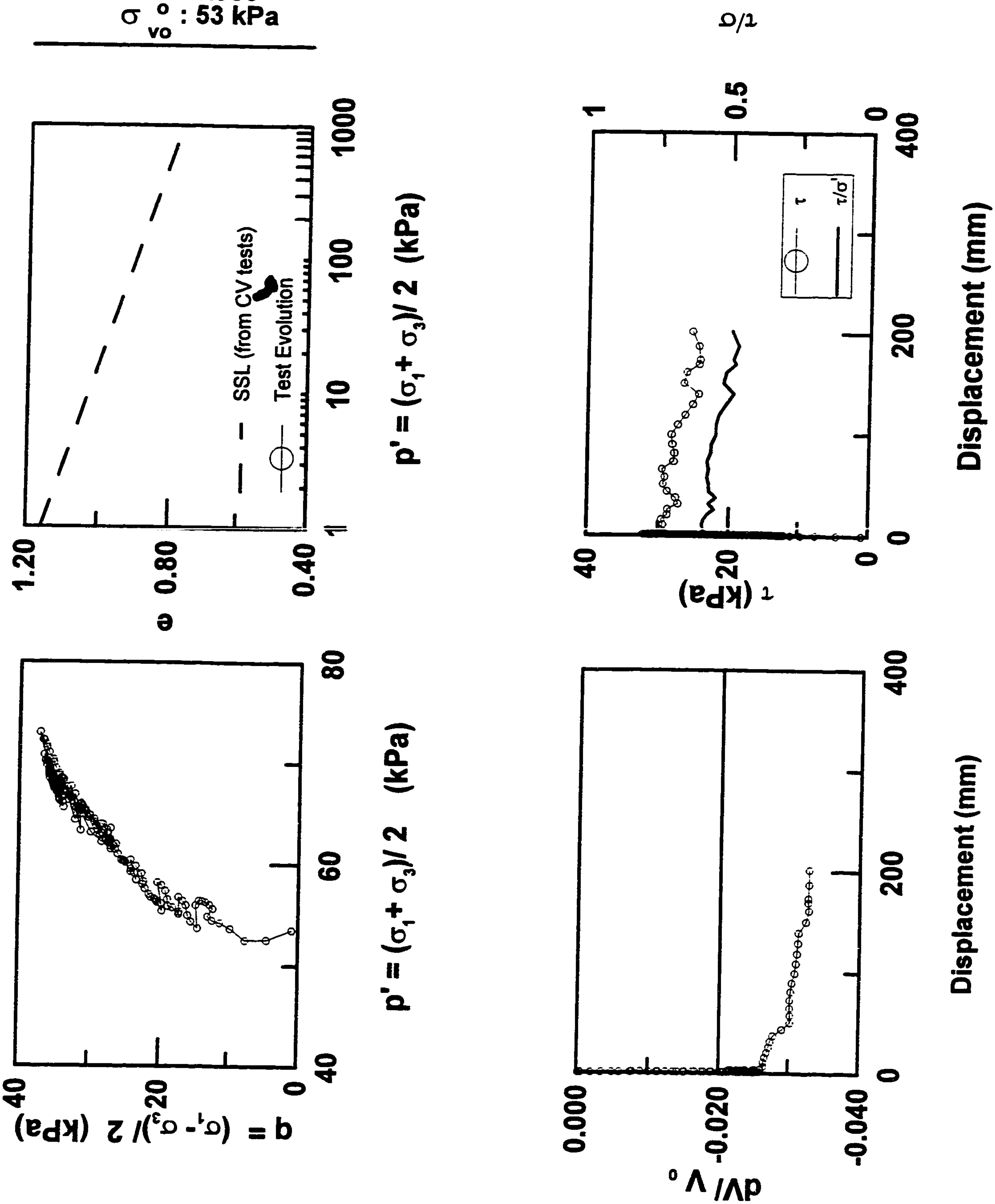

APPENDIX I

TEST: CLDF40-06

e_o : 0.527
σ_{vo} : 94 kPa

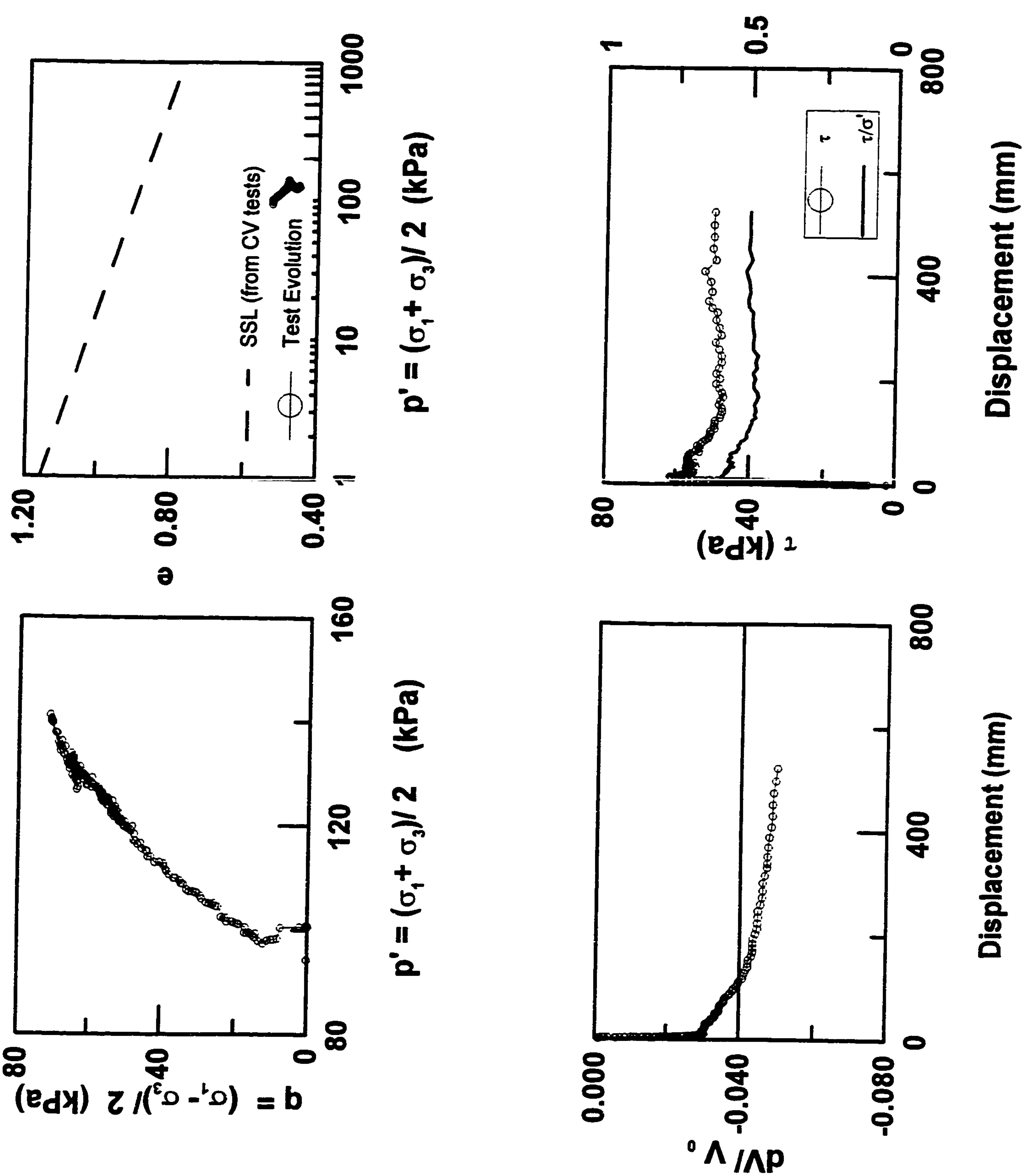

APPENDIX I

TEST: CLDF40-05

e_o : 0.557
σ_{vo} : 93 kPa

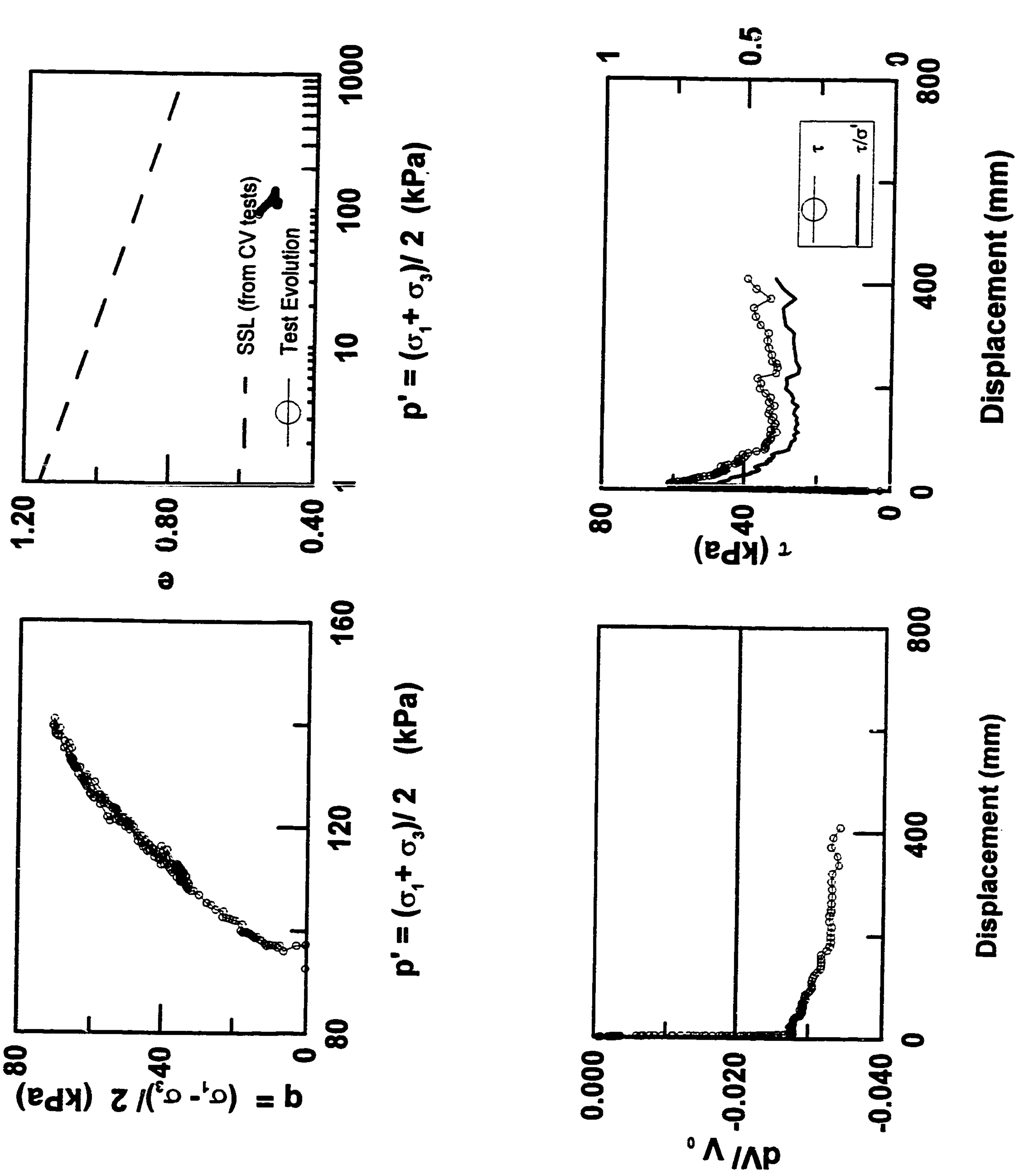

APPENDIX I

TEST: CLDF40-08

e_o : 0.573
σ_{vo}^{o}: 112 kPa

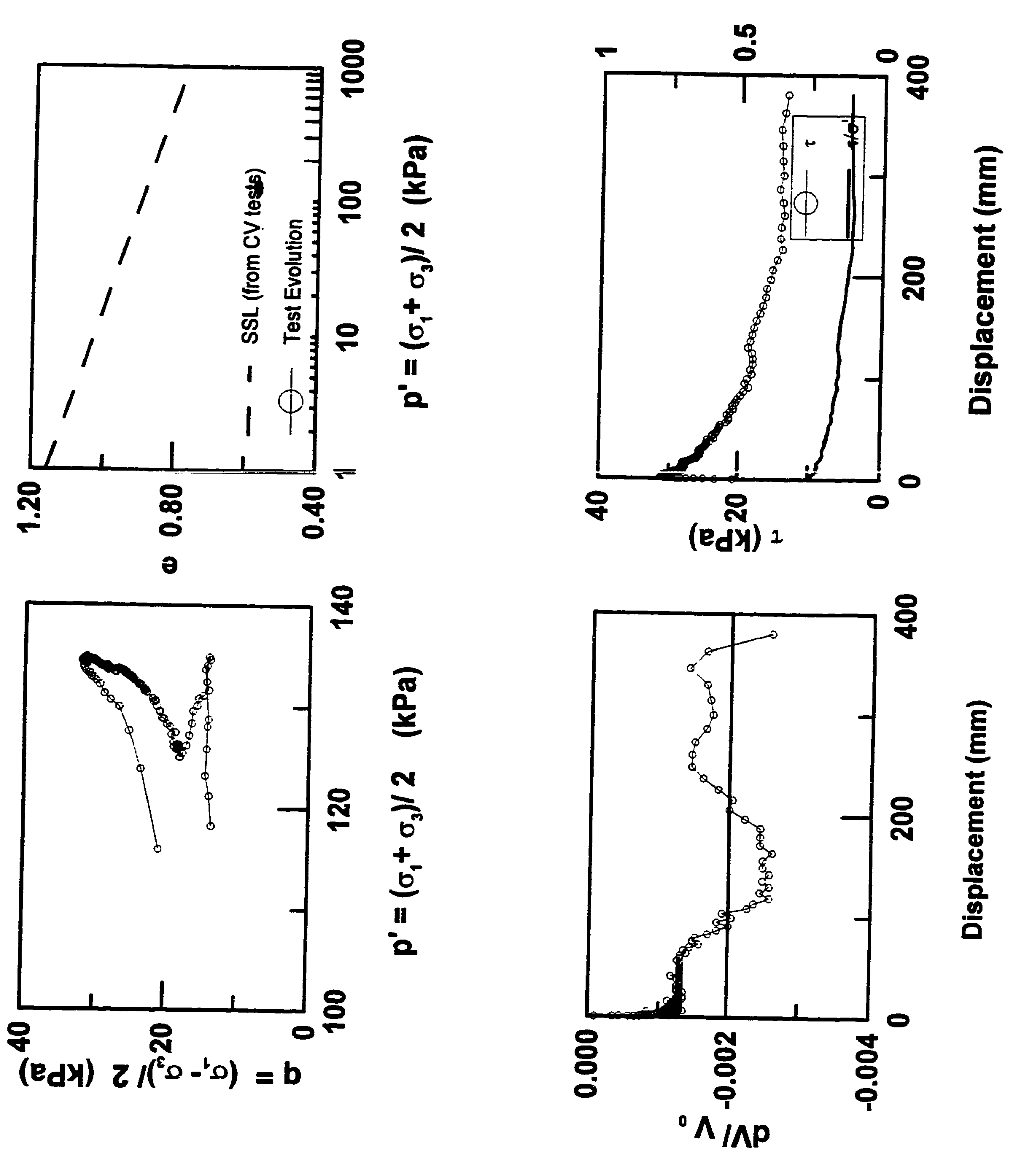

APPENDIX I

TEST: CLDF30-05

e_o : 0.492
σ'_{vo}: 106 kPa

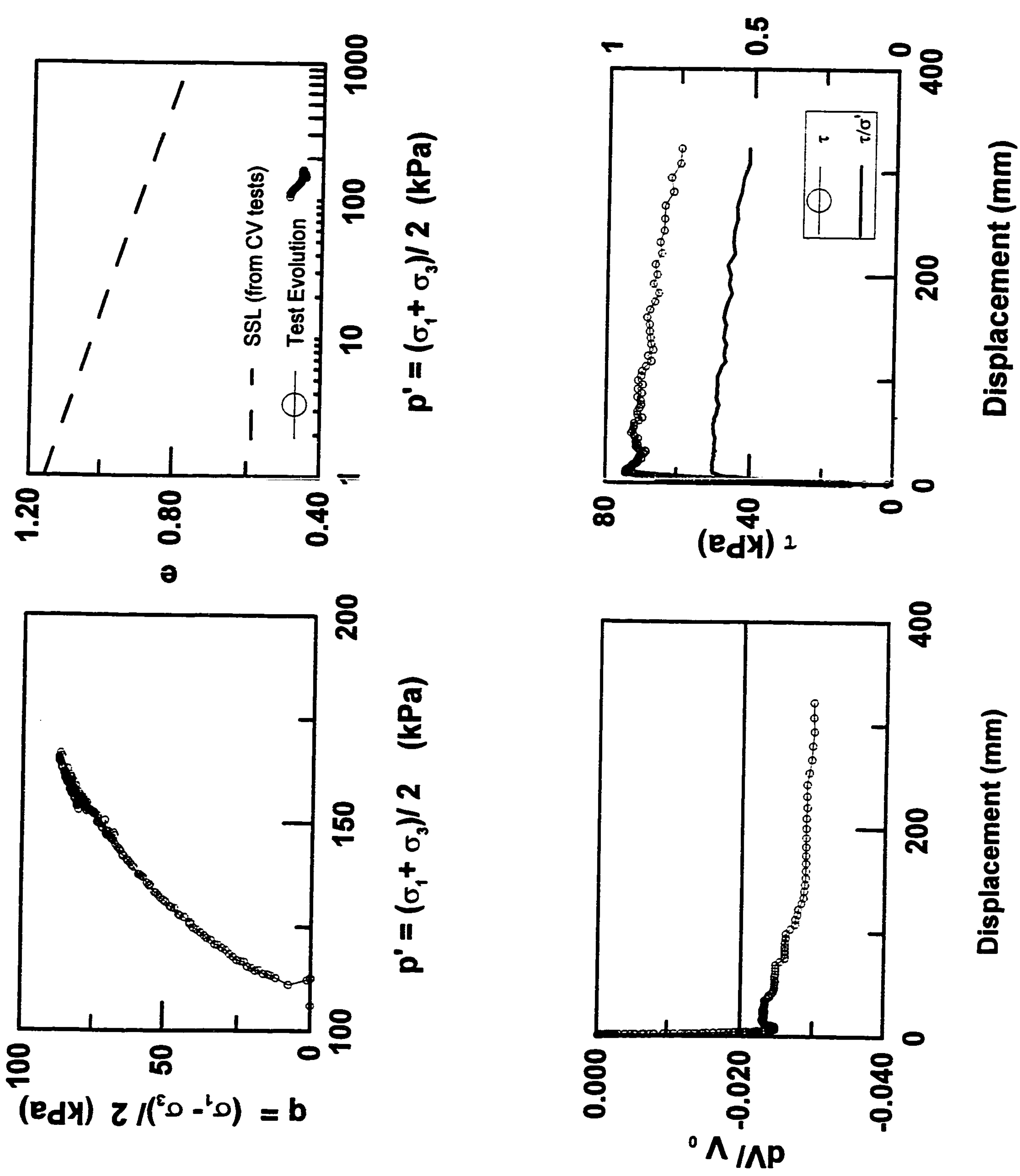

APPENDIX I

TEST: CLDF40-01

e_o : 0.613
σ_{vo} : 23 kPa

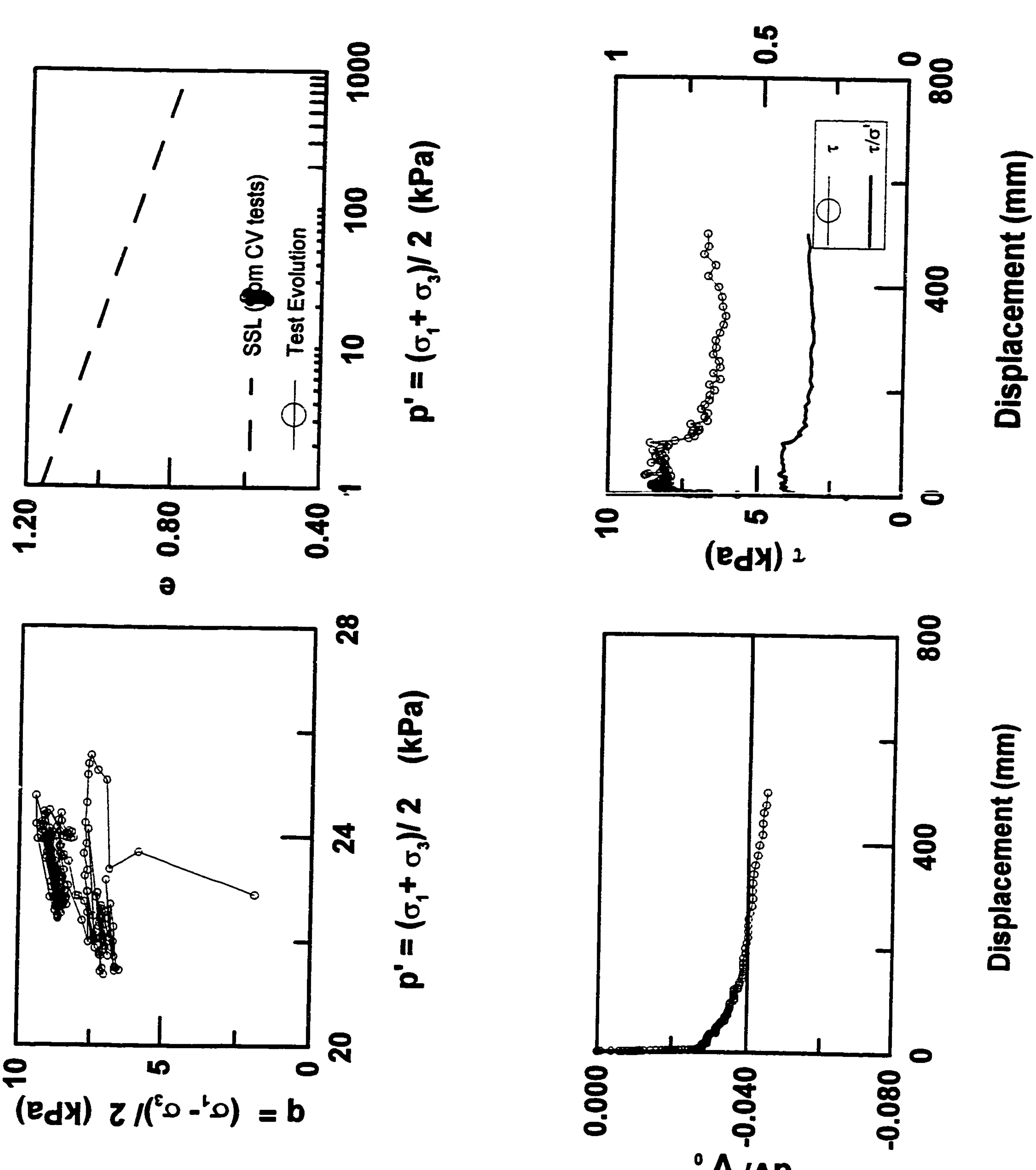

APPENDIX I

TEST: CLDF40-02

e_o : 0.497
σ_{vo} : 33 kPa

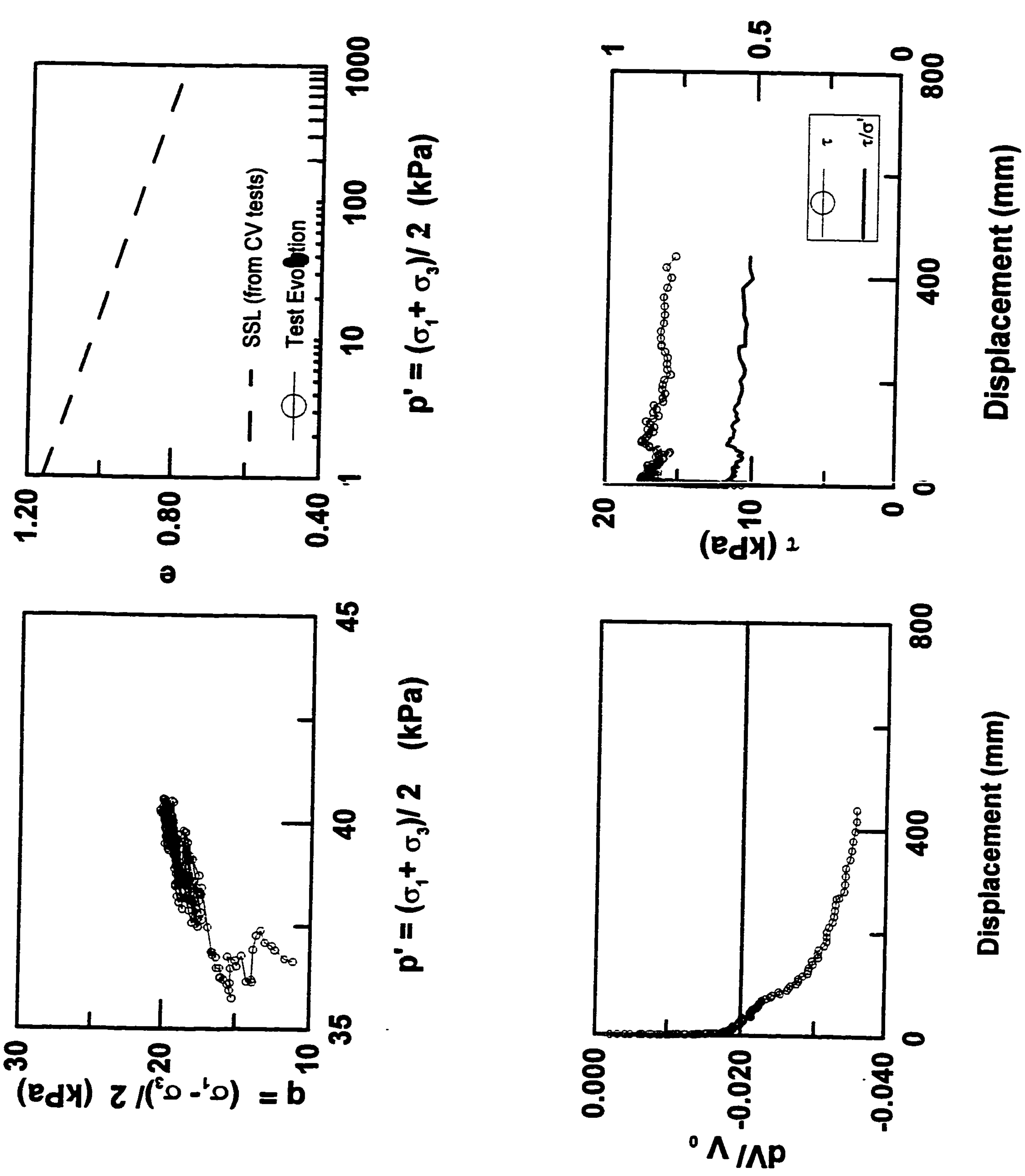

APPENDIX I

TEST: CLDF40-03

e_o : 0.590
σ'_{vo} : 38 kPa

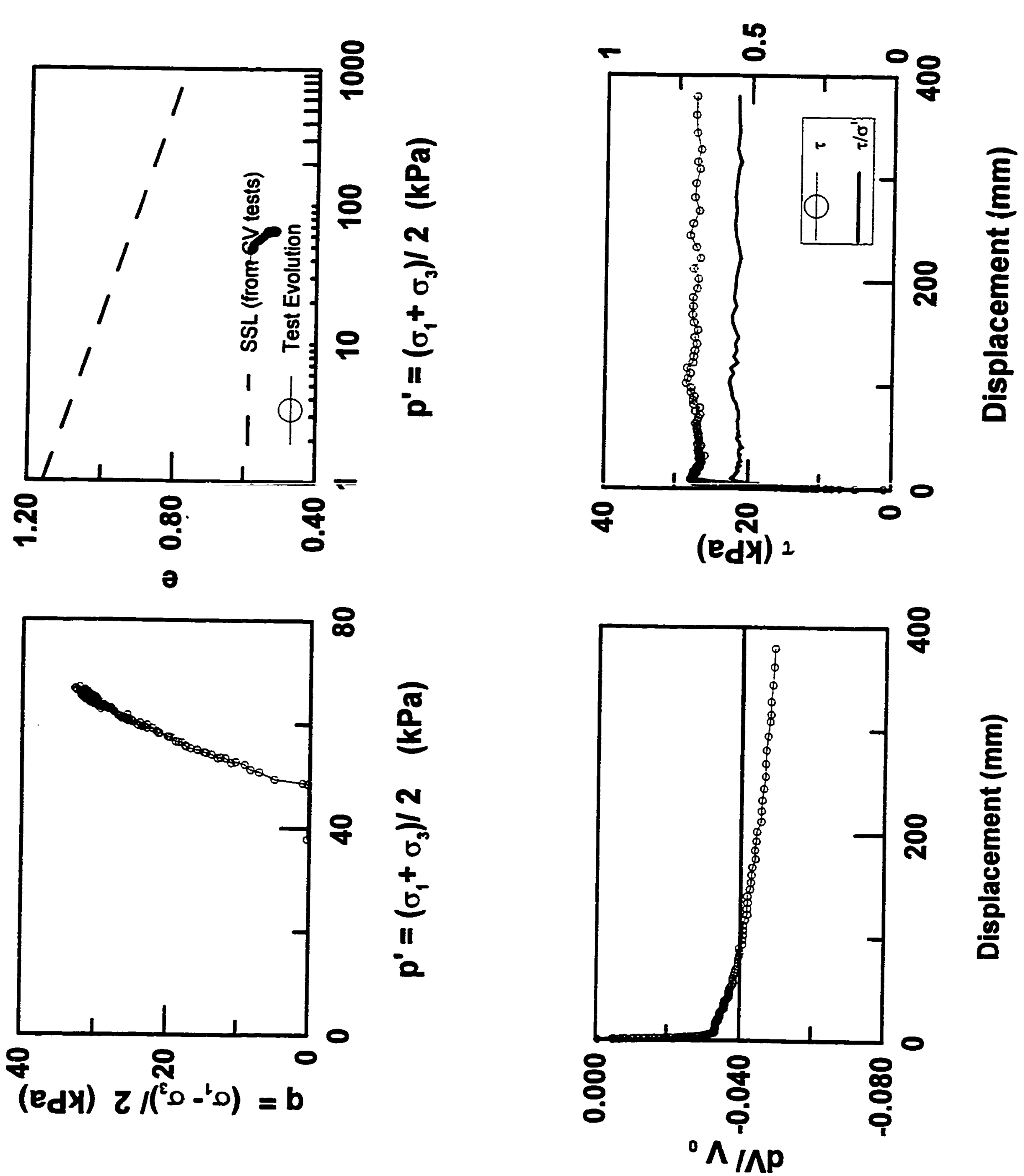

APPENDIX I

TEST: CLDF40-04

e_o : 0.557
σ'_{vo} : 71 kPa

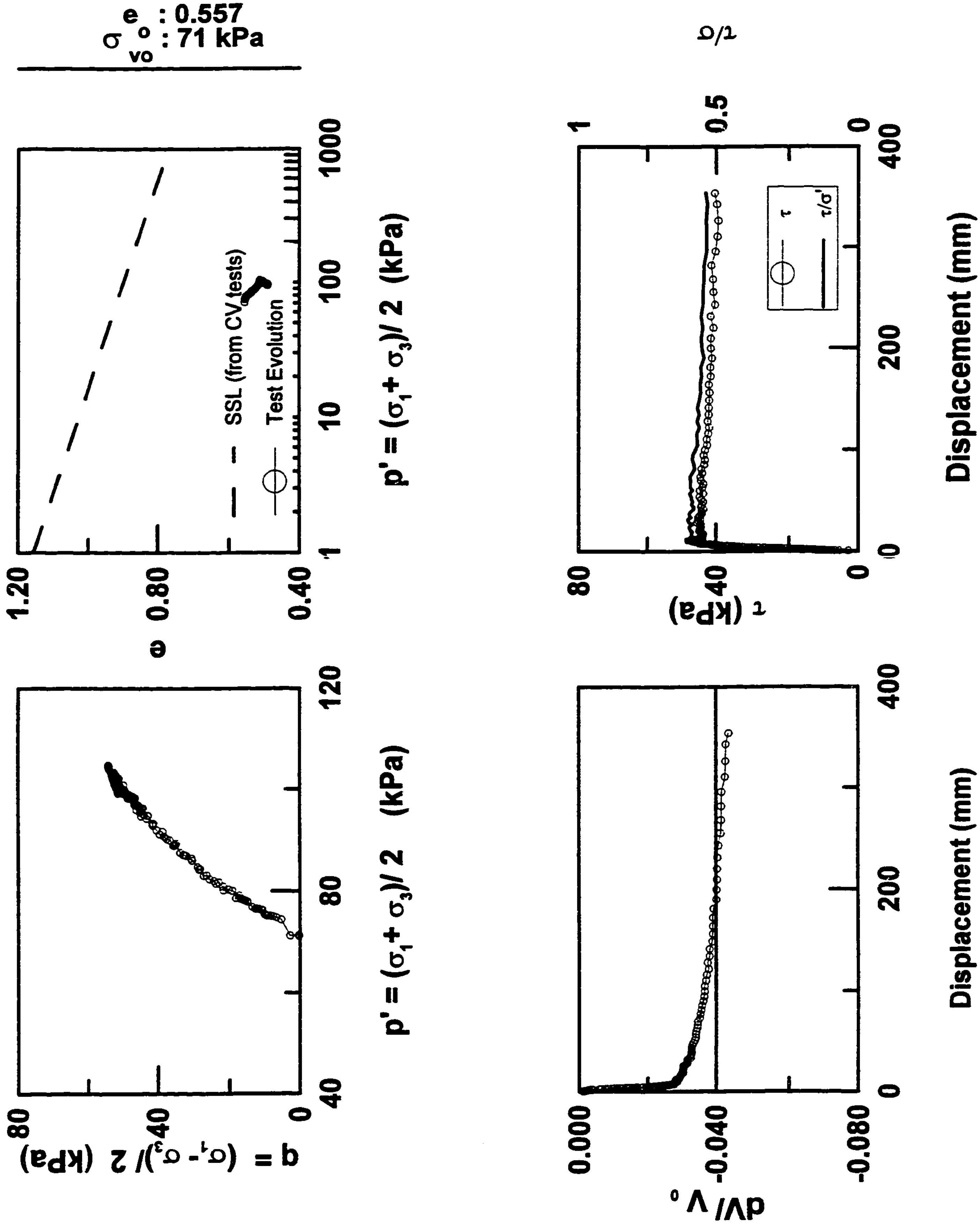

APPENDIX I

TEST: CLD-09

e_o : 0.940
σ_{vo} : 35 kPa

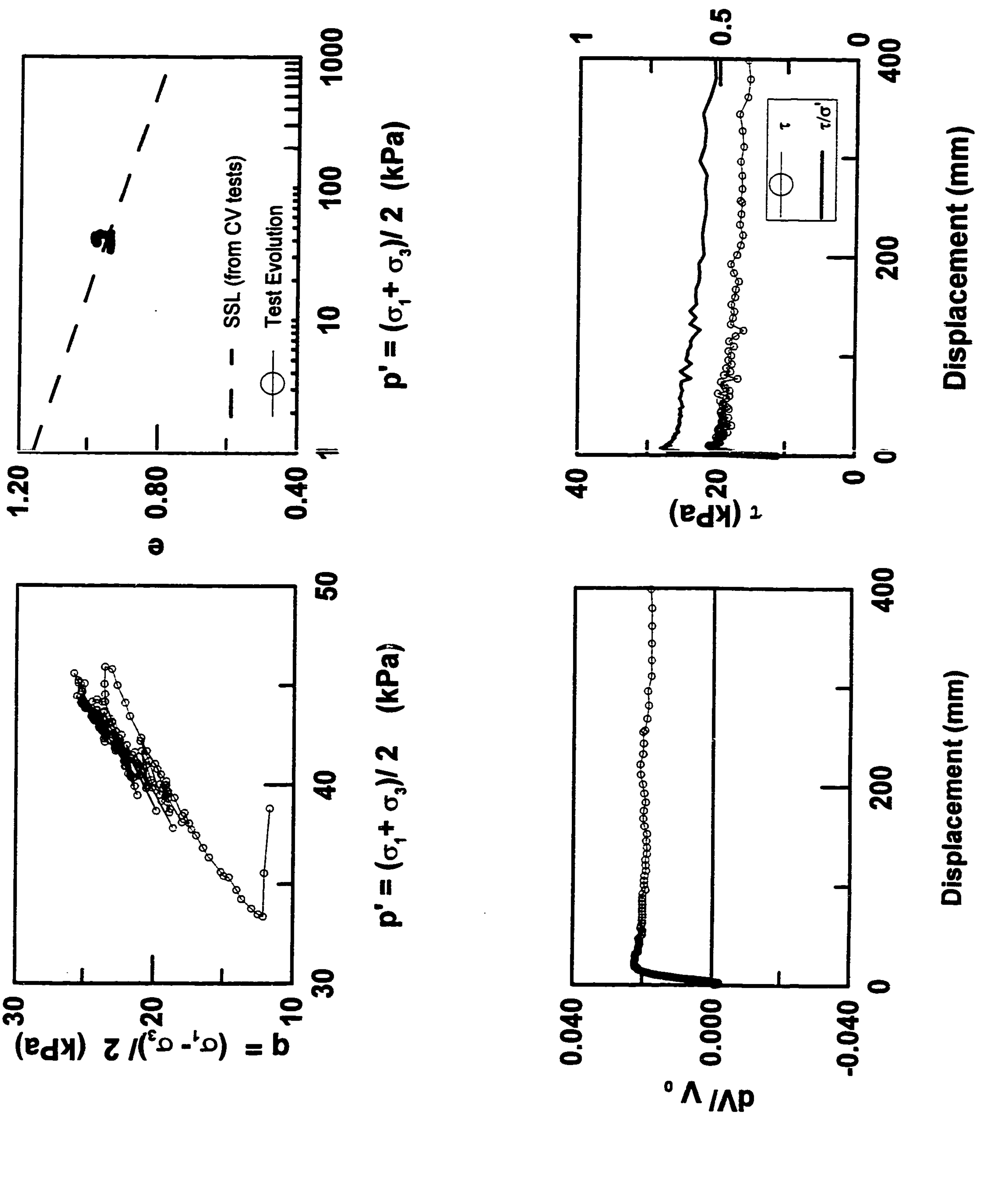

APPENDIX I

TEST: CLD-11

e_o : 0.947
σ'_{vo} : 72 kPa

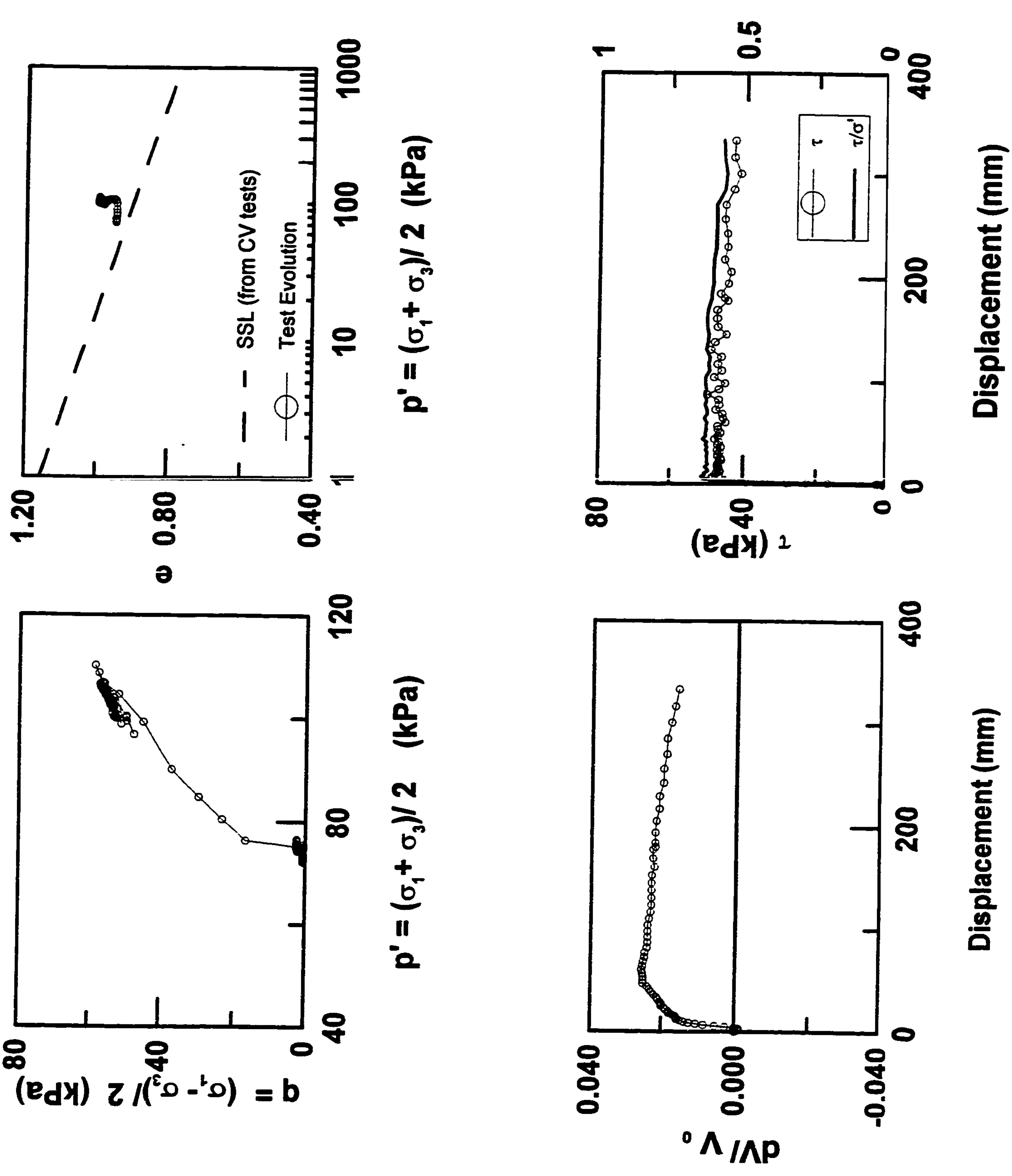

APPENDIX I

TEST: CLSR15-03

e_o : 0.797
σ_{vo}': 310 kPa

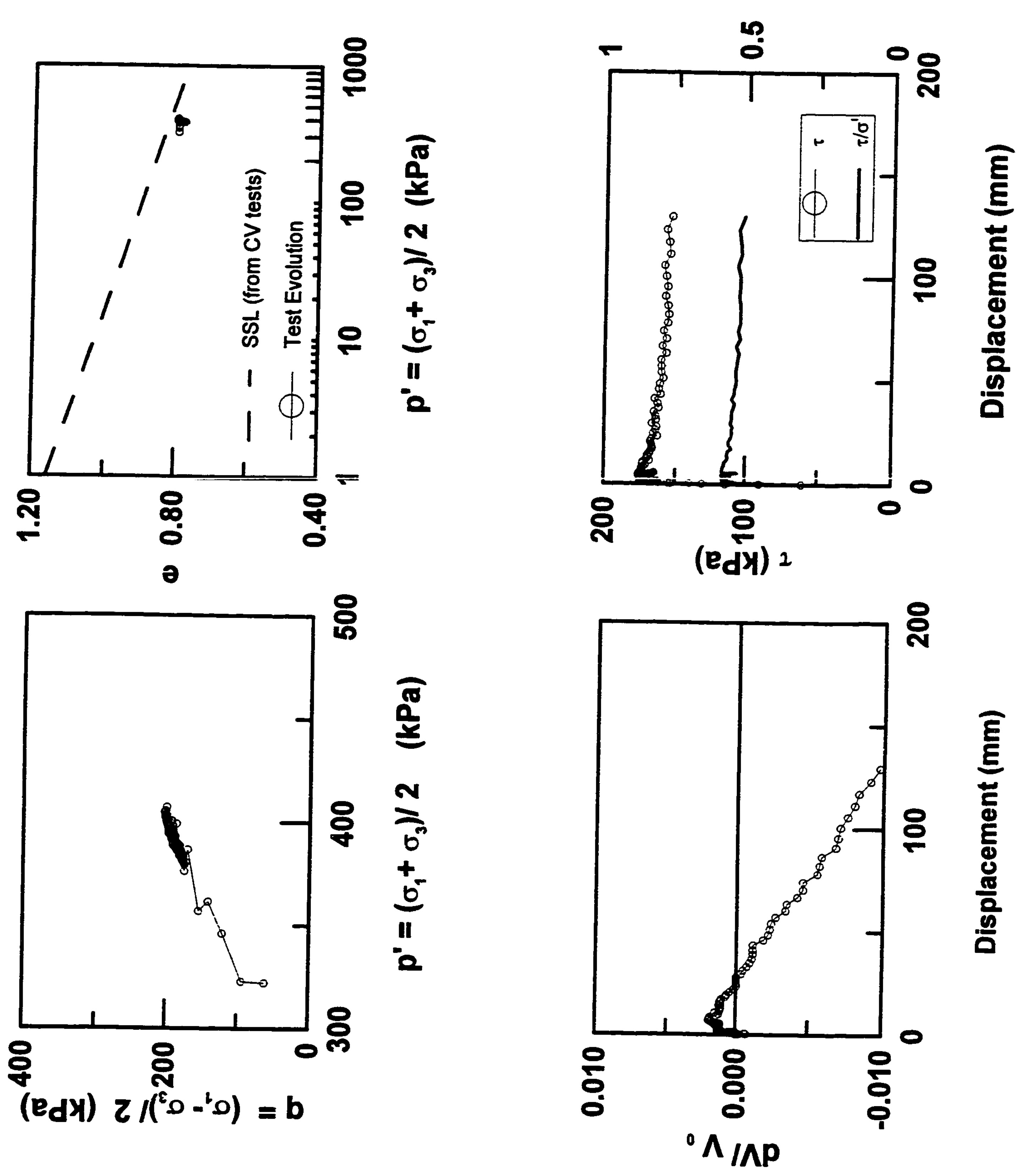

APPENDIX I

TEST: CLSR30-03

e_o : 0.770
σ_{vo}': 299 kPa